D. Primary to Secondary Side Coupling

One primary:
One secondary

One primary:
Multiple secondary

Multiple primary:
One secondary

Multiple primary:
Multiple secondary

FIG. 78

InductEV, Inc.
Exhibit 1025
Page 348

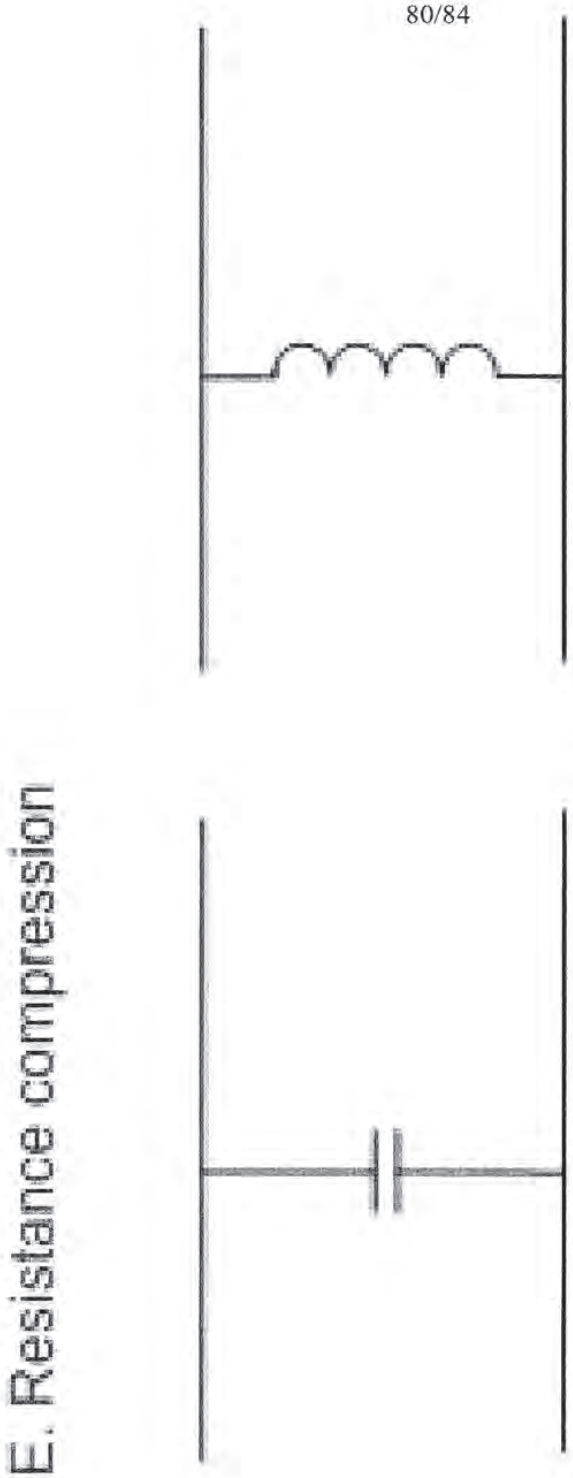


FIG. 79

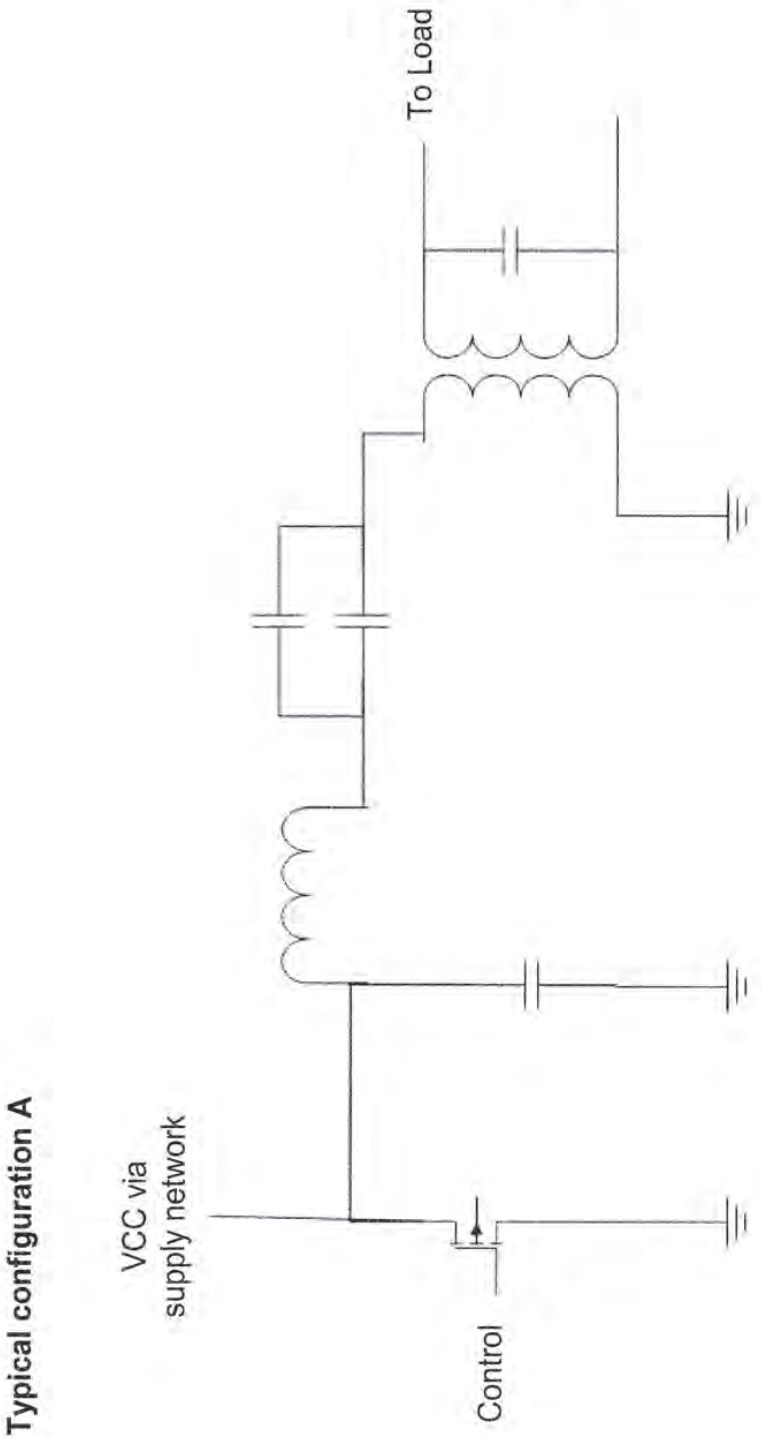

Typical configuration A
VCC via
supply network
Control
To Load

FIG. 80

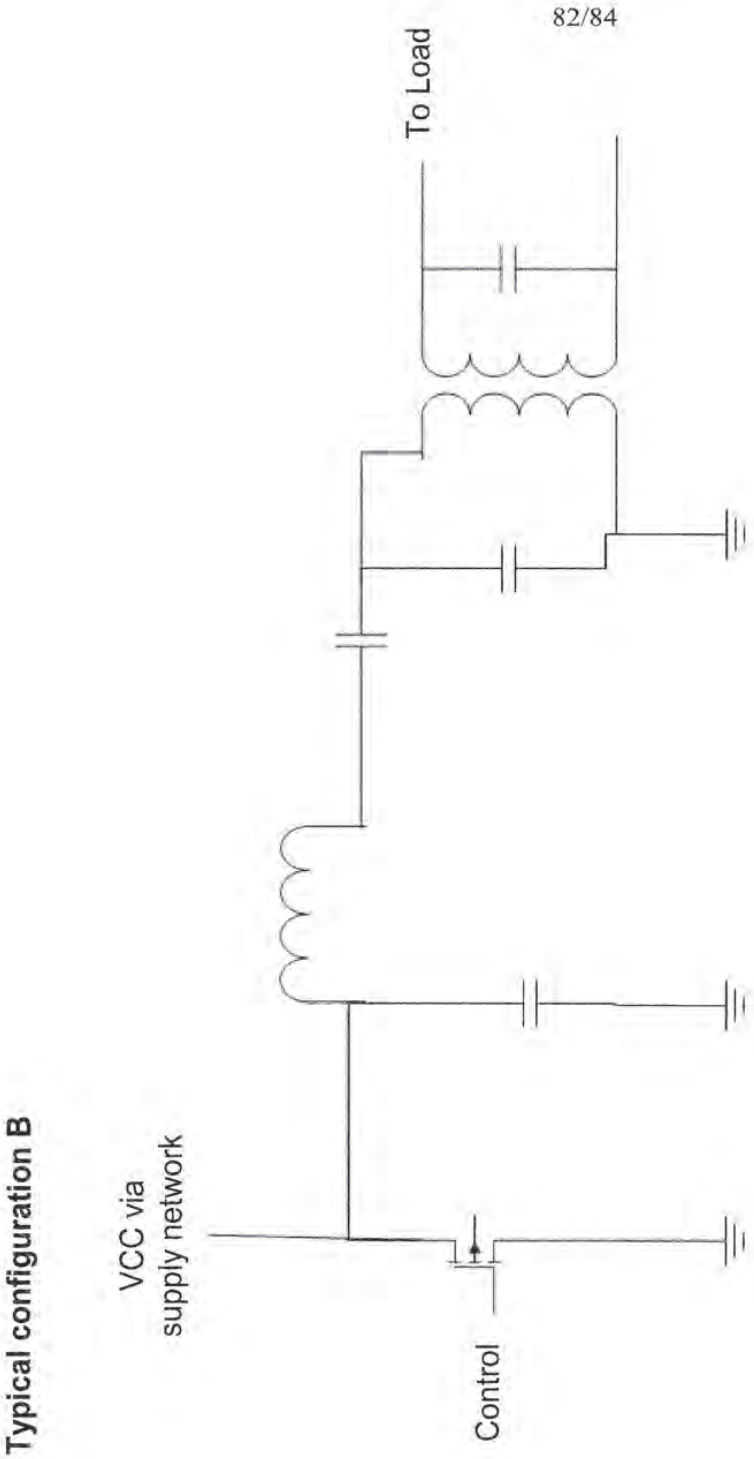

Typical configuration B
VCC via
supply network
Control
To Load

FIG. 81

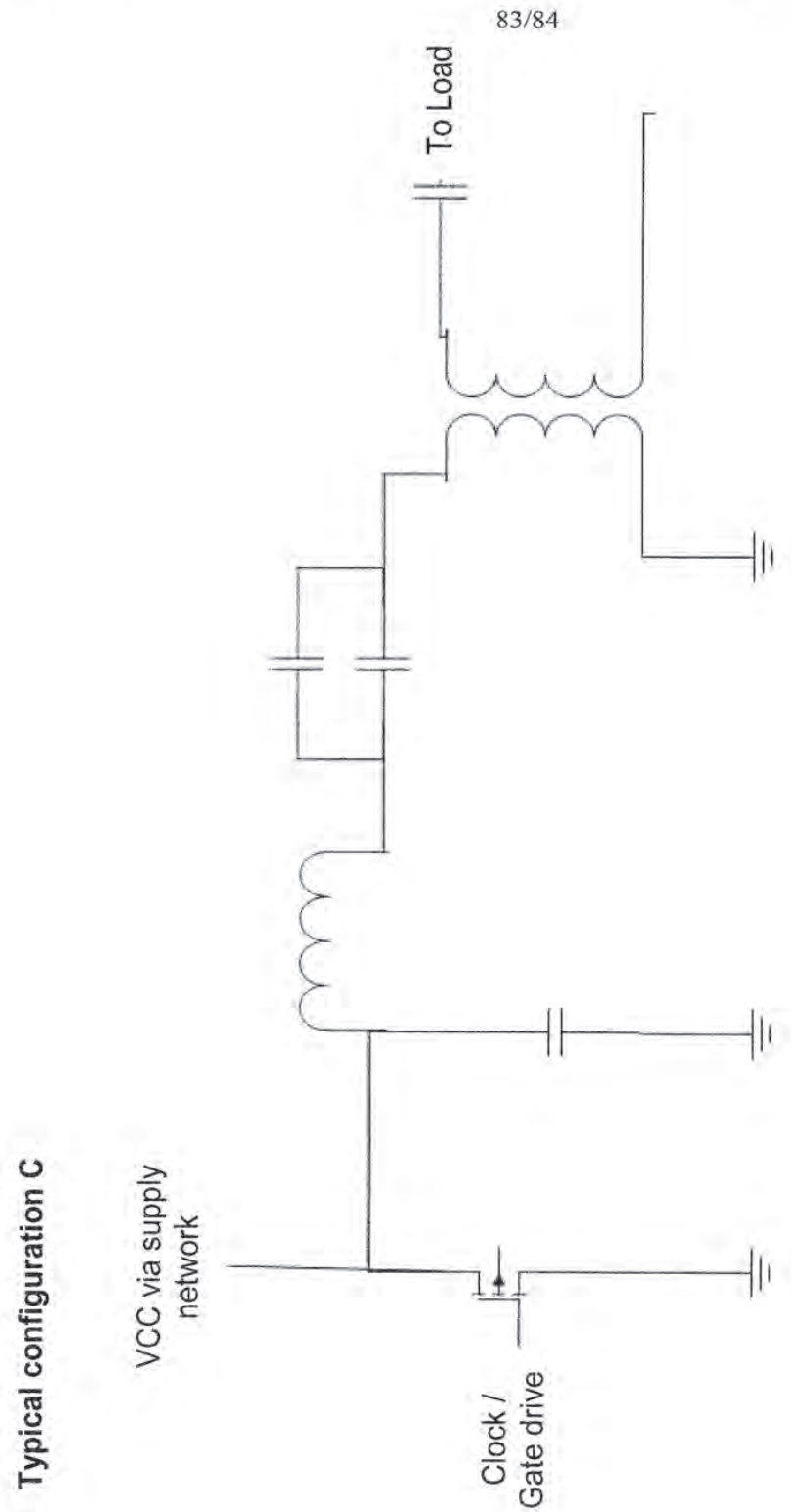


FIG. 82

InductEV, Inc.
Exhibit 1025
Page 352

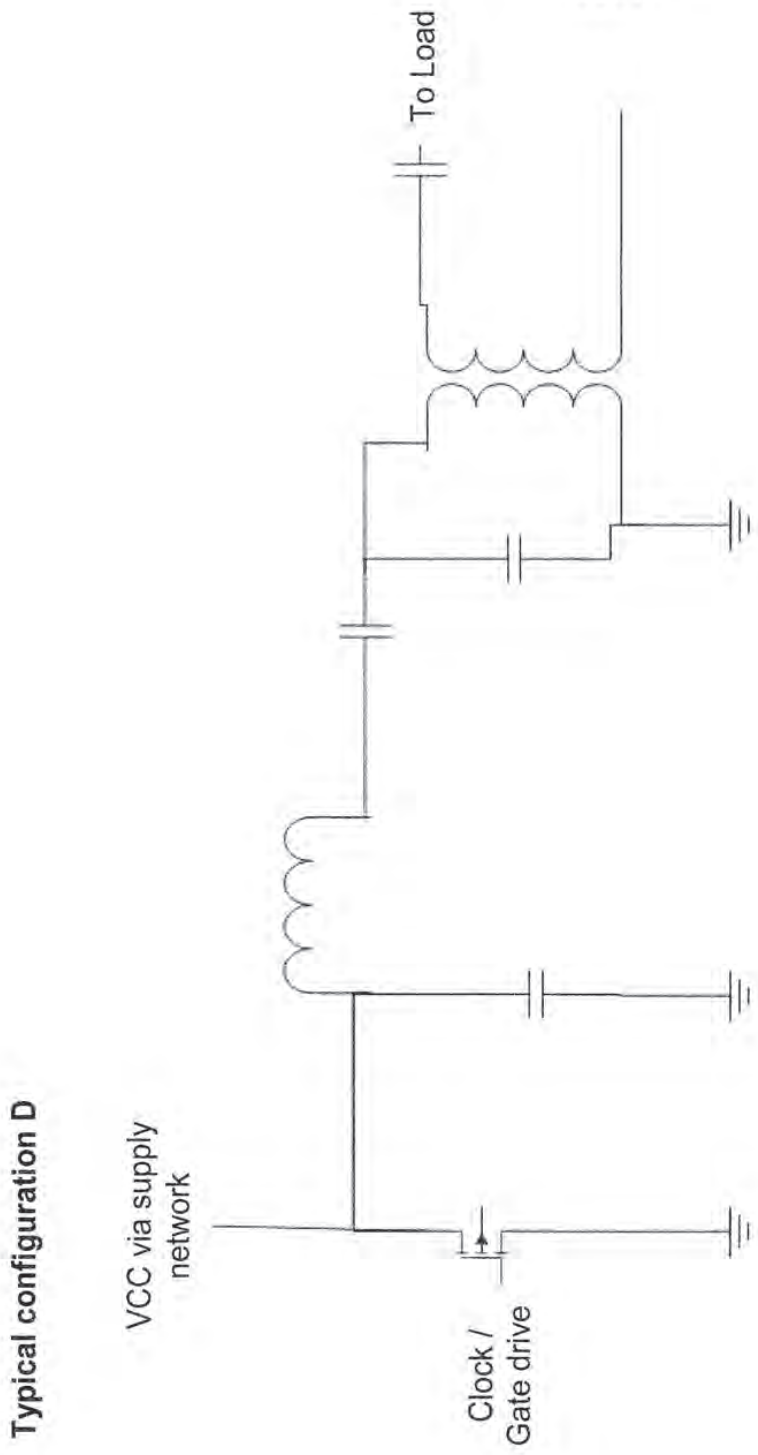


FIG. 83

InductEV, Inc.
Exhibit 1025
Page 353

(12) INTERNATIONAL APPLICATION PUBLISHED UNDER THE PATENT COOPERATION TREATY (PCT)

(19) World Intellectual Property Organization
International Bureau

(43) International Publication Date
10 December 2009 (10.12.2009)

PCT

(10) International Publication Number
WO 2009/149464 A3

(51) International Patent Classification:
H02J 17/00 (2006.01)

(21) International Application Number:
PCT/US2009/046648

(22) International Filing Date:
8 June 2009 (08.06.2009)

(25) Filing Language: English

(26) Publication Language: English

(30) Priority Data:
61/059,663 6 June 2008 (06.06.2008) US

(71) Applicant *(for all designated States except US)*: **UNIVERSITY OF FLORIDA RESEARCH FOUNDATION, INC.** [US/US]; 223 Grinter Hall, Gainesville, FL 32611 (US).

(72) Inventors; and

(75) Inventors/Applicants *(for US only)*: **LOW, Zhen, Ning** [SG/US]; 712 S.W. 16th Avenue, #311, Gainesville, FL 32601 (US). **LIN, Jenshan** [US/US]; 910 SW. 105th Terrace, Gainesville, FL 32607 (US). **CHINGA, Raul, Andres** [PE/US]; 1653 N.W. 16th Avenue, Gainesville, FL 32605 (US).

(74) Agent: **PARKER, James, S.**; Saliwanchik, Lloyd, Saliwanchik, P.O. Box 142950, Gainesville, FL 32614-2950 (US).

(81) Designated States *(unless otherwise indicated, for every kind of national protection available)*: AE, AG, AL, AM, AO, AT, AU, AZ, BA, BB, BG, BH, BR, BW, BY, BZ, CA, CH, CL, CN, CO, CR, CU, CZ, DE, DK, DM, DO, DZ, EC, EE, EG, ES, FI, GB, GD, GE, GH, GM, GT, HN, HR, HU, ID, IL, IN, IS, JP, KE, KG, KM, KN, KP, KR, KZ, LA, LC, LK, LR, LS, LT, LU, LY, MA, MD, ME, MG, MK, MN, MW, MX, MY, MZ, NA, NG, NI, NO, NZ, OM, PE, PG, PH, PL, PT, RO, RS, RU, SC, SD, SE, SG, SK, SL, SM, ST, SV, SY, TJ, TM, TN, TR, TT, TZ, UA, UG, US, UZ, VC, VN, ZA, ZM, ZW.

(84) Designated States *(unless otherwise indicated, for every kind of regional protection available)*: ARIPO (BW, GH, GM, KE, LS, MW, MZ, NA, SD, SL, SZ, TZ, UG, ZM, ZW), Eurasian (AM, AZ, BY, KG, KZ, MD, RU, TJ, TM), European (AT, BE, BG, CH, CY, CZ, DE, DK, EE, ES, FI, FR, GB, GR, HR, HU, IE, IS, IT, LT, LU, LV, MC, MK, MT, NL, NO, PL, PT, RO, SE, SI, SK, TR), OAPI (BF, BJ, CF, CG, CI, CM, GA, GN, GQ, GW, ML, MR, NE, SN, TD, TG).

Published:

— *with international search report (Art. 21(3))*

— *before the expiration of the time limit for amending the claims and to be republished in the event of receipt of amendments (Rule 48.2(h))*

(88) Date of publication of the international search report:
8 April 2010

(54) Title: METHOD AND APPARATUS FOR CONTACTLESS POWER TRANSFER

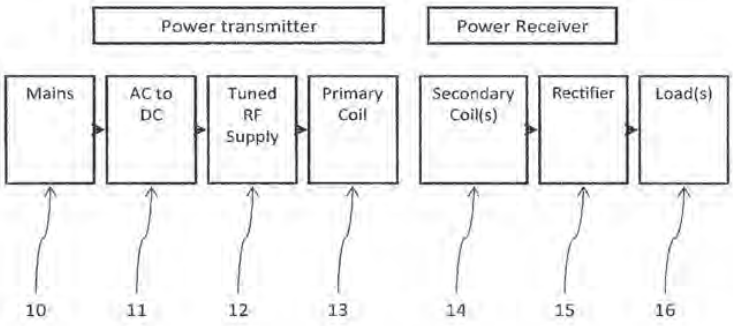


FIG. 1

(57) Abstract: Embodiments of the subject invention pertain to a method and apparatus for contactless power transfer. A specific embodiment relates to an impedance transformation network, a new class of load network for application to a contactless power system. Embodiments of the impedance transformation network enable a contactless power system to operate without encountering the common problems of: 1) over-voltage and/or under-voltage conditions; 2) over-power and/or under-power conditions; 3) power oscillations; and 4) high heat dissipation.

WO 2009/149464 A3

INTERNATIONAL SEARCH REPORT

International application No.
PCT/US2009/046648

A. CLASSIFICATION OF SUBJECT MATTER

H02J 17/00(2006.01)i

According to International Patent Classification (IPC) or to both national classification and IPC

B. FIELDS SEARCHED

Minimum documentation searched (classification system followed by classification symbols)
H02J 17/00; C12M 1/34; H02M 3/335; H02M 7/537; H03F 1/22; H05B 3/00; H05B 37/02

Documentation searched other than minimum documentation to the extent that such documents are included in the fields searched
Korean utility models and applications for utility models
Japanese utility models and applications for utility models
(Chinese Patents and application for patent)

Electronic data base consulted during the international search (name of data base and, where practicable, search terms used)
PAJ, FPD, USPAT, eKIPASS "Keyword: primary coil, secondary coil, inductive coupling, variable impedance"

C. DOCUMENTS CONSIDERED TO BE RELEVANT

Category*	Citation of document, with indication, where appropriate, of the relevant passages	Relevant to claim No.
A	US 2006-0076338 A1 (VALERY KAGAN) 13 April 2006 See the abstract; figure 1.	1-111
A	US 2005-0140456 A1 (NUNTHA KUMAR KRISHNASAMY MANIAM et al.) 30 June 2005 See the abstract; figure 1.	1-111
A	US 6088249 A (ADAMSON; HUGH PATRICK) 11 July 2000 See the abstract; figure 8.	1-111
A	US 5818702 A (FAULK; RICHARD A.) 06 October 1998 See the abstract; figures 2B, 3A.	1-111

☐ Further documents are listed in the continuation of Box C.

☒ See patent family annex.

* Special categories of cited documents:
"A" document defining the general state of the art which is not considered to be of particular relevance
"E" earlier application or patent but published on or after the international filing date
"L" document which may throw doubts on priority claim(s) or which is cited to establish the publication date of citation or other special reason (as specified)
"O" document referring to an oral disclosure, use, exhibition or other means
"P" document published prior to the international filing date but later than the priority date claimed
"T" later document published after the international filing date or priority date and not in conflict with the application but cited to understand the principle or theory underlying the invention
"X" document of particular relevance; the claimed invention cannot be considered novel or cannot be considered to involve an inventive step when the document is taken alone
"Y" document of particular relevance; the claimed invention cannot be considered to involve an inventive step when the document is combined with one or more other such documents,such combination being obvious to a person skilled in the art
"&" document member of the same patent family

Date of the actual completion of the international search	Date of mailing of the international search report
11 FEBRUARY 2010 (11.02.2010)	**17 FEBRUARY 2010 (17.02.2010)**

Name and mailing address of the ISA/KR
Korean Intellectual Property Office
Government Complex-Daejeon, 139 Seonsa-ro, Seo-gu, Daejeon 302-701, Republic of Korea
Facsimile No. 82-42-472-7140

Authorized officer
WEE Jae Woo
Telephone No. 82-42-481-8540

Form PCT/ISA/210 (second sheet) (July 2008)

INTERNATIONAL SEARCH REPORT
Information on patent family members

International application No.
PCT/US2009/046648

Patent document cited in search report	Publication date	Patent family member(s)	Publication date
US 2006-0076338 A1	13.04.2006	AU 2004-300525 A1	13.01.2005
		CA 2531096-A1	13.01.2005
		CA 2592673-A1	10.05.2007
		CN 101112123 A	23.01.2008
		CN 101112123 C0	23.01.2008
		CN 1836467 A0	20.09.2006
		EP 1649726 A2	26.04.2006
		EP 1649726 B1	03.01.2007
		EP 1649726 B8	28.02.2007
		EP 1768462 A2	28.03.2007
		EP 1768462 A3	26.09.2007
		EP 1943879 A1	16.07.2008
		JP 2007-531200 A	01.11.2007
		JP 2009-518778 A	07.05.2009
		KR 10-2006-0052721 A	19.05.2006
		KR 10-2008-0072524 A	06.08.2008
		KR20080072524A	06.08.2008
		MX2007009778A	21.08.2007
		US 2005-0000959 A1	06.01.2005
		US 2005-0006380 A1	13.01.2005
		US 2006-0219709 A1	05.10.2006
		US 2008-0238386 A1	02.10.2008
		US 7034263 B2	25.04.2006
		US 7034264 B2	25.04.2006
		US 7279665 B2	09.10.2007
		WO 2005-004540 A2	13.01.2005
		WO 2005-004540 A3	13.01.2005
		WO 2007-053583 A1	10.05.2007
		WO 2007-053583 A8	28.06.2007
US 2005-0140456 A1	30.06.2005	US 7019593 B2	28.03.2006
US 6088249 A	11.07.2000	AU 1999-31096 A1	08.11.1999
		CN 1152609 C0	02.06.2004
		CN 1306733 A0	01.08.2001
		EP 1078557 A1	28.02.2001
		EP 1078557 B1	31.07.2002
		US 5933340 A1	03.08.1999
		US 6094017 A1	25.07.2000
		US 6181066 B1	30.01.2001
		WO 99-55125 A1	28.10.1999
US 5818702 A	06.10.1998	US 5706182 A1	06.01.1998

(12) INTERNATIONAL APPLICATION PUBLISHED UNDER THE PATENT COOPERATION TREATY (PCT)

(19) World Intellectual Property Organization
International Bureau

(43) International Publication Date
23 December 2009 (23.12.2009)

PCT

(10) International Publication Number
WO 2009/155000 A2

(51) International Patent Classification:
H02J 7/00 (2006.01) *H02J 17/00* (2006.01)

(21) International Application Number:
PCT/US2009/045339

(22) International Filing Date:
27 May 2009 (27.05.2009)

(25) Filing Language: English

(26) Publication Language: English

(30) Priority Data:
61/056,354 27 May 2008 (27.05.2008) US

(71) Applicant *(for all designated States except US)*: **UNIVERSITY OF FLORIDA RESEARCH FOUNDATION, INC.** [US/US]; 223 Grinter Hall, Gainesville, FL 32611 (US).

(72) Inventor; and

(75) Inventor/Applicant *(for US only)*: **LIN, Jenshan** [US/US]; 910 S.W. 105th Terrace, Gainesville, FL 32607 (US).

(74) Agent: **PARKER, James, S.**; Saliwanchik, Lloyd, Saliwanchik, P.O. Box 142950, Gainesville, FL 32614-2950 (US).

(81) Designated States *(unless otherwise indicated, for every kind of national protection available)*: AE, AG, AL, AM, AO, AT, AU, AZ, BA, BB, BG, BH, BR, BW, BY, BZ, CA, CH, CN, CO, CR, CU, CZ, DE, DK, DM, DO, DZ, EC, EE, EG, ES, FI, GB, GD, GE, GH, GM, GT, HN, HR, HU, ID, IL, IN, IS, JP, KE, KG, KM, KN, KP, KR, KZ, LA, LC, LK, LR, LS, LT, LU, LY, MA, MD, ME, MG, MK, MN, MW, MX, MY, MZ, NA, NG, NI, NO, NZ, OM, PG, PH, PL, PT, RO, RS, RU, SC, SD, SE, SG, SK, SL, SM, ST, SV, SY, TJ, TM, TN, TR, TT, TZ, UA, UG, US, UZ, VC, VN, ZA, ZM, ZW.

(84) Designated States *(unless otherwise indicated, for every kind of regional protection available)*: ARIPO (BW, GH, GM, KE, LS, MW, MZ, NA, SD, SL, SZ, TZ, UG, ZM, ZW), Eurasian (AM, AZ, BY, KG, KZ, MD, RU, TJ, TM), European (AT, BE, BG, CH, CY, CZ, DE, DK, EE, ES, FI, FR, GB, GR, HR, HU, IE, IS, IT, LT, LU, LV, MC, MK, MT, NL, NO, PL, PT, RO, SE, SI, SK, TR), OAPI (BF, BJ, CF, CG, CI, CM, GA, GN, GQ, GW, ML, MR, NE, SN, TD, TG).

[Continued on next page]

(54) Title: METHOD AND APPARATUS FOR PRODUCING SUBSTANTIALLY UNIFORM MAGNETIC FIELD

(57) Abstract: A planar wireless power transmitter coil design and method are provided. A single spiral coil can be used to provide a uniform magnetic field across its surface area for location-independent planar wireless power charging. The spiral coil can be designed to have a non- constant gap between adjacent loops such that the gap between adjacent loops decreases towards the outer loops.

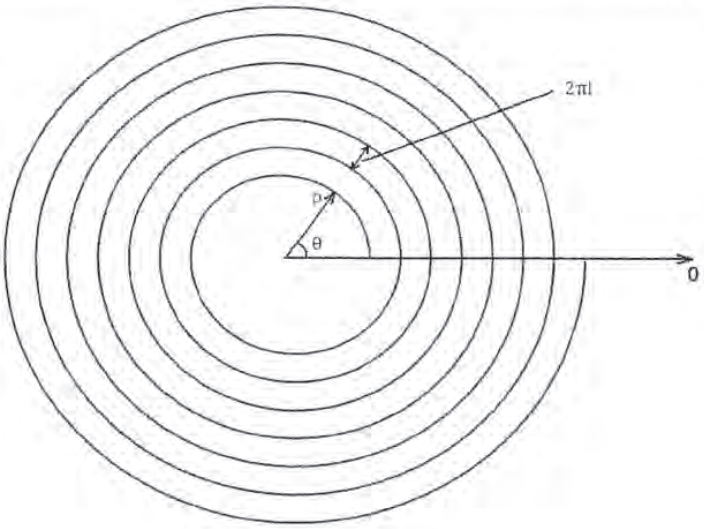


FIG. 1

WO 2009/155000 A2

Published:

— *without international search report and to be republished upon receipt of that report (Rule 48.2(g))*

DESCRIPTION

METHOD AND APPARATUS FOR PRODUCING SUBSTANTIALLY UNIFORM MAGNETIC FIELD

CROSS-REFERENCE TO RELATED APPLICATION

The present application claims the benefit of U.S. Provisional Application Serial No. 61/056,354, filed May 27, 2008, which is hereby incorporated by reference herein in its entirety, including any figures, tables, or drawings.

BACKGROUND OF INVENTION

In recent years, consumer electronics devices such as cell phones, personal digital assistants (PDAs), and laptops are using more wireless components such as a Bluetooth headset, wireless mouse, and wireless LAN. However, the wired power line remains to impair wireless freedom. Many designs and research has been conducted to provide solutions to get rid of this wire. Inductive wireless power transmission appears to be the most promising solution to this problem.

In wireless power charging, AC current passes through a transmitter coil, inducing magnetic flux on and/or above the surface of a power platform. A receiver coil generates voltage when magnetic flux passing through the receiver coil's loop(s) changes. In many cases, the transmitter coil and the receiver coil are not of the same size.

However, when the transmitter coil and receiver coil have significantly different sizes, the voltage generated on the receiving side can be greatly affected by the receiver coil's placement on the surface of the transmitter coil.

Specifically, a typical transmitter coil has a non-uniform magnetic field across its surface area, which may cause voltage variation and impedance matching difficulty.

A normal spiral coil as shown in Figure 1 usually has constant gap between adjacent loops. For example, the circular spiral coil of Figure 1 follows the equation of

$$\rho = \rho_0 + l\theta . \quad (1)$$

where ρ is the radius, θ is the angle, ρ_0 is the initial radius and l is a constant. In Figure 1, the distance between adjacent wires is a constant $2p l$.

InductEV, Inc.
Exhibit 1025
Page 359

The magnetic field near the surface for the coil shown in Figure 1 is shown in Figure 2, which illustrates a high magnetic field strength at the center of the coil. Each loop of the coil contributes magnetic field in the area it encloses, and the magnetic field in the center is the superposition of magnetic field contributions from all the loops.

For a regular coil, the density of magnetic flux generated in the coil has a maximum value at a position closest to the coil, and has a minimum value at a position at the center of the coil. Thus, the charging efficiency may be abruptly deteriorated leading to significant variation in charging efficiency.

One approach to solve this problem is discussed in WO2007/013725A1 (Gwon *et al.*), which discloses a wireless charger having decreased variation of charging efficiency. According to Gwon *et al.*, a smaller coil is placed in the center of an outer coil, which reinforces the magnetic flux density in the center of the outer and inner coils. Thus the entire magnetic flux density is flattened as a whole in comparison to the magnetic flux density formed by only the outer coil. Though the design disclosed in Gwon *et al.* reduces the effect of variation of the magnetic flux density of the outer coil, the variation can still be significant. In addition, when the receiver coil is much smaller than the transmitter coil, the location of the receiver coil can often affect its performance.

In a similar approach, WO2007/019806A1 (Hui *et al.*) provides a design of an auxiliary winding for improved performance of a planar inductive charging platform. According to Hui *et al.* an auxiliary winding is introduced to compensate the magnetic field generated by a principle winding. The design taught by Hui *et al.* uses a similar mechanism as that taught by Gwon *et al.* in that separate coils are used to improve charging efficiency.

Thus, there exists in the art a need for improved inductive wireless power transmission.

BRIEF SUMMARY

Embodiments of the subject invention relate to a method and apparatus for providing a planar spiral transmitter coil that produces a substantially uniform magnetic field over a region of interest near the surface of the coil. Embodiments of the invention provide a planar inductive wireless power transmission system incorporating a planar spiral transmitter coil and a receiver coil.

According to embodiments of the invention, a single coil design can provide improved charging efficiency to a wireless power transmission apparatus.

Coils in accordance with embodiments of the invention can provide for a system that uses near-field coupling to transfer power. Advantageously, embodiments of the invention do not require the alignment of the two axes of two coils. Certain embodiments of the invention provide improved robustness for wireless power transfer.

According to an embodiment of the invention, a single spiral coil can be used to provide a uniform magnetic field across the coil's surface area for location-independent planar wireless power charging. Embodiments of the invention generate a uniform magnetic field across an area that enables uniform wireless power transfer insensitive to the location of the device being charged.

In one embodiment, a circular spiral coil can be used. In another embodiment, a rectangular spiral coil can be used. Other shapes can also be utilized for the coil, such as elliptical, rectangular, hexagonal, and other polygonal shapes. The spiral coil can be designed to have a non-constant gap between adjacent loops such that the gap between adjacent loops decreases towards the outer loops.

BRIEF DESCRIPTION OF DRAWINGS

Figure 1 shows a normal spiral coil having a constant gap between adjacent loops.

Figure 2 shows a plot of the magnetic field of the normal spiral coil shown in Figure 1.

Figure 3 shows a spiral coil according to an embodiment of the invention.

Figure 4 shows a plot of the magnetic field of the spiral coil shown in Figure 3.

Figure 5 shows a rectangular spiral coil according to an embodiment of the invention.

Figure 6 shows a plot of the magnetic field of the rectangular spiral coil shown in Figure 5.

DETAILED DISCLOSURE

Embodiments of the subject invention relate to a spiral coil that can generate a substantially uniform magnetic field near the surface of the coil, across at least a portion of the surface area of the coil. Embodiments provide a location-independent planar wireless power charging system. Embodiments of the spiral coil can generate a substantially uniform magnetic field near the surface of the coil, across a portion of the surface area of the coil. A wireless power transmission system in accordance with an embodiment of the invention can have performance insensitive to the placement of the receiver coil within the substantially

uniform magnetic field. The transmitter coil can be driven by a driver. In specific embodiments, the driver is a current source or a voltage source.

Specific embodiments can provide magnetic fields where the magnitude of the magnetic field in a direction perpendicular to the plane of the coil is substantially uniform over the region of interest such that $\frac{MAX - MIN}{AVERAGE}$ is less than or equal to 0.2 over the region of interest, where MAX and MIN are the maximum magnitude, and minimum magnitude, of the magnet field over the region of interest, respectively, and AVERAGE is $\frac{MAX + MIN}{2}$. Further specific embodiments can have the $\frac{MAX - MIN}{AVERAGE}$ of less than or equal to 0.1 over the region of interest and the $\frac{MAX - MIN}{AVERAGE}$ is less than or equal to 0.05 over the region of interest.

In an embodiment of a wireless power charging system, AC current passes through a transmitter coil, inducing magnetic flux on the surface of a power platform. In a specific embodiment, the frequency of the transmitter is between 1kHz and 10MHz. In a preferred embodiment, the frequency of the transmitter is in the range 100 kHz to 400 kHz, and in another embodiment, less than 1MHz. In specific embodiments, the region of interest can be a plane parallel to the plane of the coil offset from the plane of the coil by less than R, less than 30 cm, and/or less than 10 cm. The region of interest can cover a portion of, or all of the area of the coil. A receiver coil generates voltage when magnetic flux passing through the loop of the receiver coil changes. In specific embodiments, the transmitter coil and the receiver coil are not of the same size. A normal coil in accordance with an embodiment of the subject charging system can have a uniform magnetic field across its surface area, which reduces voltage variation and improves impedance matching. In a specific embodiment, the uniformity of the magnetic field can be less than 10% across the surface area of the coil, where the surface of the coil is the area enclosed by the outermost turn of the coil.

According to embodiments of the invention, to generate a more uniform field near the surface of the spiral coil, the distance between two adjacent loops can be adjusted. To reduce the magnetic field density at the center, the density of the inner loops should be less than the outer loops. In a specific embodiment, the gap between two adjacent coils decreases continuously toward the outer loops of the coil. A formula that describes the curve of a

circular spiral inductor according to an embodiment of the invention is

$$\rho(\theta) = \rho_0 + l(\theta)\theta \tag{2}$$

where $l(\theta)$ is a function of θ. θ can vary from 0 to $2\pi N$, where N is the number of turns of the coil. In an embodiment, the derivative of $l(\theta)$ is positive and decreases as θ increases. Specific functions allow $l(\theta)$, the distance between adjacent loops, to be adjusted, and can allow the field across the surface of the coil to be substantially uniform. In another embodiment, the derivative of $l(\theta)$ is such that the spacing between adjacent loops can decrease or remain the same as θ increases such that as the coil moves from the innermost radius to the outermost radius the spacing decreases.

According to an embodiment of the invention, a circular spiral coil, which can be used to obtain the formula for $l(\theta)$, is

$$\rho(\theta) = r + (1 - (1 - \frac{\theta}{2\pi N})^4)(R - r) \tag{3}$$

where R is the outermost radius, r is the innermost radius, and N is the total turns of the coil. $l(\theta)$ can be obtained by setting the right side of equation (2) equal to the right side of equation (3) and solving $l(\theta)$, where r has the same meaning as ρ_0. According to one embodiment, r is 1/4 to 1/3 of R. In another embodiment, the coil can be elliptical with appropriate modifications to equations (2) and (3).

Figure 3 shows a coil with non-constant gap between adjacent loops, in accordance with an embodiment of the subject invention. The curvature of the spiral coil of Figure 3 follows equation 3, in which R = 200 mm, r = 50 mm, and N = 8. Figure 4 shows the magnetic field strength in a perpendicular direction across the surface area of the coil of Figure 3. As shown in Figure 4, the uniformity of the magnetic field for the coil of Figure 3 is significantly improved over the uniformity of the magnetic field for the coil of Figure 1.

For a rectangular spiral inductor, narrower gaps can be used between adjacent loops as the loops become farther from the center. According to an embodiment of the present invention, the gap between adjacent loops can be derived from

$$\rho(2n\pi) - \rho[2(n-1)\pi], \text{ n=1, 2,..., N.} \tag{4}$$

where ρ is the same function as Equation 3. Figure 5 shows a rectangular spiral coil according to an embodiment of the invention. The design of the coil of Figure 5 follows equation 4, in which $R = 200$ mm, $r = 50$ mm, and $N = 8$mm. The magnetic field strength in a perpendicular direction for the coil of Figure 5 is shown in Figure 6.

The results, as shown in Figures 4 and 6, demonstrate that a substantially uniform magnetic field of spiral coil can be generated in accordance with embodiments of the invention.

Additional embodiments utilize polygonal coils, such as rectangles, squares, hexagons, and other multisided shapes, to produce the magnetic fields. The spacing between adjacent coils can decrease or stay the same at each corner of the polygon such that the spacing decreases as the coil goes from the innermost radius to the outermost radius. In specific embodiments, the spacing can continuously decrease, the spacing can be the same between two corners (along one side of the polygonal) and decrease from before each corner to after each corner, the spacing can remain the same for a portion or all of a loop (as shown in Figure 5) and have decreases as the coil moves outward, and/or combinations of these changes.

In specific embodiments, a receiver coil can be inductively coupled to the transmitter coil so as to transfer power to the receiver coil. Embodiments can use receiver coils that have areas such that the transmitter coil area is 2 to 12 times as large, 2 to 8 times as large, or 2 to 4 times as large as the receiver coil area.

All patents, patent applications, provisional applications, and publications referred to or cited herein are incorporated by reference in their entirety, including all figures and tables, to the extent they are not inconsistent with the explicit teachings of this specification.

It should be understood that the examples and embodiments described herein are for illustrative purposes only and that various modifications or changes in light thereof will be suggested to persons skilled in the art and are to be included within the spirit and purview of this application.

CLAIMS

What is claimed is:

1. An apparatus for producing a magnetic field, comprising:

a coil, wherein the coil is a planar spiral coil, where the coil has at least two loops, wherein a spacing between adjacent loops decreases continuously from an inner loop toward an outer loop of the coil, and

a driver, wherein the driver drives the coil to produce a magnetic field, wherein a magnitude of the magnetic field in a direction perpendicular to a plane of the coil is substantially uniform over a region of interest.

2. The apparatus according to claim 1, wherein the magnitude of the magnetic field in a direction perpendicular to the plane of the coil is substantially uniform over the region of interest such that $\frac{MAX - MIN}{AVERAGE}$ is less than or equal to 0.2 over the region of interest, where MAX and MIN are the maximum magnitude, and minimum magnitude, of the magnet field over the region of interest, respectively, and AVERAGE is $\frac{MAX + MIN}{2}$.

3. The apparatus according to claim 2, wherein the $\frac{MAX - MIN}{AVERAGE}$ is less than or equal to 0.1 over the region of interest.

4. The apparatus according to claim 2, wherein the $\frac{MAX - MIN}{AVERAGE}$ is less than or equal to 0.05 over the region of interest.

5. The apparatus according to claim 1, wherein the magnetic field is time-varying.

6. The apparatus according to claim 5, wherein the time-varying magnetic field has a frequency in the range 1 kHz to 10 MHz.

7. The apparatus according to claim 5, wherein the time-varying magnetic field has a frequency in the range 100 kHz to 400 kHz.

8. The apparatus according to claim 5, wherein the time varying magnetic field has a frequency less than or equal to 1 MHz.

9. An apparatus according to claim 1, wherein the coil is a planar elliptical spiral coil.

10. The apparatus according to claim 1, wherein the coil is a planar circular spiral coil, wherein the coil follows the equation:

$$\rho(\theta) = \rho_0 + l(\theta)\theta$$

where $\rho(\theta)$ is the radius of the coil, ρ_0 is the initial radius of the coil, θ is the angle with respect to the initial radius of the coil, and $l(\theta)$ is a function of θ.

11. The apparatus according to claim 10, wherein a derivative of $l(\theta)$ is positive.

12. The apparatus according to claim 11, wherein the derivative of $l(\theta)$ decreases as θ increases over at least a portion of the coil.

13. The apparatus according to claim 12, wherein the derivative of $l(\theta)$ decreases as θ increases over the coil.

14. The apparatus according to claim 1, wherein the spiral coil further follows the equation:

$$\rho(\theta) = r + (1 - (1 - \frac{\theta}{2\pi N})^4)(R - r)$$

where R is an outermost radius of the coil, r is the initial radius of the coil, and N is a number of loops of the coil.

15. The apparatus according to claim 1, wherein the region of interest is a second plane parallel to a plane of the coil.

16. The apparatus according to claim 15, wherein the second plane is offset from the plane of the coil by a distance d.

17. The apparatus according to claim 16, wherein d is less than 30 cm.

18. The apparatus according to claim 16, wherein d is less than 10 cm.

19. The apparatus according to claim 16, wherein d is less than R, where R is an outermost radius of the coil.

20. The apparatus according to claim 15, wherein the region of interest is a region covering at least a portion of an area of the coil.

21. The apparatus according to claim 15, wherein the region of interest is a region covering an area of the coil.

22. The apparatus according to claim 1, wherein the coil is a polygonal spiral coil.

23. The apparatus according to claim 1, wherein the coil is a rectangular spiral coil.

24. An apparatus for producing a magnetic field, comprising:

a coil, wherein the coil is a planer polygonal spiral coil wherein the coil has at least two loops, wherein a spacing between adjacent loops either stays the same or decreases at each corner of the polygonal going from an inner loop toward an outer loop of the coil; and

a driver, wherein the driver drives the coil to produce a magnetic field, wherein a magnitude of the magnetic field in a direction perpendicular to a plane of the coil substantially is uniform over a region of interest.

25. The apparatus according to claim 24, wherein the magnitude of the magnetic field in a direction perpendicular to the plane of the coil is substantially uniform over the region of

interest such that $\frac{MAX - MIN}{AVERAGE}$ is less than or equal to 0.2 over the region of interest, where MAX and MIN are the maximum magnitude, and minimum magnitude, of the magnet field over the region of interest, respectively, and AVERAGE is $\frac{MAX + MIN}{2}$.

26. The apparatus according to claim 25, wherein the $\frac{MAX - MIN}{AVERAGE}$ is less than or equal to 0.1 over the region of interest.

27. The apparatus according to claim 25, wherein the $\frac{MAX - MIN}{AVERAGE}$ is less than or equal to 0.05 over the region of interest.

28. The apparatus according to claim 24, wherein the magnetic field is time-varying.

29. The apparatus according to claim 28, wherein the time-varying magnetic field has a frequency in the range 1 kHz to 10 MHz.

30. The apparatus according to claim 25, wherein the time-varying magnetic field has a frequency in the range 100 kHz to 400 kHz.

31. The apparatus according to claim 25, wherein the time varying magnetic field has a frequency less than or equal to 1 MHz.

32. The apparatus according to claim 24, wherein the spacing between adjacent loops follows the equation:

$\rho(2n\pi) - \rho[2(n-1)\pi]$, $n = 1, 2, \ldots, N$, where ρ is the function

$$\rho(\theta) = r + (1 - (1 - \frac{\theta}{2\pi N})^4)(R - r)$$

where R is an outermost radius of the coil, r is an innermost radius of the coil, and N is a number of loops of the coil.

33. The apparatus according to claim 24, wherein the region of interest is a second plane parallel to the plane of the coil.

34. The apparatus according to claim 33, wherein the second plane is offset from the plane of the coil by a distance d.

35. The apparatus according to claim 34, wherein d is less than 30 cm.

36. The apparatus according to claim 34, wherein d is less than 10 cm.

37. The apparatus according to claim 34, wherein d is less than R, where R is an outermost radius of the coil.

38. The apparatus according to claim 33, wherein the region of interest is a region covering at least a portion of an area of the coil.

39. The apparatus according to claim 33, wherein the region of interest is a region covering an area of the coil.

40. The apparatus according to claim 24, wherein the polygonal coil is a square coil.

41. The apparatus according to claim 24, wherein the polygonal coil is a hexagonal coil.

42. An apparatus for producing a magnetic field, comprising:

a coil, wherein the coil is a planar spiral coil, where the coil has at least two loops, wherein a spacing between starting points of adjacent loops decreases from an inner loop toward an outer loop of the coil, and

a driver, wherein the driver drives the coil to produce a magnetic field, wherein a magnitude of the magnetic field in a direction perpendicular to the plane of the coil is substantially uniform over the region of interest such that $\frac{MAX - MIN}{AVERAGE}$ is less than or equal

to 0.2 over the region of interest, where MAX and MIN are the maximum magnitude, and minimum magnitude, of the magnet field over the region of interest, respectively, and AVERAGE is $\frac{MAX + MIN}{2}$, wherein a magnitude of the magnetic field in a direction perpendicular to a plane of the coil is substantially uniform over a region of interest.

43. A method for producing a magnetic field, comprising:

providing a coil, wherein the coil is a planar spiral coil, where the coil has at least two loops, wherein a spacing between adjacent loops decreases continuously from an inner loop toward an outer loop of the coil, and

driving the coil to produce a magnetic field, wherein a magnitude of the magnetic field in a direction perpendicular to a plane of the coil is substantially uniform over a region of interest.

44. The method according to claim 43, wherein the magnitude of the magnetic field in a direction perpendicular to the plane of the coil is substantially uniform over the region of interest such that $\frac{MAX - MIN}{AVERAGE}$ is less than or equal to 0.2 over the region of interest, where MAX and MIN are the maximum magnitude, and minimum magnitude, of the magnet field over the region of interest, respectively, and AVERAGE is $\frac{MAX + MIN}{2}$.

45. The method according to claim 44, wherein the $\frac{MAX - MIN}{AVERAGE}$ is less than or equal to 0.1 over the region of interest.

46. The method according to claim 44, wherein the $\frac{MAX - MIN}{AVERAGE}$ is less than or equal to 0.05 over the region of interest.

47. The method according to claim 44, wherein the magnetic field is time-varying.

48. The method according to claim 47, wherein the time-varying magnetic field has a frequency in the range 1 kHz to 10 MHz.

49. The method according to claim 47, wherein the time-varying magnetic field has a frequency in the range 100 kHz to 400 kHz.

50. The method according to claim 47, wherein the time varying magnetic field has a frequency less than or equal to 1 MHz.

51. An method according to claim 43, wherein the coil is a planar elliptical spiral coil.

52. The method according to claim 43, wherein the coil is a planar circular spiral coil, wherein the coil follows the equation:

$$\rho(\theta) = \rho_0 + l(\theta)\theta$$

where $\rho(\theta)$ is the radius of the coil, ρ_0 is the initial radius of the coil, θ is the angle with respect to the initial radius of the coil, and $l(\theta)$ is a function of θ.

53. The method according to claim 52, wherein a derivative of $l(\theta)$ is positive.

54. The method according to claim 53, wherein the derivative of $l(\theta)$ decreases as θ increases over at least a portion of the coil.

55. The method according to claim 54, wherein the derivative of $l(\theta)$ decreases as θ increases over the coil.

56. The method according to claim 43, wherein the spiral coil further follows the equation:

$$\rho(\theta) = r + (1 - (1 - \frac{\theta}{2\pi N})^4)(R - r)$$

where R is an outermost radius of the coil, r is the initial radius of the coil, and N is a number of loops of the coil.

57. The method according to claim 43, wherein the region of interest is a second plane parallel to a plane of the coil.

58. The method according to claim 57, wherein the second plane is offset from the plane of the coil by a distance d.

59. The method according to claim 58, wherein d is less than 30 cm.

60. The method according to claim 58, wherein d is less than 10 cm.

61. The method according to claim 58, wherein d is less than R, where R is an outermost radius of the coil.

62. The method according to claim 57, wherein the region of interest is a region covering at least a portion of an area of the coil.

63. The method according to claim 57, wherein the region of interest is a region covering an area of the coil.

64. The method according to claim 43, wherein the coil is a polygonal spiral coil.

65. The method according to claim 43, wherein the coil is a rectangular spiral coil.

66. An method for producing a magnetic field, comprising:

producing a coil, wherein the coil is a planer polygonal spiral coil wherein the coil has at least two loops, wherein a spacing between adjacent loops either stays the same or decreases at each corner of the polygonal going from an inner loop toward an outer loop of the coil; and

driving the coil to produce a magnetic field, wherein a magnitude of the magnetic field in a direction perpendicular to a plane of the coil substantially is uniform over a region of interest.

67. The method according to claim 66, wherein the magnitude of the magnetic field in a direction perpendicular to the plane of the coil is substantially uniform over the region of interest such that $\frac{MAX - MIN}{AVERAGE}$ is less than or equal to 0.2 over the region of interest, where MAX and MIN are the maximum magnitude, and minimum magnitude, of the magnet field over the region of interest, respectively, and AVERAGE is $\frac{MAX + MIN}{2}$.

68. The method according to claim 67, wherein the $\frac{MAX - MIN}{AVERAGE}$ is less than or equal to 0.1 over the region of interest.

69. The method according to claim 67, wherein the $\frac{MAX - MIN}{AVERAGE}$ is less than or equal to 0.05 over the region of interest.

70. The method according to claim 66, wherein the magnetic field is time-varying.

71. The method according to claim 70, wherein the time-varying magnetic field has a frequency in the range 1 kHz to 10 MHz.

72. The method according to claim 67, wherein the time-varying magnetic field has a frequency in the range 100 kHz to 400 kHz.

73. The method according to claim 67, wherein the time varying magnetic field has a frequency less than or equal to 1 MHz.

74. The method according to claim 66, wherein the spacing between adjacent loops follows the equation:

$\rho(2n\pi) - \rho[2(n-1)\pi]$, $n = 1, 2, \ldots, N$, where ρ is the function

$$\rho(\theta) = r + (1 - (1 - \frac{\theta}{2\pi N})^4)(R - r)$$

where R is an outermost radius of the coil, r is an innermost radius of the coil, and N is a number of loops of the coil.

75. The method according to claim 66, wherein the region of interest is a second plane parallel to the plane of the coil.

76. The method according to claim 75, wherein the second plane is offset from the plane of the coil by a distance d.

77. The method according to claim 76, wherein d is less than 30 cm.

78. The method according to claim 76, wherein d is less than 10 cm.

79. The method according to claim 76, wherein d is less than R, where R is an outermost radius of the coil.

80. The method according to claim 75, wherein the region of interest is a region covering at least a portion of an area of the coil.

81. The method according to claim 75, wherein the region of interest is a region covering an area of the coil.

82. The method according to claim 66, wherein the polygonal coil is a square coil.

83. The method according to claim 66, wherein the polygonal coil is a hexagonal coil.

84. An method for producing a magnetic field, comprising:

providing a coil, wherein the coil is a planar spiral coil, where the coil has at least two loops, wherein a spacing between starting points of adjacent loops decreases from an inner loop toward an outer loop of the coil, and

driving the coil to produce a magnetic field, wherein a magnitude of the magnetic field in a direction perpendicular to the plane of the coil is substantially uniform over the region of interest such that $\frac{MAX - MIN}{AVERAGE}$ is less than or equal to 0.2 over the region of interest, where MAX and MIN are the maximum magnitude, and minimum magnitude, of the magnet field over the region of interest, respectively, and AVERAGE is $\frac{MAX + MIN}{2}$, wherein a magnitude of the magnetic field in a direction perpendicular to a plane of the coil is substantially uniform over a region of interest.

85. A system for inductive power transfer, comprising:

an apparatus for producing a magnetic field according to any of claims 1-42; and

a receiver coil, wherein when the receiver coil is positioned proximate the apparatus for producing the magnetic field, power is inductively transfer to the receiver coil.

86. The system according to claim 85, wherein the coil has an area in the range of 2 to 12 times as large as an area of the receiver coil.

87. A method for inductively transferring power, comprising:

implementing the method according to any of claims 43-84; and

providing a receiver coil proximate to the coil such that power is inductively coupled to the receiver coil.

88. The method according to claim 87, wherein the coil has an area in the range of 2 to 12 times as large as an area of the receiver coil.

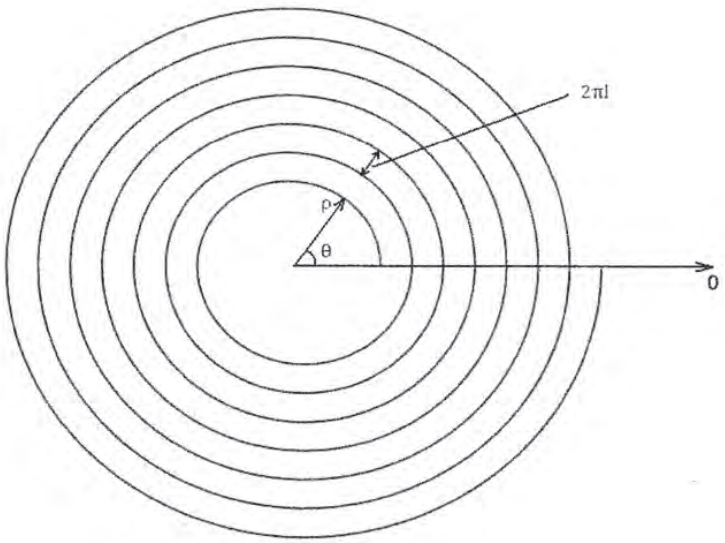

2πl
ρ
θ
0

FIG. 1

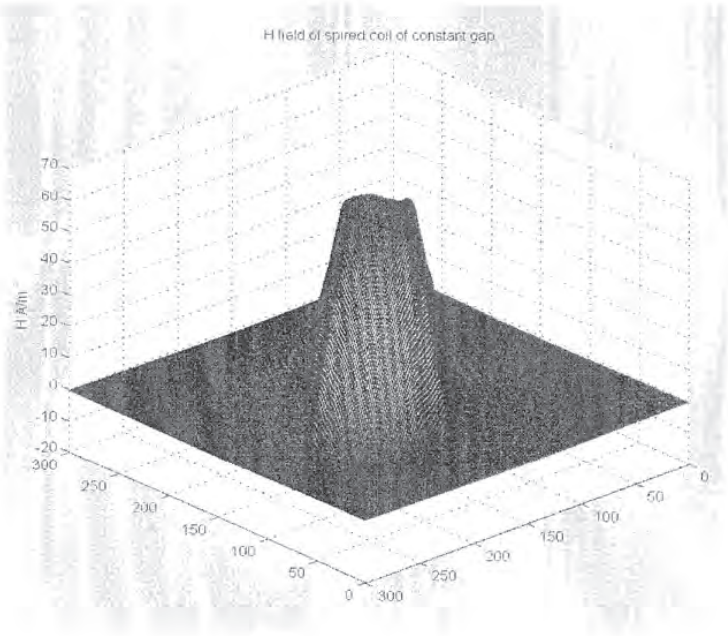

H field of spired coil of constant gap
H A/m
70
60
50
40
30
20
10
0
-10
-20
300
250
200
150
100
50
0
0
50
100
150
200
250
300

FIG. 2

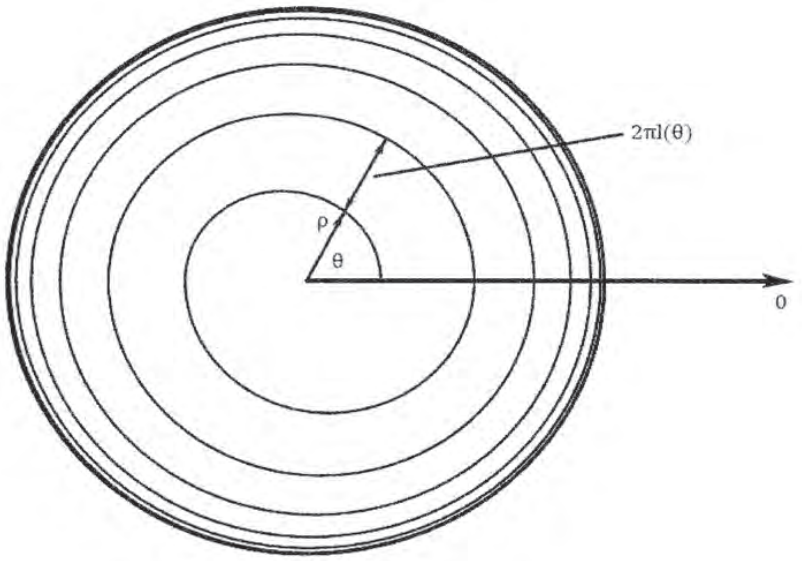


FIG. 3

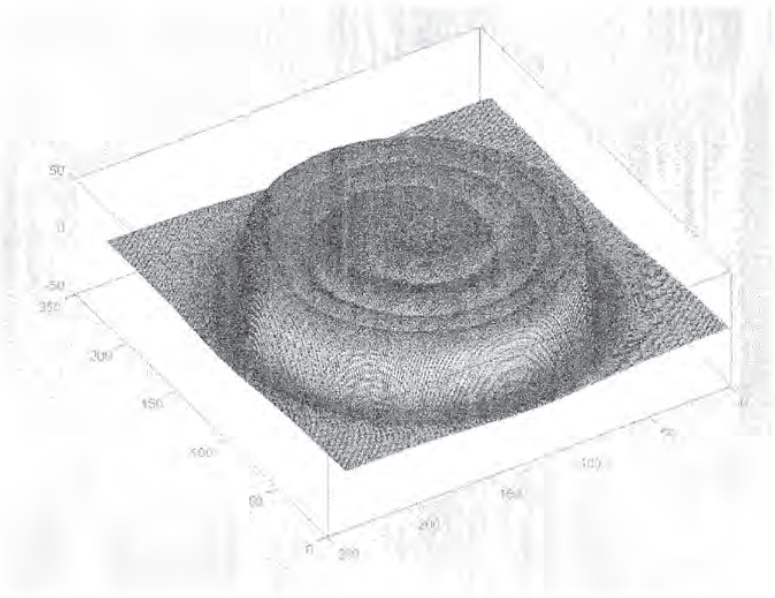


FIG. 4

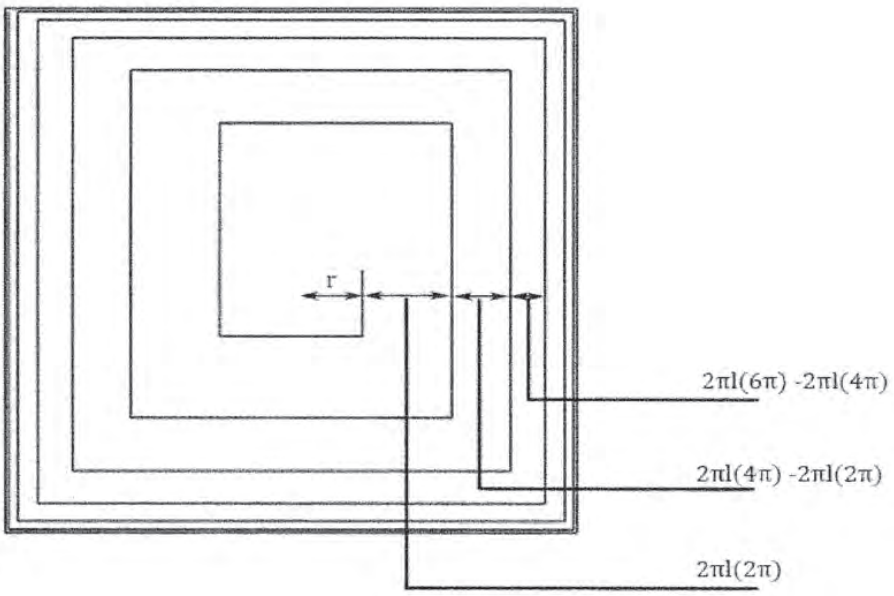

r
2πl(6π) -2πl(4π)
2πl(4π) -2πl(2π)
2πl(2π)

FIG. 5

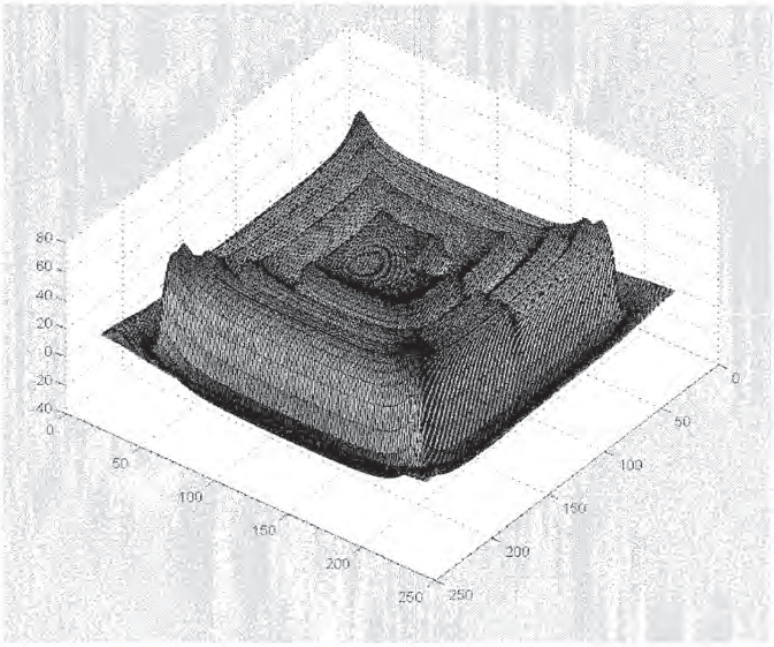

80
60
40
20
0
20
40
0
50
100
150
200
250
0
50
100
150
200
250

FIG. 6

(12) INTERNATIONAL APPLICATION PUBLISHED UNDER THE PATENT COOPERATION TREATY (PCT)

(19) World Intellectual Property Organization
International Bureau

(43) International Publication Date
23 December 2009 (23.12.2009)

PCT

(10) International Publication Number
WO 2009/155000 A3

(51) International Patent Classification:
H02J 7/00 (2006.01) *H02J 17/00* (2006.01)

(21) International Application Number:
PCT/US2009/045339

(22) International Filing Date:
27 May 2009 (27.05.2009)

(25) Filing Language: English

(26) Publication Language: English

(30) Priority Data:
61/056,354 27 May 2008 (27.05.2008) US

(71) Applicant *(for all designated States except US)*: **UNIVERSITY OF FLORIDA RESEARCH FOUNDATION, INC.** [US/US]; 223 Grinter Hall, Gainesville, FL 32611 (US).

(72) Inventor; and

(75) Inventor/Applicant *(for US only)*: **LIN, Jenshan** [US/US]; 910 S.W. 105th Terrace, Gainesville, FL 32607 (US).

(74) Agents: **PARKER, James, S.** et al.; Saliwanchik, Lloyd, Saliwanchik, P.O. Box 142950, Gainesville, FL 32614-2950 (US).

(81) Designated States *(unless otherwise indicated, for every kind of national protection available)*: AE, AG, AL, AM, AO, AT, AU, AZ, BA, BB, BG, BH, BR, BW, BY, BZ, CA, CH, CN, CO, CR, CU, CZ, DE, DK, DM, DO, DZ, EC, EE, EG, ES, FI, GB, GD, GE, GH, GM, GT, HN, HR, HU, ID, IL, IN, IS, JP, KE, KG, KM, KN, KP, KR, KZ, LA, LC, LK, LR, LS, LT, LU, LY, MA, MD, ME, MG, MK, MN, MW, MX, MY, MZ, NA, NG, NI, NO, NZ, OM, PG, PH, PL, PT, RO, RS, RU, SC, SD, SE, SG, SK, SL, SM, ST, SV, SY, TJ, TM, TN, TR, TT, TZ, UA, UG, US, UZ, VC, VN, ZA, ZM, ZW.

(84) Designated States *(unless otherwise indicated, for every kind of regional protection available)*: ARIPO (BW, GH, GM, KE, LS, MW, MZ, NA, SD, SL, SZ, TZ, UG, ZM, ZW), Eurasian (AM, AZ, BY, KG, KZ, MD, RU, TJ, TM), European (AT, BE, BG, CH, CY, CZ, DE, DK, EE, ES, FI, FR, GB, GR, HR, HU, IE, IS, IT, LT, LU, LV, MC, MK, MT, NL, NO, PL, PT, RO, SE, SI, SK, TR), OAPI (BF, BJ, CF, CG, CI, CM, GA, GN, GQ, GW, ML, MR, NE, SN, TD, TG).

[Continued on next page]

(54) Title: METHOD AND APPARATUS FOR PRODUCING SUBSTANTIALLY UNIFORM MAGNETIC FIELD

(57) Abstract: A planar wireless power transmitter coil design and method are provided. A single spiral coil can be used to provide a uniform magnetic field across its surface area for location-independent planar wireless power charging. The spiral coil can be designed to have a non- constant gap between adjacent loops such that the gap between adjacent loops decreases towards the outer loops.

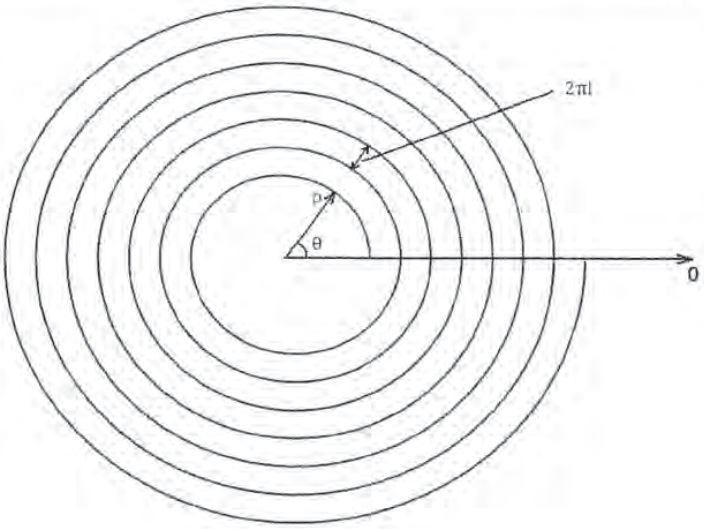


FIG. 1

WO 2009/155000 A3

Published:

— *with international search report (Art. 21(3))*

— *before the expiration of the time limit for amending the claims and to be republished in the event of receipt of amendments (Rule 48.2(h))*

(88) Date of publication of the international search report:
4 March 2010

INTERNATIONAL SEARCH REPORT

International application No.
PCT/US2009/045339

A. CLASSIFICATION OF SUBJECT MATTER

H02J 7/00(2006.01)i, H02J 17/00(2006.01)i

According to International Patent Classification (IPC) or to both national classification and IPC

B. FIELDS SEARCHED

Minimum documentation searched (classification system followed by classification symbols)
H02J 7/00; G11B 13/04; H01F 5/00; H05B 6/40; H05H 1/30; G01R 33/20; H05H 1/00

Documentation searched other than minimum documentation to the extent that such documents are included in the fields searched
Korean utility models and applications for utility models since 1975.
Japanese utility models and applications for utility models since 1975.

Electronic data base consulted during the international search (name of data base and, where practicable, search terms used)
eKOMPASS(KIPO internal) & Keywords: uniform, magnetic field, spiral coil, inductive

C. DOCUMENTS CONSIDERED TO BE RELEVANT

Category*	Citation of document, with indication, where appropriate, of the relevant passages	Relevant to claim No.
X	US 5293360 A1 (HASEGAWA; KOYO et al.) 08 March 1994 See abstract; claims 1-8; figures 1-8.	1-5,9,22-28,40-47 ,51,64-70,82-84
Y		6-8,15-21,29-31 ,33-39,48-50,57-63 ,71-73,75-81,85-88
A		10-14,32,52-56,74
Y	LIU X. and HUI S. Y., "Optimal Design of a Hybrid Winding Structure for Plan ar Contactless Battery Charging Platform", IEEE Transactions on Power Electron s,s, Vol. 23, No. 1, January 2008.	6-8,15-21,29-31 ,33-39,48-50,57-63 ,71-73,75-81,85-88
A	See abstract; pages 456-459; figures 1-9.	1-5,9-14,22-28,32 ,40-47,51-56,64-70 ,74,82-84
A	KR 10-2002-0007155 A (-) 26 January 2002 See abstract; claims 1-17; figures 1-12.	1-88
A	JP 60-234304 A (RIKO DENKI:KK) 21 November 1985 See abstract; pages 3-4; claims 1-6; figures 1-10.	1-88

☐ Further documents are listed in the continuation of Box C. ☒ See patent family annex.

* Special categories of cited documents:
"A" document defining the general state of the art which is not considered to be of particular relevance
"E" earlier application or patent but published on or after the international filing date
"L" document which may throw doubts on priority claim(s) or which is cited to establish the publication date of citation or other special reason (as specified)
"O" document referring to an oral disclosure, use, exhibition or other means
"P" document published prior to the international filing date but later than the priority date claimed
"T" later document published after the international filing date or priority date and not in conflict with the application but cited to understand the principle or theory underlying the invention
"X" document of particular relevance; the claimed invention cannot be considered novel or cannot be considered to involve an inventive step when the document is taken alone
"Y" document of particular relevance; the claimed invention cannot be considered to involve an inventive step when the document is combined with one or more other such documents,such combination being obvious to a person skilled in the art
"&" document member of the same patent family

Date of the actual completion of the international search	Date of mailing of the international search report
12 JANUARY 2010 (12.01.2010)	**13 JANUARY 2010 (13.01.2010)**

Name and mailing address of the ISA/KR
Korean Intellectual Property Office
Government Complex-Daejeon, 139 Seonsa-ro, Seo-gu, Daejeon 302-701, Republic of Korea
Facsimile No. 82-42-472-7140

Authorized officer
KOO, Young Hoi
Telephone No. 82-42-481-8376

Form PCT/ISA/210 (second sheet) (July 2008)

INTERNATIONAL SEARCH REPORT
Information on patent family members

International application No.
PCT/US2009/045339

Patent document cited in search report	Publication date	Patent family member(s)	Publication date
US 5293360 A1	08.03.1994	JP 02-859627 B2	04.12.1998
		JP 2235202 A	18.09.1990
		JP 2235203 A	18.09.1990
		JP 2235204 A	18.09.1990
		JP 2235239 A	18.09.1990
		JP 2235241 A	18.09.1990
		JP 2235242 A	18.09.1990
		JP 2859627 B2	17.02.1999
		US 5293360 A1	08.03.1994
KR 10-2002-0007155 A	26.01.2002	EP 1168415 A3	21.02.2007
		EP 1168415 A3	21.02.2007
		EP 1912246 A2	16.04.2008
		EP 1912246 A2	16.04.2008
		JP 2002-008996 A	11.01.2002
		KR 10-0516595 B1	22.09.2005
		US 2002-018025 A1	14.02.2002
		US 2006-027168 A1	09.02.2006
		US 7520246 B2	21.04.2009
JP 60-234304 A	21.11.1985	JP 60-234304 A	21.11.1985

InductEV, Inc.
Exhibit 1025
Page 382

Electronic Acknowledgement Receipt

EFS ID:	9396828
Application Number:	12639963
International Application Number:	
Confirmation Number:	7811
Title of Invention:	WIRELESS ENERGY TRANSFER WITH HIGH-Q TO MORE THAN ONE DEVICE
First Named Inventor/Applicant Name:	John D. Joannopoulos
Customer Number:	26161
Filer:	Marc M. Wefers/Cheryl Forrest
Filer Authorized By:	Marc M. Wefers
Attorney Docket Number:	01997-0359009
Receipt Date:	08-FEB-2011
Filing Date:	16-DEC-2009
Time Stamp:	12:53:37
Application Type:	Utility under 35 USC 111(a)

Payment information:

Submitted with Payment	no

File Listing:

Document Number	Document Description	File Name	File Size(Bytes)/ Message Digest	Multi Part /.zip	Pages (if appl.)
1		359009IDS.pdf	129896 234dcce3147(343)e419bbd724edfd7d012 9a11c	yes	4

	Multipart Description/PDF files in .zip description				
	Document Description		Start	End	
	Transmittal Letter		1	1	
	Information Disclosure Statement (IDS) Filed (SB/08)		2	4	
Warnings:					
Information:					
2	Foreign Reference	Art1.pdf	2263738 8926954168562cd1f10868ed9fbabeb4fbb16aa8	no	28
Warnings:					
Information:					
3	Foreign Reference	Art2.pdf	1675874 b60aa04422e3cbdb115e2ba07ceb064bf2213867	no	30
Warnings:					
Information:					
4	Foreign Reference	Art3.pdf	1424983 6ebc8a137890e1251b1330102887f22a7f12b7	no	17
Warnings:					
Information:					
5	Foreign Reference	Art4.pdf	12427844 49048073e1e5275daae44ab93107f24b075cb1929c	no	147
Warnings:					
Information:					
6	Foreign Reference	Art5.pdf	1728876 0f758dc77d2390ff084bea55c69a76e07b09265d	no	26
Warnings:					
Information:					
7	NPL Documents	NPL1.pdf	742038 4452226886476e1f355fab67cdb7a2d8d95aa9ea5	no	9
Warnings:					
Information:					
8	NPL Documents	NPL2.pdf	393690 ff2aaaf7c5a6ce5b9b4f8a096dd49001db5e320b	no	11
Warnings:					
Information:					
		Total Files Size (in bytes):	20786939		

This Acknowledgement Receipt evidences receipt on the noted date by the USPTO of the indicated documents, characterized by the applicant, and including page counts, where applicable. It serves as evidence of receipt similar to a Post Card, as described in MPEP 503.

New Applications Under 35 U.S.C. 111

If a new application is being filed and the application includes the necessary components for a filing date (see 37 CFR 1.53(b)-(d) and MPEP 506), a Filing Receipt (37 CFR 1.54) will be issued in due course and the date shown on this Acknowledgement Receipt will establish the filing date of the application.

National Stage of an International Application under 35 U.S.C. 371

If a timely submission to enter the national stage of an international application is compliant with the conditions of 35 U.S.C. 371 and other applicable requirements a Form PCT/DO/EO/903 indicating acceptance of the application as a national stage submission under 35 U.S.C. 371 will be issued in addition to the Filing Receipt, in due course.

New International Application Filed with the USPTO as a Receiving Office

If a new international application is being filed and the international application includes the necessary components for an international filing date (see PCT Article 11 and MPEP 1810), a Notification of the International Application Number and of the International Filing Date (Form PCT/RO/105) will be issued in due course, subject to prescriptions concerning national security, and the date shown on this Acknowledgement Receipt will establish the international filing date of the application.

IN THE UNITED STATES PATENT AND TRADEMARK OFFICE

Applicant	: John D. Joannopoulos et al.	Art Unit	: Unknown
Serial No.	: 12/639,963	Examiner	: Unknown
Filed	: December 16, 2009	Conf. No.	: 7811
Title	: WIRELESS ENERGY TRANSFER WITH HIGH-Q TO MORE THAN ONE DEVICE		

MAIL STOP AMENDMENT
Commissioner for Patents
P.O. Box 1450
Alexandria, VA 22313-1450

INFORMATION DISCLOSURE STATEMENT

Please consider the references listed on the enclosed PTO-1449 form. Foreign patent documents and non-patent literature are enclosed; cited U.S. patents and patent application publications will be provided on request.

This statement is being filed within three months of the filing date of the application or before the receipt of a first Office Action on the merits. Apply any charges or credits to Deposit Account No. 06-1050, referencing 01997-0359009.

Respectfully submitted,

Date: 2/7/11

Marc M. Wefers
Reg. No. 56,842

Customer Number
Fish & Richardson P.C.
Telephone: (617) 542-5070
Facsimile: (877) 769-7945

22534941.doc

Substitute Form PTO-1449 (Modified) U.S. Department of Commerce Patent and Trademark Office	Attorney Docket No. 01997-0359009	Application No. 12/639,963
Information Disclosure Statement by Applicant (Use several sheets if necessary) (37 CFR §1.98(b))	Applicant John D. Joannopoulos et al.	
	Filing Date December 16, 2009	Group Art Unit

U.S. Patent Documents

Examiner Initial	Desig. ID	Document Number	Publication Date	Patentee	Class	Subclass	Filing Date If Appropriate
	1	2009/0108679	4/30/2009	Porwal			
	2						
	3						

Foreign Patent Documents or Published Foreign Patent Applications

Examiner Initial	Desig. ID	Document Number	Publication Date	Country or Patent Office	Class	Subclass	Translation Yes	Translation No
	4							
	5							

Other Documents (include Author, Title, Date, and Place of Publication)

Examiner Initial	Desig. ID	Document
	6	
	7	

Examiner Signature	Date Considered
EXAMINER: Initials citation considered. Draw line through citation if not in conformance and not considered. Include copy of this form with next communication to applicant.	

Substitute Disclosure Form (PTO-1449)

Electronic Acknowledgement Receipt

EFS ID:	9525505
Application Number:	12639963
International Application Number:	
Confirmation Number:	7811
Title of Invention:	WIRELESS ENERGY TRANSFER WITH HIGH-Q TO MORE THAN ONE DEVICE
First Named Inventor/Applicant Name:	John D. Joannopoulos
Customer Number:	26161
Filer:	Marc M. Wefers/Cheryl Forrest
Filer Authorized By:	Marc M. Wefers
Attorney Docket Number:	01997-0359009
Receipt Date:	24-FEB-2011
Filing Date:	16-DEC-2009
Time Stamp:	15:28:05
Application Type:	Utility under 35 USC 111(a)

Payment information:

Submitted with Payment	no

File Listing:

Document Number	Document Description	File Name	File Size(Bytes)/ Message Digest	Multi Part /.zip	Pages (if appl.)
1		359009-IDS.pdf	74533 bca247ea2b5e7959e5fdb1b8d49314e8ad13616df	yes	2

	Multipart Description/PDF files in .zip description		
	Document Description	**Start**	**End**
	Transmittal Letter	1	1
	Information Disclosure Statement (IDS) Filed (SB/08)	2	2
Warnings:			
Information:			
	Total Files Size (in bytes):	74533	

This Acknowledgement Receipt evidences receipt on the noted date by the USPTO of the indicated documents, characterized by the applicant, and including page counts, where applicable. It serves as evidence of receipt similar to a Post Card, as described in MPEP 503.

New Applications Under 35 U.S.C. 111
If a new application is being filed and the application includes the necessary components for a filing date (see 37 CFR 1.53(b)-(d) and MPEP 506), a Filing Receipt (37 CFR 1.54) will be issued in due course and the date shown on this Acknowledgement Receipt will establish the filing date of the application.

National Stage of an International Application under 35 U.S.C. 371
If a timely submission to enter the national stage of an international application is compliant with the conditions of 35 U.S.C. 371 and other applicable requirements a Form PCT/DO/EO/903 indicating acceptance of the application as a national stage submission under 35 U.S.C. 371 will be issued in addition to the Filing Receipt, in due course.

New International Application Filed with the USPTO as a Receiving Office
If a new international application is being filed and the international application includes the necessary components for an international filing date (see PCT Article 11 and MPEP 1810), a Notification of the International Application Number and of the International Filing Date (Form PCT/RO/105) will be issued in due course, subject to prescriptions concerning national security, and the date shown on this Acknowledgement Receipt will establish the international filing date of the application.

IN THE UNITED STATES PATENT AND TRADEMARK OFFICE

Applicant	: John D. Joannopoulos et al.	Art Unit	: Unknown
Serial No.	: 12/639,963	Examiner	: Unknown
Filed	: December 16, 2009	Conf. No.	: 7811
Title	: WIRELESS ENERGY TRANSFER WITH HIGH-Q TO MORE THAN ONE DEVICE		

Commissioner for Patents
P.O. Box 1450
Alexandria, VA 22313-1450

INFORMATION DISCLOSURE STATEMENT

Please consider the references listed on the enclosed PTO-1449 form. Foreign patent documents and non-patent literature are enclosed; cited U.S. patents and patent application publications will be provided on request.

This Information Disclosure Statement is being filed to correct the Information Disclosure Statement that was previously filed on February 8, 2011. The applicant incorrectly listed Desig. Id. No. 21 (the Porwal reference) as U.S. Publication No. as 2009/0180679. The correct U.S. Publication No. for this reference is 2009/0108679.

This statement is being filed within three months of the filing date of the application or before the receipt of a first Office Action on the merits. Apply any charges or credits to Deposit Account No. 06-1050, referencing 01997-0359009.

Respectfully submitted,

Date: 2/22/11

Marc M. Wefers
Reg. No. 56,842

Customer Number
Fish & Richardson P.C.
Telephone: (617) 542-5070
Facsimile: (877) 769-7945

22581830.doc

Substitute Form PTO-1449 (Modified) U.S. Department of Commerce Patent and Trademark Office	Attorney Docket No. 01997-0359009	Application No. 12/639,963
Information Disclosure Statement by Applicant (Use several sheets if necessary) (37 CFR §1.98(b))	Applicant John D. Joannopoulos et al.	
	Filing Date December 16, 2009	Group Art Unit

U.S. Patent Documents

Examiner Initial	Desig. ID	Document Number	Publication Date	Patentee	Class	Subclass	Filing Date If Appropriate
	1	645,576	3/20/1900	Tesla			
	2	649,621	5/15/1900	Tesla			
	3	7,795,708	9/14/2010	Katti			
	4	2007/0145830	6/28/2007	Lee et al.			
	5						

Foreign Patent Documents or Published Foreign Patent Applications

Examiner Initial	Desig. ID	Document Number	Publication Date	Country or Patent Office	Class	Subclass	Translation Yes	Translation No
	6							

Other Documents (include Author, Title, Date, and Place of Publication)

Examiner Initial	Desig. ID	Document
	7	John C. Schuder et al., "An Inductively Coupled RF System for the Transmission of 1 kW of Power Through the Skin", IEEE Transactions on Bio-Medical Engineering, Vol. BME-18, No. 4 (July 1971)
	8	J. C. Schuder et al., "Energy Transport Into the Closed Chest From a Set of Very-Large Mutually Orthogonal Coils", Communication Electronics, Vol. 64, pp. 527-534 (January 1963)
	9	John C. Schuder "Powering an Artificial Heart: Birth of the Inductively Coupled-Radio Frequency System in 1960", Artificial Organs, Vol. 26, No. 11, pp. 909-915 (2002)
	10	

Examiner Signature	Date Considered
EXAMINER: Initials citation considered. Draw line through citation if not in conformance and not considered. Include copy of this form with next communication to applicant.	

Substitute Disclosure Form (PTO-1449)

Electronic Acknowledgement Receipt

EFS ID:	10239338
Application Number:	12639963
International Application Number:	
Confirmation Number:	7811
Title of Invention:	WIRELESS ENERGY TRANSFER WITH HIGH-Q TO MORE THAN ONE DEVICE
First Named Inventor/Applicant Name:	John D. Joannopoulos
Customer Number:	26161
Filer:	Marc M. Wefers/Cheryl Forrest
Filer Authorized By:	Marc M. Wefers
Attorney Docket Number:	01997-0359009
Receipt Date:	06-JUN-2011
Filing Date:	16-DEC-2009
Time Stamp:	14:52:52
Application Type:	Utility under 35 USC 111(a)

Payment information:

Submitted with Payment	no

File Listing:

Document Number	Document Description	File Name	File Size(Bytes)/ Message Digest	Multi Part /.zip	Pages (if appl.)
1		359009IDS.pdf	85234 6abc359c25bbb50afbad2a2c224bb2f933 1da4e	yes	2

	Multipart Description/PDF files in .zip description				
	Document Description		Start	End	
	Transmittal Letter		1	1	
	Information Disclosure Statement (IDS) Form (SB08)		2	2	
Warnings:					
Information:					
2	Non Patent Literature	Art1.pdf	15221882 d108fd0eaddc71c01cb248ac63a2c7c158c0bb80	no	9
Warnings:					
Information:					
3	Non Patent Literature	Art2.pdf	5755944 af2e3fdd3411d023cbc5b50df3fa401bce41a4bf	no	8
Warnings:					
Information:					
4	Non Patent Literature	Art3.pdf	204093 db6e163aa08fd5609297ea289e8e95fd913ab8c8541	no	7
Warnings:					
Information:					
		Total Files Size (in bytes):	21267153		

This Acknowledgement Receipt evidences receipt on the noted date by the USPTO of the indicated documents, characterized by the applicant, and including page counts, where applicable. It serves as evidence of receipt similar to a Post Card, as described in MPEP 503.

New Applications Under 35 U.S.C. 111
If a new application is being filed and the application includes the necessary components for a filing date (see 37 CFR 1.53(b)-(d) and MPEP 506), a Filing Receipt (37 CFR 1.54) will be issued in due course and the date shown on this Acknowledgement Receipt will establish the filing date of the application.

National Stage of an International Application under 35 U.S.C. 371
If a timely submission to enter the national stage of an international application is compliant with the conditions of 35 U.S.C. 371 and other applicable requirements a Form PCT/DO/EO/903 indicating acceptance of the application as a national stage submission under 35 U.S.C. 371 will be issued in addition to the Filing Receipt, in due course.

New International Application Filed with the USPTO as a Receiving Office
If a new international application is being filed and the international application includes the necessary components for an international filing date (see PCT Article 11 and MPEP 1810), a Notification of the International Application Number and of the International Filing Date (Form PCT/RO/105) will be issued in due course, subject to prescriptions concerning national security, and the date shown on this Acknowledgement Receipt will establish the international filing date of the application.

IN THE UNITED STATES PATENT AND TRADEMARK OFFICE

Applicant	: John D. Joannopoulos et al.	Art Unit	: Unknown
Serial No.	: 12/639,963	Examiner	: Unknown
Filed	: December 16, 2009	Conf. No.	: 7811
Title	: WIRELESS ENERGY TRANSFER WITH HIGH-Q TO MORE THAN ONE DEVICE		

MAIL STOP AMENDMENT
Commissioner for Patents
P.O. Box 1450
Alexandria, VA 22313-1450

INFORMATION DISCLOSURE STATEMENT

Please consider the references listed on the enclosed PTO-1449 form. Foreign patent documents and non-patent literature are enclosed; cited U.S. patents and patent application publications will be provided on request.

This statement is being filed within three months of the filing date of the application or before the receipt of a first Office Action on the merits. Apply any charges or credits to Deposit Account No. 06-1050, referencing 01997-0359009.

Respectfully submitted,

Date: 6/6/11

Marc M. Wefers
Reg. No. 56,842

Customer Number
Fish & Richardson P.C.
Telephone: (617) 542-5070
Facsimile: (877) 769-7945

22644802.doc

UNITED STATES PATENT AND TRADEMARK OFFICE

UNITED STATES DEPARTMENT OF COMMERCE
United States Patent and Trademark Office
Address: COMMISSIONER FOR PATENTS
P.O. Box 1450
Alexandria, Virginia 22313-1450
www.uspto.gov

APPLICATION NO.	FILING DATE	FIRST NAMED INVENTOR	ATTORNEY DOCKET NO.	CONFIRMATION NO.
12/639,963	12/16/2009	John D. Joannopoulos	01997-0359009	7811

26161 7590 09/30/2011

FISH & RICHARDSON P.C. (BO)
P.O. BOX 1022
MINNEAPOLIS, MN 55440-1022

EXAMINER	
PALADINI, ALBERT WILLIAM	
ART UNIT	PAPER NUMBER
2836	

NOTIFICATION DATE	DELIVERY MODE
09/30/2011	ELECTRONIC

Please find below and/or attached an Office communication concerning this application or proceeding.

The time period for reply, if any, is set in the attached communication.

Notice of the Office communication was sent electronically on above-indicated "Notification Date" to the following e-mail address(es):

PATDOCTC@fr.com

Office Action Summary	Application No.	Applicant(s)	
	12/639,963	JOANNOPOULOS ET AL.	
	Examiner	Art Unit	
	ALBERT W. PALADINI	2836	

-- The MAILING DATE of this communication appears on the cover sheet with the correspondence address --

Period for Reply

A SHORTENED STATUTORY PERIOD FOR REPLY IS SET TO EXPIRE 3 MONTH(S) OR THIRTY (30) DAYS, WHICHEVER IS LONGER, FROM THE MAILING DATE OF THIS COMMUNICATION.

- Extensions of time may be available under the provisions of 37 CFR 1.136(a). In no event, however, may a reply be timely filed after SIX (6) MONTHS from the mailing date of this communication.
- If NO period for reply is specified above, the maximum statutory period will apply and will expire SIX (6) MONTHS from the mailing date of this communication.
- Failure to reply within the set or extended period for reply will, by statute, cause the application to become ABANDONED (35 U.S.C. § 133). Any reply received by the Office later than three months after the mailing date of this communication, even if timely filed, may reduce any earned patent term adjustment. See 37 CFR 1.704(b).

Status

1)☒ Responsive to communication(s) filed on *06 December 2009*.

2a)☐ This action is **FINAL**. 2b)☒ This action is non-final.

3)☐ An election was made by the applicant in response to a restriction requirement set forth during the interview on _____; the restriction requirement and election have been incorporated into this action.

4)☐ Since this application is in condition for allowance except for formal matters, prosecution as to the merits is closed in accordance with the practice under *Ex parte Quayle*, 1935 C.D. 11, 453 O.G. 213.

Disposition of Claims

5)☒ Claim(s) *1 and 2* is/are pending in the application.

5a) Of the above claim(s) _____ is/are withdrawn from consideration.

6)☐ Claim(s) _____ is/are allowed.

7)☒ Claim(s) *1 and 2* is/are rejected.

8)☐ Claim(s) _____ is/are objected to.

9)☐ Claim(s) _____ are subject to restriction and/or election requirement.

Application Papers

10)☐ The specification is objected to by the Examiner.

11)☐ The drawing(s) filed on _____ is/are: a)☐ accepted or b)☐ objected to by the Examiner.

Applicant may not request that any objection to the drawing(s) be held in abeyance. See 37 CFR 1.85(a).

Replacement drawing sheet(s) including the correction is required if the drawing(s) is objected to. See 37 CFR 1.121(d).

12)☐ The oath or declaration is objected to by the Examiner. Note the attached Office Action or form PTO-152.

Priority under 35 U.S.C. § 119

13)☐ Acknowledgment is made of a claim for foreign priority under 35 U.S.C. § 119(a)-(d) or (f).

a)☐ All b)☐ Some * c)☐ None of:

1.☐ Certified copies of the priority documents have been received.

2.☐ Certified copies of the priority documents have been received in Application No. _____.

3.☐ Copies of the certified copies of the priority documents have been received in this National Stage application from the International Bureau (PCT Rule 17.2(a)).

* See the attached detailed Office action for a list of the certified copies not received.

Attachment(s)

1) ☒ Notice of References Cited (PTO-892)
2) ☐ Notice of Draftsperson's Patent Drawing Review (PTO-948)
3) ☒ Information Disclosure Statement(s) (PTO/SB/08) Paper No(s)/Mail Date *6/6/11,2/24/11,2/8/11,6/16/10,4/23/10*.
4) ☐ Interview Summary (PTO-413) Paper No(s)/Mail Date. _____.
5) ☐ Notice of Informal Patent Application
6) ☐ Other: _____.

InductEV, Inc.
Exhibit 1025
Page 396

DETAILED ACTION

Double Patenting

1. The nonstatutory double patenting rejection is based on a judicially created doctrine grounded in public policy (a policy reflected in the statute) so as to prevent the unjustified or improper timewise extension of the "right to exclude" granted by a patent and to prevent possible harassment by multiple assignees. A nonstatutory obviousness-type double patenting rejection is appropriate where the conflicting claims are not identical, but at least one examined application claim is not patentably distinct from the reference claim(s) because the examined application claim is either anticipated by, or would have been obvious over, the reference claim(s). See, e.g., *In re Berg*, 140 F.3d 1428, 46 USPQ2d 1226 (Fed. Cir. 1998); *In re Goodman*, 11 F.3d 1046, 29 USPQ2d 2010 (Fed. Cir. 1993); *In re Longi*, 759 F.2d 887, 225 USPQ 645 (Fed. Cir. 1985); *In re Van Ornum*, 686 F.2d 937, 214 USPQ 761 (CCPA 1982); *In re Vogel*, 422 F.2d 438, 164 USPQ 619 (CCPA 1970); and In *re Thorington*, 418 F.2d 528, 163 USPQ 644 (CCPA 1969).

A timely filed terminal disclaimer in compliance with 37 CFR 1.321(c) or 1.321(d) may be used to overcome an actual or provisional rejection based on a nonstatutory double patenting ground provided the conflicting application or patent either is shown to be commonly owned with this application, or claims an invention made as a result of activities undertaken within the scope of a joint research agreement.

Effective January 1, 1994, a registered attorney or agent of record may sign a terminal disclaimer. A terminal disclaimer signed by the assignee must fully comply with 37 CFR 3.73(b).

2. Claims 1-2 are rejected on the ground of nonstatutory obviousness-type double patenting as being unpatentable over claims 1-70 of U.S. Patent No. 7,741,734. Although the conflicting claims are not identical, they are not patentably distinct from each other.

The source high Q resonator and the second high Q resonator recited in claims 1 and 2 of the instant application are taught in claims 1 and 2 of U.S. Patent No. 7,741,734. It would have been obvious to one of ordinary skill in the art that a third high Q resonator which receives energy from the source high Q resonator could easily be added and extend the capability of energy transfer.

3. Any inquiry concerning this communication or earlier communication from the examiner should be directed to Albert W. Paladini whose telephone number is 571-272-3748. The examiner can normally be reached from 7:00 AM to 2:30 PM on Monday, Tuesday, Thursday or Friday.

If attempts to reach the examiner by telephone are unsuccessful, the examiner's supervisor, Mr. Rexford Barnie can be reached on 571-272-7492. The fax phone number for the organization where this application or proceeding is assigned is 571-273-8300.

/ALBERT W PALADINI/ 9/23/11
Primary Examiner, Art Unit 2836

Notice of References Cited	Application/Control No. 12/639,963	Applicant(s)/Patent Under Reexamination JOANNOPOULOS ET AL.	
	Examiner ALBERT W. PALADINI	Art Unit 2836	Page 1 of 1

U.S. PATENT DOCUMENTS

*		Document Number Country Code-Number-Kind Code	Date MM-YYYY	Name	Classification
*	A	US-7,741,734	06-2010	Joannopoulos et al.	307/104
	B	US-			
	C	US-			
	D	US-			
	E	US-			
	F	US-			
	G	US-			
	H	US-			
	I	US-			
	J	US-			
	K	US-			
	L	US-			
	M	US-			

FOREIGN PATENT DOCUMENTS

*		Document Number Country Code-Number-Kind Code	Date MM-YYYY	Country	Name	Classification
	N					
	O					
	P					
	Q					
	R					
	S					
	T					

NON-PATENT DOCUMENTS

*		Include as applicable: Author, Title Date, Publisher, Edition or Volume, Pertinent Pages)
	U	
	V	
	W	
	X	

*A copy of this reference is not being furnished with this Office action. (See MPEP § 707.05(a).)
Dates in MM-YYYY format are publication dates. Classifications may be US or foreign.

InductEV, Inc.
Exhibit 1025
Page 399

UNITED STATES PATENT AND TRADEMARK OFFICE

UNITED STATES DEPARTMENT OF COMMERCE
United States Patent and Trademark Office
Address: COMMISSIONER FOR PATENTS
P.O. Box 1450
Alexandria, Virginia 22313-1450
www.uspto.gov

BIB DATA SHEET

CONFIRMATION NO. 7811

SERIAL NUMBER	FILING or 371(c) DATE	CLASS	GROUP ART UNIT	ATTORNEY DOCKET NO.
12/639,963	12/16/2009 RULE	307	2836	01997-0359009

APPLICANTS

John D. Joannopoulos, Belmont, MA;
Aristeidis Karalis, Boston, MA;
Marin Soljacic, Belmont, MA;

**** CONTINUING DATA ***************************

This application is a CON of 12/553,957 09/03/2009
which is a CON of 11/481,077 07/05/2006 PAT 7,741,734
which claims benefit of 60/698,442 07/12/2005

**** FOREIGN APPLICATIONS ***************************

**** IF REQUIRED, FOREIGN FILING LICENSE GRANTED ****

01/04/2010

Foreign Priority claimed ☐ Yes ☑ No 35 USC 119(a-d) conditions met ☐ Yes ☑ No Verified and Acknowledged /ALBERT WILLIAM PALADINI/ Examiner's Signature	☐ Met after Allowance Initials	STATE OR COUNTRY	SHEETS DRAWINGS	TOTAL CLAIMS	INDEPENDENT CLAIMS
		MA	6	2	2

ADDRESS

FISH & RICHARDSON P.C. (BO)
P.O. BOX 1022
MINNEAPOLIS, MN 55440-1022
UNITED STATES

TITLE

WIRELESS ENERGY TRANSFER WITH HIGH-Q TO MORE THAN ONE DEVICE

FILING FEE RECEIVED		
1220	FEES: Authority has been given in Paper No._____ to charge/credit DEPOSIT ACCOUNT No._____ for following:	☐ All Fees ☐ 1.16 Fees (Filing) ☐ 1.17 Fees (Processing Ext. of time) ☐ 1.18 Fees (Issue) ☐ Other _____ ☐ Credit

EAST Search History

EAST Search History (Prior Art)

Ref #	Hits	Search Query	DBs	Default Operator	Plurals	Time Stamp
L1	2952	((307/104) or (333/195)).CCLS.	US-PGPUB; USPAT; FPRS; EPO; JPO; DERWENT	OR	OFF	2011/09/23 12:20
L2	215	1 and (high with q with resona $3)	US-PGPUB; USPAT; FPRS; EPO; JPO; DERWENT	OR	ON	2011/09/23 12:21

EAST Search History (Interference)

< This search history is empty>

9/23/2011 12:21:53 PM

Index of Claims	Application/Control No.	Applicant(s)/Patent Under Reexamination
	12639963	JOANNOPOULOS ET AL.
	Examiner	Art Unit
	ALBERT W PALADINI	2836

✓	Rejected	-	Cancelled	N	Non-Elected	A	Appeal
=	Allowed	÷	Restricted	I	Interference	O	Objected

☐ Claims renumbered in the same order as presented by applicant ☐ CPA ☐ T.D. ☐ R.1.47

CLAIM		DATE								
Final	Original	09/23/2011								
	1	✓								
	2	✓								

InductEV, Inc.
Exhibit 1025
Page 402

Substitute Form PTO-1449 (Modified) U.S. Department of Commerce Patent and Trademark Office	Attorney Docket No. 01997-0359009	Application No. 12/639,963
Information Disclosure Statement by Applicant (Use several sheets if necessary) (37 CFR §1.98(b))	Applicant John D. Joannopoulos et al.	
	Filing Date December 16, 2009	Group Art Unit

U.S. Patent Documents

Examiner Initial	Desig. ID	Document Number	Publication Date	Patentee	Class	Subclass	Filing Date If Appropriate
	1	645,576	3/20/1900	Tesla			
	2	649,621	5/15/1900	Tesla			
	3	7,795,708	9/14/2010	Katti			
	4	2007/0145830	6/28/2007	Lee et al.			
	5						

Foreign Patent Documents or Published Foreign Patent Applications

Examiner Initial	Desig. ID	Document Number	Publication Date	Country or Patent Office	Class	Subclass	Translation Yes	Translation No
	6							

Other Documents (include Author, Title, Date, and Place of Publication)

Examiner Initial	Desig. ID	Document
	7	John C. Schuder et al., "An Inductively Coupled RF System for the Transmission of 1 kW of Power Through the Skin", IEEE Transactions on Bio-Medical Engineering, Vol. BME-18, No. 4 (July 1971)
	8	J. C. Schuder et al., "Energy Transport Into the Closed Chest From a Set of Very-Large Mutually Orthogonal Coils", Communication Electronics, Vol. 64, pp. 527-534 (January 1963)
	9	John C. Schuder "Powering an Artificial Heart: Birth of the Inductively Coupled-Radio Frequency System in 1960", Artificial Organs, Vol. 26, No. 11, pp. 909-915 (2002)
	10	

Examiner Signature	Date Considered
/Albert Paladini/	09/23/2011

EXAMINER: Initials citation considered. Draw line through citation if not in conformance and not considered. Include copy of this form with next communication to applicant.

Substitute Disclosure Form (PTO-1449)

ALL REFERENCES CONSIDERED EXCEPT WHERE LINED THROUGH. /A.P./

Substitute Form PTO-1449 (Modified) U.S. Department of Commerce Patent and Trademark Office	Attorney Docket No. 01997-0359009	Application No. 12/639,963
Information Disclosure Statement by Applicant (Use several sheets if necessary) (37 CFR §1.98(b))	Applicant John D. Joannopoulos et al.	
	Filing Date December 16, 2009	Group Art Unit

U.S. Patent Documents

Examiner Initial	Desig. ID	Document Number	Publication Date	Patentee	Class	Subclass	Filing Date If Appropriate
	1						
	2						

Foreign Patent Documents or Published Foreign Patent Applications

Examiner Initial	Desig. ID	Document Number	Publication Date	Country or Patent Office	Class	Subclass	Translation Yes	Translation No
	3	WO 00/77910	12/21/2000	WIPO	H02J	5/00		
	4							
	5							

Other Documents (include Author, Title, Date, and Place of Publication)

Examiner Initial	Desig. ID	Document
	6	
	7	

Examiner Signature /Albert Paladini/	Date Considered 09/23/2011

EXAMINER: Initials citation considered. Draw line through citation if not in conformance and not considered. Include copy of this form with next communication to applicant.

Substitute Disclosure Form (PTO-1449)

ALL REFERENCES CONSIDERED EXCEPT WHERE LINED THROUGH. /A.P./

Substitute Form PTO-1449 (Modified)	U.S. Department of Commerce Patent and Trademark Office	Attorney Docket No. 01997-0359009	Application No. 12/639,963
Information Disclosure Statement by Applicant (Use several sheets if necessary) (37 CFR §1.98(b))		Applicant John D. Joannopoulos et al.	
		Filing Date December 16, 2009	Group Art Unit

U.S. Patent Documents

Examiner Initial	Desig. ID	Document Number	Publication Date	Patentee	Class	Subclass	Filing Date If Appropriate
	1	2009/0108679	4/30/2009	Porwal			
	2						
	3						

Foreign Patent Documents or Published Foreign Patent Applications

Examiner Initial	Desig. ID	Document Number	Publication Date	Country or Patent Office	Class	Subclass	Translation Yes	Translation No
	4							
	5							

Other Documents (include Author, Title, Date, and Place of Publication)

Examiner Initial	Desig. ID	Document
	6	
	7	

Examiner Signature	Date Considered
/Albert Paladini/	09/23/2011

EXAMINER: Initials citation considered. Draw line through citation if not in conformance and not considered. Include copy of this form with next communication to applicant.

Substitute Disclosure Form (PTO-1449)

ALL REFERENCES CONSIDERED EXCEPT WHERE LINED THROUGH. /A.P./

Substitute Form PTO-1449 (Modified) U.S. Department of Commerce Patent and Trademark Office	Attorney Docket No 01997-0359009	Application No. 12/639,963
Information Disclosure Statement by Applicant (Use several sheets if necessary)	Applicant John D. Joannopoulos et al.	
(37 CFR §1.98(b))	Filing Date December 16, 2009	Group Art Unit

U.S. Patent Documents

Examiner Initial	Desig. ID	Document Number	Publication Date	Patentee	Class	Subclass	Filing Date If Appropriate
	1	5,118,997	6/2/1992	El-Hamamsy			
	2	5,986,895	11/16/1999	Stewart et al.			
	3	7,147,604	12/12/2006	Allen et al.			
	4	7,191,007	3/13/2007	Desai et al.			
	5	7,599,743	10/6/2009	Hassler, Jr. et al.			
	6	7,639,514	12/29/2009	Baarman			
	7	7,825,543	11/2/2010	Karalis et al.			
	8	7,843,288	11/30/2010	Lee et al.			
	9	2005/0288739	12/29/2005	Hassler, Jr. et al.			
	10	2005/0288740	12/29/2005	Hassler, Jr. et al.			
	11	2007/0182367	8/9/2007	Partovi			
	12	2008/0012569	1/17/2008	Hall et al.			
	13	2008/0030415	2/7/2008	Homan et al.			
	14	2008/0067874	3/20/2008	Tseng			
	15	2008/0265684	10/30/2008	Farkas			
	16	2009/0015075	1/15/2009	Cook et al.			
	17	2009/0067198	3/12/2009	Graham et al.			
	18	2009/0085408	4/2/2009	Bruhn			
	19	2009/0085706	4/2/2009	Baarman et al.			
	20	2009/0096413	4/16/2009	Patovi et al.			
	21	2009/0180679	4/30/2009	Porwal			
	22	2009/0108997	4/30/2009	Patterson et al.			
	23	2009/0146892	6/11/2009	Shimizu et al.			
	24	2009/0160261	6/25/2009	Elo			
	25	2009/0174263	9/9/2009	Baarman et al.			
	26	2009/0189458	7/30/2009	Kawasaki			
	27	2009/0230777	9/17/2009	Baarman et al.			

Examiner Signature /Albert Paladini/	Date Considered 09/23/2011
EXAMINER: Initials citation considered. Draw line through citation if not in conformance and not considered. Include copy of this form with next communication to applicant.	

Substitute Disclosure Form (PTO-1449)

ALL REFERENCES CONSIDERED EXCEPT WHERE LINED THROUGH. /A.P./

Substitute Form PTO-1449 (Modified) U.S. Department of Commerce Patent and Trademark Office	Attorney Docket No 01997-0359009	Application No. 12/639,963
Information Disclosure Statement by Applicant (Use several sheets if necessary) (37 CFR §1.98(b))	Applicant John D. Joannopoulos et al.	
	Filing Date December 16, 2009	Group Art Unit

U.S. Patent Documents

Examiner Initial	Desig. ID	Document Number	Publication Date	Patentee	Class	Subclass	Filing Date If Appropriate
	28	2009/0237194	9/24/2009	Waffenschmidt et al.			
	29	2009/0251008	10/8/2009	Sugaya			
	30	2009/0267558	10/29/2009	Jung			
	31	2009/0271047	10/29/2009	Wakamatsu			
	32	2009/0271048	10/29/2009	Wakamatsu			
	33	2009/0281678	11/12/2009	Wakamatsu			
	34	2009/0284082	11/19/2009	Mohammadian			
	35	2009/0284218	11/19/2009	Mohammadian et al.			
	36	2009/0284220	11/19/2009	Toncich et al.			
	37	2009/0284227	11/19/2009	Mohammadian et al.			
	38	2009/0284245	11/19/2009	Kirby et al.			
	39	2009/0284369	11/19/2001	Toncich et al.			
	40	2009/0286470	11/19/2009	Mohammadian et al.			
	41	2009/0286475	11/19/2009	Toncich et al.			
	42	2009/0286476	11/19/2009	Toncich et al.			
	43	2009/0289595	11/26/2009	Chen et al.			
	44	2010/0231163	9/19/2010	Mashinsky			
	45	2010/0289449	11/18/2010	Elo			
	46						

Foreign Patent Documents or Published Foreign Patent Applications

Examiner Initial	Desig. ID	Document Number	Publication Date	Country or Patent Office	Class	Subclass	Translation Yes	Translation No
	47	WO 2009/033043	3/12/2009	WIPO				
	48	WO 2009/070730	6/4/2009	WIPO				
	49	WO 2009/126963	10/15/2009	WIPO				
	50	WO 2009/149464	12/10/2009	WIPO				
	51	WO 2009/155000	12/23/2009	WIPO				

Examiner Signature	Date Considered
/Albert Paladini/	09/23/2011

EXAMINER: Initials citation considered. Draw line through citation if not in conformance and not considered. Include copy of this form with next communication to applicant.

Substitute Disclosure Form (PTO-1449)

ALL REFERENCES CONSIDERED EXCEPT WHERE LINED THROUGH. /A.P./

Substitute Form PTO-1449 (Modified)	U.S. Department of Commerce Patent and Trademark Office	Attorney Docket No 01997-0359009	Application No. 12/639,963
Information Disclosure Statement by Applicant (Use several sheets if necessary) (37 CFR §1.98(b))		Applicant John D. Joannopoulos et al.	
		Filing Date December 16, 2009	Group Art Unit

Foreign Patent Documents or Published Foreign Patent Applications

Examiner Initial	Desig. ID	Document Number	Publication Date	Country or Patent Office	Class	Subclass	Translation Yes	Translation No
	52							
	53							

Other Documents (include Author, Title, Date, and Place of Publication)

Examiner Initial	Desig. ID	Document
	54	A. Mediano et al. "Design of class E amplifier with nonlinear and linear shunt capacitances for any duty cycle", IEEE Trans. Microwave Theor. Tech., volume 55, no. 3, pp. 484-492, (2007)
	55	H. Sekiya et al. "FM/PWM control scheme in class DE inverter", IEEE Trans. Circuits Syst. I, vol. 51, no. 7 (July 2004)
	56	

Examiner Signature	Date Considered
/Albert Paladini/	09/23/2011

EXAMINER: Initials citation considered. Draw line through citation if not in conformance and not considered. Include copy of this form with next communication to applicant.

Substitute Disclosure Form (PTO-1449)

ALL REFERENCES CONSIDERED EXCEPT WHERE LINED THROUGH. /A.P./

Search Notes	Application/Control No.	Applicant(s)/Patent Under Reexamination
	12639963	JOANNOPOULOS ET AL.
	Examiner	Art Unit
	ALBERT W PALADINI	2836

SEARCHED			
Class	Subclass	Date	Examiner
307	104	9/23/11	awp
333	195	9/23/11	awp

SEARCH NOTES		
Search Notes	Date	Examiner
EAST	9/23/11	awp

INTERFERENCE SEARCH			
Class	Subclass	Date	Examiner

Substitute Form PTO-1449 (Modified) U.S. Department of Commerce Patent and Trademark Office	Attorney Docket No. 01997-0359009	Application No. 12/639,963
Information Disclosure Statement by Applicant (Use several sheets if necessary) (37 CFR §1.98(b))	Applicant John D. Joannopoulos et al.	
	Filing Date December 16, 2009	Group Art Unit

U.S. Patent Documents

Examiner Initial	Desig. ID	Document Number	Publication Date	Patentee	Class	Subclass	Filing Date If Appropriate
	1	787,412	4/18/1905	Tesla			
	2	1,119,732	12/1/1914	Tesla			
	3	2,133,494	10/18/1938	H.F. Waters			
	4	3,517,350	6/23/1970	Beaver			
	5	3,535,543	10/20/1970	Dailey			
	6	4,088,999	5/9/1978	Fletcher et al.			
	7	5,027,709	7/2/1991	Slagle			
	8	5,070,293	12/3/1991	Ishii et al.			
	9	5,216,402	6/1/1993	Carosa			
	10	5,341,083	8/23/1994	Klontz et al.			
	11	5,367,242	11/22/1994	Hulman			
	12	5,437,057	7/25/1995	Richley et al.			
	13	5,493,691	2/20/1996	Barrett			
	14	5,528,113	6/18/1996	Boys et al.			
	15	5,550,452	8/27/1996	Shirai et al.			
	16	5,898,579	4/27/1999	Boys et al.			
	17	5,999,308	12/7/1999	Nelson et al.			
	18	6,184,651	2/6/2001	Fernandez et al.			
	19	6,436,299	8/20/2002	Baarman et al.			
	20	6,450,946	9/17/2002	Forsell			
	21	6,452,465	9/17/2002	Brown et al.			
	22	6,515,878	2/4/2003	Meins et al.			
	23	6,597,076	7/22/2003	Scheible et al.			
	24	6,673,250	1/6/2004	Kuennen et al.			
	25	6,731,071	5/4/2004	Baarman			
	26	6,749,119	6/15/2004	Scheible et al.			
	27	6,798,716	9/28/2004	Charych			

Examiner Signature	Date Considered
/Albert Paladini/	09/23/2011

EXAMINER: Initials citation considered. Draw line through citation if not in conformance and not considered. Include copy of this form with next communication to applicant.

Substitute Disclosure Form (PTO-1449)

ALL REFERENCES CONSIDERED EXCEPT WHERE LINED THROUGH. /A.P./

Substitute Form PTO-1449 (Modified) U.S. Department of Commerce Patent and Trademark Office	Attorney Docket No. 01997-0359009	Application No. 12/639,963
Information Disclosure Statement by Applicant (Use several sheets if necessary) (37 CFR §1.98(b))	Applicant John D. Joannopoulos et al.	
	Filing Date December 16, 2009	Group Art Unit

U.S. Patent Documents

Examiner Initial	Desig. ID	Document Number	Publication Date	Patentee	Class	Subclass	Filing Date If Appropriate
	28	6,806,649	10/19/2004	Mollema et al.			
	29	6,812,645	11/2/2004	Baarman			
	30	6,825,620	11/30/2004	Kuennen et al.			
	31	6,831,417	12/14/2004	Baarman			
	32	6,856,291	2/15/2005	Mickle et al.			
	33	6,844,702	1/18/2005	Giannopoulos et al.			
	34	6,906,495	6/14/2005	Cheng et al.			
	35	6,917,431	7/12/2005	Soljacic et al.			
	36	6,917,163	7/12/2005	Baarman			
	37	6,937,130	8/30/2005	Scheible et al.			
	38	6,960,968	11/1/2005	Odendaal et al.			
	39	6,975,198	12/13/2005	Baarman			
	40	7,042,196	5/9/2006	Ka-Lai et al.			
	41	7,069,064	6/27/2006	Govorgian et al.			
	42	7,116,200	10/3/2006	Baarman et al.			
	43	7,118,240	10/10/2006	Baarman et al.			
	44	7,126,450	10/24/2006	Baarman et al.			
	45	7,132,918	11/7/2006	Baarman et al.			
	46	7,180,248	2/20/2007	Kuennen et al.			
	47	7,212,414	5/1/2007	Baarman			
	48	7,239,110	7/3/2007	Cheng et al.			
	49	7,248,017	7/24/2007	Cheng et al.			
	50	7,375,492	5/20/2008	Calhoon et al.			
	51	7,375,493	5/20/2008	Calhoon et al.			
	52	7,378,817	5/27/2008	Calhoon et al.			
	53	7,382,636	6/3/2008	Baarman et al.			
	54	7,385,357	6/10/2008	Kuennen et al.			

Examiner Signature	Date Considered
/Albert Paladini/	09/23/2011

EXAMINER: Initials citation considered. Draw line through citation if not in conformance and not considered. Include copy of this form with next communication to applicant.

Substitute Disclosure Form (PTO-1449)

ALL REFERENCES CONSIDERED EXCEPT WHERE LINED THROUGH. /A.P./

Substitute Form PTO-1449 (Modified) U.S. Department of Commerce Patent and Trademark Office	Attorney Docket No. 01997-0359009	Application No. 12/639,963
Information Disclosure Statement by Applicant (Use several sheets if necessary) (37 CFR §1.98(b))	Applicant John D. Joannopoulos et al.	
	Filing Date December 16, 2009	Group Art Unit

U.S. Patent Documents

Examiner Initial	Desig. ID	Document Number	Publication Date	Patentee	Class	Subclass	Filing Date If Appropriate
	55	7,462,951	12/9/2008	Baarman			
	56	7,466,213	12/16/2008	Lobl et al.			
	57	7,474,058	1/6/2009	Baarman			
	58	7,492,247	2/17/2009	Schmidt et al.			
	59	7,518,267	4/14/2009	Baarman			
	60	7,525,283	4/28/2009	Cheng et al.			
	61	7,615,936	11/10/2009	Baarman et al.			
	62	2002/0032471	3/14/2002	Loftin et al.			
	63	2002/0105343	8/8/2002	Scheible et al.			
	64	2002/0118004	8/29/2002	Scheible et al.			
	65	2003/0038641	2/27/2003	Scheible			
	66	2003/0062794	4/3/2003	Scheible et al.			
	67	2003/0062980	4/3/2003	Scheible et al.			
	68	2003/0199778	10/23/2003	Mickle et al.			
	69	2003/0214255	11/20/2003	Baarman et al.			
	70	2004/0000974	1/1/2004	Odenaal et al.			
	71	2004/0113847	6/17/2004	Qi et al.			
	72	2004/0130915	7/8/2004	Baarman			
	73	2004/0130916	7/8/2004	Baarman			
	74	2004/0150934	8/5/2004	Baarman			
	75	2004/0201361	10/14/2004	Koh et al.			
	76	2004/0222751	11/11/2004	Mollema et al.			
	77	2004/0232845	11/25/2004	Baarman			
	78	2004/0267501	12/30/2004	Freed et al.			
	79	2005/0007067	1/13/2005	Baarman et al.			
	80	2005/0085873	4/21/2005	Gord et al.			
	81	2005/0093475	5/5/2005	Kuennen et al.			

Examiner Signature /Albert Paladini/	Date Considered 09/23/2011
EXAMINER: Initials citation considered. Draw line through citation if not in conformance and not considered. Include copy of this form with next communication to applicant.	

Substitute Disclosure Form (PTO-1449)

ALL REFERENCES CONSIDERED EXCEPT WHERE LINED THROUGH. /A.P./

Substitute Form PTO-1449 (Modified) U.S. Department of Commerce Patent and Trademark Office	Attorney Docket No. 01997-0359009	Application No. 12/639,963
Information Disclosure Statement by Applicant (Use several sheets if necessary) (37 CFR §1.98(b))	Applicant John D. Joannopoulos et al.	
	Filing Date December 16, 2009	Group Art Unit

U.S. Patent Documents

Examiner Initial	Desig. ID	Document Number	Publication Date	Patentee	Class	Subclass	Filing Date If Appropriate
	82	2005/0104064	5/19/2005	Hegarty et al.			
	83	2005/0116650	6/2/2005	Baarman			
	84	2005/0122058	6/9/2005	Baarman et al.			
	85	2005/0122059	6/9/2005	Baarman et al.			
	86	2005/0127849	6/16/2005	Baarman et al.			
	87	2005/0127850	6/16/2005	Baarman et al.			
	88	2005/0127866	6/16/2005	Hamilton et al.			
	89	2005/0156560	7/21/2005	Shimaoka et al.			
	90	2006/0022636	2/2/2006	Xian et al.			
	91	2006/0061323	3/23/2006	Cheng et al.			
	92	2006/0132045	6/22/2006	Baarman			
	93	2006/0181242	8/17/2006	Freed et al.			
	94	2006/0185809	8/24/2006	Elfrink et al.			
	95	2006/0205381	9/14/2006	Beart et al.			
	96	2006/0270440	11/30/2006	Shearer et al.			
	97	2007/0064406	3/22/2007	Beart			
	98	2007/0171681	7/26/2007	Baarman			
	99	2007/0178945	8/2/2007	Cook et al.			
	100	2007/0222542	9/27/2007	Joannopoulos et al.			
	101	2007/0267918	11/22/2007	Gyland			
	102	2007/0276538	11/29/2007	Kjellsson et al.			
	103	2008/0014897	1/7/2008	Cook et al.			
	104	2008/0191638	8/14/2008	Kuennen et al.			
	105	2008/0197710	8/21/2008	Kreitz et al.			
	106	2008/0211320	9/4/2008	Cook et al.			
	107	2008/0278264	11/13/2008	Karalis et al.			
	108	2009/0010028	1/8/2009	Baarmen et al.			

Examiner Signature	Date Considered
/Albert Paladini/	09/23/2011

EXAMINER: Initials citation considered. Draw line through citation if not in conformance and not considered. Include copy of this form with next communication to applicant.

Substitute Disclosure Form (PTO-1449)

ALL REFERENCES CONSIDERED EXCEPT WHERE LINED THROUGH. /A.P./

Substitute Form PTO-1449 (Modified) U.S. Department of Commerce Patent and Trademark Office	Attorney Docket No. 01997-0359009	Application No. 12/639,963
Information Disclosure Statement by Applicant (Use several sheets if necessary) (37 CFR §1.98(b))	Applicant John D. Joannopoulos et al.	
	Filing Date December 16, 2009	Group Art Unit

U.S. Patent Documents

Examiner Initial	Desig. ID	Document Number	Publication Date	Patentee	Class	Subclass	Filing Date If Appropriate
	109	2009/0015075	1/15/2009	Cook et al.			
	110	2009/0033564	2/5/2009	Cook et al.			
	111	2009/0045772	2/19/2009	Cook et al.			
	112	2009/0051224	2/26/2009	Cook et al.			
	113	2009/0058189	3/5/2009	Cook et al.			
	114	2009/0072627	3/19/2009	Cook et al.			
	115	2009/0072628	3/19/2009	Cook et al.			
	116	2009/0072629	3/19/2009	Cook et al.			
	117	2009/0079268	3/26/2009	Cook et al.			
	118	2009/0102292	4/23/2009	Cook et al.			
	119	2009/0127937	5/21/2009	Widmer et al.			
	120	2009/0134712	5/28/2009	Cook et al.			
	121	2009/0153273	6/18/2009	Chen			
	122	2009/0167449	7/2/2009	Cook et al.			
	123	2009/0179502	7/16/2009	Cook et al.			
	124	2009/0195332	8/6/2009	Joannopoulos et al.			
	125	2009/0195333	8/6/2009	Joannopoulos et al.			
	126	2009/0212636	8/27/2009	Cook et al.			
	127	2009/0213028	8/27/2009	Cook et al.			
	128	2009/0224856	9/10/2009	Karalis et al.			
	129	2009/0224608	9/10/2009	Cook et al.			
	130	2009/0224609	9/10/2009	Cook et al.			
	131	2009/0243394	10/1/2009	Levine			
	132	2009/0243397	10/1/2009	Cook et al.			
	133	2009/0273242	11/5/2009	Cook			
	134	2009/0299918	12/3/2009	Cook et al.			
	135	2010/0038970	2/18/2010	Cook et al.			

Examiner Signature	Date Considered
/Albert Paladini/	09/23/2011

EXAMINER: Initials citation considered. Draw line through citation if not in conformance and not considered. Include copy of this form with next communication to applicant.

Substitute Disclosure Form (PTO-1449)

ALL REFERENCES CONSIDERED EXCEPT WHERE LINED THROUGH. /A.P./

Substitute Form PTO-1449 (Modified) U.S. Department of Commerce Patent and Trademark Office	Attorney Docket No. 01997-0359009	Application No. 12/639,963
Information Disclosure Statement by Applicant (Use several sheets if necessary) (37 CFR §1.98(b))	Applicant John D. Joannopoulos et al.	
	Filing Date December 16, 2009	Group Art Unit

U.S. Patent Documents

Examiner Initial	Desig. ID	Document Number	Publication Date	Patentee	Class	Subclass	Filing Date If Appropriate
	136						

Foreign Patent Documents or Published Foreign Patent Applications

Examiner Initial	Desig. ID	Document Number	Publication Date	Country or Patent Office	Class	Subclass	Translation Yes	Translation No
	137	CA 142352	08/13/1912	Canada				
	138	DE 10 2005 036290	02/15/2007	Germany				
	139	DE 38 24 972	01/12/1989	Germany				
	140	DE 100 29147	12/21/2001	Germany				
	141	DE 102006044057	4/10/2008	Germany				
	142	DE 103 04584	08/19/2004	Germany				
	143	EP 1,335,477	08/13/2003	Europe				
	144	WO 92/17929	10/15/1992	WIPO				
	145	WO 93/23908	11/25/1993	WIPO				
	146	WO 94/28560	12/08/1994	WIPO				
	147	WO 96/02970	02/01/1996	WIPO				
	148	WO 98/50993	11/12/1998	WIPO				
	149	WO 00/79910	12/21/2000	WIPO				
	150	WO 03/092329	11/6/2003	WIPO				
	151	WO 03/096361	11/20/2003	WIPO				
	152	WO 03/096512	11/20/2003	WIPO				
	153	WO 2004/038888	5/6/2004	WIPO				
	154	WO 2004/055654	7/1/2004	WIPO				
	155	WO 2004/073150	8/26/2004	WIPO				
	156	WO 2004/073166	8/26/2004	WIPO				
	157	WO 2004/073176	8/26/2004	WIPO				
	158	WO 2004/073177	8/26/2004	WIPO				
	159	WO 2004/112216	12/23/2004	WIPO				

Examiner Signature	Date Considered
/Albert Paladini/	09/23/2011

EXAMINER: Initials citation considered. Draw line through citation if not in conformance and not considered. Include copy of this form with next communication to applicant.

Substitute Disclosure Form (PTO-1449)

ALL REFERENCES CONSIDERED EXCEPT WHERE LINED THROUGH. /A.P./

Substitute Form PTO-1449 (Modified) U.S. Department of Commerce Patent and Trademark Office	Attorney Docket No. 01997-0359009	Application No. 12/639,963
Information Disclosure Statement by Applicant (Use several sheets if necessary) (37 CFR §1.98(b))	Applicant John D. Joannopoulos et al.	
	Filing Date December 16, 2009	Group Art Unit

Foreign Patent Documents or Published Foreign Patent Applications

Examiner Initial	Desig. ID	Document Number	Publication Date	Country or Patent Office	Class	Subclass	Translation Yes	Translation No
	160	WO 2005/024865	3/17/2005	WIPO				
	161	WO 2005/060068	6/30/2005	WIPO				
	162	WO 2005/109597	11/17/2005	WIPO				
	163	WO 2005/109598	11/17/2005	WIPO				
	164	WO 2007/008646	01/18/2007	WIPO				
	165	WO 2007/084716	7/26/2007	WIPO				
	166	WO 2007/084717	7/26/2007	WIPO				
	167	WO 2007/020583	2/22/2007	WIPO				
	168	WO 2007/042952	4/19/2007	WIPO				
	169	WO 2008/109489	9/12/2008	WIPO				
	170	WO 2008/118178	10/02/2008	WIPO				
	171	WO 2009/009559	1/5/2009	WIPO				
	172	WO 2009/018568	2/5/2009	WIPO				
	173	WO 2009/023155	2/19/2009	WIPO				
	174	WO 2009/023646	2/19/2009	WIPO				
	175							

Other Documents (include Author, Title, Date, and Place of Publication)

Examiner Initial	Desig. ID	Document
	176	Abe et al. "A Noncontact Charger Using a Resonant Converter with Parallel Capacitor of the Secondary Coil". IEEE, 36(2):444-451, March/April 2000.
	177	Altchev et al. "Efficient Resonant Inductive Coupling Energy Transfer Using New Magnetic and Design Criteria". IEEE, pp. 1293-1298, 2005.
	178	T. Aoki et al. "Observation of strong coupling between one atom and a monolithic microresonator'. Nature 443:671-674 (2006).
	179	Apneseth et al. "Introducing wireless proximity switches" ABB Review 4/2002.
	180	Baker et al., "Feedback Analysis and Design of RF Power Links for Low-Power Bionic Systems," IEEE Transactions on Biomedical Circuits and Systems, 1(1):28-38 (March 2007)
	181	Balanis, C.A., "Antenna Theory: Analysis and Design," 3rd Edition, Sections 4.2, 4.3, 5.2, 5.3 (Wiley, New Jersey, 2005).
	182	Burri et al. "Invention Description" February 5, 2008

Examiner Signature	Date Considered
/Albert Paladini/	09/23/2011

EXAMINER: Initials citation considered. Draw line through citation if not in conformance and not considered. Include copy of this form with next communication to applicant.

Substitute Disclosure Form (PTO-1449)

ALL REFERENCES CONSIDERED EXCEPT WHERE LINED THROUGH. /A.P./

Substitute Form PTO-1449 (Modified) U.S. Department of Commerce Patent and Trademark Office	Attorney Docket No. 01997-0359009	Application No. 12/639,963
Information Disclosure Statement by Applicant (Use several sheets if necessary) (37 CFR §1.98(b))	Applicant John D. Joannopoulos et al.	
	Filing Date December 16, 2009	Group Art Unit

Other Documents (include Author, Title, Date, and Place of Publication)		
Examiner Initial	Desig. ID	Document
	183	Electricity Unplugged, Feature: Wireless Energy, Physics World, pp. 23-25 (February 2009)
	184	Esser et al. "A New Approach to Power Supplies for Robots". IEEE, 27(5):872-875, September/October 1991.
	185	Fenske et al. "Dielectric Materials at Microwave Frequencies". Applied Microwave & Wireless, pp. 92-100, 2000.
	186	C. Fernandez et al., "A simple dc-dc converter for the power supply of a cochlear implant", IEEE, pp. 1965-1970 (2003)
	187	D.H.Freedman. "Power on a Chip". MIT Technology Review, November 2004.
	188	Geyi, Wen. A Method for the Evaluation of Small Antenna Q. IEEE Transactions on Antennas and Propagation, Vol. 51, No. 8, August 2003.
	189	Haus, H.A., "Waves and Fields in Optoelectronics," Chapter 7 "Coupling of Modes --- Reasonators and Couplers" (Prentice-Hall, New Jersey, 1984).
	190	Heikkinen et al. "Performance and Efficiency of Planar Rectennas for Short-Range Wireless Power Transfer at 2.45 GHz". Microwave and Optical Technology Letters, 31(2):86-91, October 20, 2001.
	191	Hirai et al. "Integral Motor with Driver and Wireless Transmission of Power and Information for Autonomous Subspindle Drive". IEEE, 15(1):13-20, January 2000.
	192	Hirai et al. "Practical Study on Wireless Transmission of Power and Information for Autonomous Decentralized Manufacturing System". IEEE, 46(2):349-359, April 1999.
	193	Hirai et al. "Study on Intelligent Battery Charging Using Inductive Transmission of Power and Information". IEEE, 15(2):335-345, March 2000.
	194	Hirai et al. "Wireless Transmission of Power and Information and Information for Cableless Linear Motor Drive". IEEE 15(1):21-27, January 2000.
	195	"Intel CTO Says Gap between Humans, Machines Will Close by 2050", Intel News Release, (See intel.com/.../20080821comp.htm?iid=S...) (Printed 11/6/2009)
	196	M. V. Jacob et al. "Lithium Tantalate – A High Permittivity Dielectric Material for Microwave Communication Systems". Proceedings of IEEE TENCON – Poster Papers, pp. 1362-1366, 2003.
	197	Jackson, J.D., "Classical Electrodynamics," 3rd Edition, Sections 1.11, 5.5, 5.17, 6.9, 8.1, 8.8, 9.2, 9.3 (Wiley, New York, 1999).
	198	Aristeidis Karalis et al., "Efficient Wireless *non-radiative mid-range* energy transfer", Annals of Physics, Vol. 323, pp. 34-48 (2008)
	199	Kawamura et al. "Wireless Transmission of Power and Information Through One High-Frequency Resonant AC Link Inverter for Robot Manipulator Applications". IEEE, 32(3):503-508, May/June 1996.
	200	Yoshihiro Konishi, Microwave Electronic Circuit Technology, Chapter 4, pp. 145-197 (Marcel Dekker, Inc., New York, NY 1998)
	201	Andre Kurs et al., "Wireless Power Transfer via Strongly Coupled Magnetic Resonances", Science Vol. 317, pp. 83-86 (July 6, 2007)
	202	Lee, "Antenna Circuit Design for RFID Applications," Microchip Technology Inc., AN710, 50 pages (2003)
	203	Lee, "RFID Coil Design," Microchip Technology Inc., AN678, 21 pages (1998)
	204	Liang et al., "Silicon waveguide two-photon absorption detector at 1.5 μm wavelength for autocorrelation measurements," Applied Physics Letters, 81(7):1323-1325 (August 12, 2002)

Examiner Signature	Date Considered
/Albert Paladini/	09/23/2011

EXAMINER: Initials citation considered. Draw line through citation if not in conformance and not considered. Include copy of this form with next communication to applicant.

Substitute Disclosure Form (PTO-1449)

ALL REFERENCES CONSIDERED EXCEPT WHERE LINED THROUGH. /A.P./

Substitute Form PTO-1449 (Modified) U.S. Department of Commerce Patent and Trademark Office	Attorney Docket No. 01997-0359009	Application No. 12/639,963
Information Disclosure Statement by Applicant (Use several sheets if necessary) (37 CFR §1.98(b))	Applicant John D. Joannopoulos et al.	
	Filing Date December 16, 2009	Group Art Unit

Other Documents (include Author, Title, Date, and Place of Publication)		
Examiner Initial	Desig. ID	Document
	205	Microchip Technology Inc., "microID 13.56 MHz Design Guide - MCRF355/360 Reader Reference Design," 24 pages (2001)
	206	MIT Team Experimentally Demonstrates Wireless Power Transfer, Potentially Useful for Power Laptops, Cell-Phones Without Cords - Goodbye Wires ..., by Franklin Hadley, Institute for Soldier Nanotechnologies, Massachusetts Institute of Technology (June 7, 2007)
	207	O'Brien et al. "Analysis of Wireless Power Supplies for Industrial Automation Systems". IEEE, pp. 367-372, 2003.
	208	O'Brien et al. "Design of Large Air-Gap Transformers for Wireless Power Supplies". IEEE, pp. 1557-1562, 2003.
	209	J. B. Pendry. "A Chiral Route to Negative Refraction". Science 306:1353-1355 (2004).
	210	Gary Peterson, "MIT WiTricity Not So Original After All", Feed Line No. 9, (See http://www.tfcbooks.com/articles/witricity.htm) printed 11/12/2009
	211	"Physics Update, Unwired Energy", Physics Today, pp. 26, (January 2007) (See http://arxiv.org/abs/physics/0611063.)
	212	Powercast LLC. "White Paper" Powercast simply wire free, 2003.
	213	Sakamoto et al. "A Novel Circuit for Non-Contact Charging Through Electro-Magnetic Coupling". IEEE, pp. 168-174, 1992.
	214	Sekitani et al. "A large-area flexible wireless power transmission sheet using printed plastic MEMS switches and organic field-effect transistors". [PUBLICATION UNKNOWN]
	215	Sekitani et al. "A large-area wireless power-transmission sheet using printed organic transistors and plastic MEMS switches" www.nature.com/naturematerials. Published online April 29, 2007.
	216	S. Sensiper. Electromagnetic wave propogation on helical conductors. PhD Thesis, Massachusetts Institute of Technology, 1951.
	217	Soljacic. "Wireless Non-Radiative Energy Transfer – PowerPoint presentation". Massachusetts Institute of Technology, October 6, 2005.
	218	Someya, Takao. "The world's first sheet-type wireless power transmission system". University of Tokyo, December 12, 2006
	219	Splashpower, "Splashpower - World Leaders in Wireless Power," PowerPoint presentation, 30 pages (September 3, 2007)
	220	David H. Staelin et al., Electromagnetic Waves, Chapters 2, 3, 4, and 8, pp. 46-176 and 336-405 (Prentice Hall Upper Saddle River, New Jersey 1998)
	221	Nikola Tesla, "High Frequency Oscillators for Electro-Therapeutic and Other Purposes", The Electrical Engineer, Vol. XXVI, No. 50 (November 17, 1898)
	222	Nikola Tesla, "High Frequency Oscillators for Electro-Therapeutic and Other Purposes", Proceedings of the IEEE, Vol. 87, No. 7, pp 1282-1292 (July 1999)
	223	Texas Instruments, "HF Antenna Design Notes - Technical Application Report," Literature Number 11-08-26-003, 47 pages (September 2003)
	224	"The Big Story for CES 2007: The public debut of eCoupled Intelligent Wireless Power" Press Release, Fulton Innovation LLC, Las Vegas, NV, December 27, 2006.
	225	"The world's first sheet-type wireless power transmission system: Will a socket be replaced by e-wall?" Press Release, Tokyo, Japan, December 12, 2006.

Examiner Signature /Albert Paladini/	Date Considered 09/23/2011
EXAMINER: Initials citation considered. Draw line through citation if not in conformance and not considered. Include copy of this form with next communication to applicant.	

Substitute Disclosure Form (PTO-1449)

ALL REFERENCES CONSIDERED EXCEPT WHERE LINED THROUGH. /A.P./

Substitute Form PTO-1449 (Modified) U.S. Department of Commerce Patent and Trademark Office	Attorney Docket No. 01997-0359009	Application No. 12/639,963
Information Disclosure Statement by Applicant (Use several sheets if necessary) (37 CFR §1.98(b))	Applicant John D. Joannopoulos et al.	
	Filing Date December 16, 2009	Group Art Unit

Other Documents (include Author, Title, Date, and Place of Publication)		
Examiner Initial	Desig. ID	Document
	226	Thomsen et al., "Ultrahigh speed all-optical demultiplexing based on two-photon absorption in a laser diode," Electronics Letters, 34(19):1871-1872 (September 17, 1998)
	227	"Unwired energy questions asked, answered", Physics Today, pp. 16-17 (September 2007)
	228	UPM Rafsec, "Tutorial overview of inductively coupled RFID Systems," 7 pages (May 2003)
	229	Vandevoorde et al. "Wireless energy transfer for stand-alone systems: a comparison between low and high power applicability". Sensors and Actuators, A 92:305-311, 2001.
	230	David Vilkomerson et al., "Implantable Doppler System for Self-Monitoring Vascular Grafts", IEEE Ultrasonics Symposium, pp. 461-465 (2004)
	231	"Wireless Energy Transfer Can Potentially Recharge Laptops, Cell Phones Without Cords", by Marin Soljacic of Massachusetts Institute of Technology and Davide Castelvecchi of American Institute of Physics (November 14, 2006)
	232	Clemens M. Zierhofer et al., "High-Efficiency Coupling-Insensitive Transcutaneous Power and Data Transmission Via an Inductive Link", IEEE Transactions on Biomedical Engineering, Vol. 37, No. 7, pp. 716-722 (July 1990)
	233	Copy of Examination Report for Australia Application No. 2006269374, dated September 18, 2008
	234	Copy of International Search Report and Written Opinion for International Application No. PCT/US2006/026480, dated December 21, 2007
	235	Copy of International Preliminary Report on Patentability for International Application No. PCT/US2006/026480, dated January 29, 2008
	236	Copy of International Search Report and Written Opinion for International Application No. PCT/US2007/070892, dated March 3, 2008
	237	Copy of International Search Report and Written Opinion for International Application No. PCT/US09/43970, dated July 14, 2009
	238	European Examination Report dated January 15, 2009 in connection with Application No. 06 786 588.1 – 1242, Examined by Michael Lund.
	239	Copy of International Preliminary Report on Patentability with regard to International Application No. PCT/US2007/070892 by Examiner Philippe Becamel dated September 29, 2009
	240	"Recharging, The Wireless Way – Even physicists forget to recharge their cell phones sometimes." By Angela Chang – PC Magazine, ABC News Internet Ventures, (2006)
	241	"Physics Promises Wireless Power" by Jonathan Fildes, Science and Technology Reporter, BBC News, (November 15, 2006)
	242	"Wireless energy promise powers up" by Jonathan Fildes, Science and Technology Report, BBC News, (See http://news.bbc.co.uk/2/hi/technology/6725955.stm) (June 7, 2007)
	243	"The technology with impact 2007", by Jonathan Fildes, BBC News, (December 27, 2007)
	244	"In pictures: A year in technology", BBC News, (December 28, 2007)
	245	"Man tries wirelessly boosting batteries", by Seth Borenstein, AP Science Writer, Boston.com, (See http://www.boston.com/business/technology/articles/2006/11/15/man_tries_wirelessly_b...) (November 15, 2006)
	246	"The vision of an MIT physicist: Getting rid of pesky rechargers" by Gareth Cooks, Globe Staff, Boston.com, (December 11, 2006)

Examiner Signature	Date Considered
/Albert Paladini/	09/23/2011

EXAMINER: Initials citation considered. Draw line through citation if not in conformance and not considered. Include copy of this form with next communication to applicant.

Substitute Disclosure Form (PTO-1449)

ALL REFERENCES CONSIDERED EXCEPT WHERE LINED THROUGH. /A.P./

Substitute Form PTO-1449 (Modified) U.S. Department of Commerce Patent and Trademark Office	Attorney Docket No. 01997-0359009	Application No. 12/639,963
Information Disclosure Statement by Applicant (Use several sheets if necessary) (37 CFR §1.98(b))	Applicant John D. Joannopoulos et al.	
	Filing Date December 16, 2009	Group Art Unit

Other Documents (include Author, Title, Date, and Place of Publication)		
Examiner Initial	Desig. ID	Document
	247	"MIT discovery could unplug your iPod forever", by Chris Reidy, Globe staff, Boston.com, (See http://www.boston.com/business/ticker/2007/06/mit_discovery_c.html) (June 7, 2007)
	248	"Scientists light bulb with 'wireless electricity' ", www.Chinaview.cn, (See http://news.xinhuanet.com/english/2007-06/08/content_6215681.htm) (June, 2007)
	249	"Look, Ma – no wires! - Electricity broadcast through the air may someday run your home", by Gregory M. Lamb, Staff writer, The Christian Science Monitor, (See http://www.csmonitor.com/2006/1116/p14s01-stct.html) (November 15, 2006)
	250	"The end of the plug? Scientists invent wireless device that beams electricity through your home", by David Derbyshire, Daily Mail, (See http://www.dailymail.co.uk/pages/live/articles/technology/technology.html?in_article_id=4...) (June 7, 2007)
	251	"Lab report: Pull the plug for a positive charge", by James Morgan, The Herald, Web Issue 2680 (November 16, 2006)
	252	"Recharging gadgets without cables", Infotech Online, Printed from infotech.indiatimes.com (November 17, 2006)
	253	"Electro-nirvana? Not so fast", by Alan Boyle, MSNBC, (June 8, 2007)
	254	" 'Evanescent coupling' could power gadgets wirelessly" by Celeste Biever, NewScientistsTech.com, (see http://www.newscientisttech.com/article.ns?id=dn10575&print=true) (November 15, 2006)
	255	"Wireless Energy", by Clay Risen, The New York Times, (December 9, 2007)
	256	"Wireless power transfer possible", PressTV, (See http://www.presstv.ir/detail.aspx?id=12754&sectionid=3510208) (June 11, 2007)
	257	"Outlets Are Out", by Phil Berardelli, ScienceNOW Daily News, Science Now, (See http://sciencenow.sciencemag.org/cgi/content/full/2006/1114/2) (November 14, 2006)
	258	"The Power of Induction – Cutting the last cord could resonate with our increasingly gadget-dependent lives", by Davide Castelvecchi, Science News Online, Vol. 172, No. 3, (Week of July 21, 2007)
	259	"Wireless Energy Transfer May Power Devices at a Distance", ScientificAmerican.com, (November 14, 2006)
	260	"Wireless Energy Lights Bulb from Seven Feet Away – Physicists vow to cut the cord between your laptop battery and the wall socket – with just a simple loop of wire", by JR Minkel, ScientificAmerican.com, (See http://www.sciam.com/article.cfm?articleid=07511C52-E7F2-99DF-3FA6ED2D7DC9AA2...) (June 7, 2007)
	261	"Air Power – Wireless data connections are common -- now scientists are working on wireless power", by Stephen Cass, Sponsored by Spectrum, (See http://spectrum.ieee.org/computing/hardware/air-power) (November 2006)
	262	"Wireless revolution could spell end of plugs", by Roger Highfield, Science Editor, Telegraph.co.uk, (See http://www.telegraph.co.uk/news/main.jhtml?xml=/news/2007/06/07/nwireless107.xml) (June 7, 2007)

Examiner Signature /Albert Paladini/	Date Considered 09/23/2011

EXAMINER: Initials citation considered. Draw line through citation if not in conformance and not considered. Include copy of this form with next communication to applicant.

Substitute Disclosure Form (PTO-1449)

ALL REFERENCES CONSIDERED EXCEPT WHERE LINED THROUGH. /A.P./

Substitute Form PTO-1449 (Modified) U.S. Department of Commerce Patent and Trademark Office	Attorney Docket No. 01997-0359009	Application No. 12/639,963
Information Disclosure Statement by Applicant (Use several sheets if necessary) (37 CFR §1.98(b))	Applicant John D. Joannopoulos et al.	
	Filing Date December 16, 2009	Group Art Unit

Other Documents (include Author, Title, Date, and Place of Publication)		
Examiner Initial	Desig. ID	Document
	263	"Man tries wirelessly boosting batteries", by Seth Borenstein, The Associated Press, USA Today, (November 16, 2006)
	264	"MIT's wireless electricity for mobile phones", by Miebi Senge, Vanguard, (See http://www.vanguardngr.com/articles/2002/features/gsm/gsm211062007.htm) (June 11, 2007)
	265	"MIT Scientists Pave the Way For Wireless Battery Charging", by William M. Bulkeley, The Wall Street Journal, (See http://online.wsj.com/article/SB118123955549228045.html?mod=googlenews_wsj) (June 8,2007)
	266	Copy of Provisional Application, Application Serial No. 60/908,383 filed on March 27, 2007
	267	"Intel Moves to Free Gadgets of Their Recharging Cords", By John Markoff, The New York Times - nytimes.com, August 21, 2008
	268	G. Scheible et al., "Novel Wireless Power Supply System for Wireless Communication Devices in Industrial Automation Systems", IEEE, (2002)
	269	J. Schutz et al., "Load Adaptive Medium Frequency Resonant Power Supply", IEEE, (2002)
	270	Marin Soljacic et al., "Photonic-crystal slow-light enhancement of nonlinear phase sensitivity", J. Opt. Soc. Am B, Vol. 19, No. 9, pp. 2052-2059 (September 2002)
	271	Amnon Yariv et al., "Coupled-resonator optical waveguide: a proposal and analysis", Optics Letters, Vol. 24, No. 11, pp. 711-713 (June 1, 1999)
	272	Copy of International Search Report for International Application No. PCT/US09/58499 by Examiner Lee W. Young dated December 10, 2009
	273	Copy of PCT International Search Report and Written Opinion for PCT/US09/59244, December 7, 2009, 12 pages.
	274	

Examiner Signature /Albert Paladini/	Date Considered 09/23/2011
EXAMINER: Initials citation considered. Draw line through citation if not in conformance and not considered. Include copy of this form with next communication to applicant.	

Substitute Disclosure Form (PTO-1449)

ALL REFERENCES CONSIDERED EXCEPT WHERE LINED THROUGH. /A.P./

IN THE UNITED STATES PATENT AND TRADEMARK OFFICE

Applicant	: John D. Joannopoulos et al.	Art Unit	: 2836
Serial No.	: 12/639,963	Examiner	: Albert W. Paladini
Filed	: December 16, 2009	Conf. No.	: 7811
Title	: WIRELESS ENERGY TRANSFER WITH HIGH-Q TO MORE THAN ONE DEVICE		

Mail Stop Amendment
Commissioner for Patents
P.O. Box 1450
Alexandria, VA 22313-1450

AMENDMENT IN REPLY TO ACTION OF SEPTEMBER 30, 2011

Please amend the above-identified application as follows:

Amendments to the Claims:

This listing of claims replaces all prior versions and listings of claims in the application:

Listing of Claims:

1. (Currently Amended) A system, comprising:

a source high-Q resonator, optionally coupled to an energy source;

a second high-Q resonator, optionally coupled to an energy drain, located a distance from the source resonator; and

a third high-Q resonator, optionally coupled to an energy drain, located a distance from the source resonator,

wherein the source resonator and at least one of the second resonator and third resonator are coupled to wirelessly transfer electromagnetic energy from said source resonator to said at least one of the second resonator and third resonator.

2. (Currently Amended) A method, comprising:

providing a source high-Q resonator, optionally coupled to an energy source;

providing a second high-Q resonator, optionally coupled to an energy drain, located a distance from the source resonator; and

providing a third high-Q resonator, optionally coupled to an energy drain, located a distance from the source resonator,

wherein the source resonator and at least one of the second resonator and third resonator are coupled to wirelessly transfer electromagnetic energy from said source resonator to said at least one of the second resonator and third resonator.

3. (New) The system of claim 1, further comprising the energy source coupled to the source resonator.

4. (New) The system of claim 1, further comprising the first-mentioned energy drain coupled to the second resonator and the second-mentioned energy drain coupled to the third resonator.

5. (New) The system of claim 4, wherein at least one of the energy drains comprises a robot, vehicle, computer, cell phone, or a portable electronic device.

6. (New) The system of claim 1, wherein at least one of the high-Q resonators has a Q-factor $Q_i > 100$.

7. (New) The system of claim 6, wherein another one of the high-Q resonators has a Q-factor $Q_j > 100$.

8. (New) The system of claim 1, wherein the source resonator is electromagnetically coupled to each of the second and third resonators.

9. (New) The system of claim 8, wherein the source resonator is configured to wirelessly transfer electromagnetic energy from the source resonator to each of the second and third resonators.

10. (New) The system of claim 8, wherein at least one of the high-Q resonators has a Q-factor $Q_i > 100$.

11. (New) The system of claim 10, wherein another one of the high-Q resonators has a Q-factor $Q_j > 100$.

12. (New) The system of claim 1, wherein at least one of the resonators is tunable.

13. (New) The system of claim 1, wherein the resonators are movable relative to one another and wherein the wireless energy transfer occurs over a range of distances.

14. (New) The system of claim 13, wherein the range of distances includes 5 cm.

15. (New) The system of claim 13, wherein the range of distances includes 10 cm.

16. (New) The system of claim 13, wherein the range of distances includes 30 cm.

17. (New) The system of claim 13, wherein $\kappa/\sqrt{\Gamma_1\Gamma_2} > 0.2$ over the range of distances, wherein κ is the wireless energy transfer rate, Γ_1 is the intrinsic loss rate of the source resonator, and Γ_2 is the intrinsic loss rate of said at least one of the second resonator and the third resonator.

18. (New) The system of claim 17, wherein $\kappa/\sqrt{\Gamma_1\Gamma_2} > 0.5$ over the range of distances.

19. (New) The system of claim 17, wherein $\kappa/\sqrt{\Gamma_1\Gamma_2} > 1$ over the range of distances.

20. (New) The system of claim 13, wherein the efficiency of the wireless energy transfer is at least 20% over the range of distances..

21. (New) The system of claim 1, wherein the resonant frequencies $f_1 = \omega_1/2\pi$, $f_2 = \omega_2/2\pi$, and $f_3 = \omega_3/2\pi$ of the resonators are each at least 5 MHz.

22. (New) The system of claim 1, further comprising a feedback mechanism coupled to at least one of the resonators to correct for detuning.

23. (New) The system of claim 1, wherein the energy source is coupled to the source resonator, the energy drain is coupled to the second resonator, and the source resonator is electromagnetically coupled to the second resonator, and wherein the energy source and energy drain are configured to be driven to increase the ratio of useful-to-lost power for varying wireless energy transfer rates κ between the source resonator and the second resonator.

24. (New) The system of claim 1, wherein the source resonator is electromagnetically coupled to the second resonator, and wherein the source resonator and second resonator are configured to be adjustably tuned to increase the ratio of useful-to-lost power for varying wireless energy transfer rates κ between the source resonator and the second resonator.

25. (New) The method of claim 2, wherein the energy source is coupled to the source resonator.

26. (New) The method of claim 2, wherein the first-mentioned energy drain is coupled to the second resonator and the second-mentioned energy drain is coupled to the third resonator.

27. (New) The method of claim 26, wherein at least one of the energy drains comprises a robot, vehicle, computer, cell phone, or a portable electronic device.

28. (New) The method of claim 2, wherein at least one of the high-Q resonators has a Q-factor $Q_i > 100$.

29. (New) The method of claim 28, wherein another one of the high-Q resonators has a Q-factor $Q_j > 100$.

30. (New) The method of claim 2, wherein source resonator is electromagnetically coupled to each of the second and third resonators.

31. (New) The method of claim 30, wherein the source resonator is configured to wirelessly transfer electromagnetic energy from the source resonator to each of the second and third resonators.

32. (New) The method of claim 30, wherein at least one of the high-Q resonators has a Q-factor $Q_i > 100$.

33. (New) The method of claim 32, wherein another one of the high-Q resonators has a Q-factor $Q_j > 100$.

34. (New) The method of claim 2, wherein at least one of the resonators is tunable.

35. (New) The method of claim 2, wherein the resonators are movable relative to one another and wherein the wireless energy transfer occurs over a range of distances.

36. (New) The method of claim 35, wherein the range of distances includes 5 cm.

37. (New) The method of claim 35, wherein the range of distances includes 10 cm.

38. (New) The method of claim 35, wherein the range of distances includes 30 cm.

39. (New) The method of claim 35, wherein $\kappa/\sqrt{\Gamma_1\Gamma_2} > 0.2$ over the range of distances, wherein κ is the wireless energy transfer rate, Γ_1 is the intrinsic loss rate of the source resonator, and Γ_2 is the intrinsic loss rate of said at least one of the second resonator and the third resonator.

40. (New) The method of claim 39, wherein $\kappa/\sqrt{\Gamma_1\Gamma_2} > 0.5$ over the range of distances.

41. (New) The method of claim 39, wherein $\kappa/\sqrt{\Gamma_1\Gamma_2} > 1$ over the range of distances.

42. (New) The method of claim 35, wherein the efficiency of the wireless energy transfer is at least 20% over the range of distances.

43. (New) The method of claim 2, wherein the resonant frequencies $f_1 = \omega_1/2\pi$, $f_2 = \omega_2/2\pi$, and $f_3 = \omega_3/2\pi$ of the resonators are each at least 5 MHz.

44. (New) The method of claim 2, wherein a feedback mechanism is coupled to at least one of the resonators to correct for detuning.

45. (New) The method of claim 2, wherein the energy source is coupled to the source resonator, the energy drain is coupled to the second resonator, and the source resonator is electromagnetically coupled to the second resonator, and wherein the energy source and energy drain is driven to increase the ratio of useful-to-lost power for varying wireless energy transfer rates κ between the source resonator and the second resonator.

46. (New) The method of claim 2, wherein the source resonator is electromagnetically coupled to the second resonator, and wherein the source resonator and second resonator are adjustably tuned to increase the ratio of useful-to-lost power for varying wireless energy transfer rates κ between the source resonator and the second resonator.

47. (New) The system of claim 1, wherein the source resonator and the second resonator have different characteristic sizes.

48. (New) The method of claim 2, wherein the source resonator and the second resonator have different characteristic sizes.

REMARKS

Claims 1-48 are pending.

Claims 1 and 2 are the independent claims.

Claims 3-48 are new dependent claims.

The only outstanding rejection was an obviousness-type double patenting rejection over the parent application, which issued as U.S. Patent No. 7,741,734. Filed herewith is a Terminal Disclaimer to moot the rejection.

Accordingly, we ask that the application be allowed.

An Information Disclosure Statement is being filed together with this Reply.

The fees in the amount of $1,680.00 for excess claim fees are being paid concurrently herewith on the Electronic Filing System (EFS) by way of Deposit Account authorization. Please apply any necessary charges or credits to Deposit Account 06-1050, referencing the above attorney docket number.

Respectfully submitted,

Date: November 23, 2011

/Marc M. Wefers Reg. No. 56,842/
Marc M. Wefers
Reg. No. 56,842

Customer Number 26161
Fish & Richardson P.C.
Telephone: (617) 542-5070
Facsimile: (877) 769-7945

22714869.doc

(12) INTERNATIONAL APPLICATION PUBLISHED UNDER THE PATENT COOPERATION TREATY (PCT)

(19) World Intellectual Property Organization
International Bureau

(43) International Publication Date
26 May 2011 (26.05.2011)

PCT

(10) International Publication Number
WO 2011/062827 A2

(51) International Patent Classification:
G06F 1/26 (2006.01)

(21) International Application Number:
PCT/US2010/056240

(22) International Filing Date:
10 November 2010 (10.11.2010)

(25) Filing Language: English

(26) Publication Language: English

(30) Priority Data:
61/262,086 17 November 2009 (17.11.2009) US

(71) Applicant *(for all designated States except US)*: **APPLE INC.** [US/US]; 1 Infinite Loop, Cupertino, California 95014 (US).

(72) Inventors; and

(75) Inventors/Applicants *(for US only)*: **CULBERT, Michael F.** [US/US]; 1 Infinite Loop, MS 305-2GM, Cupertino, California 95014 (US). **BILBREY, Brett C.** [US/US]; 1 Infinite Loop, MS 305-2GM, Cupertino, California 95014 (US). **SIMON, David I.** [US/US]; 1 Infinite Loop, MS 305-2GM, Cupertino, California 95014 (US). **ARNOLD, Peter M.** [US/US]; 1 Infinite Loop, MS 306-3P, Cupertino, California 95014 (US).

(74) Agents: **FERRAZANO, Michael J.** et al.; Beyer Law Group LLP, P.O. Box 1687, Cupertino, California 95015-1687 (US).

(81) Designated States *(unless otherwise indicated, for every kind of national protection available)*: AE, AG, AL, AM, AO, AT, AU, AZ, BA, BB, BG, BH, BR, BW, BY, BZ, CA, CH, CL, CN, CO, CR, CU, CZ, DE, DK, DM, DO, DZ, EC, EE, EG, ES, FI, GB, GD, GE, GH, GM, GT, HN, HR, HU, ID, IL, IN, IS, JP, KE, KG, KM, KN, KP, KR, KZ, LA, LC, LK, LR, LS, LT, LU, LY, MA, MD, ME, MG, MK, MN, MW, MX, MY, MZ, NA, NG, NI, NO, NZ, OM, PE, PG, PH, PL, PT, RO, RS, RU, SC, SD, SE, SG, SK, SL, SM, ST, SV, SY, TH, TJ, TM, TN, TR, TT, TZ, UA, UG, US, UZ, VC, VN, ZA, ZM, ZW.

(84) Designated States *(unless otherwise indicated, for every kind of regional protection available)*: ARIPO (BW, GH, GM, KE, LR, LS, MW, MZ, NA, SD, SL, SZ, TZ, UG, ZM, ZW), Eurasian (AM, AZ, BY, KG, KZ, MD, RU, TJ,

[Continued on next page]

(54) Title: WIRELESS POWER UTILIZATION IN A LOCAL COMPUTING ENVIRONMENT

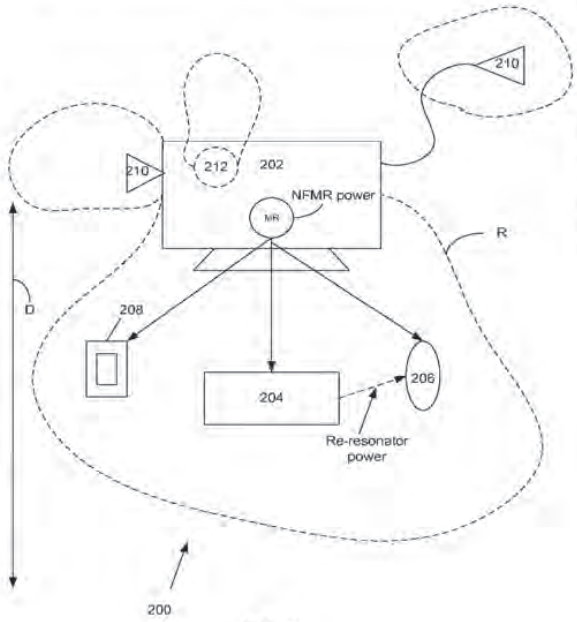


Fig. 2

(57) Abstract: Various embodiments of a wirelessly powered local computing environment are described. The wireless powered local computing environment includes at least a near field magnetic resonance (NFMR) power supply arranged to wirelessly provide power to any of a number of suitably configured devices. In the described embodiments, the devices arranged to receive power wirelessly from the NFMR power supply must be located in a region known as the near field that extends no further than a distance D of a few times a characteristic size of the NFMR power supply transmission device. Typically, the distance D can be on the order of 1 meter or so.

WO 2011/062827 A2

TM), European (AL, AT, BE, BG, CH, CY, CZ, DE, DK, EE, ES, FI, FR, GB, GR, HR, HU, IE, IS, IT, LT, LU, LV, MC, MK, MT, NL, NO, PL, PT, RO, RS, SE, SI, SK, SM, TR), OAPI (BF, BJ, CF, CG, CI, CM, GA, GN, GQ, GW, ML, MR, NE, SN, TD, TG).

Declarations under Rule 4.17:

— *as to the applicant's entitlement to claim the priority of the earlier application (Rule 4.17(iii))*

Published:

— *without international search report and to be republished upon receipt of that report (Rule 48.2(g))*

WIRELESS POWER UTILIZATION IN A LOCAL COMPUTING ENVIRONMENT

TECHNICAL FIELD

[0001] The described embodiments relate generally to utilizing a wireless power transmission in a portable computing environment.

BACKGROUND

[0002] Historically, transferring power wirelessly has been successful for fairly limited applications. In particular, only those applications where a wireless power source and a wireless power receiver are located very close to each other have been successful. In this arrangement, the wireless power source and the wireless power receiver are typically coupled inductively by way of a magnetic field that can entangle both the power source and receiver. Although well suited for applications requiring relatively low power (on the order of mW), this same process is not suitable for those applications requiring either more power (on the order of at least a few watts to hundreds of watts) or where the power source and power receiver are located further apart from each other, such as a few inches to a few feet.

[0003] However, it has been discovered (see "Efficient wireless non-radiative mid-range energy transfer" by Karalis et al., Annals of Physics 323 (2008) pgs. 34 - 38) that useable power can be transferred wirelessly from a power source to a receiver located within a distance referred to as a near field. By near field it is meant that within a distance a few times larger than that of both objects involved in the transfer (about one meter or so for most applications) a relatively large amount of power (at least on the order of a few watts) can be transferred between a wireless source device and a receiver with an acceptable efficiency. In this way, a realistic and practical approach to wireless transferring useable amounts of power over distances suitable for limited applications can be realized. Typically, each battery powered device such as a wireless electronic device requires its own charger and power source, which is usually an alternating current (AC) power outlet. Such a wired configuration becomes unwieldy when many devices need charging.

[0004] Various over-the-air or wireless power transmission between a transmitter and a receiver coupled to the electronic device to be charged have been carried out that generally fall into two categories. One category is based on the coupling of plane wave radiation between a transmit antenna and a receive antenna on the device to be

InductEV, Inc.
Exhibit 1025
Page 432

charged. The receive antenna collects the radiated power and rectifies it for charging the battery. Antennas are generally of resonant length in order to improve the coupling efficiency. This approach suffers from the fact that the power coupling falls off quickly with distance between the antennas, so charging over reasonable distances (e.g., less than 1 to 2 meters) becomes difficult.

[0005] Other techniques rely upon inductive coupling between a transmit antenna embedded, for example, in a "charging" mat or surface and a receive antenna (plus a rectifying circuit) embedded in the electronic device to be charged. This approach has the disadvantage that the spacing between transmit and receive antennas must be very close (e.g., within thousandths of meters). Though this approach does have the capability to simultaneously charge multiple devices in the same area, this area is typically very small and requires the user to accurately locate the devices to a specific area.

[0006] With wireless power transmission there is a need for apparatuses and methods for transmitting and relaying wireless power at varying power levels and multiplexed times to increase power transmission efficiency.

[0007] Furthermore, what is desired are methods, systems, and apparatus for efficient and user friendly interaction between peripheral devices in a wirelessly powered local computing environment. In particular, in order to enhance the user's experience and provide efficient power utilization, cooperation between the plurality of peripheral devices in the context of the wireless power environment is desired.

SUMMARY

[0008] The present invention provides a system and method for utilizing wireless near field magnetic resonance (NFMR) power transmission in a computing environment.

[0009] In various embodiments, methods, systems, and apparatus for interacting between a plurality of peripheral devices receiving power wirelessly from a wireless power supply is described. In one embodiment, a virtual charging area can be created. The virtual charging area can extend to about about one (1) meter from a central station that incorporates a NFMR power supply. The virtual charging area can define a region in which suitably configured peripheral devices, such as a mouse, keyboard, and so on can receive power by way of a NFMR channel formed between the NFRM power supply and a NFMR resonator circuit included in the peripheral

InductEV, Inc.
Exhibit 1025
Page 433

device. In this way, when both the NFMR power supply and the NFMR resonator circuit are tuned to each other, then useable power can be transferred over a power conduction channel formed between the two resonant devices.

[0010] In some embodiments, at least one of the peripheral devices can have a tunable resonator circuit having at least one circuit element (such as a resistor, inductor, or capacitor) having a value that can be changed. In this way, the tunable resonator circuit can be de-coupled from the NFMR power supply by de-tuning the tunable resonator circuit in relation to the resonance frequency of the NFMR power supply. In this way, the effective Q value of the tunable circuit is reduced to the point that essentially no power is transferred. In one embodiment, at least one of the plurality of peripheral devices can include a secondary NFMR resonator circuit adapted to re-resonant power to another one of the plurality of peripheral devices by establishing a NFMR channel to the other peripheral device over which useable power can be transferred. In some embodiments, the NFMR power supply can eliminate any voids in the virtual charging area by modifying resonance characteristics such as frequency.

[0011] A method of wirelessly transmitting power can be performed by creating a first coupling mode region of an electromagnetic field within a near field of a power supply transmit antenna, coupling the electromagnetic field and a receiver antenna of a first receiver device within the coupling mode region, creating a second coupling mode region of the electromagnetic field different from the first coupling mode region within a near field of a transmit antenna of the first receiver device, coupling the electromagnetic field to a receive antenna of second receiver device in the near field of the transmit antenna of the first receiver device, wirelessly delivering power from the power supply to the first receiver device by way of the power supply transmit antenna using the first coupling mode region of the electromagnetic field; and wirelessly delivering at least some of the power wirelessly delivered to the first receiver device is wirelessly by re-transmitting the at least some power to the second receiver device by way of the first receiver transmit antenna using the second coupling mode region of the electromagnetic field.

BRIEF DESCRIPTION OF THE DRAWINGS

[0012] The included drawings are for illustrative purposes and serve only to provide examples of possible structures and arrangements for the disclosed

InductEV, Inc.
Exhibit 1025
Page 434

embodiments. These drawings in no way limit any changes in form and detail that may be made to the described embodiments by one skilled in the art without departing from the spirit and scope of the embodiments.

[0013] Fig. 1 illustrates representative tunable resonator circuits in accordance with the described embodiments.

[0014] Fig. 2 shows representative virtual charging area in accordance with the described embodiments.

[0015] Fig. 3 shows representative hybrid power circuit in accordance with the described embodiments.

[0016] Fig. 4 shows representative time multiplexing for distributing power in accordance with the described embodiments.

[0017] Fig. 5 illustrates a wireless transmission or charging system, in accordance with various exemplary embodiments.

[0018] Fig. 6 shows a simplified schematic diagram of a wireless power transfer system.

[0019] Fig. 7 shows an antenna used in exemplary embodiments configured as a "loop" antenna that can also be referred to herein as a "magnetic" antenna.

[0020] Fig. 8 shows a flowchart detailing process 800 in accordance with the described embodiments.

DETAILED DESCRIPTION

[0021] Various embodiments of a wirelessly powered local computing environment are described. The wireless powered local computing environment includes at least a near field magnetic resonance (NFMR) power supply arranged to wirelessly provide power to any of a number of suitably configured devices. In the described embodiments, the devices arranged to receive power wirelessly from the NFMR power supply can be located in a region known as the near field that extends no further than a distance D that can be a few times a characteristic size of the NFMR power supply transmission device. Typically, the distance D can be on the order of 1 meter or so.

[0022] Fig. 1 shows various representative tunable circuits in accordance with the described embodiments. The representative tunable circuits can include series RLC (resistor (R), inductor (L), capacitor(C)) circuit 102. In this arrangement, a resonant frequency can be tuned (i.e., changed) by changing any of the component values. For

InductEV, Inc.
Exhibit 1025
Page 435

example, circuit 102, capacitor C can be a variable capacitor used to tune circuit 102. Similarly, circuit 104 (known as a Hartley oscillator) can be used as a tunable circuit in the described embodiments as can tuned LC circuit 106.

[0023] Fig. 2 shows representative virtual charging area 200 in accordance with the described embodiments. Virtual charging area 200 provides region R of charging for suitably configured devices placed within the region R. NFMR power supply can be placed in central unit such as desktop computer. In this way, the desktop computer can provide the NFMR power supply with computing resources. It should be noted that the near field magnetic resonance (NFMR) power supply can include high Q circuit that relies upon near field magnetic coupling by way of a resonance channel formed between resonances of the power source and sink to transfer power. The NFMR power supply can be a standalone unit such as, for example, included in a desk top computer, laptop computer, tablet computer, and so on. In other embodiments, the NFMR power supply can take the form of a portable type unit such as a dongle that can be connected to a legacy device such as a desktop computer thereby providing the ability to retrofit devices. In still other embodiments, housing or a portion of a housing used to enclose the NFMR power source can act to extend a useful range of the NFMR power supply.

[0024] In this way, suitably configured peripheral devices can be powered directly from the NFMR power supply. In so doing, the peripheral devices when tuned to the appropriate frequency can receive power wirelessly from the NFMR power supply. In so doing, the appropriately tuned peripheral device can be considered to be part of a resonance circuit that can include the NFMR power supply and any other peripheral devices so tuned. As part of such a circuit, each device has associated with it a corresponding load that can be sensed by the NFMR power supply. As such, the resonance circuit can have a characteristic load that can change by the addition or deletion of devices from the resonance circuit. For example, if a suitably configured device such as a portable media player is brought within range of the NFMR power supply, then the load associated with the portable media player can be sensed by the NFMR power supply when (and if) the portable media player is appropriately tuned. It should be noted that in some cases, the device being brought into the range of the NFMR power supply can communicate its initial presence using a standard communication protocol such as WiFi or Bluetooth. However, once incorporated into

InductEV, Inc.
Exhibit 1025
Page 436

the resonance circuit, the device can use a communication back channel described in detail below. Accordingly, any change in the characteristic load factor of the resonance circuit can convey information that can be used by the NFMR power supply to control the various devices in the resonance circuit by, for example, distributing power, and so on.

[0025] In some embodiments, certain of the peripheral devices can be configured to include a re-resonator circuit that can receive power directly from the NFMR power supply. Such devices can also transfer a portion of the power received to other of the peripheral devices. For example, as shown in Fig. 2 virtual charging area 200 includes central unit 202 (desktop computer) that can include the NFMR power supply, keyboard 204, mouse 206, and portable media player 208. In one embodiment, keyboard 204 can be configured to receive power directly from the NFMR power supply included in desktop computer 202 as can mouse 206 and portable media player 208 (when located within range R).

[0026] In some cases, the ability of desktop computer 202 to provide power directly to mouse 206, for example, can be reduced due to any number of factors. Such factors can include, for example, the addition of other devices into region R that require power from the NFMR power supply, obstacles interfering with the direct power channel formed between the NFMR and mouse 206, and so on. In this case, keyboard 204 can act as a re-resonator such that a portion of the power delivered to keyboard 204 from the NFMR power supply can be passed on by way of a re-resonator transmission unit (not shown) in keyboard 204. In this way, any power loss experienced by mouse 206 can be ameliorated by the power received from keyboard 204. This arrangement can be transitory or can last for as long as mouse 206 is not able to receive adequate power directly from the NFMR power supply. In other cases, the locating of portable media player 208 within region R can reduce the amount of power available to keyboard 204 and mouse 206. In this case, if a battery in keyboard 206 is fully charged (or additional charge is not necessary) then keyboard 206 can decouple a charging circuit while still maintaining a re-resonator circuit providing power to mouse 206.

[0027] In some embodiments, dongle 210 can be connected to desktop computer 202 (by way of a USB port or cable, for example). So connected, dongle 210 can, in turn, act as a range extender for the NFMR power supply. In this way, dongle 210

InductEV, Inc.
Exhibit 1025
Page 437

can extend a range that power can be provided by the NFMR power supply included in desktop computer 202. In some cases, dongle 210 can re-resonate power already received from the NFMR power supply while in other cases, dongle 210 can include its own NFMR power supply. By having its own NFMR power supply, dongle 210 can provide additional power wirelessly to those devices within virtual charging region 200 separate from the power provided by the NFMR power supply included in desktop 202. It should be noted that in some embodiments, the housing of desktop computer 202 (or a portion thereof) can be used as a resonator as part of the NFMR power supply.

[0028] Fig. 3 shows representative hybrid power circuit 300 in accordance with the described embodiments. As described, hybrid power circuit 300 can match the low power delivery capability of the NFMR power supply to a large power requirement of required for long term storage devices, such as lithium ion polymer (LiPO) battery. Batteries in such devices as portable phones, portable media players, and so on, can require relatively large amount of power to charge that can be greater than that available from the NFMR power supply. Therefore, it is difficult to charge these high capacity batteries such as LiPO using the NFMR power supply. However, a short term charge storage device (such as a capacitor, ultra capacitor, and so on) that can be charged up by power delivered by the NFMR power supply can be used to temporarily store charge prior to being passed to the battery. In this way, once sufficient charge is stored in the short term charge storage device, the stored charge can be used to charge a long term charge storage device (such as a LiPO battery). For example, Fig. 3 shows representative hybrid power circuit 300 having capacitor 302, capacitor charging circuit 304 (that can receive power P from the NFMR power supply), long term power storage unit 306 (that can take the form of battery 306), and battery charging circuit 308. In the described embodiment, power P provided by the NFMR power supply can "trickle" charge capacitor 302. Once sufficient charge is stored in capacitor 302, capacitor charging circuit 304 can sense capacitor voltage VC and switch fully charged capacitor 302 to battery 306 by way of battery charging circuit 308. In this way, charge Q stored in capacitor 302 can be used to increase the charge of battery 306. Once capacitor 302 is discharged (as determined by capacitor charging circuit 304), capacitor 302 can again receive power P from the NFMR power supply.

InductEV, Inc.
Exhibit 1025
Page 438

[0029] One of the advantages of a wirelessly powered local computing environment is the potential to provide an enhanced user experience. For example, by doing away with clumsy and annoying cables and eliminating the need to replace batteries, an easy to use and efficient local computing environment can be provided to the user. However, in order to provide this enhanced user experience, it would be advantageous for the various devices that make up the wirelessly powered local computing environment to be able to interact with each other as well as with the NFMR power supply. Such interaction can include, for example, providing power by the NFMR power supply to any of the devices within range in whatever amount is required. For example, an amount of power transferred between the NFMR power supply (having a first resonator circuit) and receiving device (having a second resonator circuit) can be controlled by tuning (or de-tuning) the second resonator circuit along the lines described above. It should be noted that when a device is tuned, the tuned device can become part of the resonance circuit. As part of the resonance circuit, a load associated with the device can be "seen" by the NFMR power supply. This load can, in turn, be used by the NFMR power supply to determine the power requirements of the resonance circuit as well as how the required power must be distributed amongst the various devices included in the resonance circuit. On the other hand, when a device "de-tunes", then the device no longer resonates with the NFMR power supply and is effectively removed from the resonance circuit and receives little or no additional power.

[0030] It should be noted that various environmental factors can have an effect on the efficiency of power transfer from the NFMR power supply to those devices included in the resonance circuit. For example, any object (metallic, for example) that can interfere with the magnetic coupling between the NFMR power supply and those device wirelessly receiving power can adversely affect both the amount of power supplied and the efficiency of the power transfer. This reduction in power transferred or power transfer efficiency can put an undue strain on the NFMR power supply as well as increase the likelihood that particular devices may not have sufficient power to operate at peak efficiency, to execute important functions, or in some cases, not be able to operate at all. In one embodiment, feedback provided by a device to the NFMR power supply indicating that the device requires more power or has experienced a reduction in power can cause the NFMR power supply to try to

InductEV, Inc.
Exhibit 1025
Page 439

ascertain the reason or reasons why the device has experienced this reduction in power. For example, if the device is moving within a void region (a void being defined as that region having a substantially reduced power transmission or efficiency factor), then the NFMR power supply can attempt to move the void region by modifying selected resonance factors (such as resonance frequency) thereby having the effect of moving the void region (hopefully beyond the range of the operating region of the devices wirelessly coupled to the NFMR power supply). In one embodiment, the NFMR power supply can determine that the power transfer efficiency has dropped below a threshold for a device(s) based upon, for example, feedback from the affected device(s). In response, the NFMR power supply can respond by modifying the frequency of the magnetic resonance signal until the power efficiency has recovered to above the threshold, by increasing power, or by, in some cases, causing less important or less used devices, to de-tune themselves (thereby removing themselves from the resonance circuit) so as to free up power that can be provided to those devices requiring more power. It should be noted that these operations can be carried out in the background in such a way that the user is unaware of the operations taking place. In still another embodiment, the power source can alter phase, frequency and or signal amplitude relative to other links in order to optimize power delivery.

[0031] In order to provide more robust communication between the various devices coupled with the NFMR power supply, each device can provide affirmative feedback to the NFMR power supply using a direct communication channel such as Bluetooth or WiFi. It should be noted, however, that an indirect communication channel can also be used. Such an indirect communication channel can be formed using the resonance circuit load factor mediated by the number (and type) of devices wirelessly coupled with the NFMR power supply. Since each device has an associated resonance load (i.e., load perceived by the NFMR power supply when a device is tuned to the proper resonance frequency), an indirect communication channel mediated by load state of the device, or devices in the resonance circuit can be established with the NFMR power supply. For example, the NFMR power supply can characterize a particular load state of a resonance circuit by ascertaining the overall resonance load (i.e., sense load on resonant circuit). Any changes to the load state can indicate a change in the status of the resonance circuit which, in turn, can

InductEV, Inc.
Exhibit 1025
Page 440

infer that one or more of the devices previously included in the resonance circuit (i.e., tuned to the NFMR power supply resonant frequency) has dropped out, or de-tuned. In some cases, a Morse code like communication protocol can be established between the NFRM power supply and each of the devices. This Morse code like communication protocol can be based upon a device tuning and de-tuning itself using an identifiable pattern. In this way, a simple device identifier, for example, can be communicated to the NFMR power supply. Using this arrangement, a device that has determined to de-tune itself and to remove itself from the resonance circuit, can signal the NFMR power supply its intent as well as identify itself. In this way, the NFRM power supply can have a more clear understanding of the condition of the resonance circuit and the devices included therein. This device to device communication channel (also referred to as a back channel) can be capable of communicating simple information. Such information can include, for example, a device identifier, a synchronization flag, and so on. It should be noted that this communication channel is independent and separate from other communication channels provided by, for example, WiFi or Bluetooth.

[0032] For example, if keyboard is using power wirelessly provide by the NFMR power supply to charge its battery, when the keyboard determines that the battery is substantially fully charged, then the keyboard can determine that power from the NFMR power supply is no longer required (at least until the battery discharges to a pre-set level). In this case, the keyboard can notify the NFMR power supply that it no longer requires power (or at least until it signals that it requires power at some future point in time). In this case, the NFMR can redirect power away from the keyboard (using, for example, a different resonant frequency when the NFMR power supply is equipped to transmit power on a number of frequency ranges, or bands) or the keyboard can remove itself from the resonance circuit (either on its own or as directed) by de-tuning itself. In this way, the load of the resonance circuit can be reduced allowing more power to be wirelessly delivered to the other devices in the resonance circuit. It should be noted that for efficiency and environmental reasons, the NFMR power supply will provide only as much power as is needed. For example, as battery charges up then less power is required. In this way, the charge state of the battery can be communicated to the NFMR power supply that can respond by reducing, or throttling back, the power provided to the keyboard.

InductEV, Inc.
Exhibit 1025
Page 441

[0033] It should be noted that while a device can be removed from the resonance circuit by the process of de-tuning, the device can be added to the resonance circuit by tuning it. By tuning (and conversely de-tuning) it is meant that circuit characteristics (such as resistance) can be changed resulting in the circuit Q increasing in the case of tuning or decreasing in the case of de-tuning. It should be noted that the relative increase or decrease in Q for a circuit can be dependent upon the circuit and applications to which the circuit is used.

[0034] When a device is brought within range R of the power supply, then the load experienced by the power supply increases by that amount corresponding to the device. In this way, proximity detection can be thought as having taken place that can trigger an action to be taken. For example, if a portable media player is brought within range R of a desktop computer, then the proximity signal generated by the change in load experienced by the power supply can cause the desktop computer to initiate a synchronization process, for example, between the portable media player and the desktop computer.

[0035] The communication channels established between the various devices in the resonance circuit can be used for the devices to determine amongst themselves which device takes priority with regards to power supplied by the NFMR power supply. In other cases, a host device (that includes the NFMR power supply and any associated computing resources) can act as aggregator. By aggregator, it is meant that the host device can determine the priority of those devices for receiving power, how much power to receive, and for how long. It should be noted that some devices and or some operations performed by a device can have a higher priority than other devices and or operations. For example, a high priority device(s) may require guaranteed power for operation (such as using a mouse vs charging a portable media player). The host device can use any suitable priority mechanism (round robin, for example).

[0036] In another embodiment, the devices receiving power can communicate amongst themselves to determine which device has priority. The devices understand their own operating points, such as a minimum amount of power to perform certain function, maximum power required to perform all functions. In this way, each device can provide a desired amount of power, a list of functions that can be performed, and a minimum amount of power required for operation. The source can determine how much power can be delivered and which device can get the power it needs. In some

InductEV, Inc.
Exhibit 1025
Page 442

cases, the devices themselves set the priority, in other cases, the host device sets the priority. When a device is not receiving power, it removes itself from the resonance circuit by de-tuning, and returns to the circuit by re-tuning.

[0037] It should be noted that the NFMR power supply can use any number of protocols to wirelessly provide power to the various devices included in the resonance circuit. For example, the NFMR power supply can include a plurality of resonator circuits each arranged to resonate at a particular frequency. In this way, the NFMR power supply can provide power orthogonally using different frequency bands. In this way, a device can have multiple resonant frequencies in order to take advantage of the frequency bands provided by the NFMR power supply. For example, the NFMR power supply can wirelessly provide power using multiple frequency bands where a number of devices can each tune themselves to a particular frequency. In this way, frequency shifting techniques can be used to more efficiently transfer power to the plurality of devices within range of the NFMR power supply.

[0038] Other mechanisms for a single NFMR power supply to independently transmit power to more than one device includes time multiplexing as shown in Fig. 4. As illustrated, devices 400, 402 and 404 can each take turns tuning and de-tuning themselves such that at any one time only one of the devices if receiving power. For example, during a period 1, device 400 receives power by tuning itself to at least one of the available resonant frequencies while devices 402 and 404 are de-tuned. Once device 400 has completed its power cycle, device 400 de-tunes itself and device 402 tunes itself and receives power wirelessly from the NFMR power supply. Once device 402 completes its power cycle, device 402 de-tunes itself and device 404 tunes itself to at least one of the resonance frequencies to receive power from the NFMR power supply. In other embodiments, the NFMR power supply can use frequency multiplexing in which the NFMR can toggle amongst a number of frequencies each one tuned to a particular device. The device can receive power only when the device resonates with a current frequency of the power supply.

[0039] The closed loop control can also affect the modes of operation of the devices in the resonance circuit. For example, a keyboard can determine an amount of power received from the source which will depend upon the distance between the source and the keyboard (as well as the presence of any interfering objects). If the power received falls below a threshold, then the keyboard can use more battery power

InductEV, Inc.
Exhibit 1025
Page 443

or request that the source increase power. In some cases, if the power provided can not be increased to meet the current operating requirements of the keyboard, then the keyboard can take action to reduce its power requirements by, for example, reducing backlight, etc. It should be noted that as discussed above, the reduction on power received by the keyboard can be caused by many other factors other than an increase in distance. Such factors can include, for example, the presence of voids, objects, other devices added to the circuit, and so on.

[0040] Fig. 5 illustrates a wireless transmission or charging system 500, in accordance with various exemplary embodiments. Input power 502 is provided to a transmitter 504 for generating a radiated field 506 for providing energy transfer. A receiver 508 couples to the radiated field 506 and generates an output power 510 for storing or consumption by a device (not shown) coupled to the output power 510. Both the transmitter 504 and the receiver 508 are separated by a distance 512. In one exemplary embodiment, transmitter 504 and receiver 508 are configured according to a mutual resonant relationship and when the resonant frequency of receiver 508 and the resonant frequency of transmitter 504 are very close, transmission losses between the transmitter 504 and the receiver 508 are minimal when the receiver 508 is located in the "near-field" of the radiated field 506.

[0041] Transmitter 504 further includes a transmit antenna 514 for providing a means for energy transmission and receiver 508 further includes a receive antenna 518 for providing a means for energy reception. The transmit and receive antennas are sized according to applications and devices to be associated therewith. As stated, an efficient energy transfer occurs by coupling a large portion of the energy in the near-field of the transmitting antenna to a receiving antenna rather than propagating most of the energy in an electromagnetic wave to the far field. When in this near-field a coupling mode may be developed between the transmit antenna 514 and the receive antenna 518. The area around the antennas 514 and 518 where this near-field coupling may occur is referred to herein as a coupling-mode region.

[0042] Fig. 6 shows a simplified schematic diagram of a wireless power transfer system. The transmitter 604 includes an oscillator 622, a power amplifier 624 and a filter and matching circuit 626. The oscillator is configured to generate a desired frequency, which may be adjusted in response to adjustment signal 623. The oscillator signal may be amplified by the power amplifier 624 with an amplification

InductEV, Inc.
Exhibit 1025
Page 444

amount responsive to control signal 625. The filter and matching circuit 626 may be included to filter out harmonics or other unwanted frequencies and match the impedance of the transmitter 604 to the transmit antenna 514.

[0043] The receiver 608 may include a matching circuit 632 and a rectifier and switching circuit 634 to generate a DC power output to charge a battery 636 as shown in FIG. 6 or power a device coupled to the receiver (not shown). The matching circuit 632 may be included to match the impedance of the receiver 508 to the receive antenna 518. The receiver 508 and transmitter 504 may communicate on a separate communication channel 619 (e.g., Bluetooth, zigbee, cellular, etc).

[0044] As illustrated in Fig. 7, antennas used in exemplary embodiments may be configured as a "loop" antenna 750, which may also be referred to herein as a "magnetic" antenna. Loop antennas may be configured to include an air core or a physical core such as a ferrite core. Air core loop antennas may be more tolerable to extraneous physical devices placed in the vicinity of the core. Furthermore, an air core loop antenna allows the placement of other components within the core area. In addition, an air core loop may more readily enable placement of the receive antenna 518 (FIG. 5, 6) within a plane of the transmit antenna5 (FIG. 5, 6) where the coupled-mode region of the transmit antenna 514 (FIG. 5, 6) may be more powerful.

[0045] As stated, efficient transfer of energy between the transmitter 104 and receiver 508 occurs during matched or nearly matched resonance between the transmitter 504 and the receiver 508. However, even when resonance between the transmitter 504 and receiver 508 are not matched, energy may be transferred at a lower efficiency. Transfer of energy occurs by coupling energy from the near-field of the transmitting antenna to the receiving antenna residing in the neighborhood where this near-field is established rather than propagating the energy from the transmitting antenna into free space.

[0046] The resonant frequency of the loop or magnetic antennas is based on the inductance and capacitance. Inductance in a loop antenna is generally simply the inductance created by the loop, whereas, capacitance is generally added to the loop antenna's inductance to create a resonant structure at a desired resonant frequency. As a non-limiting example, capacitor 752 and capacitor 754 may be added to the antenna to create a resonant circuit that generates resonant signal 756. Accordingly, for larger diameter loop antennas, the size of capacitance needed to induce resonance decreases

InductEV, Inc.
Exhibit 1025
Page 445

as the diameter or inductance of the loop increases. Furthermore, as the diameter of the loop or magnetic antenna increases, the efficient energy transfer area of the near-field increases. Of course, other resonant circuits are possible. As another non-limiting example, a capacitor may be placed in parallel between the two terminals of the loop antenna. In addition, those of ordinary skill in the art will recognize that for transmit antennas the resonant signal 756 may be an input to the loop antenna 750.

[0047] Exemplary embodiments of the invention include coupling power between two antennas that are in the near-fields of each other. As stated, the near-field is an area around the antenna in which electromagnetic fields exist but may not propagate or radiate away from the antenna. They are typically confined to a volume that is near the physical volume of the antenna. In the exemplary embodiments of the invention, magnetic type antennas such as single and multi-turn loop antennas are used for both transmit (Tx) and receive (Rx) antenna systems since magnetic near-field amplitudes tend to be higher for magnetic type antennas in comparison to the electric near-fields of an electric-type antenna (e.g., a small dipole). This allows for potentially higher coupling between the pair. Furthermore, "electric" antennas (e.g., dipoles and monopoles) or a combination of magnetic and electric antennas is also contemplated.

[0048] The Tx antenna can be operated at a frequency that is low enough and with an antenna size that is large enough to achieve good coupling (e.g., >-4 dB) to a small Rx antenna at significantly larger distances than allowed by far field and inductive approaches mentioned earlier. If the Tx antenna is sized correctly, high coupling levels (e.g., -1 to -4 dB) can be achieved when the Rx antenna on a host device is placed within a coupling-mode region (i.e., in the near-field) of the driven Tx loop antenna.

[0049] Fig. 8 shows a flowchart detailing process 800 in accordance with the described embodiments. Process 800 can begin at 802 by creating a first coupling mode region of an electromagnetic field within a near field of a power supply transmit antenna. Next at 804, the electromagnetic field and a receiver antenna of a first receiver device are coupled with the coupling mode region. At 806, a second coupling mode region of the electromagnetic field different from the first coupling mode region is created with a near field of a transmit antenna of the first receiver device. At 808, the electromagnetic field is coupled to a receive antenna of second receiver device in the near field of the transmit antenna of the first receiver device. At

InductEV, Inc.
Exhibit 1025
Page 446

810, power is wirelessly delivered from the power supply to the first receiver device by way of the power supply transmit antenna using the first coupling mode region of the electromagnetic field. At 812, at least some of the power wirelessly delivered to the first receiver device is wirelessly re-transmitted to the second receiver device by way of the first receiver transmit antenna using the second coupling mode region of the electromagnetic field.

InductEV, Inc.
Exhibit 1025
Page 447

WHAT IS CLAIMED IS:

1. A wirelessly powered local computing environment, the local computing environment including a near field magnetic resonance wireless power supply arranged to use a resonance channel to transfer useable energy to resonance circuits within a near field distance D, the distance D defining an outermost range of the NFMR power supply, comprising:

a central processing unit, the central processing unit providing processing resources to the NFMR power supply; and

a plurality of peripheral devices each having a tunable resonance circuit suitably adapted to receive power wirelessly from the NFMR power supply, wherein when at least one of the plurality of devices is within range of the NFMR power supply, the device tunes the resonance circuit to at least one of the resonance frequencies of the NFMR power supply and subsequently de-tunes the resonance circuit to provide a device identification to the NFMR power supply using a change in a resonance circuit load factor.

2. The local computing environment as recited in claim 1, wherein at least one of the peripheral devices includes a re-resonator circuit, the re-resonator circuit arranged to wirelessly provide a portion of the power received by the peripheral device from the NFMR power supply to at least one other peripheral client device.

3. A battery charging circuit, comprising:

a first node arranged to receive wirelessly provided power;

a short term charge storage device having a first charge capacity; and

a long term storage device having a second charge capacity, wherein the second charge capacity is substantially greater than the first charge capacity, wherein the long term storage device is charged by,

(A) storing charge corresponding to the power wirelessly received at the first node into the short term charge storage device,

(B) when the stored charge is equal to about the first charge capacity, then passing the stored charge from the short term storage device to the long term storage device, and

(C) repeating (A) and (B) until the charge stored in the long term storage device is about equal to the second charge capacity.

InductEV, Inc.
Exhibit 1025
Page 448

4. The circuit as recited in claim 3, wherein the short term charge storage device is an ultracapacitor and wherein the long term charge storage device is a LiPO battery.

5. A method of wirelessly transmitting power, comprising:

creating a first coupling mode region of an electromagnetic field within a near field of a power supply transmit antenna;

coupling the electromagnetic field and a receiver antenna of a first receiver device within the coupling mode region;

creating a second coupling mode region of the electromagnetic field different from the first coupling mode region within a near field of a transmit antenna of the first receiver device;

coupling the electromagnetic field to a receive antenna of second receiver device in the near field of the transmit antenna of the first receiver device;

wirelessly delivering power from the power supply to the first receiver device by way of the power supply transmit antenna using the first coupling mode region of the electromagnetic field; and

wirelessly delivering at least some of the power wirelessly delivered to the first receiver device is wirelessly by re-transmitting the at least some power to the second receiver device by way of the first receiver transmit antenna using the second coupling mode region of the electromagnetic field.

6. The method as recited in claim 5, wherein the first receiver device is a keyboard.

7. The method as recited in claim 6, wherein the second receiver device is a mouse.

8. The method as recited in claim 7, wherein the power supply is included in a host computing device.

9. The method as recited in claim 8, wherein the second coupling mode region is between the keyboard and the mouse.

10. The method as recited in claim 9, wherein the first coupling mode region is between the host computing device and the keyboard.

11. The method as recited in claim 9, wherein the first coupling mode region is between the host computing device and the mouse.

InductEV, Inc.
Exhibit 1025
Page 449

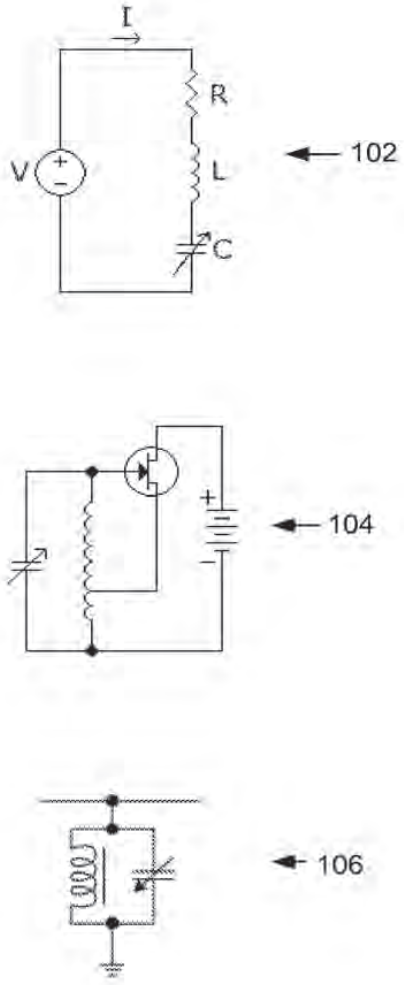


Fig. 1

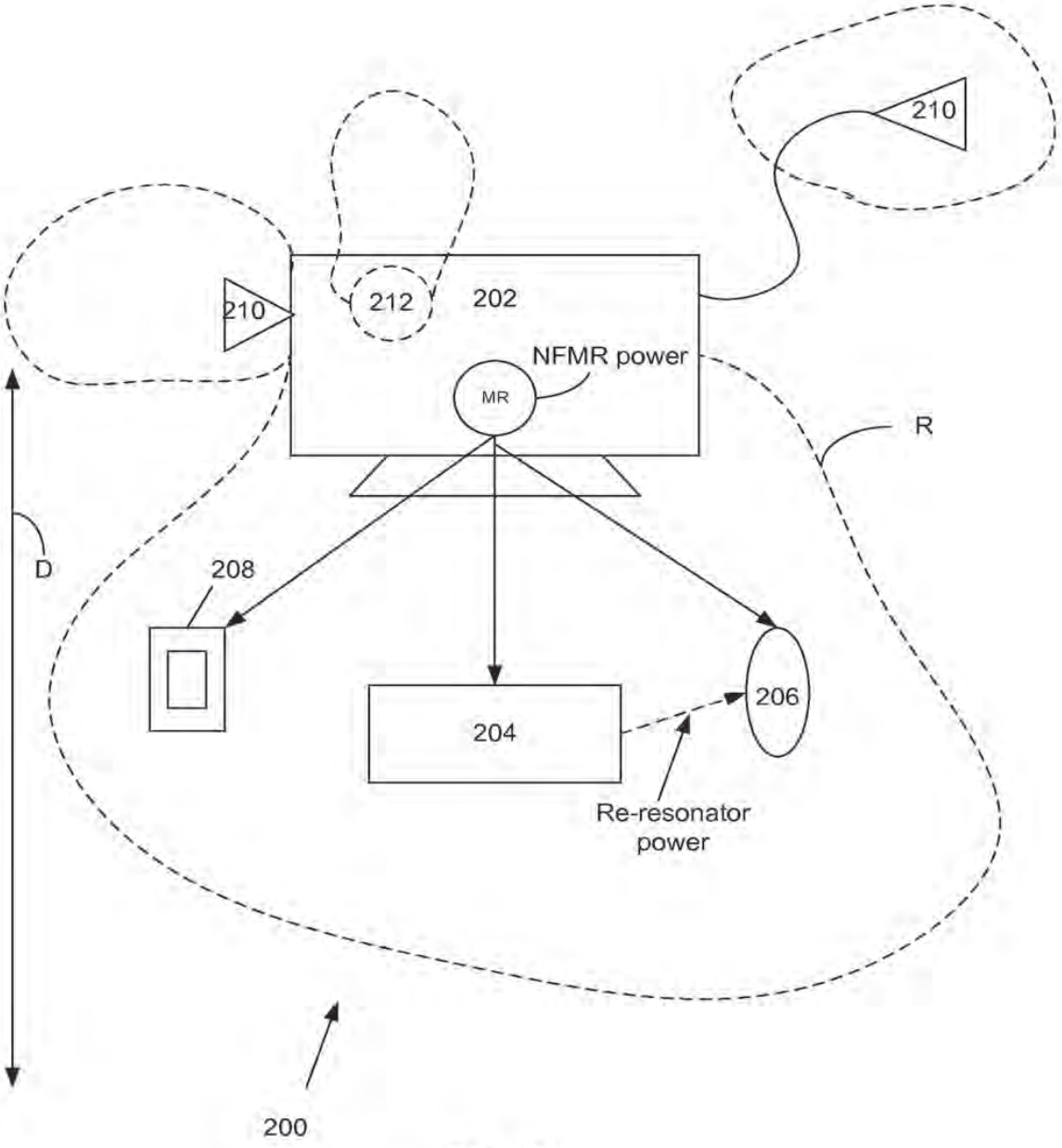

210
210
212
202
NFMR power
MR
R
D
208
206
204
Re-resonator
power
200

Fig. 2

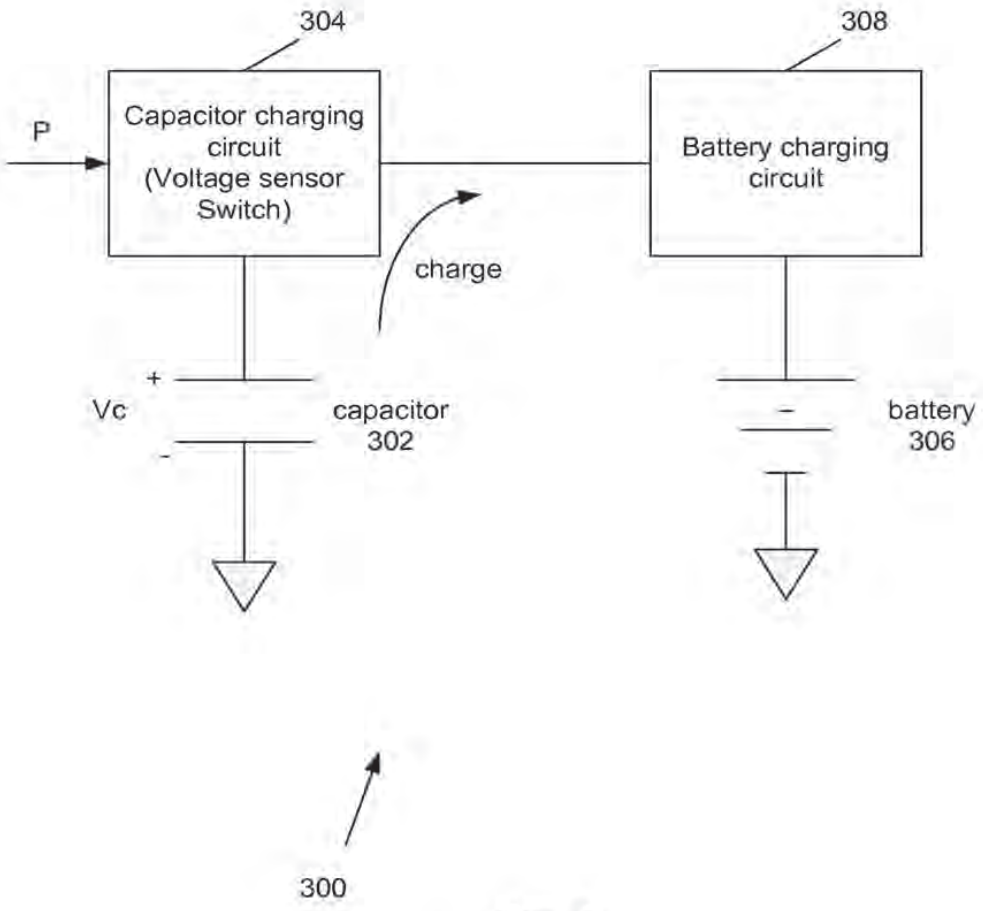

304
308
P
Capacitor charging circuit (Voltage sensor Switch)
Battery charging circuit
charge
+
Vc
-
capacitor 302
-
battery 306
300

Fig. 3

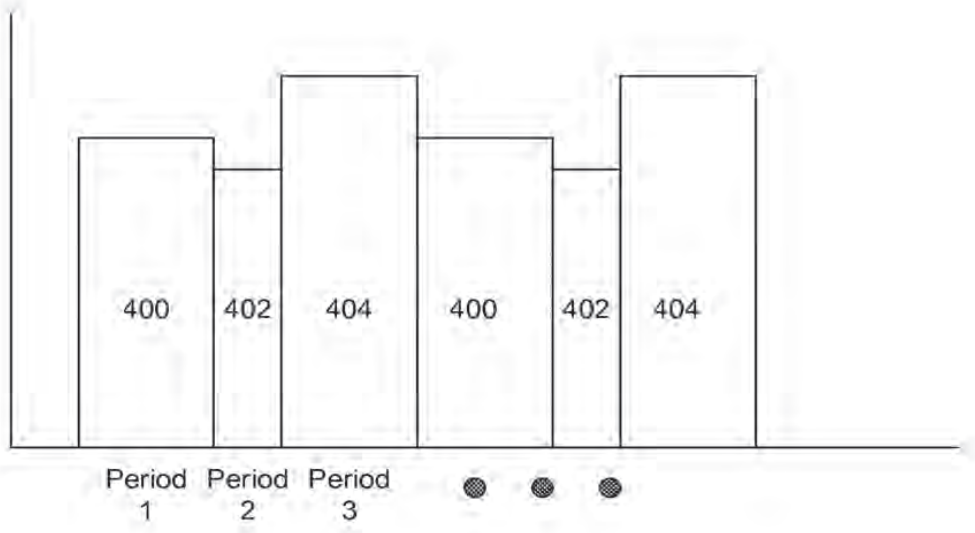


Fig. 4

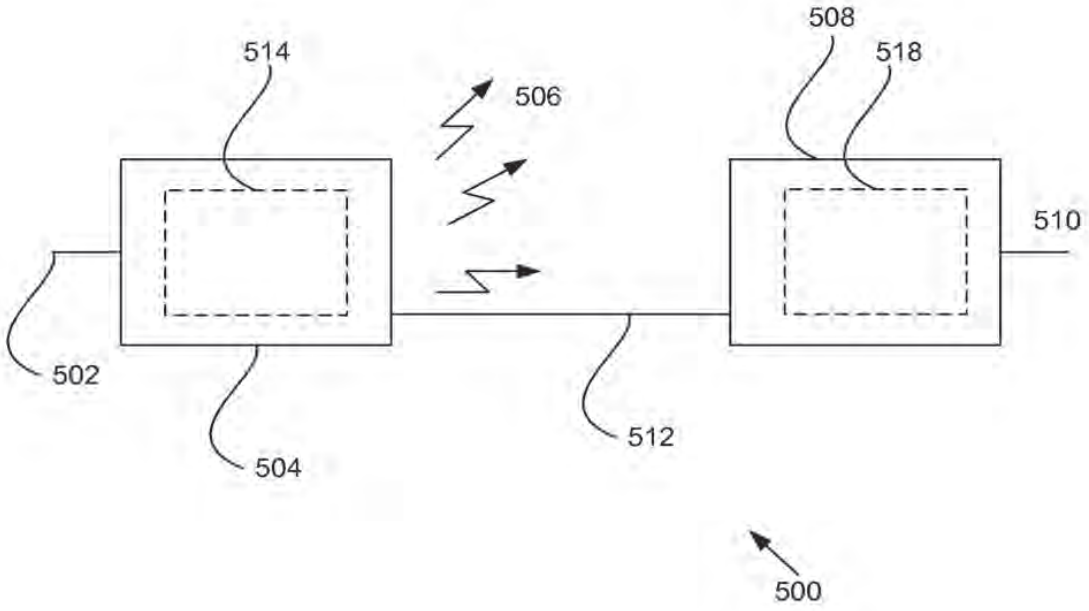


Fig. 5

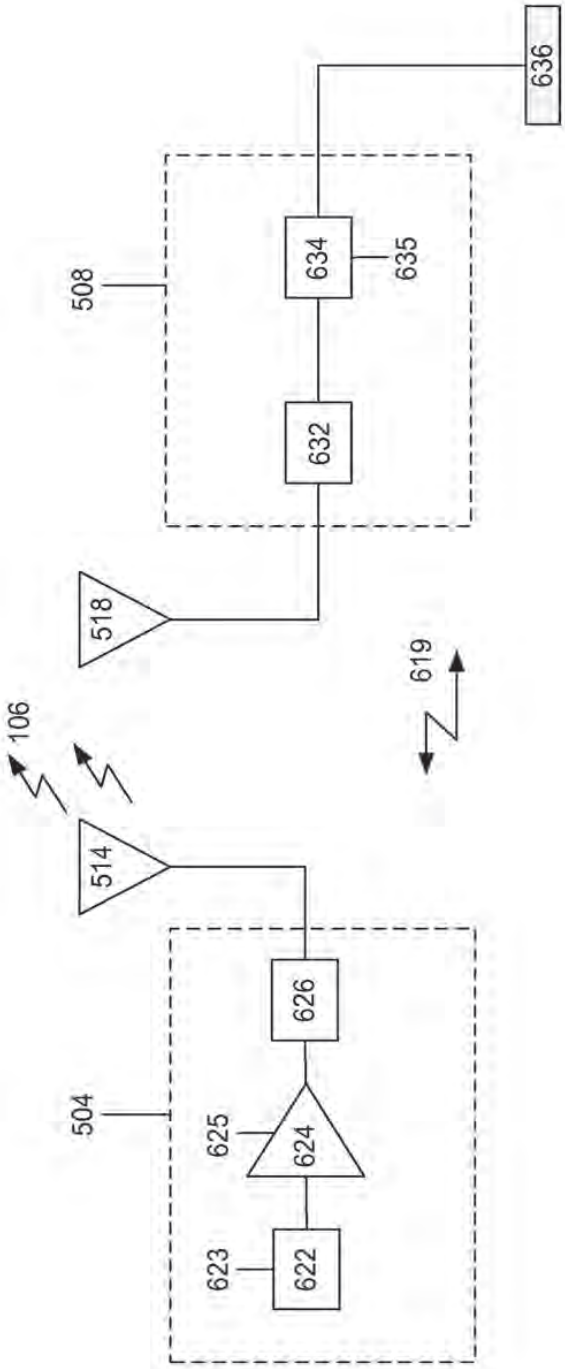


Fig. 6

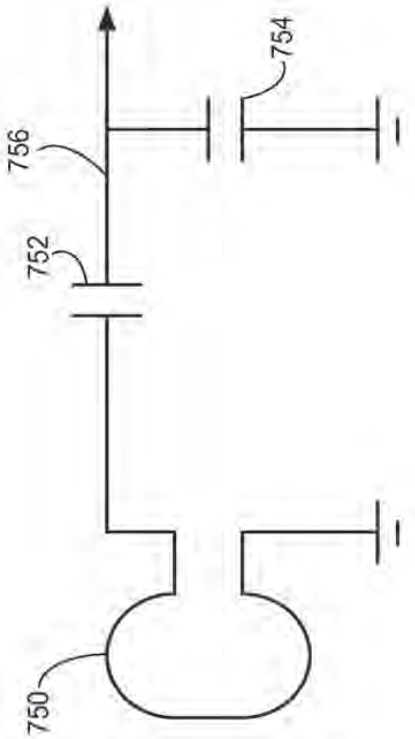


Fig. 7

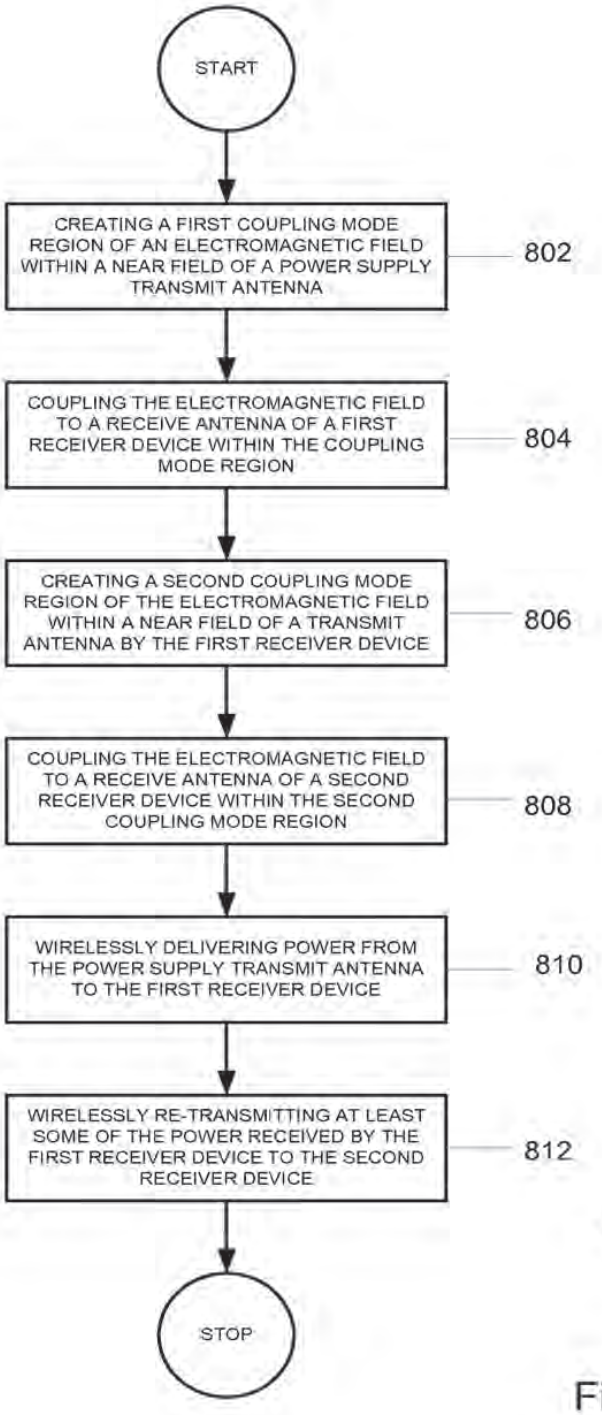

START
CREATING A FIRST COUPLING MODE REGION OF AN ELECTROMAGNETIC FIELD WITHIN A NEAR FIELD OF A POWER SUPPLY TRANSMIT ANTENNA
802
COUPLING THE ELECTROMAGNETIC FIELD TO A RECEIVE ANTENNA OF A FIRST RECEIVER DEVICE WITHIN THE COUPLING MODE REGION
804
CREATING A SECOND COUPLING MODE REGION OF THE ELECTROMAGNETIC FIELD WITHIN A NEAR FIELD OF A TRANSMIT ANTENNA BY THE FIRST RECEIVER DEVICE
806
COUPLING THE ELECTROMAGNETIC FIELD TO A RECEIVE ANTENNA OF A SECOND RECEIVER DEVICE WITHIN THE SECOND COUPLING MODE REGION
808
WIRELESSLY DELIVERING POWER FROM THE POWER SUPPLY TRANSMIT ANTENNA TO THE FIRST RECEIVER DEVICE
810
WIRELESSLY RE-TRANSMITTING AT LEAST SOME OF THE POWER RECEIVED BY THE FIRST RECEIVER DEVICE TO THE SECOND RECEIVER DEVICE
812
STOP
800

Fig. 8

(12) INTERNATIONAL APPLICATION PUBLISHED UNDER THE PATENT COOPERATION TREATY (PCT)

(19) World Intellectual Property Organization
International Bureau

(43) International Publication Date
26 May 2011 (26.05.2011)

PCT

(10) International Publication Number
WO 2011/062827 A3

(51) International Patent Classification:
G06F 1/26 (2006.01)

(21) International Application Number:
PCT/US2010/056240

(22) International Filing Date:
10 November 2010 (10.11.2010)

(25) Filing Language: English

(26) Publication Language: English

(30) Priority Data:
61/262,086 17 November 2009 (17.11.2009) US

(71) Applicant *(for all designated States except US)*: **APPLE INC.** [US/US]; 1 Infinite Loop, Cupertino, California 95014 (US).

(72) Inventors; and

(75) Inventors/Applicants *(for US only)*: **CULBERT, Michael F.** [US/US]; 1 Infinite Loop, MS 305-2GM, Cupertino, California 95014 (US). **BILBREY, Brett C.** [US/US]; 1 Infinite Loop, MS 305-2GM, Cupertino, California 95014 (US). **SIMON, David I.** [US/US]; 1 Infinite Loop, MS 305-2GM, Cupertino, California 95014 (US). **ARNOLD, Peter M.** [US/US]; 1 Infinite Loop, MS 306-3P, Cupertino, California 95014 (US).

(74) Agents: **FERRAZANO, Michael J.** et al.; Beyer Law Group LLP, P.O. Box 1687, Cupertino, California 95015-1687 (US).

(81) Designated States *(unless otherwise indicated, for every kind of national protection available)*: AE, AG, AL, AM, AO, AT, AU, AZ, BA, BB, BG, BH, BR, BW, BY, BZ, CA, CH, CL, CN, CO, CR, CU, CZ, DE, DK, DM, DO, DZ, EC, EE, EG, ES, FI, GB, GD, GE, GH, GM, GT, HN, HR, HU, ID, IL, IN, IS, JP, KE, KG, KM, KN, KP, KR, KZ, LA, LC, LK, LR, LS, LT, LU, LY, MA, MD, ME, MG, MK, MN, MW, MX, MY, MZ, NA, NG, NI, NO, NZ, OM, PE, PG, PH, PL, PT, RO, RS, RU, SC, SD, SE, SG, SK, SL, SM, ST, SV, SY, TH, TJ, TM, TN, TR, TT, TZ, UA, UG, US, UZ, VC, VN, ZA, ZM, ZW.

(84) Designated States *(unless otherwise indicated, for every kind of regional protection available)*: ARIPO (BW, GH, GM, KE, LR, LS, MW, MZ, NA, SD, SL, SZ, TZ, UG, ZM, ZW), Eurasian (AM, AZ, BY, KG, KZ, MD, RU, TJ,

[Continued on next page]

(54) Title: WIRELESS POWER UTILIZATION IN A LOCAL COMPUTING ENVIRONMENT

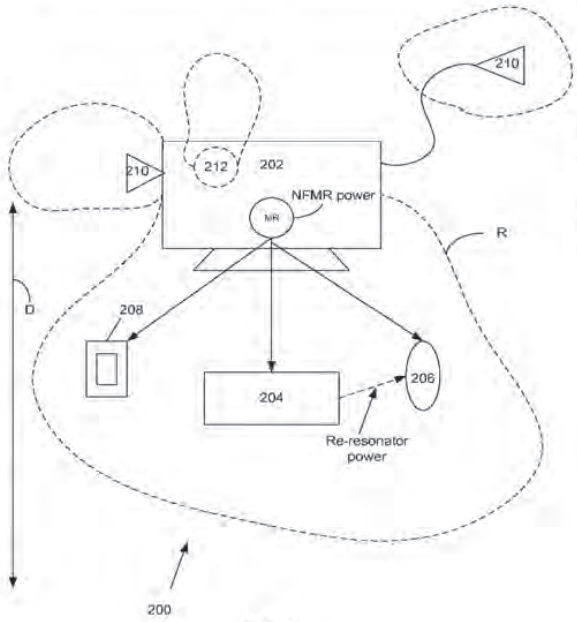


Fig. 2

(57) Abstract: Various embodiments of a wirelessly powered local computing environment are described. The wireless powered local computing environment includes at least a near field magnetic resonance (NFMR) power supply arranged to wirelessly provide power to any of a number of suitably configured devices. In the described embodiments, the devices arranged to receive power wirelessly from the NFMR power supply must be located in a region known as the near field that extends no further than a distance D of a few times a characteristic size of the NFMR power supply transmission device. Typically, the distance D can be on the order of 1 meter or so.

WO 2011/062827 A3

TM), European (AL, AT, BE, BG, CH, CY, CZ, DE, DK, EE, ES, FI, FR, GB, GR, HR, HU, IE, IS, IT, LT, LU, LV, MC, MK, MT, NL, NO, PL, PT, RO, RS, SE, SI, SK, SM, TR), OAPI (BF, BJ, CF, CG, CI, CM, GA, GN, GQ, GW, ML, MR, NE, SN, TD, TG).

Declarations under Rule 4.17:

— *as to the applicant's entitlement to claim the priority of the earlier application (Rule 4.17(iii))*

Published:

— *with international search report (Art. 21(3))*

— *before the expiration of the time limit for amending the claims and to be republished in the event of receipt of amendments (Rule 48.2(h))*

(88) Date of publication of the international search report:
14 July 2011

INTERNATIONAL SEARCH REPORT

International application No
PCT/US2010/056240

A. CLASSIFICATION OF SUBJECT MATTER
INV. G06F1/26
ADD.

According to International Patent Classification (IPC) or to both national classification and IPC

B. FIELDS SEARCHED

Minimum documentation searched (classification system followed by classification symbols)
G06F H02J H04B

Documentation searched other than minimum documentation to the extent that such documents are included in the fields searched

Electronic data base consulted during the international search (name of data base and, where practical, search terms used)
EPO-Internal

C. DOCUMENTS CONSIDERED TO BE RELEVANT

Category*	Citation of document, with indication, where appropriate, of the relevant passages	Relevant to claim No.
Y	US 2009/271048 A1 (WAKAMATSU MASATAKA [JP]) 29 October 2009 (2009-10-29) Paragraph [0044] - [0046]; Paragraph [0107] - [0109]; Paragraph [0116] - [0141]; Paragraph [0160] - [0167]; paragraph [0177] - paragraph [0180]; figures 1,7,10,12,14	1,2
Y	US 5 701 121 A (MURDOCH GRAHAM ALEXANDER M [AU]) 23 December 1997 (1997-12-23) column 11, line 60 - column 13, line 19	1
X Y	US 2009/134712 A1 (COOK NIGEL P [US] ET AL) 28 May 2009 (2009-05-28) paragraph [0019] - paragraph [0041]; figure 1	5-11 2

-/--

[X] Further documents are listed in the continuation of Box C.

[X] See patent family annex.

* Special categories of cited documents :

"A" document defining the general state of the art which is not considered to be of particular relevance

"E" earlier document but published on or after the international filing date

"L" document which may throw doubts on priority claim(s) or which is cited to establish the publication date of another citation or other special reason (as specified)

"O" document referring to an oral disclosure, use, exhibition or other means

"P" document published prior to the international filing date but later than the priority date claimed

"T" later document published after the international filing date or priority date and not in conflict with the application but cited to understand the principle or theory underlying the invention

"X" document of particular relevance; the claimed invention cannot be considered novel or cannot be considered to involve an inventive step when the document is taken alone

"Y" document of particular relevance; the claimed invention cannot be considered to involve an inventive step when the document is combined with one or more other such documents, such combination being obvious to a person skilled in the art.

"&" document member of the same patent family

Date of the actual completion of the international search	Date of mailing of the international search report
5 May 2011	24/05/2011

Name and mailing address of the ISA/	Authorized officer
European Patent Office, P.B. 5818 Patentlaan 2 NL - 2280 HV Rijswijk Tel. (+31-70) 340-2040, Fax: (+31-70) 340-3016	Alonso Nogueiro, M

Form PCT/ISA/210 (second sheet) (April 2005)

INTERNATIONAL SEARCH REPORT

International application No.
PCT/US2010/056240

Box No. II Observations where certain claims were found unsearchable (Continuation of item 2 of first sheet)

This international search report has not been established in respect of certain claims under Article 17(2)(a) for the following reasons:

1. ☐ Claims Nos.:
because they relate to subject matter not required to be searched by this Authority, namely:

2. ☐ Claims Nos.:
because they relate to parts of the international application that do not comply with the prescribed requirements to such an extent that no meaningful international search can be carried out, specifically:

3. ☐ Claims Nos.:
because they are dependent claims and are not drafted in accordance with the second and third sentences of Rule 6.4(a).

Box No. III Observations where unity of invention is lacking (Continuation of item 3 of first sheet)

This International Searching Authority found multiple inventions in this international application, as follows:

see additional sheet

1. ☒ As all required additional search fees were timely paid by the applicant, this international search report covers all searchable claims.

2. ☐ As all searchable claims could be searched without effort justifying an additional fees, this Authority did not invite payment of additional fees.

3. ☐ As only some of the required additional search fees were timely paid by the applicant, this international search report covers only those claims for which fees were paid, specifically claims Nos.:

4. ☐ No required additional search fees were timely paid by the applicant. Consequently, this international search report is restricted to the invention first mentioned in the claims; it is covered by claims Nos.:

Remark on Protest

☐ The additional search fees were accompanied by the applicant's protest and, where applicable, the payment of a protest fee.

☐ The additional search fees were accompanied by the applicant's protest but the applicable protest fee was not paid within the time limit specified in the invitation.

☒ No protest accompanied the payment of additional search fees.

InductEV, Inc.
Exhibit 1025
Page 461

INTERNATIONAL SEARCH REPORT

International application No
PCT/US2010/056240

C(Continuation). DOCUMENTS CONSIDERED TO BE RELEVANT

Category*	Citation of document, with indication, where appropriate, of the relevant passages	Relevant to claim No.
X	EP 0 903 830 A2 (NOKIA TECHNOLOGY GMBH [DE] SALCOMP OY [FI]) 24 March 1999 (1999-03-24) paragraph [0018] - paragraph [0029]; figure 1	3,4
X	US 2003/214821 A1 (GIANNOPOULOS DEMETRI [US] ET AL) 20 November 2003 (2003-11-20) paragraph [0012] - paragraph [0019]; paragraph [0029] - paragraph [0031];figures 1,5	3,4
X	US 6 633 155 B1 (LIANG HUI-PIN [TW]) 14 October 2003 (2003-10-14) column 2, line 24 - column 2, line 58; figure 2	3,4
X	US 2009/058189 A1 (COOK NIGEL P [US] ET AL) 5 March 2009 (2009-03-05) paragraph [0038]; paragraph [0010] - paragraph [0017]; figure 1	5-11
X,P	US 2009/286470 A1 (MOHAMMADIAN ALIREZA HORMOZ [US] ET AL) 19 November 2009 (2009-11-19) paragraph [0136] - paragraph [0145]; figures 17a,17b,18a,18b	5-11

InductEV, Inc.
Exhibit 1025
Page 462

INTERNATIONAL SEARCH REPORT

Information on patent family members

International application No
PCT/US2010/056240

Patent document cited in search report	Publication date	Patent family member(s)	Publication date
US 2009271048 A1	29-10-2009	JP 4544339 B2	15-09-2010
		JP 2009268311 A	12-11-2009
US 5701121 A	23-12-1997	NONE	
US 2009134712 A1	28-05-2009	CN 101911387 A	08-12-2010
		EP 2232636 A1	29-09-2010
		JP 2011505103 T	17-02-2011
		KR 20100090711 A	16-08-2010
		WO 2010036279 A1	01-04-2010
EP 0903830 A2	24-03-1999	AT 283567 T	15-12-2004
		DE 19836401 A1	17-02-2000
		US 6028413 A	22-02-2000
US 2003214821 A1	20-11-2003	AU 2003230103 A1	02-12-2003
		CN 1653670 A	10-08-2005
		EP 1506606 A1	16-02-2005
		WO 03098773 A1	27-11-2003
		JP 2005526474 T	02-09-2005
US 6633155 B1	14-10-2003	NONE	
US 2009058189 A1	05-03-2009	CN 101803224 A	11-08-2010
		EP 2186211 A2	19-05-2010
		JP 2010537496 T	02-12-2010
		KR 20100042292 A	23-04-2010
		US 2009170148 A1	02-07-2009
		WO 2009023646 A2	19-02-2009
US 2009286470 A1	19-11-2009	CN 102027683 A	20-04-2011
		CN 102027684 A	20-04-2011
		CN 102027685 A	20-04-2011
		CN 102027686 A	20-04-2011
		CN 102027687 A	20-04-2011
		CN 102027688 A	20-04-2011
		CN 102027689 A	20-04-2011
		CN 102027690 A	20-04-2011
		CN 102027691 A	20-04-2011
		EP 2294709 A2	16-03-2011
		EP 2294710 A2	16-03-2011
		EP 2294711 A1	16-03-2011
		EP 2294712 A1	16-03-2011
		EP 2294713 A1	16-03-2011
		EP 2294714 A2	16-03-2011
		EP 2286521 A1	23-02-2011
US 2009286470 A1		EP 2294715 A1	16-03-2011
		EP 2294708 A1	16-03-2011
		KR 20110014641 A	11-02-2011
		KR 20110014642 A	11-02-2011
		KR 20110010104 A	31-01-2011
		KR 20110009225 A	27-01-2011
		KR 20110010105 A	31-01-2011
		KR 20110009226 A	27-01-2011
		KR 20110009227 A	27-01-2011
		KR 20110009228 A	27-01-2011
		KR 20110009229 A	27-01-2011

INTERNATIONAL SEARCH REPORT

Information on patent family members

International application No
PCT/US2010/056240

Patent document cited in search report	Publication date	Patent family member(s)	Publication date
		US 2009284369 A1	19-11-2009
		US 2009286475 A1	19-11-2009
		US 2009286476 A1	19-11-2009
		US 2009284218 A1	19-11-2009
		US 2009284227 A1	19-11-2009
		US 2009284220 A1	19-11-2009
		US 2009284082 A1	19-11-2009
		US 2009284245 A1	19-11-2009
		WO 2009140216 A2	19-11-2009
		WO 2009140217 A2	19-11-2009
		WO 2009140218 A1	19-11-2009
		WO 2009140219 A1	19-11-2009
		WO 2010047850 A1	29-04-2010
		WO 2009140220 A1	19-11-2009
		WO 2009140221 A2	19-11-2009
		WO 2009140222 A1	19-11-2009
		WO 2009140223 A1	19-11-2009

Form PCT/ISA/210 (patent family annex) (April 2005)

FURTHER INFORMATION CONTINUED FROM PCT/ISA/ 210

This International Searching Authority found multiple (groups of) inventions in this international application, as follows:

1. claims: 1, 2

   The invention is directed to a wireless power transmission system using magnetic resonance power transmission to a plurality of tunable power receiver apparatuses. The invention furthermore tunes and detunes the resonant circuit of the power receiver devices to communicate with the wireless power supply.

   ---

2. claims: 3, 4

   The invention is directed to a battery charging circuit arranged to receive wireless power. The invention furthermore comprises a short term charge storage device where wirelessly transmitted power is stored before recharging the internal battery.

   ---

3. claims: 5-11

   The invention is directed to a wireless power transmission system using magnetic resonance power transmission to a plurality of tunable power receiver apparatuses. The invention furthermore creates a second coupling mode region in the near of a power receiver device to wirelessly deliver some of the wirelessly received power from the transmitter to a second power receiver device.

P80157.V01W01

PATENT COOPERATION TREATY

From the INTERNATIONAL SEARCHING AUTHORITY

To: JOHN NORTRUP
STRATEGIC PATENTS, P.C.
C/O CPA GLOBAL
P.O. BOX 52050
MINNEAPOLIS, MN 55402

PCT

NOTIFICATION OF TRANSMITTAL OF THE INTERNATIONAL SEARCH REPORT AND THE WRITTEN OPINION OF THE INTERNATIONAL SEARCHING AUTHORITY, OR THE DECLARATION

(PCT Rule 44.1)

Date of mailing *(day/month/year)* 05 JUL 2011	
Applicant's or agent's file reference WTCY0053PWO	**FOR FURTHER ACTION** See paragraphs 1 and 4 below
International application No. PCT/US2011/027868	International filing date *(day/month/year)* 10 March 2011
Applicant WITRICITY CORPORATION	

1. ☒ The applicant is hereby notified that the international search report and the written opinion of the International Searching Authority have been established and are transmitted herewith.

   Filing of amendments and statement under Article 19:
   The applicant is entitled, if he so wishes, to amend the claims of the international application (see Rule 46):

   When? The time limit for filing such amendments is normally two months from the date of transmittal of the international search report.

   Where? Directly to the International Bureau of WIPO, 34 chemin des Colombettes 1211 Geneva 20, Switzerland, Facsimile No.: +41 22 338 82 70

   For more detailed instructions, see *PCT Applicant's Guide*, International Phase, paragraphs 9.004 – 9.011.

2. ☐ The applicant is hereby notified that no international search report will be established and that the declaration under Article 17(2)(a) to that effect and the written opinion of the International Searching Authority are transmitted herewith.

3. ☐ **With regard to any protest** against payment of (an) additional fee(s) under Rule 40.2, the applicant is notified that:

   ☐ the protest together with the decision thereon has been transmitted to the International Bureau together with any request to forward the texts of both the protest and the decision thereon to the designated Offices.

   ☐ no decision has been made yet on the protest; the applicant will be notified as soon as a decision is made.

4. **Reminders**

   The applicant may submit comments on an informal basis on the written opinion of the International Searching Authority to the International Bureau. The International Bureau will send a copy of such comments to all designated Offices unless an international preliminary examination report has been or is to be established. Following the expiration of 30 months from the priority date, these comments will also be made available to the public.

   Shortly after the expiration of **18 months** from the priority date, the international application will be published by the International Bureau. If the applicant wishes to avoid or postpone publication, a notice of withdrawal of the international application, or of the priority claim, must reach the International Bureau before the completion of the technical preparations for international publication (Rules 90*bis*.1 and 90*bis*.3).

   Within **19 months** from the priority date, but only in respect of some designated Offices, a demand for international preliminary examination must be filed if the applicant wishes to postpone the entry into the national phase **until 30 months** from the priority date (in some Offices even later); otherwise, the applicant must, **within 20 months** from the priority date, perform the prescribed acts for entry into the national phase before those designated Offices.

   In respect of other designated Offices, the time limit of **30 months** (or later) will apply even if no demand is filed within 19 months.

   For details about the applicable time limits, Office by Office, see www.wipo.int/pct/en/texts/time_limits.html and the *PCT Applicant's Guide*, National Chapters.

Name and mailing address of the ISA/ Mail Stop PCT, Attn: ISA/US Commissioner for Patents P.O. Box 1450, Alexandria, Virginia 22313-1450	Authorized officer Blaine R. Copenheaver
Facsimile No. 571-273-3201	Telephone No. PCT Helpdesk: 571-272-4300 PCT OSP: 571-272-7774

Form PCT/ISA/220 (July 2010)



PATENT COOPERATION TREATY

From the INTERNATIONAL SEARCHING AUTHORITY

To: JOHN NORTRUP
STRATEGIC PATENTS, P.C.
C/O CPA GLOBAL
P.O. BOX 52050
MINNEAPOLIS, MN 55402

PCT

NOTIFICATION OF TRANSMITTAL OF THE INTERNATIONAL SEARCH REPORT AND THE WRITTEN OPINION OF THE INTERNATIONAL SEARCHING AUTHORITY, OR THE DECLARATION

(PCT Rule 44.1)

	Date of mailing *(day/month/year)* 05 JUL 2011
Applicant's or agent's file reference WTCY0053PWO	**FOR FURTHER ACTION** See paragraphs 1 and 4 below
International application No. PCT/US2011/027868	International filing date *(day/month/year)* 10 March 2011
Applicant WITRICITY CORPORATION	

1. ☒ The applicant is hereby notified that the international search report and the written opinion of the International Searching Authority have been established and are transmitted herewith.

   Filing of amendments and statement under Article 19:
   The applicant is entitled, if he so wishes, to amend the claims of the international application (see Rule 46):

   When? The time limit for filing such amendments is normally two months from the date of transmittal of the international search report.

   Where? Directly to the International Bureau of WIPO, 34 chemin des Colombettes 1211 Geneva 20, Switzerland, Facsimile No.: +41 22 338 82 70

   For more detailed instructions, see *PCT Applicant's Guide*, International Phase, paragraphs 9.004 – 9.011.

2. ☐ The applicant is hereby notified that no international search report will be established and that the declaration under Article 17(2)(a) to that effect and the written opinion of the International Searching Authority are transmitted herewith.

3. ☐ **With regard to any protest** against payment of (an) additional fee(s) under Rule 40.2, the applicant is notified that:

   ☐ the protest together with the decision thereon has been transmitted to the International Bureau together with any request to forward the texts of both the protest and the decision thereon to the designated Offices.

   ☐ no decision has been made yet on the protest; the applicant will be notified as soon as a decision is made.

4. **Reminders**

   The applicant may submit comments on an informal basis on the written opinion of the International Searching Authority to the International Bureau. The International Bureau will send a copy of such comments to all designated Offices unless an international preliminary examination report has been or is to be established. Following the expiration of 30 months from the priority date, these comments will also be made available to the public.

   Shortly after the expiration of **18 months** from the priority date, the international application will be published by the International Bureau. If the applicant wishes to avoid or postpone publication, a notice of withdrawal of the international application, or of the priority claim, must reach the International Bureau before the completion of the technical preparations for international publication (Rules 90*bis*.1 and 90*bis*.3).

   Within **19 months** from the priority date, but only in respect of some designated Offices, a demand for international preliminary examination must be filed if the applicant wishes to postpone the entry into the national phase **until 30 months** from the priority date (in some Offices even later); otherwise, the applicant must, **within 20 months** from the priority date, perform the prescribed acts for entry into the national phase before those designated Offices.

   In respect of other designated Offices, the time limit of **30 months** (or later) will apply even if no demand is filed within 19 months.

   For details about the applicable time limits, Office by Office, see www.wipo.int/pct/en/texts/time_limits.html and the *PCT Applicant's Guide*, National Chapters.

Name and mailing address of the ISA/ Mail Stop PCT, Attn: ISA/US Commissioner for Patents P.O. Box 1450, Alexandria, Virginia 22313-1450	Authorized officer Blaine R. Copenheaver PCT Helpdesk: 571-272-4300
Facsimile No. 571-273-3201	Telephone No. PCT OSP: 571-272-7774

Form PCT/ISA/220 (July 2010)

PATENT COOPERATION TREATY

PCT

INTERNATIONAL SEARCH REPORT

(PCT Article 18 and Rules 43 and 44)

Applicant's or agent's file reference WTCY0053PWO	**FOR FURTHER ACTION**	see Form PCT/ISA/220 as well as, where applicable, item 5 below.
International application No. PCT/US2011/027868	International filing date *(day/month/year)* 10 March 2011	(Earliest) Priority Date *(day/month/year)* 10 March 2010
Applicant WITRICITY CORPORATION		

This international search report has been prepared by this International Searching Authority and is transmitted to the applicant according to Article 18. A copy is being transmitted to the International Bureau.

This international search report consists of a total of 2 sheets.

☐ It is also accompanied by a copy of each prior art document cited in this report.

1. **Basis of the report**

a. With regard to the **language**, the international search was carried out on the basis of:

☒ the international application in the language in which it was filed.

☐ a translation of the international application into _____ which is the language of a translation furnished for the purposes of international search (Rules 12.3(a) and 23.1(b)).

b. ☐ This international search report has been established taking into account the **rectification of an obvious mistake** authorized by or notified to this Authority under Rule 91 (Rule 43.6*bis*(a)).

c. ☐ With regard to any **nucleotide and/or amino acid sequence** disclosed in the international application, see Box No. I.

2. ☐ **Certain claims were found unsearchable** (see Box No. II).

3. ☐ **Unity of invention is lacking** (see Box No. III).

4. With regard to the **title,**

☒ the text is approved as submitted by the applicant.

☐ the text has been established by this Authority to read as follows:

5. With regard to the **abstract,**

☒ the text is approved as submitted by the applicant.

☐ the text has been established, according to Rule 38.2, by this Authority as it appears in Box No. IV. The applicant may, within one month from the date of mailing of this international search report, submit comments to this Authority.

6. With regard to the **drawings,**

a. the figure of the **drawings** to be published with the abstract is Figure No. 1

☒ as suggested by the applicant.

☐ as selected by this Authority, because the applicant failed to suggest a figure.

☐ as selected by this Authority, because this figure better characterizes the invention.

b. ☐ none of the figures is to be published with the abstract.

InductEV, Inc.
Exhibit 1025
Page 468

INTERNATIONAL SEARCH REPORT

International application No.
PCT/US2011/027868

A. CLASSIFICATION OF SUBJECT MATTER
IPC(8) - H04B 5/00 (2011.01)
USPC - 307/104
According to International Patent Classification (IPC) or to both national classification and IPC

B. FIELDS SEARCHED

Minimum documentation searched (classification system followed by classification symbols)
IPC(8) - H04B 5/00; H01F 38/00; H02J 17/00; H01P 7/00, 7/06 (2011.01)
USPC - 307/104, 333/219, 230; 455/41.1

Documentation searched other than minimum documentation to the extent that such documents are included in the fields searched

Electronic data base consulted during the international search (name of data base and, where practicable, search terms used)
MicroPatent, Questel Orbit, USPTO EAST System (US-PGPUB; USPAT; USOCR; EPO; JPO; DERWENT), Google Patent

C. DOCUMENTS CONSIDERED TO BE RELEVANT

Category*	Citation of document, with indication, where appropriate, of the relevant passages	Relevant to claim No.
X -- Y	US 2009/0085408 A1 (BRUHN) 02 April 2009 (02.04.2009) entire document	1-4, 11-12, 14-15, 17 ---- 5-10, 13, 16, 18-19
Y	US 2009/0243397 A1 (COOK et al) 01 October 2009 (01.10.2009) entire document	5, 8-10, 16, 18
Y	US 2007/0021140 A1 (KEYES, IV et al) 25 January 2007 (25.01.2007) entire document	6-7
Y	US 2008/0266748 A1 (LEE) 30 October 2008 (30.10.2008) entire document	13, 19
A	US 2008/0036588 A1 (IVERSON et al) 14 February 2008 (14.02.2008) entire document	20-25
A	US 6,664,770 B1 (BARTELS) 16 December 2003 (16.12.2003) entire document	1-25
A	US 2004/0000974 A1 (ODENAAL et al) 01 January 2004 (01.01.2004) entire document	1-25

☐ Further documents are listed in the continuation of Box C. ☐

* Special categories of cited documents:
"A" document defining the general state of the art which is not considered to be of particular relevance
"E" earlier application or patent but published on or after the international filing date
"L" document which may throw doubts on priority claim(s) or which is cited to establish the publication date of another citation or other special reason (as specified)
"O" document referring to an oral disclosure, use, exhibition or other means
"P" document published prior to the international filing date but later than the priority date claimed
"T" later document published after the international filing date or priority date and not in conflict with the application but cited to understand the principle or theory underlying the invention
"X" document of particular relevance; the claimed invention cannot be considered novel or cannot be considered to involve an inventive step when the document is taken alone
"Y" document of particular relevance; the claimed invention cannot be considered to involve an inventive step when the document is combined with one or more other such documents, such combination being obvious to a person skilled in the art
"&" document member of the same patent family

Date of the actual completion of the international search	Date of mailing of the international search report
27 June 2011	05 JUL 2011
Name and mailing address of the ISA/US Mail Stop PCT, Attn: ISA/US, Commissioner for Patents P.O. Box 1450, Alexandria, Virginia 22313-1450 Facsimile No. 571-273-3201	Authorized officer: Blaine R. Copenheaver PCT Helpdesk: 571-272-4300 PCT OSP: 571-272-7774

Form PCT/ISA/210 (second sheet) (July 2009)

PATENT COOPERATION TREATY

From the
INTERNATIONAL SEARCHING AUTHORITY

To: JOHN NORTRUP
STRATEGIC PATENTS, P.C.
C/O CPA GLOBAL
P.O. BOX 52050
MINNEAPOLIS, MN 55402

PCT

WRITTEN OPINION OF THE
INTERNATIONAL SEARCHING AUTHORITY

(PCT Rule 43*bis*.1)

Date of mailing *(day/month/year)*	05 JUL 2011
Applicant's or agent's file reference: WTCY0053PWO	**FOR FURTHER ACTION** See paragraph 2 below

International application No.	International filing date *(day/month/year)*	Priority date *(day/month/year)*
PCT/US2011/027868	10 March 2011	10 March 2010

International Patent Classification (IPC) or both national classification and IPC
IPC(8) - H04B 5/00 (2011.01)
USPC - 307/104

Applicant WITRICITY CORPORATION

1. This opinion contains indications relating to the following items:

- ☒ Box No. I Basis of the opinion
- ☐ Box No. II Priority
- ☐ Box No. III Non-establishment of opinion with regard to novelty, inventive step and industrial applicability
- ☐ Box No. IV Lack of unity of invention
- ☒ Box No. V Reasoned statement under Rule 43*bis*.1(a)(i) with regard to novelty, inventive step or industrial applicability; citations and explanations supporting such statement
- ☐ Box No. VI Certain documents cited
- ☐ Box No. VII Certain defects in the international application
- ☐ Box No. VIII Certain observations on the international application

2. **FURTHER ACTION**

If a demand for international preliminary examination is made, this opinion will be considered to be a written opinion of the International Preliminary Examining Authority ("IPEA") except that this does not apply where the applicant chooses an Authority other than this one to be the IPEA and the chosen IPEA has notified the International Bureau under Rule 66.1*bis*(b) that written opinions of this International Searching Authority will not be so considered.

If this opinion is, as provided above, considered to be a written opinion of the IPEA, the applicant is invited to submit to the IPEA a written reply together, where appropriate, with amendments, before the expiration of 3 months from the date of mailing of Form PCT/ISA/220 or before the expiration of 22 months from the priority date, whichever expires later.

For further options, see Form PCT/ISA/220.

3. For further details, see notes to Form PCT/ISA/220.

Name and mailing address of the ISA/US	Date of completion of this opinion	Authorized officer:
Mail Stop PCT, Attn: ISA/US Commissioner for Patents P.O. Box 1450, Alexandria, Virginia 22313-1450 Facsimile No. 571-273-3201	27 June 2011	Blaine R. Copenheaver PCT Helpdesk: 571-272-4300 PCT OSP: 571-272-7774

Form PCT/ISA/237 (cover sheet) (July 2009)

WRITTEN OPINION OF THE INTERNATIONAL SEARCHING AUTHORITY

International application No.
PCT/US2011/027868

Box No. I Basis of this opinion

1. With regard to the **language**, this opinion has been established on the basis of:

   ☒ the international application in the language in which it was filed.

   ☐ a translation of the international application into _____ which is the language of a translation furnished for the purposes of international search (Rules 12.3(a) and 23.1(b)).

2. ☐ This opinion has been established taking into account the **rectification of an obvious mistake** authorized by or notified to this Authority under Rule 91 (Rule 43*bis*.1(a))

3. With regard to any **nucleotide and/or amino acid sequence** disclosed in the international application, this opinion has been established on the basis of a sequence listing filed or furnished:

   a. (means)

      ☐ on paper

      ☐ in electronic form

   b. (time)

      ☐ in the international application as filed

      ☐ together with the international application in electronic form

      ☐ subsequently to this Authority for the purposes of search

4. ☐ In addition, in the case that more than one version or copy of a sequence listing has been filed or furnished, the required statements that the information in the subsequent or additional copies is identical to that in the application as filed or does not go beyond the application as filed, as appropriate, were furnished.

5. Additional comments:

InductEV, Inc.
Exhibit 1025
Page 471

WRITTEN OPINION OF THE INTERNATIONAL SEARCHING AUTHORITY

International application No.
PCT/US2011/027868

Box No. V **Reasoned statement under Rule 43*bis*.1(a)(i) with regard to novelty, inventive step or industrial applicability; citations and explanations supporting such statement**

1. Statement

Novelty (N)	Claims	3, 5-10, 13, 16, 18-19	YES
	Claims	1-2, 4, 11-12, 14-15, 17	NO
Inventive step (IS)	Claims	20-25	YES
	Claims	1-19	NO
Industrial applicability (IA)	Claims	1-25	YES
	Claims	None	NO

2. Citations and explanations:

Claims 1-2, 4, 11-12, 14-15, 17 lack novelty under PCT Article 33(2) as being anticipated by Bruhn.

Regarding claim 1, Bruhn discloses a wireless power converter (apparatus for wireless energy transmission, para 0017, Fig. 9) comprising at least one receiving magnetic resonator 130, 132 configured to capture electrical energy received wirelessly (resonator is "electrically isolated", i.e. galvanically isolated from the primary and secondary circuits, Fig. 9, para 0034) through a first oscillating magnetic field (developed by generator 16 and primary winding 18, Fig. 9, para 0034) characterized by a first plurality of parameters (operating at the fundamental frequency, para 0017, 0031, Fig. 9); and at least one transferring magnetic resonator 126, 128 (Fig. 9) configured to generate (through resonance, para 0017-0018, Fig. 9) a second oscillating magnetic field (transferred to the secondary winding 20, para 0017-0018, 0031, Fig. 9) characterized by a second plurality of parameters different from the first plurality of parameters (different at least for operating at the second harmonic or other multiple of the fundamental frequency, para 0017-0018), wherein the electrical energy from the at least one receiving magnetic resonator 130, 132 is used to energize the at least one transferring magnetic resonator 126, 128 (Fig. 9) to generate the second oscillating magnetic field (energy coupling is present between the first and second magnetic resonators when they are arranged in the near field, as they are here: the free-space wavelength at even the 60th harmonic of the shortest wavelength contemplated (at 5 MHz) would be 1 meter, such that the spacing here would be understood to be "sub-wavelength" or "near-field", para 0018, Fig. 9).

Regarding claim 2, Bruhn discloses wherein the first plurality of parameters includes a first frequency (operating at the fundamental frequency, para 0017, 0031, Fig. 9) different from a second frequency of the second plurality of parameters (different at least for operating at the second harmonic or other multiple of the fundamental frequency, para 0017-0018).

Regarding claim 4, Bruhn discloses wherein the second frequency is approximately an integer multiple of the first frequency (second resonator has twice the resonant frequency of first resonator, para 0018).

Regarding claim 11, Bruhn discloses wherein the at least one receiving magnetic resonator 130, 132 is configurable to capture energy from magnetic fields with different parameters (resonator 130 can receive energies with different frequencies, para 0017-0018, 0040, Fig. 9).

Regarding claim 12, Bruhn discloses wherein the at least one transferring magnetic resonator 126, 128 is configurable to generate magnetic fields with different parameters (resonator 126 can generate and transmit energy with different frequencies, para 0017-0018, 0040, Fig. 9).

Regarding claim 14, Bruhn discloses a system (para 0017, 0043) comprising a source resonator 126, 128 configured to generate a first oscillating magnetic field (transferred to the secondary winding 20, para 0017-0018, 0031, Fig. 9) characterized by a first plurality of parameters (operating at the fundamental frequency, para 0017, 0031, Fig. 9); a device resonator 130, 132 configured to capture electrical energy received wirelessly (resonator is "electrically isolated", i.e. galvanically isolated from the primary and secondary circuits, Fig. 9, para 0034) through a second oscillating magnetic field (developed by generator 16 and primary winding 18, Fig. 9, para 0034) characterized by a second plurality of parameters different from the first plurality of parameters (different at least for operating at the second harmonic or other multiple of the fundamental frequency, para 0017-0018); and a wireless power converter (apparatus for wireless energy transmission, para 0017, Fig. 9) including conversion circuitry (circuits as seen in Fig. 9) configured to capture energy from the second oscillating magnetic field (developed by generator 16 and primary winding 18, Fig. 9, para 0034) and to energize the source resonator 126, 128 to generate the first oscillating magnetic field (transferred to the secondary winding 20, energy coupling is present between the first and second magnetic resonators when they are arranged in the near field, as they are here: the free-space wavelength at even the 60th harmonic of the shortest wavelength contemplated (at 5 MHz) would be 1 meter, such that the spacing here would be understood to be "sub-wavelength" or "near-field", para 0017-0018, 0031, Fig. 9).

Regarding claim 15, Bruhn discloses wherein the first plurality of parameters (operating at the fundamental frequency, para 0017, 0031, Fig. 9) and the second plurality of parameters are different in at least a frequency (different at least for operating at the second harmonic or other multiple of the fundamental frequency, para 0017-0018).

InductEV, Inc.
Exhibit 1025
Page 472

WRITTEN OPINION OF THE INTERNATIONAL SEARCHING AUTHORITY

International application No.
PCT/US2011/027868

Supplemental Box

In case **the space in any of the preceding boxes is not sufficient.**
Continuation of:

Regarding claim 17, Bruhn discloses wherein the wireless power converter (apparatus for wireless energy transmission, para 0017, Fig. 9) is powered by electrical energy captured by the device resonator 130, 132 (transferred to the secondary winding 20, energy coupling is present between the first and second magnetic resonators when they are arranged in the near field, as they are here: the free-space wavelength at even the 60th harmonic of the shortest wavelength contemplated (at 5 MHz) would be 1 meter, such that the spacing here would be understood to be "sub-wavelength" or "near-field", para 0017-0018, 0031, Fig. 9).

Claim 3 lacks an inventive step under PCT Article 33(3) as being obvious over Bruhn.

Regarding claim 3, Bruhn discloses the invention above, the invention above, and discloses a first frequency (operating at the fundamental frequency, para 0017, 0031, Fig. 9) and a second frequency (different at least for operating at the second harmonic or other multiple of the fundamental frequency, para 0017-0018), but does not disclose wherein the first frequency is approximately an integer multiple of the second frequency. It would have been obvious to one of ordinary skill in the art at the time of the invention to provide a first frequency that is approximately an integer multiple of the second frequency, in order to provide a system that can handle different power levels for providing wireless energy to multiple devices, and because discovering the optimal value of a result effective variable involves only routine skill in the art.

Claims 5, 8-10, 16, 18 lack an inventive step under PCT Article 33(3) as being obvious over Bruhn in view of Cook et al. (hereinafter referred to as Cook).

Regarding claim 5, Bruhn discloses the invention above, but does not specifically disclose wherein the first plurality of parameters includes a first magnitude different from a second magnitude of the second plurality of parameters. Cook is in the field of wireless power systems (para 0044) and teaches wherein the first plurality of parameters includes a first magnitude different from a second magnitude of the second plurality of parameters (transmit power converter unit converts the supply voltage and frequency, such as 110V/60Hz, into another voltage [different voltage] and into another frequency, such as under 50Hz, that is more appropriate for wireless transmission, para 0155-0158). It would have been obvious to one of ordinary skill in the art at the time of the invention to combine the different magnitudes as taught in Cook with the invention of Bruhn in order to provide an efficient power transfer system to charge electronic devices (see Cook, para 0017, 0042).

Regarding claim 8, Bruhn discloses the invention above, and further discloses electrical energy captured by the at least one receiving magnetic resonator 130 (resonator 130 captures energy developed by generator 16 and primary winding 18, Fig. 9, para 0034), but does not specifically disclose a first converter circuit configured to convert the electrical energy into a direct current signal. Cook teaches a first converter circuit 1550 configured to convert the electrical energy into a direct current signal (a DC/DC or DC/AC converter 1550 converts the electrical energy received by resonator antenna into direct current, para 0194-0195, Fig. 15). It would have been obvious to one of ordinary skill in the art at the time of the invention to combine the direct current conversion as taught in Cook with the invention of Bruhn in order to provide an efficient power transfer system to charge electronic devices (see Cook, para 0017, 0042).

Regarding claim 9, Bruhn discloses the invention above, and further discloses wherein the alternating current signal (power source 16^ provides AC current signal, Fig. 9, para 0040) is used to energize the at least one transferring magnetic resonator 126, 128 (energy coupling is present between the first and second magnetic resonators when they are arranged in the near field, as they are here: the free-space wavelength at even the 60th harmonic of the shortest wavelength contemplated (at 5 MHz) would be 1 meter, such that the spacing here would be understood to be "sub-wavelength" or "near-field", para 0018, Fig. 9), but does not disclose a second converter circuit configured to convert the direct current signal from the first converter circuit into an alternating current signal. Cook teaches a second converter circuit (two converter circuits for converting current signals, para 0194-0195, as shown in Fig. 15) configured to convert the direct current signal from the first converter circuit into an alternating current signal (a DC/DC or DC/AC converter 1550 can convert the electrical energy received by resonator antenna into alternating current, para 0194-0195, Fig. 15). It would have been obvious to one of ordinary skill in the art at the time of the invention to combine the direct current conversion as taught in Cook with the invention of Bruhn in order to provide an efficient power transfer system to charge electronic devices (see Cook, para 0017, 0042).

Regarding claim 10, Bruhn discloses the invention above, and further discloses at least one receiving magnetic resonator 130, 132 (resonator is "electrically isolated", i.e. galvanically isolated from the primary and secondary circuits, Fig. 9, para 0034) and at least one transferring magnetic resonator 126, 128 (Fig. 9), but does not disclose wherein at least one of the resonators has a quality factor Q>100. Cook teaches a resonator with a quality factor Q>100 (magnetic resonant antennas used in system must provide a Q-factor as high as possible, and can provide Q-factors up to 300, para 0060-0061). It would have been obvious to one of ordinary skill in the art at the time of the invention to combine the high quality factor resonator as taught in Cook with the invention of Bruhn in order to provide a very efficient wireless power transmission system with minimal power losses (see Cook, para 0047).

Regarding claim 16, Bruhn discloses the invention above, but does not specifically disclose wherein the first plurality of parameters and the second plurality of parameters of the oscillating magnetic fields are different in at least a magnitude. Cook teaches wherein the first plurality of parameters and the second plurality of parameters of the oscillating magnetic fields are different in at least a magnitude (transmit power converter unit converts the supply voltage and frequency, such as 110V/60Hz, into another voltage [different voltage] and into another frequency, such as under 50Hz, that is more appropriate for wireless transmission, para 0155-0158). It would have been obvious to one of ordinary skill in the art at the time of the invention to combine the different magnitudes as taught in Cook with the invention of Bruhn in order to provide an efficient power transfer system to charge electronic devices (see Cook, para 0017, 0042).

Supplemental Box

In case the space in any of the preceding boxes is not sufficient.
Continuation of:

Regarding claim 18, Bruhn discloses the invention above, and further discloses the source resonator 126, 128 and the device resonator 130, 132 (Fig. 9), but does not disclose wherein at least one of the resonators has a quality factor Q>100. Cook teaches a resonator with a quality factor Q>100 (magnetic resonant antennas used in system must provide a Q-factor as high as possible, and can provide Q-factors up to 300, para 0060-0061). It would have been obvious to one of ordinary skill in the art at the time of the invention to combine the high quality factor resonator as taught in Cook with the invention of Bruhn in order to provide a very efficient wireless power transmission system with minimal power losses (see Cook, para 0047).

Claims 6-7 lack an inventive step under PCT Article 33(3) as being obvious over Bruhn in view of Keyes, IV et al. (hereinafter referred to as Keyes).

Regarding claim 6, Bruhn discloses the invention above, and discloses wherein the first plurality of parameters includes a first frequency (operating at the fundamental frequency, para 0017, 0031, Fig. 9) different from a second frequency of the second plurality of parameters (different at least for operating at the second harmonic or other multiple of the fundamental frequency, para 0017-0018), but does not disclose a frequency hopping sequence. Keyes is in the field of wireless energy transfer systems (para 0008-0009, Fig. 43), and teaches a frequency hopping sequence (power transmitted wirelessly using frequency hopping technique, para 0056-0058). It would have been obvious to one of ordinary skill in the art at the time of the invention to combine the frequency hopping sequence as taught in Keyes with the invention of Bruhn in order to avoid wireless interference (see Keyes, para 0056).

Regarding claim 7, Bruhn discloses the invention above, and discloses wherein the first plurality of parameters (operating at the fundamental frequency, para 0017, 0031, Fig. 9) includes a sequence different from a second sequence of the second plurality of parameters (different at least for operating at the second harmonic or other multiple of the fundamental frequency, para 0017-0018), but does not disclose an on/off sequence. Keyes teaches an on/off sequence (wireless reception of on or off control commands for wireless base units, para 0094). It would have been obvious to one of ordinary skill in the art at the time of the invention to combine the on/off sequence as taught in Keyes with the invention of Bruhn in order to provide a method of wirelessly powering devices on and off (see Keyes, para 0007-0008).

Claims 13, 19 lack an inventive step under PCT Article 33(3) as being obvious over Bruhn in view of Lee.

Regarding claim 13, Bruhn discloses the invention above, and discloses a loop inductor 130 (Fig. 9), but does not disclose wherein the at least one receiving magnetic resonator and the at least one transferring resonator share a loop inductor. Lee is in the field of wireless power converters (para 0001) and teaches wherein the at least one receiving magnetic resonator and the at least one transferring resonator share a loop inductor (transmitter and receiver are combined, para 0048, and constructed by winding transmission coil outputting power generated from electromagnetic wave generating source, para 0051, Fig. 10). It would have been obvious to one of ordinary skill in the art at the time of the invention to combine the shared loop as taught in Lee with the invention of Bruhn to provide a more efficient wireless power system for transferring power by maximizing generation and reception of electromagnetic waves in the resonance circuit (see Lee, para 0051).

Regarding claim 19, Bruhn discloses the invention above, and discloses a loop inductor 130 (Fig. 9), but does not disclose wherein the source resonator and the device resonator include a shared loop inductor. Lee teaches wherein the at least one receiving magnetic resonator and the at least one transferring resonator share a loop inductor (transmitter and receiver are combined, para 0048, and constructed by winding transmission coil outputting power generated from electromagnetic wave generating source, para 0051, Fig. 10). It would have been obvious to one of ordinary skill in the art at the time of the invention to combine the shared loop as taught in Lee with the invention of Bruhn to provide a more efficient wireless power system for transferring power by maximizing generation and reception of electromagnetic waves in the resonance circuit (see Lee, para 0051).

Claims 20-25 meet the criteria set out in PCT Article 33(2)-(3), because the prior art does not teach or fairly suggest:

Regarding claim 20, a method of wireless power conversion comprising: providing a configurable magnetic resonator; tuning the configurable magnetic resonator to capture a first oscillating magnetic field characterized by a first plurality of parameters; converting the oscillating magnetic field into electrical energy; storing the electrical energy as stored energy in an energy storage element; tuning the configurable magnetic resonator to generate a second oscillating magnetic field characterized by a second plurality of parameters; and energizing the configurable magnetic resonator using the stored energy to produce the second oscillating magnetic field.

Claims 21-25 meet the criteria due to their dependence on novel claim 20.

The prior art, as shown below, details some aspects of the invention, however, none of the prior art teaches all the missing limitations either alone or in combination as specified.

InductEV, Inc.
Exhibit 1025
Page 474

WRITTEN OPINION OF THE INTERNATIONAL SEARCHING AUTHORITY

International application No.
PCT/US2011/027868

Supplemental Box

In case **the space in any of the preceding boxes is not sufficient.**
Continuation of:

Bruhn (US 2009/0085408 A1) teaches a method of wireless power conversion (method for wireless energy transmission, para 0017, Fig. 9) comprising providing a configurable magnetic resonator 130, 132 (resonators can be configured for different frequencies, para 0017, Fig. 9); tuning the configurable magnetic resonator 130, 132 to capture (resonator is "electrically isolated", i.e. galvanically isolated from the primary and secondary circuits, Fig. 9, para 0034) a first oscillating magnetic field (developed by generator 16 and primary winding 18, Fig. 9, para 0034) characterized by a first plurality of parameters (operating at the fundamental frequency, para 0017, 0031, Fig. 9); converting the oscillating magnetic field into electrical energy (magnetic field converted induces voltage to provide current flow, para 0005, 0017-0018); tuning a [different, second] configurable magnetic resonator 126, 128 (Fig. 9) to generate (through resonance, para 0017-0018, Fig. 9) a second oscillating magnetic field (transferred to the secondary winding 20, para 0017-0018, 0031, Fig. 9) characterized by a second plurality of parameters (different at least for operating at the second harmonic or other multiple of the fundamental frequency, para 0017-0018); and energizing the [different, second] configurable magnetic resonator to produce the second oscillating magnetic field (energy coupling is present between the first and second magnetic resonators when they are arranged in the near field, as they are here: the free-space wavelength at even the 60th harmonic of the shortest wavelength contemplated (at 5 MHz) would be 1 meter, such that the spacing here would be understood to be "sub-wavelength" or "near-field", para 0018, Fig. 9), but does not disclose tuning a magnetic resonator to capture energy, storing the energy, and then tuning the same magnetic resonator to generate energy using the stored energy to wirelessly transfer power.

Cook (US 2009/0243397 A1) teaches a method (para 0249) of wireless power conversion (wireless power system including power converter, para 0153-0158, Fig. 13, Fig. 15) comprising providing a configurable magnetic resonator (resonant magnetic antenna is adjustable to provide different operational parameters and configurations, para 0143-0144, 0210); tuning the configurable magnetic resonator (resonator receives tuning through tuning network, para 0194, Fig. 15) to capture a first oscillating magnetic field (receive antenna unit is a resonant magnetic antenna for receiving energy in form of magnetic field, para 0143-0144, 0191, Fig. 15) characterized by a first plurality of parameters (energy is in form of magnetic field which is oscillating or resonating and characterized by parameters such as frequency, para 0143-0144, 0157); converting the oscillating magnetic field into electrical energy (power converter receives energy in form of magnetic field and converts to DC current to be used by devices, para 0129, 0143-0144); tuning a [different, second] configurable magnetic resonator (resonator receives tuning through tuning network, para 0175, Fig. 13) to generate a second oscillating magnetic field characterized by a second plurality of parameters (energy transmitted is in form of magnetic field and is characterized by parameters such as frequency, para 0143-0144, 0156); and energizing the [different, second] configurable magnetic resonator using the stored energy to produce the second oscillating magnetic field (wireless energy transfer system relays energy from the energy receiver which receives power source supply and sends it to the energy receiver which powers the device, para 0129, 0143-0144), but does not disclose tuning a magnetic resonator to capture energy, storing the energy, and then tuning the same magnetic resonator to generate energy using the stored energy to wirelessly transfer power.

Iverson (US 2008/0036588 A1) teaches storing the electrical energy as stored energy in an energy storage element 302 (energy harvesting unit 302 stores the energy electromagnetically received by antenna coil 106 from master antenna coil 104, para 0005, 0019, Fig. 3), and using the stored energy (stored energy is used to power remote unit 306 and to transmit message wirelessly through antenna 106, para 0005, 0019, Fig. 3), but does not disclose tuning a magnetic resonator to capture energy, storing the energy, and then tuning the same magnetic resonator to generate energy using the stored energy to wirelessly transfer power.

Claims 1-25 meet the criteria set out in PCT Article 33(4), and thus have industrial applicability because the subject matter claimed can be made or used in industry.

Electronic Patent Application Fee Transmittal

Application Number:	12639963
Filing Date:	16-Dec-2009
Title of Invention:	WIRELESS ENERGY TRANSFER WITH HIGH-Q TO MORE THAN ONE DEVICE
First Named Inventor/Applicant Name:	John D. Joannopoulos
Filer:	Marc M. Wefers/Cheryl Forrest
Attorney Docket Number:	01997-0359009

Filed as Large Entity

Utility under 35 USC 111(a) Filing Fees

Description	Fee Code	Quantity	Amount	Sub-Total in USD($)
Basic Filing:				
Pages:				
Claims:				
Claims in excess of 20	1202	28	60	1680
Miscellaneous-Filing:				
Petition:				
Patent-Appeals-and-Interference:				
Post-Allowance-and-Post-Issuance:				
Extension-of-Time:				

Description	Fee Code	Quantity	Amount	Sub-Total in USD($)
Miscellaneous:				
Submission- Information Disclosure Stmt	1806	1	180	180
Statutory or terminal disclaimer	1814	1	160	160
		Total in USD ($)		**2020**

Electronic Acknowledgement Receipt

EFS ID:	11473504
Application Number:	12639963
International Application Number:	
Confirmation Number:	7811
Title of Invention:	WIRELESS ENERGY TRANSFER WITH HIGH-Q TO MORE THAN ONE DEVICE
First Named Inventor/Applicant Name:	John D. Joannopoulos
Customer Number:	26161
Filer:	Marc M. Wefers/Cheryl Forrest
Filer Authorized By:	Marc M. Wefers
Attorney Docket Number:	01997-0359009
Receipt Date:	23-NOV-2011
Filing Date:	16-DEC-2009
Time Stamp:	11:47:47
Application Type:	Utility under 35 USC 111(a)

Payment information:

Submitted with Payment	yes
Payment Type	Deposit Account
Payment was successfully received in RAM	$2020
RAM confirmation Number	9808
Deposit Account	061050
Authorized User	

File Listing:

Document Number	Document Description	File Name	File Size(Bytes)/ Message Digest	Multi Part /.zip	Pages (if appl.)

1		IDS.pdf	152481 9bc14dca4e9eb8f3f4402b7f6ca1709d1674e259	yes	3
	Multipart Description/PDF files in .zip description				
	Document Description		Start	End	
	Transmittal Letter		1	1	
	Information Disclosure Statement (IDS) Form (SB08)		2	3	
Warnings:					
Information:					
2	Terminal Disclaimer Filed	TermDisc.pdf	55079 7e4695dd7afedcd5a98e5a9f5970308f868cb7e84	no	2
Warnings:					
Information:					
3		Reply.pdf	82956 3fc49b7b9d5074c20c30e29982a8fc30ab9c7bc2	yes	8
	Multipart Description/PDF files in .zip description				
	Document Description		Start	End	
	Amendment/Req. Reconsideration-After Non-Final Reject		1	1	
	Claims		2	7	
	Applicant Arguments/Remarks Made in an Amendment		8	8	
Warnings:					
Information:					
4	Foreign Reference	Art1.pdf	1353597 a6e51da4660f2e07a9cbfd803c52d16444c628a	no	36
Warnings:					
Information:					
5	Non Patent Literature	NPL1.pdf	120017 7cc0a22a5c3149f376a911bb186ef90869d1f72c6f	no	3
Warnings:					
Information:					
6	Non Patent Literature	NPL2.pdf	495064 6d0c5eb5052be2a3167ca1365cf7d8807f1860	no	6
Warnings:					

Information:					
7	Non Patent Literature	NPL3.pdf	2636887 ebbafc12e22fcf1fe4bd84656daa0ff8f1177...268	no	15
Warnings:					
Information:					
8	Non Patent Literature	NPL4.pdf	12318505 0974348632240c412b243b9907a8aa16914...0acac	no	247
Warnings:					
Information:					
9	Non Patent Literature	NPL5.pdf	669587 98b68a462217df3b8216be4d6088d5550a3...fccf0	no	10
Warnings:					
Information:					
10	Fee Worksheet (SB06)	fee-info.pdf	33665 ea8804ab815a974f8feb91f6aa94e0116ca61...0328	no	2
Warnings:					
Information:					
		Total Files Size (in bytes):	17917838		

This Acknowledgement Receipt evidences receipt on the noted date by the USPTO of the indicated documents, characterized by the applicant, and including page counts, where applicable. It serves as evidence of receipt similar to a Post Card, as described in MPEP 503.

New Applications Under 35 U.S.C. 111
If a new application is being filed and the application includes the necessary components for a filing date (see 37 CFR 1.53(b)-(d) and MPEP 506), a Filing Receipt (37 CFR 1.54) will be issued in due course and the date shown on this Acknowledgement Receipt will establish the filing date of the application.

National Stage of an International Application under 35 U.S.C. 371
If a timely submission to enter the national stage of an international application is compliant with the conditions of 35 U.S.C. 371 and other applicable requirements a Form PCT/DO/EO/903 indicating acceptance of the application as a national stage submission under 35 U.S.C. 371 will be issued in addition to the Filing Receipt, in due course.

New International Application Filed with the USPTO as a Receiving Office
If a new international application is being filed and the international application includes the necessary components for an international filing date (see PCT Article 11 and MPEP 1810), a Notification of the International Application Number and of the International Filing Date (Form PCT/RO/105) will be issued in due course, subject to prescriptions concerning national security, and the date shown on this Acknowledgement Receipt will establish the international filing date of the application.

IN THE UNITED STATES PATENT AND TRADEMARK OFFICE

Applicant	: John D. Joannopoulos et al.	Art Unit	: 2836
Serial No.	: 12/639,963	Examiner	: Albert W. Paladini
Filed	: December 16, 2009	Conf. No.	: 7811
Title	: WIRELESS ENERGY TRANSFER WITH HIGH-Q TO MORE THAN ONE DEVICE		

MAIL STOP AMENDMENT
Commissioner for Patents
P.O. Box 1450
Alexandria, VA 22313-1450

INFORMATION DISCLOSURE STATEMENT

Please consider the references listed on the enclosed PTO-1449 form. Foreign patent documents and non-patent literature are enclosed; cited U.S. patents and patent application publications will be provided on request. A copy of a communication from a foreign patent office in a counterpart application is also enclosed.

Applicant notes that Desig. Id. No. 6 (the Baarman reference) was previously submitted in an Information Disclosure Statement filed on February 8, 2011. However, the applicant incorrectly listed the Publication Date as 9/9/2009 rather than the correct publication date of 7/9/2009. The correct publication date is submitted herewith in the attached Form PTO-1449.

This statement is being filed after a first Office action on the merits, but before receipt of a final Office action or a Notice of Allowance. The fees in the amount of $180 in payment of the late submission fee of §1.17(p) are being paid concurrently herewith on the Electronic Filing System (EFS) by way of Deposit Account authorization. Please apply any necessary charges or credits to Deposit Account 06-1050, referencing the above attorney docket number.

Respectfully submitted,

Date: November 23, 2011

/Marc M. Wefers Reg. No. 56,842/
Marc M. Wefers
Reg. No. 56,842

Customer Number 26161
Fish & Richardson P.C.
Telephone: (617) 542-5070
Facsimile: (877) 769-7945
22715791.doc

Substitute Form PTO-1449 (Modified)	U.S. Department of Commerce Patent and Trademark Office	Attorney Docket No. 01997-0359009	Application No. 12/639,963
Information Disclosure Statement by Applicant (Use several sheets if necessary) (37 CFR §1.98(b))		Applicant John D. Joannopoulos et al.	
		Filing Date December 16, 2009	Group Art Unit 2836

U.S. Patent Documents

Examiner Initial	Desig. ID	Document Number	Publication Date	Patentee	Class	Subclass	Filing Date If Appropriate
	1	6,664,770	12/16/2003	Bartels			
	2	7,514,818	4/7/2009	Abe et al.			
	3	8,022,576	9/20/2011	Joannopoulos et al.			
	4	2007/0021140	1/25/2007	Keyes, IV et al.			
	5	2008/0266748	10/30/2008	Lee			
	6	2009/0174263	7/9/2009	Baarman et al.			
	7	2009/0267709	10/29/2009	Joannopoulos et al.			
	8	2009/0267710	10/29/2009	Joannopoulos et al.			
	9	2009/0284083	11/19/2009	Karalis et al.			
	10	2010/0096934	4/22/2010	Joannopoulos et al.			
	11	2010/0102640	4/29/2010	Joannopoulos et al.			
	12	2010/0102641	4/29/2010	Joannopoulos et al.			
	13	2010/0123353	5/20/2010	Joannopoulos et al.			
	14	2010/0123354	5/20/2010	Joannopoulos et al.			
	15	2010/0123355	5/20/2010	Joannopoulos et al.			
	16	2010/0127573	5/27/2010	Joannopoulos et al.			
	17	2010/0127574	5/27/2010	Joannopoulos et al.			
	18	2010/0133918	6/3/2010	Joannopoulos et al.			
	19	2010/0133919	6/3/2010	Joannopoulos et al.			
	20	2010/0133920	6/3/2010	Joannopoulos et al.			
	21	2010/0148589	6/17/2010	Hamam et al.			
	22	2010/0187911	7/29/2010	Joannopoulos et al.			
	23	2010/0207458	8/19/2010	Joannopoulos et al.			
	24	2011/0043046	2/24/2011	Joannopoulos et al.			
	25	2011/0074218	3/31/2011	Karalis et al.			
	26	2011/0074347	3/31/2011	Karalis et al.			
	27	2011/0089895	4/21/2011	Karalis et al.			

Examiner Signature	Date Considered
EXAMINER: Initials citation considered. Draw line through citation if not in conformance and not considered. Include copy of this form with next communication to applicant.	

Substitute Disclosure Form (PTO-1449)

Substitute Form PTO-1449 (Modified) U.S. Department of Commerce Patent and Trademark Office	Attorney Docket No. 01997-0359009	Application No. 12/639,963
Information Disclosure Statement by Applicant (Use several sheets if necessary) (37 CFR §1.98(b))	Applicant John D. Joannopoulos et al.	
	Filing Date December 16, 2009	Group Art Unit 2836

U.S. Patent Documents

Examiner Initial	Desig. ID	Document Number	Publication Date	Patentee	Class	Subclass	Filing Date If Appropriate
	28	2011/0193419	8/11/2011	Karalis et al.			
	29						

Foreign Patent Documents or Published Foreign Patent Applications

Examiner Initial	Desig. ID	Document Number	Publication Date	Country or Patent Office	Class	Subclass	Translation Yes	Translation No
	30	2011/062827	5/26/2011	WIPO	G06F	1/26		

Other Documents (include Author, Title, Date, and Place of Publication)

Examiner Initial	Desig. ID	Document
	31	Andre Kurs et al., "Simultaneous mid-range power transfer to multiple devices", Applied Physics Letters, Vol. 96, No. 044102 (2010)
	32	David Schneider, "A Critical Look at Wireless Power", IEEE Spectrum, (May 2010)
	33	Marin Soljacic, "Wireless nonradiative energy transfer", Visions of Discovery New Light on Physics, Cosmology, and Consciousness, Cambridge University Press, New York, NY pp. 530-542 (2011)
	34	Joseph C. Stark III, "Wireless Power Transmission Utilizing a Phased Array of Tesla Coils", Master Thesis, Massachusetts Institute of Technology (2004)
	35	Copy of International Search Report and Written Opinion of the International Searching Authority for International Application No. PCT/US2011/027868 by Examiner Blaine R. Copenheaver dated July 5, 2011

Examiner Signature	Date Considered
EXAMINER: Initials citation considered. Draw line through citation if not in conformance and not considered. Include copy of this form with next communication to applicant.	

Substitute Disclosure Form (PTO-1449)

IN THE UNITED STATES PATENT AND TRADEMARK OFFICE

Applicant	: John D. Joannopoulos et al.	Art Unit	: 2836
Serial No.	: 12/639,963	Examiner	: Albert W. Paladini
Filed	: December 16, 2009	Conf. No.	: 7811
Title	: WIRELESS ENERGY TRANSFER WITH HIGH-Q TO MORE THAN ONE DEVICE		

Commissioner for Patents
P.O. Box 1450
Alexandria, VA 22313-1450

TERMINAL DISCLAIMER UNDER 37 C.F.R. §§ 3.73(b) AND 1.321(c)

Pursuant to 37 C.F.R. § 3.73(b), MASSACHUSETTS INSTITUTE OF TECHNOLOGY, a university, certifies that it is the assignee of the entire right, title, and interest in the present application (a 100% ownership interest by virtue of:

☒ An assignment from the inventors of the present patent application. The assignment was recorded in the Patent and Trademark Office at Reel 024271, Frame 0854 on April 22, 2010, or a copy thereof is attached.

To the best of undersigned's knowledge and belief, title is in the assignee identified above.

The undersigned is empowered to act on behalf of the assignee.

Pursuant to 37 C.F.R. § 1.321(c), and to obviate a double patenting rejection, the assignee identified above hereby disclaims, except as provided below, the terminal portion of the statutory term of any patent granted on the instant application that would extend beyond the expiration date of the full statutory term of U.S. Patent No. 7,741,734. The assignee hereby agrees that any patent granted on the instant application shall be enforceable only for and during such period that it is commonly owned with U.S. Patent No. 7,741,734.

The assignee identified above does not disclaim any terminal part of any patent granted on the present application that would extend to the expiration date of the full statutory term of U.S. Patent No. 7,741,734 in the event that U.S. Patent No. 7,741,734 later: expires for failure to pay a maintenance fee, is held unenforceable, is found invalid by a court of competent jurisdiction, is statutorily disclaimed in whole or terminally disclaimed under 37 C.F.R. § 1.321, has all claims cancelled by a reexamination certificate, is reissued, or is otherwise terminated prior to expiration of its statutory term. The full statutory term of any patent includes any term

adjustment as defined in 35 U.S.C. § 154 and § 173. Assignee herein does not disclaim or otherwise affect any part of U.S. Patent No. 7,741,734.

This disclaimer runs with any patent granted on the above application and is binding upon the grantee, its successors or assigns.

The fees in the amount of $160 required under 37 C.F.R. § 1.20(d) are being paid concurrently herewith on the Electronic Filing System (EFS) by way of Deposit Account authorization. Please apply any necessary charges or credits to Deposit Account 06-1050, referencing the above attorney docket number.

Respectfully submitted,

Date: November 23, 2011

/Marc M. Wefers Reg. No. 56,842/
Marc M. Wefers
Reg. No. 56,842

Customer Number 26161
Fish & Richardson P.C.
Telephone: (617) 542-5070
Facsimile: (877) 769-7945

22714872.doc

PTO/SB/06 (07-06)
Approved for use through 1/31/2007. OMB 0651-0032
U.S. Patent and Trademark Office; U.S. DEPARTMENT OF COMMERCE
Under the Paperwork Reduction Act of 1995, no persons are required to respond to a collection of information unless it displays a valid OMB control number.

PATENT APPLICATION FEE DETERMINATION RECORD
Substitute for Form PTO-875

Application or Docket Number	Filing Date	☐ To be Mailed
12/639,963	12/16/2009	

APPLICATION AS FILED – PART I

	(Column 1)	(Column 2)	SMALL ENTITY ☐		OR	OTHER THAN SMALL ENTITY	
FOR	NUMBER FILED	NUMBER EXTRA	RATE ($)	FEE ($)		RATE ($)	FEE ($)
☐ BASIC FEE (37 CFR 1.16(a), (b), or (c))	N/A	N/A	N/A			N/A	
☐ SEARCH FEE (37 CFR 1.16(k), (l), or (m))	N/A	N/A	N/A			N/A	
☐ EXAMINATION FEE (37 CFR 1.16(o), (p), or (q))	N/A	N/A	N/A			N/A	
TOTAL CLAIMS (37 CFR 1.16(i))	minus 20 =	*	X $ =		OR	X $ =	
INDEPENDENT CLAIMS (37 CFR 1.16(h))	minus 3 =	*	X $ =			X $ =	
☐ APPLICATION SIZE FEE (37 CFR 1.16(s))	If the specification and drawings exceed 100 sheets of paper, the application size fee due is $250 ($125 for small entity) for each additional 50 sheets or fraction thereof. See 35 U.S.C. 41(a)(1)(G) and 37 CFR 1.16(s).						
☐ MULTIPLE DEPENDENT CLAIM PRESENT (37 CFR 1.16(j))							
* If the difference in column 1 is less than zero, enter "0" in column 2.			TOTAL			TOTAL	

APPLICATION AS AMENDED – PART II

		(Column 1)		(Column 2)	(Column 3)	SMALL ENTITY		OR	OTHER THAN SMALL ENTITY	
	11/23/2011	CLAIMS REMAINING AFTER AMENDMENT		HIGHEST NUMBER PREVIOUSLY PAID FOR	PRESENT EXTRA	RATE ($)	ADDITIONAL FEE ($)		RATE ($)	ADDITIONAL FEE ($)
AMENDMENT	Total (37 CFR 1.16(i))	- 48	Minus	** 20	= 28	X $ =		OR	X $60=	1680
	Independent (37 CFR 1.16(h))	- 2	Minus	***3	= 0	X $ =		OR	X $250=	0
	☐ Application Size Fee (37 CFR 1.16(s))									
	☐ FIRST PRESENTATION OF MULTIPLE DEPENDENT CLAIM (37 CFR 1.16(j))							OR		
						TOTAL ADD'L FEE		OR	TOTAL ADD'L FEE	1680

		(Column 1)		(Column 2)	(Column 3)					
		CLAIMS REMAINING AFTER AMENDMENT		HIGHEST NUMBER PREVIOUSLY PAID FOR	PRESENT EXTRA	RATE ($)	ADDITIONAL FEE ($)		RATE ($)	ADDITIONAL FEE ($)
AMENDMENT	Total (37 CFR 1.16(i))	-	Minus	**	=	X $ =		OR	X $ =	
	Independent (37 CFR 1.16(h))	-	Minus	***	=	X $ =		OR	X $ =	
	☐ Application Size Fee (37 CFR 1.16(s))									
	☐ FIRST PRESENTATION OF MULTIPLE DEPENDENT CLAIM (37 CFR 1.16(j))							OR		
						TOTAL ADD'L FEE		OR	TOTAL ADD'L FEE	

* If the entry in column 1 is less than the entry in column 2, write "0" in column 3.
** If the "Highest Number Previously Paid For" IN THIS SPACE is less than 20, enter "20".
*** If the "Highest Number Previously Paid For" IN THIS SPACE is less than 3, enter "3".
The "Highest Number Previously Paid For" (Total or Independent) is the highest number found in the appropriate box in column 1.

Legal Instrument Examiner:
/CHARLENE HERBERT/

This collection of information is required by 37 CFR 1.16. The information is required to obtain or retain a benefit by the public which is to file (and by the USPTO to process) an application. Confidentiality is governed by 35 U.S.C. 122 and 37 CFR 1.14. This collection is estimated to take 12 minutes to complete, including gathering, preparing, and submitting the completed application form to the USPTO. Time will vary depending upon the individual case. Any comments on the amount of time you require to complete this form and/or suggestions for reducing this burden, should be sent to the Chief Information Officer, U.S. Patent and Trademark Office, U.S. Department of Commerce, P.O. Box 1450, Alexandria, VA 22313-1450. DO NOT SEND FEES OR COMPLETED FORMS TO THIS ADDRESS. **SEND TO: Commissioner for Patents, P.O. Box 1450, Alexandria, VA 22313-1450.**

If you need assistance in completing the form, call 1-800-PTO-9199 and select option 2.

Application Number	Application/Control No.	Applicant(s)/Patent under Reexamination
	12/639,963	JOANNOPOULOS ET AL.

Document Code - DISQ	Internal Document – DO NOT MAIL

TERMINAL DISCLAIMER	☒ APPROVED	☐ DISAPPROVED
Date Filed : 11/23/11	This patent is subject to a Terminal Disclaimer	

Approved/Disapproved by:

Angie Walker

U.S. Patent and Trademark Office

PLUS Search Results for S/N 12639963, Searched Mon Mar 19 10:40:14 EDT 2012

The Patent Linguistics Utility System (PLUS) is a USPTO automated search system for U.S. Patents from 1971 to the present PLUS is a query-by-example search system which produces a list of patents that are most closely related linguistically to the application searched. This search was prepared by the staff of the Scientific and Technical Information Center, SIRA.

6021612 99	6057629 88	3840828 84
4296386 95	6094113 88	3835416 84
5912602 95	6101300 88	3835415 84
6052043 95	6109304 88	3829792 84
4760360 92	6130969 88	3823470 84
4862122 92	6144687 88	3819977 84
5280249 92	6163276 88	3819009 84
5357532 92	6181258 88	3818372 84
6060882 92	6239673 88	3813613 84
6101014 92	3628186 84	3812516 84
4293820 88	3628167 84	3805148 84
4331943 88	3624557 84	3801928 84
4342010 88	3612914 84	3798578 84
4352209 88	3599112 84	3798550 84
4481488 88	3593189 84	3792375 84
4494235 88	3585537 84	3784452 84
4598405 88	3585418 84	3783419 84
4599582 88	3581236 84	3783351 84
4776691 88	3581228 84	4019181 84
4839618 88	3576502 84	4022707 84
4896125 88	3571702 84	4025939 84
4955057 88	3560695 84	4034226 84
5266921 88	3560694 84	4035740 84
5317266 88	3704996 84	4048516 84
5349260 88	3704433 84	4059803 84
5363074 88	3702445 84	4143344 84
5379110 88	3699480 84	4145668 84
5425044 88	3696314 84	4149127 84
5511084 88	3668565 84	4167686 84
5566265 88	3668564 84	4180324 84
5576680 88	3668547 84	4072911 84
5585770 88	3652940 84	4081573 84
5598097 88	3651941 84	4082633 84
5659275 88	3648184 84	4084131 84
5748654 88	3639132 84	4095195 84
5752180 88	3638137 84	4096046 84
5781011 88	3928816 84	4099144 84
5780072 88	3919665 84	4100507 84
5841330 88	3916351 84	4100509 84
5912603 88	3904987 84	4110761 84
5914554 88	3899748 84	4114112 84
5920243 88	3892487 84	4118672 84
5936486 88	3885874 84	4127452 84
5943351 88	3879653 84	4266208 84
6014237 88	3878481 84	4268801 84
6018413 88	3868595 84	4272733 84
6023208 88	3850261 84	4286230 84
6037541 88	3849667 84	4292561 84
6054910 88	3845419 84	4294330 84

4302667 84
4318016 84
4330047 84
4338258 84
4378532 84
4422360 84
4423396 84
4445122 84
4446556 84
4462097 84
4465725 84
4479220 84
4483234 84
4484382 84
4494338 84
4500996 84
4514848 84
4530097 84
4541879 84
4558923 84
4564271 84
4590597 84
4606105 84
4769620 84
4769621 84
4772121 84
4787473 84
4794618 84
4805084 84
4844079 84
4848902 84
4859548 84
4875055 84
4914663 84
4943956 84
4945545 84
4973832 84
4999588 84
5004342 84
5012212 84
5022033 84
5070505 84
5069527 84
5068864 84
5064284 84
5063568 84
5057804 84
5057466 84
5056400 84
5054912 84
5053938 84
5053734 84
5052008 84
5048045 84
5048034 84
5043997 84
5043995 84
5038712 84
5034954 84
5034949 84
5034707 84
5033061 84
5031186 84
5031185 84
5030876 84
5030851 84
5029174 84
5194830 84
5220572 84
5233364 84
5251120 84
5260658 84
5261006 84
5263043 84
5268693 84
5274660 84
5276904 84
5287412 84
5289491 84
5309466 84
5333576 84
5343490 84
5352996 84
5371379 84
5392011 84
5410277 84
5420878 84
5425042 84
5430753 84
5436926 84
5448410 84
5450090 84
5465417 84
5469116 84
5483503 84
5491467 84
5499002 84
5543963 84
5546057 84
5550550 84
5563899 84
5565987 84
5614877 84
5635096 84
5635885 84
5642193 84
5657334 84
5675601 84
5721514 84
5742634 84
5748057 84
5754575 84
5764360 84
5777798 84
5781461 84
5781018 84
5790585 84
5821836 84
5828266 84
5856728 84
5855706 84
5864399 84
5875274 84
5892419 84
5903347 84
5905573 84
5914520 84
5920244 84
5920587 84
5937815 84
5949309 84
5957664 84
5970081 84
5972568 84
5977465 84
5991061 84
5995692 84
6028870 84
6046067 84
6051515 84
6057724 84
6057745 84
6062338 84
6064350 84
6064271 84
6081379 84
6081361 84
6105546 84
6106149 84
6111472 84
6117806 84
6137383 84
6150817 84

Substitute Form PTO-1449 (Modified)	U.S. Department of Commerce Patent and Trademark Office	Attorney Docket No. 01997-0359009	Application No. 12/639,963
Information Disclosure Statement by Applicant (Use several sheets if necessary) (37 CFR §1.98(b))		Applicant John D. Joannopoulos et al.	
		Filing Date December 16, 2009	Group Art Unit 2836

U.S. Patent Documents

Examiner Initial	Desig. ID	Document Number	Publication Date	Patentee	Class	Subclass	Filing Date If Appropriate
	1	5,053,774	10/1/1991	Schuermann et al.			
	2	5,287,112	2/15/1994	Schuermann			
	3	5,455,467	10/3/1995	Young et al.			
	4	6,772,011	8/3/2004	Dolgin			
	5	8,076,800	12/13/2011	Joannopoulos et al.			
	6	8,076,801	12/13/2011	Karalis et al.			
	7	8,084,889	12/27/2011	Joannopoulos et al.			
	8	8,097,983	1/17/2012	Karalis et al.			
	9	2003/0124050	7/3/2003	Yadav et al.			
	10	2003/0126948	7/10/2003	Yadav et al.			
	11	2004/0100338	5/27/2004	Clark			
	12	2004/0233043	11/25/2004	Yazawa et al.			
	13	2006/0202665	9/14/2006	Hsu			
	14	2012/0068549	3/22/2012	Karalis et al.			

Foreign Patent Documents or Published Foreign Patent Applications

Examiner Initial	Desig. ID	Document Number	Publication Date	Country or Patent Office	Class	Subclass	Translation Yes	Translation No
	15	JP 02-097005	04/09/1990	Japan	H01F	21/06		X
	16	WO 2009/140506	11/19/2009	WIPO				
	17	WO 2010/039967	4/8/2010	WIPO				

Other Documents (include Author, Title, Date, and Place of Publication)

Examiner Initial	Desig. ID	Document
	18	Copy of Non-Final Office Action for U.S. Application Serial No. 12/648,604 by Examiner Justen Fauth dated December 5, 2011
	19	Copy of Non-Final Office Action for U.S. Application Serial No. 13/036,177 by Examiner Fritz M. Fleming dated May 15, 2012
	20	Copy of Non-Final Office Action for U.S. Application Serial No. 13/078,511 by Examiner Fritz M. Fleming dated May 15, 2012
	21	Copy of Non-Final Office Action for U.S. Application Serial No. 12/726,742 by Examiner Fritz M. Fleming dated May 11, 2012

Examiner Signature	Date Considered

EXAMINER: Initials citation considered. Draw line through citation if not in conformance and not considered. Include copy of this form with next communication to applicant.

Substitute Disclosure Form (PTO-1449)

Substitute Form PTO-1449 (Modified) U.S. Department of Commerce Patent and Trademark Office	Attorney Docket No. 01997-0359009	Application No. 12/639,963
Information Disclosure Statement by Applicant (Use several sheets if necessary) (37 CFR §1.98(b))	Applicant John D. Joannopoulos et al.	
	Filing Date December 16, 2009	Group Art Unit 2836

Other Documents (include Author, Title, Date, and Place of Publication)		
Examiner Initial	Desig. ID	Document
	22	Copy of Non-Final Office Action for U.S. Application Serial No. 13/030,395 by Examiner Fritz M. Fleming dated May 17, 2012
	23	Copy of Non-Final Office Action for U.S. Application Serial No. 13/040,810 by Examiner Fritz M. Fleming dated May 17, 2012

Examiner Signature	Date Considered
EXAMINER: Initials citation considered. Draw line through citation if not in conformance and not considered. Include copy of this form with next communication to applicant.	

Substitute Disclosure Form (PTO-1449)

⑲日本国特許庁（JP）　⑪特許出願公開

⑫公開特許公報（A）　平2−97005

⑤Int. Cl.⁵　識別記号　庁内整理番号　⑬公開　平成2年(1990)4月9日
H 01 F 21/06　D　6447−5E

審査請求　未請求　請求項の数 1　（全4頁）

⑭発明の名称　可変インダクタンス

⑳特　願　昭63−249463
㉒出　願　昭63(1988)10月3日

㉑発明者　長田　尚一郎　神奈川県座間市相武台2−268　東京コスモス電機株式会社神奈川工場内
㉑発明者　竹内　誠　東京都八王子市戸吹町1387番地　東京コスモス電機株式会社内
㉑発明者　市倉　学　東京都八王子市戸吹町1387番地　東京コスモス電機株式会社内
㉑出願人　東京コスモス電機株式会社　東京都八王子市戸吹町1387番地

明細書

1．発明の名称　可変インダクタンス

2．特許請求の範囲

空芯コイルのコイル同軸方向の延長線上に、ネジ穴を施した支持体を設け、調整ネジが前記ネジ穴に回動自在に取付けられた事を特徴とする可変インダクタンス。

3．発明の詳細な説明

［産業上の利用分野］

この発明は可変インダクタンスに関し、更に詳しくは、短波帯、超短波、極超短波帯の発振、同調、及び共振回路に用いられる高周波用可変インダクタンスに関する。

［従来の技術］

一般に短波帯以下の高周波用のコイルにおいては、鉄芯やフェライトコア等、空芯コイルの場合に比して透磁率の高い物質を設けることにより、コイル内部の磁束密度を増加させることで小型のコイルでも十分なインダクタンスを得ることができる。この場合、インダクタンスの調整においてはコイル内のコアの位置を変更することにより、磁束密度が変化するため、容易に調整できる。

短波帯以上になると鉄芯などのバルク材においては渦電流による反磁界、フェライトにおいては磁気余効の効果のため、磁束密度は必ずしも増加しない。そのため１００ＭＨｚ以上の周波数では専ら空芯コイルが用いられ、比較的少ない巻数でも十分なインダクタンスが得られる。

共振や同調、発振などの用途で高周波コイルを用いる場合、コイルとコンデンサでタンク回路を構成する。周知の通り、タンク回路の周波数ｆは次式で与えられる。

$$f = 1 / (2\pi \sqrt{LC})$$

ここでＬはコイルのインダクタンス、Ｃはコンデンサの容量である。

周波数調整においてはコイルのインダクタンスＬを一定にして、コンデンサの容量Ｃをトリマコ

InductEV, Inc.
Exhibit 1025
Page 492

ンデンサなどで可変することが一般的である。

また一方、コンデンサの容量Cを一定にし、コイルのインダクタンスLを変化させることによって周波数調整を行う方式がある。短波帯以下の場合はコイル内部のコアの位置を変えることによって容易に調整できるが、短波帯以上の空芯コイルではこの手段を用いることができないため、巻数や巻径、ピッチなどコイルの形状に関する点を変更する方法がある。

高周波コイルの調整として一般的な空芯コイルのピッチを変える方法について第2図を用いて説明する。第2図（a）のように雑音除去の目的で回路をシールドケース1で包囲している場合は調整用ドライバ9が出入りできる程度の調整穴10を設けておく。調整用ドライバ9をコイルの巻線間に挿入し、第2図（b）の様に巻線の間隔を広げることにより、インダクタンスを減少させることができる。

[発明が解決しようとする問題]

近年、伝送線路が大幅に短縮できることから、高周波回路にも高密度実装方式が取り入れられており、トリマコンデンサは比較的大きな部品のため、高密度実装を行う上で不都合である。このため、短波帯以上の高周波回路ではインダクタンスLを可変にする方式が有利である。

コイルのインダクタンスLを変化させることによって周波数調整を行う方式では、空芯コイルの巻数、巻径、ピッチなどコイルの形状に関する点を変更せざるをえず、正確な調整が困難で手間がかかり、経時変化も大きい等の問題がある。

例えばコイルの巻径、巻数を変えて調整する方法では、一旦基板に装着したコイルを外し、巻径や巻数が適切なコイルに取り替える必要がある。ところが、コイル部品はインダクタンスのバラツキが大きいため、この方法を行うと取り替え作業の手間が大きく、精密な調整も困難である。

コイルのピッチを変える方法によればコイルを取り替える必要はないが、精密な調整には熟練を要す。またコイルを無理に変形させるため、ピッチの戻りが現れ調整周波数がずれ、不安定要因となるばかりでなく、振動、衝撃に対しても変動が生じる。

この発明はこの問題を克服すべく考案されたもので、高周波用空芯コイルにインダクタンス調整機構を設けることにより、周波数設定を安定かつ精密に行うことができ、併せて調整作業を簡単化できることにより、信頼性の高い優れた高周波コイルを提供することを目的とする。

[問題を解決するための手段]

この発明は、空芯コイルのコイル同軸方向の延長線上にネジを支え、さらに固定するための支持体を設け、コイルの同軸中心に対向する部分にネジ穴を施し、ネジ穴に金属などの導電性のネジを差し込み、ネジの先端がコイルに対向する配置を構成する。

[作用]

上記のように構成したこの発明によれば、コイルから発生される高周波交番磁界によって、導電体でできたネジの内部に渦電流が生じ、反抗磁界を発生する。渦電流による反磁界は短波帯以上の周波数帯域では無視できない大きさになるため、コイルに鎖交する磁束密度は減少する。これによりコイルのインダクタンスが減少するため、発振周波数は上昇する。

ネジとコイルの相対位置を変化させることにより、周波数上昇分を正確に調整することができ、また、調整後はネジを接着剤や半田、溶接などで支持体に固定することにより、外部環境の変動に対しても安定に動作するようになる。

この発明によれば、通信機器をはじめとする高周波の発振周波数が安定し、製品相互間のバラツキも少なくなり、ひいては色々の機器の作動における高い信頼性が得られるといった優れた効果を奏する高周波コイルを提供することができる。

[実施例]

以下この発明の実施例を図面に基づいて説明する。第一図に本発明の実施例を示し、同図（a）にその断面図、同図（b）に正面図を示す。

この実施例は調整ネジ2の支持体として、高周波発振回路の雑音対策に使われるシールドケース

InductEV, Inc.
Exhibit 1025
Page 493

1で代用している。

予め空芯コイル5をシールドケース1の近辺に配置されるように設計しておく。空芯コイル5は回路基板4に半田付け部6によって固定し、更に回路基板4の裏面の銅箔7とシールドケース1とを半田付け8で固定することにより、空芯コイル5に及ぼす周囲の影響を固定する。

空芯コイル5の同軸中心の延長線とシールドケース1の交差する点にネジ穴3を設ける。ネジ穴3は貫通穴にめねじを切っても良いし、ナットを接着固定しても良い。このネジ穴は導電性の調整ネジ2を挿入し、支持することを目的とする。これによって、外部から調整ネジ2のネジ頭をドライバで回すことでネジの先端部と空芯コイル5の巻口との間隔を変えることができる。

[発明の効果]

調整ネジを空芯コイルに近付けると発振周波数は上昇し、遠ざけると下降する。調整ネジを取り去った場合が最も発振周波数が低くなるため、この状態で目標とする発振周波数を越えないよう、予め空芯コイルのインダクタンスを大きめに設計することが必要である。

金属ネジを取付ける支持体は、高周波回路によく用いられるシールドケースで代用することができ、特に局部発振回路等の外部雑音を除外したい用途に用いることができる。ネジ頭がケース外部に突出するため、回路をケースに封入した後、金属ケースの影響でインダクタンスが変動しても再調整が行える利点を持つ。さらに、この場合、トリマコンデンサ等で調整する場合に比べて、シールドケースにドライバが通る程度の調整用の穴を設ける必要がなく、完全密閉することができるため外部雑音の侵入を防止することができる。よって、VCOのように外部雑音を極度に嫌い、安定性、高精度の設定性が求められる高周波発振回路に適している。

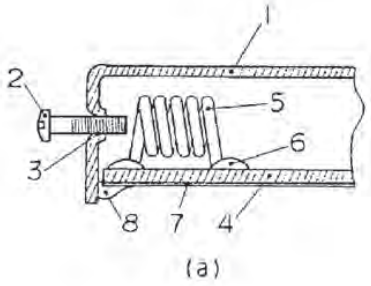
第1図の実施例では、目標とする発振周波数を360MHzとして、調整ネジ1回転で約1MHzの調整が可能で、10KHzの精度での精密調整が可能となった。

なお調整ネジに鉄等の磁性体を用いた場合、非線形歪みやバルクハウゼン雑音等の影響により不要輻射が増加し、C／N比やS／N比に劣化を来すため、黄銅等の非磁性体を用いることで良好な結果が得られる。

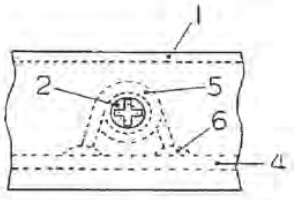
4．図面の簡単な説明

第1図は本発明の実施例を示す図で、同図（a）は部分側断面図、同図（b）は正面図である。第2図は、来の調整方法を示す部分側断面図で、同図（a）は調整前の状態、同図（b）は調整後の状態を示す。

1…シールドケース、2…調整ネジ、3…ネジ穴、4…回路基板、5…空芯コイル、6…半田付け部、7…銅箔、8…半田付け部、9…調整用ドライバ、10…調整穴



(a)

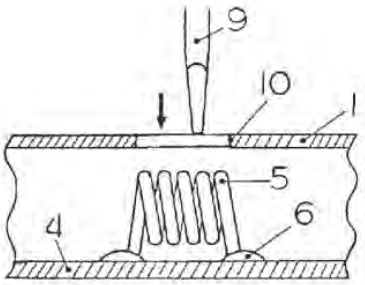


(b)

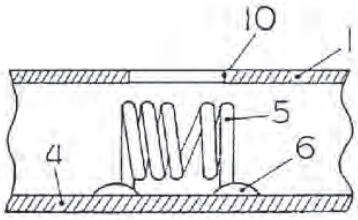
第1図

特許出願人　東京コスモス電機株式会社

InductEV, Inc.
Exhibit 1025
Page 494



(a)



(b)

第2図

InductEV, Inc.
Exhibit 1025
Page 495

DERWENT-ACC-NO: 1990-151957

DERWENT-WEEK: 199020

COPYRIGHT 2012 DERWENT INFORMATION LTD

TITLE: Variable inductor for RF resonance circuit has inductance adjustment screw movable along axis of air-core coil NoAbstract Dwg 1/2

INVENTOR: ICHIKURA M; OSADA S ; TAKEUCHI M

PATENT-ASSIGNEE: TOKYO COSMOS DENKI KK[TOKCN]

PRIORITY-DATA: 1988JP-249463 (October 3, 1988)

PATENT-FAMILY:

PUB-NO	PUB-DATE	LANGUAGE
JP 02097005 A	April 9, 1990	JA

APPLICATION-DATA:

PUB-NO	APPL-DESCRIPTOR	APPL-NO	APPL-DATE
JP 02097005A	N/A	1988JP-249463	October 3, 1988

INT-CL-CURRENT:

TYPE	IPC DATE
CIPP	H01F21/06 20060101

ABSTRACTED-PUB-NO:

EQUIVALENT-ABSTRACTS:

TITLE-TERMS: VARIABLE INDUCTOR RF RESONANCE CIRCUIT INDUCTANCE ADJUST SCREW MOVE AXIS AIR CORE COIL NOABSTRACT

DERWENT-CLASS: V02

EPI-CODES: V02-F01;

SECONDARY-ACC-NO:

Non-CPI Secondary Accession Numbers: 1990-118088

(12) INTERNATIONAL APPLICATION PUBLISHED UNDER THE PATENT COOPERATION TREATY (PCT)

(19) World Intellectual Property Organization
International Bureau

(43) International Publication Date
19 November 2009 (19.11.2009)

PCT

(10) International Publication Number
WO 2009/140506 A1

(51) International Patent Classification:
H01P 7/00 (2006.01)

(21) International Application Number:
PCT/US2009/043970

(22) International Filing Date:
14 May 2009 (14.05.2009)

(25) Filing Language: English

(26) Publication Language: English

(30) Priority Data:
61/127,661 14 May 2008 (14.05.2008) US

(71) Applicant *(for all designated States except US)*: **MASSACHUSETTS INSTITUTE OF TECHNOLOGY** [US/US]; 77 Massachusetts Avenue, Cambridge, Massachusetts 02142-1324 (US).

(72) Inventors; and

(75) Inventors/Applicants *(for US only)*: **KARALIS, Aristeidis** [GR/US]; 151 Tremont Street, Apt. 21F, Boston, Massachusetts 02111 (US). **HAMAM, Rafif, E.** [LB/US]; 550 Memorial Drive, Apt. 9C-2, Cambridge, Massachusetts 02139 (US). **JOANNOPOULOS, John, D.** [US/US]; 64 Douglas Road, Belmont, Massachusetts 02478 (US). **SOLJACIC, Marin** [HR/US]; 44 Westlund Road, Belmont, Massachusetts 02478 (US).

(74) Agent: **WEFERS, Marc, M.**; Fish & Richardson P.C., PO Box 1022, Minneapolis, Minnesota 55440-1022 (US).

(81) Designated States *(unless otherwise indicated, for every kind of national protection available)*: AE, AG, AL, AM, AO, AT, AU, AZ, BA, BB, BG, BH, BR, BW, BY, BZ, CA, CH, CN, CO, CR, CU, CZ, DE, DK, DM, DO, DZ, EC, EE, EG, ES, FI, GB, GD, GE, GH, GM, GT, HN, HR, HU, ID, IL, IN, IS, JP, KE, KG, KM, KN, KP, KR, KZ, LA, LC, LK, LR, LS, LT, LU, LY, MA, MD, ME, MG, MK, MN, MW, MX, MY, MZ, NA, NG, NI, NO, NZ, OM, PG, PH, PL, PT, RO, RS, RU, SC, SD, SE, SG, SK, SL, SM, ST, SV, SY, TJ, TM, TN, TR, TT, TZ, UA, UG, US, UZ, VC, VN, ZA, ZM, ZW.

(84) Designated States *(unless otherwise indicated, for every kind of regional protection available)*: ARIPO (BW, GH, GM, KE, LS, MW, MZ, NA, SD, SL, SZ, TZ, UG, ZM, ZW), Eurasian (AM, AZ, BY, KG, KZ, MD, RU, TJ, TM), European (AT, BE, BG, CH, CY, CZ, DE, DK, EE, ES, FI, FR, GB, GR, HR, HU, IE, IS, IT, LT, LU, LV, MC, MK, MT, NL, NO, PL, PT, RO, SE, SI, SK, TR), OAPI (BF, BJ, CF, CG, CI, CM, GA, GN, GQ, GW, ML, MR, NE, SN, TD, TG).

Published:

— *with international search report (Art. 21(3))*

WO 2009/140506 A1

(54) **Title**: WIRELESS ENERGY TRANSFER, INCLUDING INTERFERENCE ENHANCEMENT

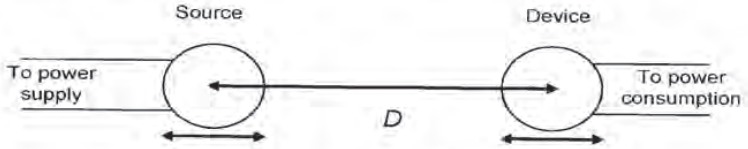


FIG. 1

(57) **Abstract**: Disclosed is an apparatus for use in wireless energy transfer, which includes a first resonator structure configured for energy transfer with a second resonator structure over a distance D larger than characteristic sizes, [insert formula] and [insert formula], of the first and second resonator structures. A power generator is coupled to the first structure and configured to drive the first resonator structure or the second resonator structure at an angular frequency away from the resonance angular frequencies and shifted towards a frequency corresponding to an odd normal mode for the resonator structures to reduce radiation from the resonator structures by destructive far-field interference.

WIRELESS ENERGY TRANSFER, INCLUDING INTERFERENCE ENHANCEMENT

CROSS REFERENCE TO RELATED APPLICATIONS

Pursuant to U.S.C. § 119(e), this application claims priority to U.S. Provisional Application Serial No. 61/127,661, filed May 14, 2008.

This application is also related by subject matter to the following commonly owned applications: U.S. Utility Patent Application Serial No. 12/055,963, filed March 26, 2008; U.S. Utility Patent Application Serial No. 11/481,077, filed July 5, 2006; U.S. Provisional Application Serial No. 60/698,442, filed July 12, 2005; U.S. Provisional Application Serial No. 60/908,383, filed March 27, 2007; U.S. Provisional Application Serial No. 60/908,666, filed March 28, 2007; and International Application No. PCT/US2007/070892, filed June 11, 2007.

The contents of the prior applications are incorporated herein by reference in their entirety.

BACKGROUND

The disclosure relates to wireless energy transfer. Wireless energy transfer can for example, be useful in such applications as providing power to autonomous electrical or electronic devices.

Radiative modes of omni-directional antennas (which work very well for information transfer) are not suitable for such energy transfer, because a vast majority of energy is wasted into free space. Directed radiation modes, using lasers or highly-directional antennas, can be efficiently used for energy transfer, even for long distances (transfer distance $L_{TRANS} \gg L_{DEV}$, where L_{DEV} is the characteristic size of the device and/or the source), but require existence of an uninterruptible line-of-sight and a complicated tracking system in the case of mobile objects. Some transfer schemes rely on induction, but are typically restricted to very close-range ($L_{TRANS} \ll L_{DEV}$) or low power (~mW) energy transfers.

The rapid development of autonomous electronics of recent years (e.g. laptops, cell-phones, house-hold robots, that all typically rely on chemical energy storage) has led to an increased need for wireless energy transfer.

SUMMARY

Efficient wireless energy-transfer between two resonant objects can be achieved at mid-range distances, provided these resonant objects are designed to operate in the 'strong-coupling' regime. We describe an implementation of a method to increase the efficiency of energy-transfer or to suppress the power radiated, which can be harmful or a cause of interference to other communication systems, by utilizing destructive interference between the radiated far-fields of the resonant coupled objects. 'Strong coupling' is a necessary condition for efficient energy-transfer, in the absence of far-field interference. 'Strong coupling' can be demonstrated in the case of realistic systems: self-resonant conducting coils, capacitively-loaded conducting coils, inductively-loaded conducting rods and dielectric disks, all bearing high-Q electromagnetic resonant modes. Also, an analytical model can be developed to take far-field interference into account for wireless energy-transfer systems. The analytical model can be used to demonstrate the efficiency enhancement and radiation suppression, in the presence of interference. In an example implementation, we describe improved performance based on the above principles in the case of two realistic systems: capacitively-loaded conducting coils and dielectric disks, both bearing high-Q electromagnetic resonant modes and far-field interference.

In an aspect, an apparatus for use in wireless energy transfer includes a first resonator structure configured for energy transfer with a second resonator structure, over a distance D larger than a characteristic size L_1 of said first resonator structure and larger than a characteristic size L_2 of said second resonator structure. The energy transfer has a rate κ and is mediated by evanescent-tail coupling of a resonant field of the first resonator structure and a resonant field of the second resonator structure. The resonant field of the first resonator structure has a resonance angular frequency ω_1, a resonance frequency-width Γ_1, and a resonance quality factor $Q_1 = \omega_1 / 2\Gamma_1$ at least larger than 300, and the said resonant field of the second resonator structure has a resonance angular frequency ω_2, a resonance frequency-width Γ_2, and a resonance quality factor $Q_2 = \omega_2 / 2\Gamma_2$ at least larger than 300. The absolute value of the difference of said angular frequencies ω_1 and ω_2 is smaller than the broader of said resonant widths Γ_1 and

InductEV, Inc.
Exhibit 1025
Page 500

Γ_2, and the quantity $\kappa/\sqrt{\Gamma_1\Gamma_2}$ is at least larger than 20. The apparatus also includes a power supply coupled to the first structure and configured to drive the first resonator structure or the second resonator structure at an angular frequency away from the resonance angular frequencies and shifted towards a frequency corresponding to an odd normal mode for the resonator structures to reduce radiation from the resonator structures by destructive far-field interference.

In some examples, the power supply is configured to drive the first resonator structure or the second resonator structure at the angular frequency away from the resonance angular frequencies and shifted towards the frequency corresponding to an odd normal mode for the resonator structures to substantially suppress radiation from the resonator structures by destructive far-field interference.

In an aspect, a method for wireless energy transfer involves a first resonator structure configured for energy transfer with a second resonator structure, over a distance D larger than a characteristic size L_1 of said first resonator structure and larger than a characteristic size L_2 of said second resonator structure, wherein the energy transfer has a rate κ and is mediated by evanescent-tail coupling of a resonant field of the first resonator structure and a resonant field of the second resonator structure, said resonant field of the first resonator structure has a resonance angular frequency ω_1, a resonance frequency-width Γ_1, and a resonance quality factor $Q_1 = \omega_1/2\Gamma_1$ at least larger than 300, and said resonant field of the second resonator structure has a resonance angular frequency ω_2, a resonance frequency-width Γ_2, and a resonance quality factor $Q_2 = \omega_2/2\Gamma_2$ at least larger than 300, the absolute value of the difference of said angular frequencies ω_1 and ω_2 is smaller than the broader of said resonant widths Γ_1 and Γ_2, and the quantity $\kappa/\sqrt{\Gamma_1\Gamma_2}$ is at least larger than 20. The method includes driving the first resonator structure or the second resonator structure at an angular frequency away from the resonance angular frequencies and shifted towards a frequency corresponding to an odd normal mode for the resonator structures to reduce radiation from the resonator structures by destructive far-field interference.

InductEV, Inc.
Exhibit 1025
Page 501

In some examples, the first resonator structure or the second resonator structure is driven at the angular frequency away from the resonance angular frequencies and shifted towards the frequency corresponding to an odd normal mode for the resonator structures to substantially suppress radiation from the resonator structures by destructive far-field interference.

In an aspect, an apparatus for use in wireless energy transfer includes a first resonator structure configured for energy transfer with a second resonator structure, over a distance D larger than a characteristic size L_1 of said first resonator structure and larger than a characteristic size L_2 of said second resonator structure. The energy transfer has a rate κ and is mediated by evanescent-tail coupling of a resonant field of the first resonator structure and a resonant field of the second resonator structure. The resonant field of the first resonator structure has a resonance angular frequency ω_1, a resonance frequency-width Γ_1, and a resonance quality factor $Q_1 = \omega_1 / 2\Gamma_1$ at least larger than 300, and the resonant field of the second resonator structure has a resonance angular frequency ω_2, a resonance frequency-width Γ_2, and a resonance quality factor $Q_2 = \omega_2 / 2\Gamma_2$ at least larger than 300. The absolute value of the difference of said angular frequencies ω_1 and ω_2 is smaller than the broader of said resonant widths Γ_1 and Γ_2, and the quantity $\kappa / \sqrt{\Gamma_1 \Gamma_2}$ is at least larger than 20. For a desired range of the distances D, the resonance angular frequencies for the resonator structures increase transmission efficiency T by accounting for radiative interference, wherein the increase is relative to a transmission efficiency T calculated without accounting for the radiative interference.

In some examples, the resonance angular frequencies for the resonator structures are selected by optimizing the transmission efficiency T to account for both a resonance quality factor U and an interference factor V.

In an aspect, a method involves designing a wireless energy transfer apparatus, the apparatus including a first resonator structure configured for energy transfer with a second resonator structure, over a distance D larger than a characteristic size L_1 of said first resonator structure and larger than a characteristic size L_2 of said second resonator structure, wherein the energy transfer has a rate κ and is mediated by evanescent-tail

InductEV, Inc.
Exhibit 1025
Page 502

coupling of a resonant field of the first resonator structure and a resonant field of the second resonator structure, wherein said resonant field of the first resonator structure has a resonance angular frequency ω_1, a resonance frequency-width Γ_1, and a resonance quality factor $Q_1 = \omega_1 / 2\Gamma_1$ at least larger than 300, and said resonant field of the second resonator structure has a resonance angular frequency ω_2, a resonance frequency-width Γ_2, and a resonance quality factor $Q_2 = \omega_2 / 2\Gamma_2$ at least larger than 300, wherein the absolute value of the difference of said angular frequencies ω_1 and ω_2 is smaller than the broader of said resonant widths Γ_1 and Γ_2, and the quantity $\kappa / \sqrt{\Gamma_1 \Gamma_2}$ is at least larger than 20. The method includes selecting the resonance angular frequencies for the resonator structures to substantially optimize the transmission efficiency by accounting for radiative interference between the resonator structures.

In some examples, the resonance angular frequencies for the resonator structures are selected by optimizing the transmission efficiency T to account for both a resonance quality factor *U* and an interference factor *V*.

In an aspect, an apparatus for use in wireless energy transfer includes a first resonator structure configured for energy transfer with a second resonator structure over a distance *D*. The energy transfer is mediated by evanescent-tail coupling of a resonant field of the first resonator structure and a resonant field of the second resonator structure, with a coupling factor *k*. The resonant field of the first resonator structure has a resonance angular frequency ω_1, a resonance frequency-width Γ_1, and a resonance quality factor $Q_1 = \omega_1 / 2\Gamma_1$, and is radiative in the far field, with an associated radiation quality factor $Q_{1,\mathrm{rad}} \geq Q_1$, and the resonant field of the second resonator structure has a resonance angular frequency ω_2, a resonance frequency-width Γ_2, and a resonance quality factor $Q_2 = \omega_2 / 2\Gamma_2$, and is radiative in the far field, with an associated radiation quality factor $Q_{2,\mathrm{rad}} \geq Q_2$. An absolute value of a difference of said angular frequencies ω_1 and ω_2 is smaller than broader of said resonant widths Γ_1 and Γ_2, and an average resonant angular frequency is defined as $\omega_o = \sqrt{\omega_1 \omega_2}$, corresponding to an average resonant wavelength $\lambda_o = 2\pi c / \omega_o$, where *c* is the speed of light in free space, and a

InductEV, Inc.
Exhibit 1025
Page 503

strong-coupling factor being defined as $U = k\sqrt{Q_1 Q_2}$. The apparatus is configured to employ interference between said radiative far fields of the resonant fields of the first and second resonator, with an interference factor V_{rad}, to reduce a total amount of radiation from the apparatus compared to an amount of radiation from the apparatus in the absence of interference, a strong-interference factor being defined as $V = V_{rad}\sqrt{\left(Q_1 / Q_{1,rad}\right)\left(Q_2 / Q_{2,rad}\right)}$.

The following are examples within the scope of this aspect.

The apparatus has $Q_1 / Q_{1,rad} \geq 0.01$ and $Q_2 / Q_{2,rad} \geq 0.01$. The apparatus has $Q_1 / Q_{1,rad} \geq 0.1$ and $Q_2 / Q_{2,rad} \geq 0.1$. The apparatus has D / λ_o larger than 0.001 and the strong-interference factor V is larger than 0.01. The apparatus has D / λ_o larger than 0.001 and the strong-interference factor V is larger than 0.1. The apparatus includes the second resonator structure.

During operation, a power generator is coupled to one of the first and second resonant structure, with a coupling rate κ_g, and is configured to drive the resonator structure, to which it is coupled, at a driving frequency f, corresponding to a driving angular frequency $\omega = 2\pi f$, wherein U_g is defined as κ_g / Γ_1, if the power generator is coupled to the first resonator structure and defined as κ_g / Γ_2, if the power generator is coupled to the second resonator structure. The driving frequency is different from the resonance frequencies of the first and second resonator structures and is closer to a frequency corresponding to an odd normal mode of the system of the two resonator structures, wherein the detuning of the first resonator from the driving frequency is defined as $D_1 = \left(\omega - \omega_1\right) / \Gamma_1$ and the detuning of the second resonator structure from the driving frequency is defined as $D_2 = \left(\omega - \omega_2\right) / \Gamma_2$.

D_1 is approximately equal to UV_{rad} and D_2 is approximately equal to UV_{rad}. U_g is chosen to maximize the ratio of the energy-transfer efficiency to the radiation efficiency. U_g is approximately equal to $\sqrt{1+U^2-V_{rad}^2U^2+V^2-2VV_{rad}}$. f is at least larger than 100 kHz and smaller than 500MHz. f is at least larger than 1MHz and smaller

InductEV, Inc.
Exhibit 1025
Page 504

than 50MHz. The apparatus further includes the power generator. During operation, a power load is coupled to the resonant structure to which the power generator is not coupled, with a coupling rate κ_l, and is configured to receive from the resonator structure, to which it is coupled, a usable power, wherein U_l is defined as κ_l / Γ_1, if the power load is coupled to the first resonator structure and defined as κ_l / Γ_2, if the power load is coupled to the second resonator structure. U_l is chosen to maximize the ratio of the energy-transfer efficiency to the radiation efficiency. The driving frequency is different from the resonance frequencies of the first and second resonator structures and is closer to a frequency corresponding to an odd normal mode of the system of the two resonator structures, wherein the detuning of the first resonator from the driving frequency is defined as $D_1 = (\omega - \omega_1)/\Gamma_1$ and is approximately equal to UV_{rad}, and the detuning of the second resonator structure from the driving frequency is defined as $D_2 = (\omega - \omega_2)/\Gamma_2$ and is approximately equal to UV_{rad}, and U_l is approximately equal to $\sqrt{1+U^2-V_{rad}^2U^2+V^2-2VV_{rad}}$.

At least one of the first and second resonator structures comprises a capacitively loaded loop or coil of at least one of a conducting wire, a conducting Litz wire, and a conducting ribbon. The characteristic size of said loop or coil is less than 30 cm and the width of said conducting wire or Litz wire or ribbon is less than 2cm. The characteristic size of said loop or coil is less than 1m and the width of said conducting wire or Litz wire or ribbon is less than 2cm.

The apparatus further includes a feedback mechanism for maintaining the resonant frequency of one or more of the resonant objects. The feedback mechanism comprises an oscillator with a fixed driving frequency and is configured to adjust the resonant frequency of the one or more resonant objects to be detuned by a fixed amount with respect to the fixed frequency.

In an aspect, an apparatus for use in wireless energy transfer includes a first resonator structure configured for energy transfer with a second resonator structure over a distance *D*. The energy transfer is mediated by evanescent-tail coupling of a resonant field of the first resonator structure and a resonant field of the second resonator structure,

InductEV, Inc.
Exhibit 1025
Page 505

with a coupling factor k. The resonant field of the first resonator structure has a resonance angular frequency ω_1, a resonance frequency-width Γ_1, and a resonance quality factor $Q_1 = \omega_1 / 2\Gamma_1$, and is radiative in the far field, with an associated radiation quality factor $Q_{1,\text{rad}} \geq Q_1$, and the resonant field of the second resonator structure has a resonance angular frequency ω_2, a resonance frequency-width Γ_2, and a resonance quality factor $Q_2 = \omega_2 / 2\Gamma_2$, and is radiative in the far field, with an associated radiation quality factor $Q_{2,\text{rad}} \geq Q_2$. An absolute value of a difference of said angular frequencies ω_1 and ω_2 is smaller than the broader of said resonant widths Γ_1 and Γ_2, and an average resonant angular frequency is defined as $\omega_o = \sqrt{\omega_1 \omega_2}$, corresponding to an average resonant wavelength $\lambda_o = 2\pi c / \omega_o$, where c is the speed of light in free space, and a strong-coupling factor is defined as $U = k\sqrt{Q_1 Q_2}$. The apparatus is configured to employ interference between said radiative far fields of the resonant fields of the first and second resonator, with an interference factor V_{rad}, to increase efficiency of energy transfer for the apparatus compared to efficiency for the apparatus in the absence of interference, the strong-interference factor being defined as $V = V_{\text{rad}} \sqrt{\left(Q_1 / Q_{1,\text{rad}}\right)\left(Q_2 / Q_{2,\text{rad}}\right)}$.

The following are examples within the scope of this aspect.

The apparatus has $Q_1 / Q_{1,\text{rad}} \geq 0.05$ and $Q_2 / Q_{2,\text{rad}} \geq 0.05$. The apparatus has $Q_1 / Q_{1,\text{rad}} \geq 0.5$ and $Q_2 / Q_{2,\text{rad}} \geq 0.5$. The apparatus has D / λ_o larger than 0.01 and the strong-interference factor V is larger than 0.05. The apparatus has D / λ_o larger than 0.01 and the strong-interference factor V is larger than 0.5. The apparatus further includes the second resonator structure.

During operation, a power generator is coupled to one of the first and second resonant structure, with a coupling rate κ_g, and is configured to drive the resonator structure, to which it is coupled, at a driving frequency f, corresponding to a driving angular frequency $\omega = 2\pi f$, wherein U_g is defined as κ_g / Γ_1, if the power generator is coupled to the first resonator structure and defined as κ_g / Γ_2, if the power generator is coupled to the second resonator structure. The driving frequency is different from the

InductEV, Inc.
Exhibit 1025
Page 506

resonance frequencies of the first and second resonator structures and is closer to a frequency corresponding to an odd normal mode of the system of the two resonator structures, wherein the detuning of the first resonator from the driving frequency is defined as $D_1 = (\omega - \omega_1)/\Gamma_1$ and the detuning of the second resonator structure from the driving frequency is defined as $D_2 = (\omega - \omega_2)/\Gamma_2$.

D_1 is approximately equal to UV and D_2 is approximately equal to UV. U_g is chosen to maximize the energy-transfer efficiency. U_g is approximately equal to $\sqrt{(1+U^2)(1-V^2)}$. f is at least larger than 100 kHz and smaller than 500MHz. f is at least larger than 1MHz and smaller than 50MHz. The apparatus further includes the power generator.

During operation, a power load is coupled to the resonant structure to which the power generator is not coupled, with a coupling rate κ_l, and is configured to receive from the resonator structure, to which it is coupled, a usable power, wherein U_l is defined as κ_l/Γ_1, if the power load is coupled to the first resonator structure and defined as κ_l/Γ_2, if the power load is coupled to the second resonator structure. U_l is chosen to maximize the energy-transfer efficiency. The driving frequency is different from the resonance frequencies of the first and second resonator structures and is closer to a frequency corresponding to an odd normal mode of the system of the two resonator structures, wherein the detuning of the first resonator from the driving frequency is defined as $D_1 = (\omega - \omega_1)/\Gamma_1$ and is approximately equal to UV, and the detuning of the second resonator structure from the driving frequency is defined as $D_2 = (\omega - \omega_2)/\Gamma_2$ and is approximately equal to UV, and U_l is approximately equal to $\sqrt{(1+U^2)(1-V^2)}$.

At least one of the first and second resonator structures comprises a capacitively loaded loop or coil of at least one of a conducting wire, a conducting Litz wire, and a conducting ribbon. The characteristic size of said loop or coil is less than 30 cm and the width of said conducting wire or Litz wire or ribbon is less than 2cm. The characteristic size of said loop or coil is less than 1m and the width of said conducting wire or Litz wire

InductEV, Inc.
Exhibit 1025
Page 507

or ribbon is less than 2cm. The apparatus includes a feedback mechanism for maintaining the resonant frequency of one or more of the resonant objects. The feedback mechanism comprises an oscillator with a fixed driving frequency and is configured to adjust the resonant frequency of the one or more resonant objects to be detuned by a fixed amount with respect to the fixed frequency. The feedback mechanism is configured to monitor an efficiency of the energy transfer, and adjust the resonant frequency of the one or more resonant objects to maximize the efficiency. The resonance angular frequencies for the resonator structures are selected to optimize the energy-transfer efficiency by accounting for both the strong-coupling factor U and the strong-interference interference factor V.

In an aspect, a method for wireless energy transfer includes providing a first resonator structure configured for energy transfer with a second resonator structure over a distance D, wherein the energy transfer is mediated by evanescent-tail coupling of a resonant field of the first resonator structure and a resonant field of the second resonator structure, with a coupling factor k, wherein said resonant field of the first resonator structure has a resonance angular frequency ω_1, a resonance frequency-width Γ_1, and a resonance quality factor $Q_1 = \omega_1 / 2\Gamma_1$, and is radiative in the far field, with an associated radiation quality factor $Q_{1,\mathrm{rad}} \geq Q_1$, and resonant field of the second resonator structure has a resonance angular frequency ω_2, a resonance frequency-width Γ_2, and a resonance quality factor $Q_2 = \omega_2 / 2\Gamma_2$, and is radiative in the far field, with an associated radiation quality factor $Q_{2,\mathrm{rad}} \geq Q_2$, wherein an absolute value of a difference of said angular frequencies ω_1 and ω_2 is smaller than broader of said resonant widths Γ_1 and Γ_2, and an average resonant angular frequency is defined as $\omega_o = \sqrt{\omega_1 \omega_2}$, corresponding to an average resonant wavelength $\lambda_o = 2\pi c / \omega_o$, where c is the speed of light in free space, and the strong-coupling factor is defined as $U = k\sqrt{Q_1 Q_2}$, and employing interference between said radiative far fields of the resonant fields of the first and second resonator, with an interference factor V_{rad}, to reduce a total amount of radiation from the first and second resonator compared to an amount of radiation from the first and second resonator in the absence of interference, a strong-interference factor being defined as

InductEV, Inc.
Exhibit 1025
Page 508

$V = V_{\text{rad}} \sqrt{\left(Q_1 / Q_{1,\text{rad}}\right)\left(Q_2 / Q_{2,\text{rad}}\right)}$.

The following are examples within the scope of this aspect.

The method has $Q_1 / Q_{1,\text{rad}} \geq 0.01$ and $Q_2 / Q_{2,\text{rad}} \geq 0.01$. During operation, a power generator is coupled to one of the first and second resonant structure and is configured to drive the resonator structure, to which it is coupled, at a driving frequency *f*, corresponding to a driving angular frequency $\omega = 2\pi f$, wherein the driving frequency is different from the resonance frequencies of the first and second resonator structures and is closer to a frequency corresponding to an odd normal mode of the system of the two resonator structures. During operation, a power load is coupled to the resonant structure to which the power generator is not coupled and is configured to receive from the resonator structure, to which it is coupled, a usable power.

In an aspect, a method for wireless energy transfer includes providing a first resonator structure configured for energy transfer with a second resonator structure over a distance *D*, wherein the energy transfer is mediated by evanescent-tail coupling of a resonant field of the first resonator structure and a resonant field of the second resonator structure, with a coupling factor *k*, wherein said resonant field of the first resonator structure has a resonance angular frequency ω_1, a resonance frequency-width Γ_1, and a resonance quality factor $Q_1 = \omega_1 / 2\Gamma_1$, and is radiative in the far field, with an associated radiation quality factor $Q_{1,\text{rad}} \geq Q_1$, and said resonant field of the second resonator structure has a resonance angular frequency ω_2, a resonance frequency-width Γ_2, and a resonance quality factor $Q_2 = \omega_2 / 2\Gamma_2$, and is radiative in the far field, with an associated radiation quality factor $Q_{2,\text{rad}} \geq Q_2$, wherein an absolute value of the difference of said angular frequencies ω_1 and ω_2 is smaller than the broader of said resonant widths Γ_1 and Γ_2,and an average resonant angular frequency is defined as $\omega_o = \sqrt{\omega_1 \omega_2}$, corresponding to an average resonant wavelength $\lambda_o = 2\pi c / \omega_o$, where *c* is the speed of light in free space, and the strong-coupling factor is defined as $U = k\sqrt{Q_1 Q_2}$, and employing interference between said radiative far fields of the resonant fields of the first and second resonator, with an interference factor V_{rad}, to increase efficiency of energy transfer between the first

InductEV, Inc.
Exhibit 1025
Page 509

and second resonator compared to efficiency of energy transfer between the first and second resonator in the absence of interference, a strong-interference factor being defined as $V = V_{\text{rad}}\sqrt{\left(Q_1 / Q_{1,\text{rad}}\right)\left(Q_2 / Q_{2,\text{rad}}\right)}$.

The following are examples within the scope of this aspect.

The method has $Q_1 / Q_{1,\text{rad}} \geq 0.05$ and $Q_2 / Q_{2,\text{rad}} \geq 0.05$. During operation, a power generator is coupled to one of the first and second resonant structure and is configured to drive the resonator structure, to which it is coupled, at a driving frequency f, corresponding to a driving angular frequency $\omega = 2\pi f$, wherein the driving frequency is different from the resonance frequencies of the first and second resonator structures and is closer to a frequency corresponding to an odd normal mode of the system of the two resonator structures. During operation, a power load is coupled to the resonant structure to which the power generator is not coupled and is configured to receive from the resonator structure, to which it is coupled, a usable power. The resonance angular frequencies for the resonator structures are selected to optimize the energy-transfer efficiency by accounting for both the strong-coupling factor U and the strong-interference interference factor V.

Various examples may include any of the above features, alone or in combination. Other features, objects, and advantages of the disclosure will be apparent from the following detailed description.

BRIEF DESCRIPTION OF THE DRAWINGS

Fig. 1 shows a schematic of an example wireless energy transfer scheme.

Figs. 2(a)-(b) show the efficiency of power transmission η_P for (a) $U = 1$ and (b) $U = 3$, as a function of the frequency detuning D_ω and for different values of the loading rate U_ρ.

Fig. 2(c) shows the optimal (for zero detuning and under conditions of impedance matching) efficiency for energy transfer η_{E^*} and power transmission η_{P^*}, as a function of the coupling-to-loss figure-of-merit U.

Fig. 3 shows an example of a self-resonant conducting-wire coil.

InductEV, Inc.
Exhibit 1025
Page 510

Fig. 4 shows an example of a wireless energy transfer scheme featuring two self-resonant conducting-wire coils

Fig. 5 is a schematic of an experimental system demonstrating wireless energy transfer.

Fig. 6 shows a comparison between experimental and theoretical results for the coupling rate of the system shown schematically in Fig. 5.

Fig. 7 shows a comparison between experimental and theoretical results for the strong-coupling factor of the system shown schematically in Fig. 5.

Fig. 8 shows a comparison between experimental and theoretical results for the power-transmission efficiency of the system shown schematically in Fig. 5.

Fig. 9 shows an example of a capacitively loaded conducting-wire coil, and illustrates the surrounding field.

Fig. 10 shows an example wireless energy transfer scheme featuring two capacitively loaded conducting-wire coils, and illustrates the surrounding field.

Fig. 11 illustrates an example circuit model for wireless energy transfer.

Fig. 12 shows the efficiency, total (loaded) device Q, and source and device currents, voltages and radiated powers (normalized to 1Watt of output power to the load) as functions of the resonant frequency, for a particular choice of source and device loop dimensions, wp and N_s and different choices of N_d=1,2,3,4,5,6,10 (red, green, blue, magenta, yellow, cyan, black respectively).

Fig.13 shows the efficiency, total (loaded) device Q, and source and device currents, voltages and radiated powers (normalized to 1Watt of output power to the load) as functions of frequency and wp for a particular choice of source and device loop dimensions, and number of turns N_s and N_d.

Fig. 14 shows an example of an inductively-loaded conducting-wire coil.

Fig. 15 shows (a) an example of a resonant dielectric disk, and illustrates the surrounding field and (b) a wireless energy transfer scheme featuring two resonant dielectric disks, and illustrates the surrounding field.

Figs. 16(a)-(b) show the efficiency of power transmission η_P for (a) U = 1, V = 0.5 and (b) U = 3, V = 0.5, as a function of the frequency detuning Do and for different values of the loading rate U_o. (The dotted lines show, for comparison, the results when

InductEV, Inc.
Exhibit 1025
Page 511

there is no interference, as shown in Fig.2(a)-(b).) and Figs. 16(c)-(d) show the optimal (for optimal detuning and under conditions of impedance matching) efficiency for energy transfer (only in (c)) and power transmission, as a function of the strong-coupling factor U and the strong-interference factor V.

Fig. 17 shows coupled-mode theory (CMT) results for (a) the coupling factor k and (b) the strong-coupling factor U as a function of the relative distance D/r between two identical capacitively-loaded conducting single-turn loops, for three different dimensions of the loops. Note that, for conducting material, copper ($\sigma = 5.998 \cdot 10^7$ S/m) was used.

Fig. 18 shows AT results for the interference factor V_{rad} as a function of the distance D (normalized to the wavelength λ) between two capacitively-loaded conducting loops.

Fig. 19 shows CMT results for the strong-coupling factor U and AT results for the interference factor V_{rad} and strong-interference factor V as a function of the resonant eigenfrequency of two identical capacitively-loaded conducting single-turn loops with $r = 30$cm and $a = 2$cm , at a relative distance $D/r = 5$ between them. Note that, for conducting material, copper ($\sigma = 5.998 \cdot 10^7$ S/m) was used.

Fig. 20 shows the power-transmission efficiency as a function of the resonant eigenfrequency of two identical capacitively-loaded conducting single-turn loops. Results for two different loop dimensions are shown and for two relative distances between the identical loops. For each loops dimension and distance, four different cases are examined: without far-field interference (dotted), with far-field interference but no driving-frequency detuning (dashed) and with driving-frequency detuning to maximize either the efficiency (solid) or the ratio of efficiency over radiation (dash-dotted).

Fig. 21 shows the driving-frequency detunings required in the presence of far-field interference as a function of the resonant eigenfrequency of two identical capacitively-loaded conducting single-turn loops of Fig. 20 to maximize either the efficiency (solid) or the ratio of efficiency over radiation (dash-dotted).

Fig. 22(a) shows the resonant eigenfrequencies f_U and f_η, where the strong-coupling factor U and the power-transmission efficiency η peak respectively, as a

InductEV, Inc.
Exhibit 1025
Page 512

function of the relative distance D/r between two identical loops with $r = 30\text{cm}$ and $a = 2\text{cm}$.

Fig. 22(b) illustrates the strong-coupling factor U and the strong-interference factor V as a curve in the $U-V$ plane, parametrized with the relative distance D/r between the two loops, for the cases with interference and eigenfrequency f_η (solid), with interference and eigenfrequency f_U (dashed), and without interference and eigenfrequency f_U (dotted).

Fig. 22(c) shows the efficiency enhancement ratio of the solid curve in Fig. 22(b) relative to the dashed and dotted curves in Fig. 22(b).

Fig. 23 shows the radiation efficiency as a function of the resonant eigenfrequency of two identical capacitively-loaded conducting single-turn loops. Results for two different loop dimensions are shown and for two relative distances between the identical loops. For each loops dimension and distance, four different cases are examined: without far-field interference (dotted), with far-field interference but no driving-frequency detuning (dashed) and with driving-frequency detuning to maximize either the efficiency (solid) or the ratio of efficiency over radiation (dash-dotted).

Fig. 24 shows CMT results for (a) the coupling factor k and (b) the strong-coupling factor U, for three different m values of subwavelength resonant modes of two same dielectric disks at distance $D/r = 5$ (and also a couple more distances for $m = 2$), when varying their ϵ in the range $250 \geq \epsilon \geq 35$. Note that disk-material loss-tangent $\tan\delta = 6{\cdot}10^{-6}\epsilon - 2{\cdot}10^{-4}$ was used. (c) Relative U error between CMT and numerical FEFD calculations of part (b).

Fig. 25 shows Antenna Theory (AT) results for (a) the normalized interference term $2\Lambda/\sqrt{\omega_1\omega_2}$ and (b) magnitude of the strong-interference factor $|V|$, as a function of frequency, for the exact same parameters as in Fig.24. (c) Relative V error between AT and numerical FEFD calculations of part (b).

Fig. 26 shows results for the overall power transmission as a function of frequency, for the same set of resonant modes and distances as in Figs.24 and 25, based on the predictions including interference (solid lines) and without interference, just from U (dotted lines).

InductEV, Inc.
Exhibit 1025
Page 513

Fig. 27 (a) shows the frequencies f_U and f_η, where the strong-coupling factor U and the power-transmission efficiency η are respectively maximized, as a function of the transfer distance between the $m = 2$ disks of Fig. 15. Fig. 27(b) shows the efficiencies achieved at the frequencies of (a) and, in inset, the enhancement ratio of the optimal (by definition) efficiency for f_η versus the achievable efficiency at f_U. Fig. 27(c) shows the D-parametrized path of the transmission efficiency for the frequency choices of (a) on the $U-V$ efficiency map.

Fig. 28 shows results for the radiation efficiency as a function of the transfer distance at resonant frequency f_U, when the operating frequency is detuned (solid line), when it is not (dashed line), and when there is no interference whatsoever (dotted line). In the inset, we show the corresponding radiation suppression factors.

Figs. 29(a)-(b) show schematics for frequency control mechanisms.

Figs. 30(a)-(c) illustrate a wireless energy transfer scheme using two dielectric disks in the presence of various extraneous objects.

DETAILED DESCRIPTION

1. Efficient energy-transfer by 'strongly coupled' resonances

Fig. 1 shows a schematic that generally describes one example of the invention, in which energy is transferred wirelessly between two resonant objects. Referring to Fig. 1, energy is transferred, over a distance D, between a resonant source object having a characteristic size r_1 and a resonant device object of characteristic size r_2. Both objects are resonant objects. The wireless non-radiative energy transfer is performed using the field (e.g. the electromagnetic field or acoustic field) of the system of two resonant objects.

The characteristic size of an object can be regarded as being equal to the radius of the smallest sphere which can fit around the entire object. The characteristic thickness of an object can be regarded as being, when placed on a flat surface in any arbitrary configuration, the smallest possible height of the highest point of the object above a flat surface. The characteristic width of an object can be regarded as being the radius of the

InductEV, Inc.
Exhibit 1025
Page 514

smallest possible circle that the object can pass through while traveling in a straight line. For example, the characteristic width of a cylindrical object is the radius of the cylinder.

It is to be understood that while two resonant objects are shown in the example of Fig. 1, and in many of the examples below, other examples can feature three or more resonant objects. For example, in some examples, a single source object can transfer energy to multiple device objects. In some examples, energy can be transferred from a first resonant object to a second resonant object, and then from the second resonant object to a third resonant object, and so forth.

Initially, we present a theoretical framework for understanding non-radiative wireless energy transfer. Note however that it is to be understood that the scope of the invention is not bound by theory.

Different temporal schemes can be employed, depending on the application, to transfer energy between two resonant objects. Here we will consider two particularly simple but important schemes: a one-time finite-amount energy-transfer scheme and a continuous finite-rate energy-transfer (power) scheme.

1.1 Finite-amount energy-transfer efficiency

Let the source and device objects be 1, 2 respectively and their resonance eigemodes, which we will use for the energy exchange, have angular frequencies $\omega_{1,2}$, frequency-widths due to intrinsic (absorption, radiation etc.) losses $\Gamma_{1,2}$ and (generally) vector fields $\mathbf{F}_{1,2}(\mathbf{r})$, normalized to unity energy. Once the two resonant objects are brought in proximity, they can interact and an appropriate analytical framework for modeling this resonant interaction is that of the well-known coupled-mode theory (CMT). In this picture, the field of the system of the two resonant objects 1, 2 can be approximated by $\mathbf{F}(\mathbf{r},t) = a_1(t)\mathbf{F}_1(\mathbf{r}) + a_2(t)\mathbf{F}_2(\mathbf{r})$, where $a_{1,2}(t)$ are the field amplitudes, with $|a_{1,2}(t)|^2$ equal to the energy stored inside the object 1, 2 respectively, due to the normalization. Then, using $e^{-i\omega t}$ time dependence, the field amplitudes can be shown to satisfy, to lowest order:

InductEV, Inc.
Exhibit 1025
Page 515

$$\begin{aligned}\frac{d}{dt}a_1(t) &= -i(\omega_1 - i\Gamma_1)a_1(t) + i\kappa_{11}a_1(t) + i\kappa_{12}a_2(t)\\ \frac{d}{dt}a_2(t) &= -i(\omega_2 - i\Gamma_2)a_2(t) + i\kappa_{21}a_1(t) + i\kappa_{22}a_2(t)\end{aligned} \quad (1)$$

where $\kappa_{11,22}$ are the shifts in each object's frequency due to the presence of the other, which are a second-order correction and can be absorbed into the eigenfrequencies by setting $\omega_{1,2} \to \omega_{1,2} + \kappa_{11,22}$, and $\kappa_{12,21}$ are the coupling coefficients, which from the reciprocity requirement of the system must satisfy $\kappa_{21} = \kappa_{12} \equiv \kappa$.

The normal modes of the combined system are found, by substituting $[a_1(t), a_2(t)] = [A_1, A_2]e^{-i\bar{\omega}t}$, to have complex frequencies

$$\bar{\omega}_{\pm} = \frac{\omega_1 + \omega_2}{2} - i\frac{\Gamma_1 + \Gamma_2}{2} \pm \sqrt{\left(\frac{\omega_1 - \omega_2}{2} - i\frac{\Gamma_1 - \Gamma_2}{2}\right)^2 + \kappa^2} \quad (2)$$

whose splitting we denote as $\delta_E \equiv \bar{\omega}_+ - \bar{\omega}_-$. Note that, at exact resonance $\omega_1 = \omega_2$ and for $\Gamma_1 = \Gamma_2$, we get $\delta_E = 2\kappa$.

Assume now that at time $t = 0$ the source object 1 has finite energy $|a_1(0)|^2$, while the device object has $|a_2(0)|^2 = 0$. Since the objects are coupled, energy will be transferred from 1 to 2. With these initial conditions, Eqs.(1) can be solved, predicting the evolution of the device field-amplitude to be

$$\frac{a_2(t)}{|a_1(0)|} = \frac{2\kappa}{\delta_E}\sin\left(\frac{\delta_E t}{2}\right)e^{-\frac{\Gamma_1+\Gamma_2}{2}t}. \quad (3)$$

The energy-transfer efficiency will be $\eta_E \equiv |a_2(t)|^2/|a_1(0)|^2$. Note that, at exact resonance $\omega_1 = \omega_2$ and in the special case $\Gamma_1 = \Gamma_2 \equiv \Gamma_o$, Eq.(3) can be written as

$$\frac{a_2(T)}{|a_1(0)|} = \sin(UT)e^{-T} \quad (4)$$

where $T \equiv \Gamma_o t$ and $U = \kappa/\Gamma_o$.

InductEV, Inc.
Exhibit 1025
Page 516

In some examples, the system designer can adjust the duration of the coupling t at will. In some examples, the duration t can be adjusted to maximize the device energy (and thus efficiency η_E). Then, in the special case $\Gamma_1 = \Gamma_2 = \Gamma_o$, it can be inferred from Eq.(4) that η_E is maximized for

$$T_* = \frac{\tan^{-1} U}{U} \tag{5}$$

resulting in an optimal energy-transfer efficiency

$$\eta_{E^*} \equiv \eta_E(T_*) = \frac{U^2}{1+U^2} \exp\left(-\frac{2\tan^{-1} U}{U}\right) \tag{6}$$

which is only a function of the coupling-to-loss ratio $U = \kappa/\Gamma_o$ and tends to unity when $U \gg 1$, as depicted in Fig.2(c). In general, also for $\Gamma_1 \neq \Gamma_2$, the energy transfer is nearly perfect, when the coupling rate is much faster than all loss rates ($\kappa/\Gamma_{1,2} \gg 1$).

In a real wireless energy-transfer system, the source object can be connected to a power generator (not shown in Fig.1), and the device object can be connected to a power consuming load (e.g. a resistor, a battery, an actual device, not shown in Fig.1). The generator will supply the energy to the source object, the energy will be transferred wirelessly and non-radiatively from the source object to the device object, and the load will consume the energy from the device object. To incorporate such supply and consumption mechanisms into this temporal scheme, in some examples, one can imagine that the generator is very briefly but very strongly coupled to the source at time $t = 0$ to almost instantaneously provide the energy, and the load is similarly very briefly but very strongly coupled to the device at the optimal time $t = t_*$ to almost instantaneously drain the energy. For a constant powering mechanism, at time $t = t_*$ also the generator can again be coupled to the source to feed a new amount of energy, and this process can be repeated periodically with a period t_*.

1.2 Finite-rate energy-transfer (power-transmission) efficiency

Let the generator be continuously supplying energy to the source object 1 at a rate κ_1 and the load continuously draining energy from the device object 2 at a rate κ_2. Field amplitudes $s_{+1,2}(t)$ are then defined, so that $|s_{+1,2}(t)|^2$ is equal to the power ingoing to

InductEV, Inc.
Exhibit 1025
Page 517

(for the + sign) or outgoing from (for the - sign) the object 1, 2 respectively, and the CMT equations are modified to

$$\begin{aligned}
\frac{d}{dt}a_1(t) &= -i(\omega_1 - i\Gamma_1)a_1(t) + i\kappa_{11}a_1(t) + i\kappa_{12}a_2(t) - \kappa_1 a_1(t) + \sqrt{2\kappa_1}s_{+1}(t) \\
\frac{d}{dt}a_2(t) &= -i(\omega_2 - i\Gamma_2)a_2(t) + i\kappa_{21}a_1(t) + i\kappa_{22}a_2(t) - \kappa_2 a_2(t) \\
s_{-1}(t) &= \sqrt{2\kappa_1}a_1(t) - s_{+1}(t) \\
s_{-2}(t) &= \sqrt{2\kappa_2}a_2(t)
\end{aligned} \tag{7}$$

where again we can set $\omega_{1,2} \to \omega_{1,2} + \kappa_{11,22}$ and $\kappa_{21} = \kappa_{12} \equiv \kappa$.

Assume now that the excitation is at a fixed frequency ω, namely has the form $s_{+1}(t) = S_{+1}e^{-i\omega t}$. Then the response of the linear system will be at the same frequency, namely $a_{1,2}(t) = A_{1,2}e^{-i\omega t}$ and $s_{-1,2}(t) = S_{-1,2}e^{-i\omega t}$. By substituting these into Eqs.(7), using $\delta_{1,2} \equiv \omega - \omega_{1,2}$, and solving the system, we find the field-amplitude transmitted to the load (S_{21} scattering-matrix element)

$$\begin{aligned}
S_{21} \equiv \frac{S_{-2}}{S_{+1}} &= \frac{2i\kappa\sqrt{\kappa_1\kappa_2}}{(\Gamma_1 + \kappa_1 - i\delta_1)(\Gamma_2 + \kappa_2 - i\delta_2) + \kappa^2} \\
&= \frac{2iU\sqrt{U_1U_2}}{(1 + U_1 - iD_1)(1 + U_2 - iD_2) + U^2}
\end{aligned} \tag{8}$$

and the field-amplitude reflected to the generator (S_{11} scattering-matrix element)

$$\begin{aligned}
S_{11} \equiv \frac{S_{-1}}{S_{+1}} &= \frac{(\Gamma_1 - \kappa_1 - i\delta_1)(\Gamma_2 + \kappa_2 - i\delta_2) + \kappa^2}{(\Gamma_1 + \kappa_1 - i\delta_1)(\Gamma_2 + \kappa_2 - i\delta_2) + \kappa^2} \\
&= \frac{(1 - U_1 - iD_1)(1 + U_2 - iD_2) + U^2}{(1 + U_1 - iD_1)(1 + U_2 - iD_2) + U^2}
\end{aligned} \tag{9}$$

where $D_{1,2} \equiv \delta_{1,2}/\Gamma_{1,2}$, $U_{1,2} \equiv \kappa_{1,2}/\Gamma_{1,2}$ and $U \equiv \kappa/\sqrt{\Gamma_1\Gamma_2}$. Similarly, the scattering-matrix elementsS_{12}, S_{22} are given by interchanging $1 \leftrightarrow 2$ in Eqs.(8),(9) and, as expected from reciprocity, $S_{21} = S_{12}$. The coefficients for power transmission (efficiency) and reflection and loss are respectively $\eta_P \equiv |S_{21}|^2 = |S_{-2}|^2/|S_{+1}|^2$ and $|S_{11}|^2 = |S_{-1}|^2/|S_{+1}|^2$ and $1 - |S_{21}|^2 - |S_{11}|^2 = (2\Gamma_1|A_1|^2 + 2\Gamma_2|A_2|^2)/|S_{+1}|^2$.

In practice, in some implementations, the parameters $D_{1,2}$, $U_{1,2}$ can be designed (engineered), since one can adjust the resonant frequencies $\omega_{1,2}$ (compared to the desired

InductEV, Inc.
Exhibit 1025
Page 518

operating frequency ω) and the generator/load supply/drain rates $\kappa_{1,2}$. Their choice can target the optimization of some system performance-characteristic of interest:

In some examples, a goal can be to maximize the power transmission (efficiency) $\eta_P \equiv |S_{21}|^2$ of the system, so one would require

$$\eta_P'(D_{1,2}) = \eta_P'(U_{1,2}) = 0 \tag{10}$$

Since S_{21} (from Eq.(8)) is symmetric upon interchanging $1 \leftrightarrow 2$, the optimal values for $D_{1,2}$ (determined by Eqs.(10)) will be equal, namely $D_1 = D_2 \equiv D_o$, and similarly $U_1 = U_2 \equiv U_o$. Then,

$$S_{21} = \frac{2iUU_o}{(1+U_o-iD_o)^2+U^2} \tag{11}$$

and from the condition $\eta_P'(D_o) = 0$ we get that, for fixed values of U and U_o, the efficiency can be maximized for the following values of the symmetric detuning

$$D_o = \begin{cases} \pm\sqrt{U^2-(1+U_o)^2}, & \text{if } U > 1+U_o \\ 0, & \text{if } U \le 1+U_o \end{cases}, \tag{12}$$

which, in the case $U > 1 + U_o$, can be rewritten for the two frequencies at which the efficiency peaks as

$$\omega_\pm = \frac{\omega_1\Gamma_2+\omega_2\Gamma_1}{\Gamma_1+\Gamma_2} \pm \frac{2\sqrt{\Gamma_1\Gamma_2}}{\Gamma_1+\Gamma_2}\sqrt{\kappa^2-(\Gamma_1+\kappa_1)(\Gamma_2+\kappa_2)}, \tag{13}$$

whose splitting we denote as $\delta_P \equiv \bar{\omega}_+ - \bar{\omega}_-$. Note that, at exact resonance $\omega_1 = \omega_2$, and for $\Gamma_1 = \Gamma_2 \equiv \Gamma_o$ and $\kappa_1 = \kappa_2 \equiv \kappa_o$, we get $\delta_P = 2\sqrt{\kappa^2 - (\Gamma_o + \kappa_o)^2} < \delta_E$, namely the transmission-peak splitting is smaller than the normal-mode splitting. Then, by substituting D_o into η_P from Eq.(12), from the condition $\eta_P'(U_o) = 0$ we get that, for fixed value of U, the efficiency can be maximized for

$$U_{o*} = \sqrt{1+U^2} \quad \overset{\text{Eq.(12)}}{\Rightarrow} \quad D_{o*} = 0 \tag{14}$$

which is known as 'critical coupling' condition, whereas for $U_o < U_{o*}$ the system is called 'undercoupled' and for $U_o > U_{o*}$ it is called 'overcoupled'. The dependence of the efficiency on the frequency detuning D_o for different values of U_o (including the

InductEV, Inc.
Exhibit 1025
Page 519

'critical-coupling' condition) are shown in Fig. 2(a,b). The overall optimal power efficiency using Eqs.(14) is

$$\eta_{P^*} \equiv \eta_P\left(D_{o^*}, U_{o^*}\right) = \frac{U_{o^*}-1}{U_{o^*}+1} = \left(\frac{U}{1+\sqrt{1+U^2}}\right)^2, \tag{15}$$

which is again only a function of the coupling-to-loss ratio $U = \kappa/\sqrt{\Gamma_1\Gamma_2}$ and tends to unity when $U \gg 1$, as depicted in Fig. 2(c).

In some examples, a goal can be to minimize the power reflection at the side of the generator $|S_{11}|^2$ and the load $|S_{22}|^2$, so one would then need

$$S_{11,22} = 0 \Rightarrow \left(1 \mp U_1 - iD_1\right)\left(1 \pm U_2 - iD_2\right) + U^2 = 0, \tag{16}$$

The equations above present 'impedance matching' conditions. Again, the set of these conditions is symmetric upon interchanging $1 \leftrightarrow 2$, so, by substituting $D_1 = D_2 \equiv D_o$ and $U_1 = U_2 \equiv U_o$ into Eqs.(16), we get

$$\left(1 - iD_o\right)^2 - U_o^2 + U^2 = 0, \tag{17}$$

from which we easily find that the values of D_o and U_o that cancel all reflections are again exactly those in Eqs.(14).

It can be seen that, for this particular problem, the two goals and their associated sets of conditions (Eqs.(10) and Eqs.(16)) result in the same optimized values of the intra-source and intra-device parameters $D_{1,2}$, $U_{1,2}$. Note that for a lossless system this would be an immediate consequence of power conservation (Hermiticity of the scattering matrix), but this is not apparent for a lossy system.

Accordingly, for any temporal energy-transfer scheme, once the parameters specific only to the source or to the device (such as their resonant frequencies and their excitation or loading rates respectively) have been optimally designed, the efficiency monotonically increases with the ratio of the source-device coupling-rate to their loss rates. Using the definition of a resonance quality factor $Q = \omega/2\Gamma$ and defining by analogy the coupling factor $k \equiv 1/Q_\kappa \equiv 2\kappa/\sqrt{\omega_1\omega_2}$, it is therefore exactly this ratio

InductEV, Inc.
Exhibit 1025
Page 520

$$U = \frac{\kappa}{\sqrt{\Gamma_1 \Gamma_2}} = k\sqrt{Q_1 Q_2} \tag{18}$$

that has been set as a figure-of-merit for any system under consideration for wireless energy-transfer, along with the distance over which this ratio can be achieved (clearly, U will be a decreasing function of distance). The desired optimal regime $U > 1$ is called 'strong-coupling' regime and it is a necessary and sufficient condition for efficient energy-transfer. In particular, for $U > 1$ we get, from Eq.(15), $\eta_{P*} > 17\%$, large enough for practical applications. The figure-of-merit U is called the strong-coupling factor. We will further show how to design systems with a large strong-coupling factor.

To achieve a large strong-coupling factor U, in some examples, the energy-transfer application preferably uses resonant modes of high quality factors Q, corresponding to low (i.e. slow) intrinsic-loss rates Γ. This condition can be satisfied by designing resonant modes where all loss mechanisms, typically radiation and absorption, are sufficiently suppressed.

This suggests that the coupling be implemented using, not the lossy radiative far-field, which should rather be suppressed, but the evanescent (non-lossy) stationary near-field. To implement an energy-transfer scheme, usually more appropriate are finite objects, namely ones that are topologically surrounded everywhere by air, into where the near field extends to achieve the coupling. Objects of finite extent do not generally support electromagnetic states that are exponentially decaying in *all* directions in air away from the objects, since Maxwell's Equations in free space imply that $\mathbf{k}^2 = \omega^2/c^2$, where $\mathbf{k}$ is the wave vector, ω the angular frequency, and c the speed of light, because of which one can show that such finite objects cannot support states of infinite Q, rather there always is some amount of radiation. However, very long-lived (so-called "high-Q") states can be found, whose tails display the needed exponential or exponential-like decay away from the resonant object over long enough distances before they turn oscillatory (radiative). The limiting surface, where this change in the field behavior happens, is called the "radiation caustic", and, for the wireless energy-transfer scheme to be based on the near field rather than the far/radiation field, the distance between the coupled objects must be such that one lies within the radiation caustic of the other. One typical way of achieving a high radiation-Q (Q_{rad}) is to design subwavelength resonant objects. When

InductEV, Inc.
Exhibit 1025
Page 521

the size of an object is much smaller than the wavelength of radiation in free space, its electromagnetic field couples to radiation very weakly. Since the extent of the near-field into the area surrounding a finite-sized resonant object is set typically by the wavelength, in some examples, resonant objects of subwavelength size have significantly longer evanescent field-tails. In other words, the radiation caustic is pushed far away from the object, so the electromagnetic mode enters the radiative regime only with a small amplitude.

Moreover, most realistic materials exhibit some nonzero amount of absorption, which can be frequency dependent, and thus cannot support states of infinite Q, rather there always is some amount of absorption. However, very long-lived ("high-Q") states can be found, where electromagnetic modal energy is only weakly dissipated. Some typical ways of achieving a high absorption-Q (Q_{abs}) is to use materials which exhibit very small absorption at the resonant frequency and/or to shape the field to be localized more inside the least lossy materials.

Furthermore, to achieve a large strong-coupling factor U, in some examples, the energy-transfer application preferably uses systems that achieve a high coupling factor k, corresponding to strong (i.e. fast) coupling rate κ, over distances larger than the characteristic sizes of the objects.

Since finite-sized subwavelength resonant objects can often be accompanied with a high Q, as was discussed above and will be seen in examples later on, such an object will typically be the appropriate choice for the possibly-mobile resonant device-object. In these cases, the electromagnetic field is, in some examples, of quasi-static nature and the distance, up to which sufficient coupling can be achieved, is dictated by the decay-law of this quasi-static field.

Note, though, that in some examples, the resonant source-object will be immobile and thus less restricted in its allowed geometry and size. It can be therefore chosen large enough that the near-field extent is not limited by the wavelength, and can thus have nearly infinite radiation-Q. Some objects of nearly infinite extent, such as dielectric waveguides, can support guided modes, whose evanescent tails are decaying exponentially in the direction away from the object, slowly if tuned close to cutoff,

InductEV, Inc.
Exhibit 1025
Page 522

therefore a good coupling can also be achieved over distances quite a few times larger than a characteristic size of the source- and/or device-object.

2 'Strongly-coupled' resonances at mid-range distances for realistic systems

In the following, examples of systems suitable for energy transfer of the type described above are described. We will demonstrate how to compute the CMT parameters $\omega_{1,2}$, $Q_{1,2}$ and k described above and how to choose or design these parameters for particular examples in order to produce a desirable figure-of-merit $U = \kappa/\sqrt{\Gamma_1\Gamma_2} = k\sqrt{Q_1Q_2}$ at a desired distance D. In some examples, this figure-of-merit is maximized when $\omega_{1,2}$ are tuned close to a particular angular frequency ω_U.

2.1 Self-resonant conducting coils

In some examples, one or more of the resonant objects are self-resonant conducting coils. Referring to Fig. 3, a conducting wire of length l and cross-sectional radius a is wound into a helical coil of radius r and height h (namely with $N = \sqrt{l^2 - h^2}/2\pi r$ number of turns), surrounded by air. As described below, the wire has distributed inductance and distributed capacitance, and therefore it supports a resonant mode of angular frequency ω. The nature of the resonance lies in the periodic exchange of energy from the electric field within the capacitance of the coil, due to the charge distribution $\rho(\mathbf{x})$ across it, to the magnetic field in free space, due to the current distribution $\mathbf{j}(\mathbf{x})$ in the wire. In particular, the charge conservation equation $\nabla \cdot \mathbf{j} = i\omega\rho$ implies that: (i) this periodic exchange is accompanied by a $\pi/2$ phase-shift between the current and the charge density profiles, namely the energy W contained in the coil is at certain points in time completely due to the current and at other points in time completely due to the charge, and (ii) if $\rho_l(x)$ and $I(x)$ are respectively the linear charge and current densities in the wire, where x runs along the wire, $q_o = \frac{1}{2}\int dx|\rho_l(x)|$ is the maximum amount of positive charge accumulated in one side of the coil (where an equal amount of negative charge always also accumulates in the other side to make the system neutral) and $I_o = \max\{|I(x)|\}$ is the maximum positive value of the linear current distribution, then

InductEV, Inc.
Exhibit 1025
Page 523

$I_o = \omega q_o$. Then, one can define an effective total inductance L and an effective total capacitance C of the coil through the amount of energy W inside its resonant mode:

$$W \equiv \frac{1}{2} I_o^2 L \Rightarrow L = \frac{\mu_o}{4\pi I_o^2} \iint d\mathbf{x} d\mathbf{x}' \frac{\mathbf{j}(\mathbf{x}) \cdot \mathbf{j}(\mathbf{x}')}{|\mathbf{x} - \mathbf{x}'|}, \tag{19}$$

$$W \equiv \frac{1}{2} q_o^2 \frac{1}{C} \Rightarrow \frac{1}{C} = \frac{1}{4\pi\varepsilon_o q_o^2} \iint d\mathbf{x} d\mathbf{x}' \frac{\rho(\mathbf{x})\rho(\mathbf{x}')}{|\mathbf{x} - \mathbf{x}'|}, \tag{20}$$

where μ_o and ε_o are the magnetic permeability and electric permittivity of free space.

With these definitions, the resonant angular frequency and the effective impedance can be given by the formulas $\omega = 1/\sqrt{LC}$ and $Z = \sqrt{L/C}$ respectively.

Losses in this resonant system consist of ohmic (material absorption) loss inside the wire and radiative loss into free space. One can again define a total absorption resistance R_{abs} from the amount of power absorbed inside the wire and a total radiation resistance R_{rad} from the amount of power radiated due to electric- and magnetic-dipole radiation:

$$P_{abs} \equiv \frac{1}{2} I_o^2 R_{abs} \Rightarrow R_{abs} \approx \zeta_c \frac{l}{2\pi a} \cdot \frac{I_{rms}^2}{I_o^2} \tag{21}$$

$$P_{rad} \equiv \frac{1}{2} I_o^2 R_{rad} \Rightarrow R_{rad} \approx \frac{\zeta_o}{6\pi} \left[\left(\frac{\omega |\mathbf{p}|}{c} \right)^2 + \left(\frac{\omega \sqrt{|\mathbf{m}|}}{c} \right)^4 \right], \tag{22}$$

where $c = 1/\sqrt{\mu_o \varepsilon_o}$ and $\zeta_o = \sqrt{\mu_o / \varepsilon_o}$ are the light velocity and light impedance in free space, the impedance ζ_c is $\zeta_c = 1/\sigma\delta = \sqrt{\mu_o \omega / 2\sigma}$ with σ the conductivity of the conductor and δ the skin depth at the frequency ω, $I_{rms}^2 = \frac{1}{l} \int dx |I(x)|^2$, $\mathbf{p} = \int dx\, \mathbf{r} \rho_l(x)$ is the electric-dipole moment of the coil and $\mathbf{m} = \frac{1}{2} \int dx\, \mathbf{r} \times \mathbf{j}(x)$ is the magnetic-dipole moment of the coil. For the radiation resistance formula Eq.(22), the assumption of operation in the quasi-static regime ($h, r \ll \lambda = 2\pi c/\omega$) has been used, which is the desired regime of a subwavelength resonance. With these definitions, the absorption and

InductEV, Inc.
Exhibit 1025
Page 524

radiation quality factors of the resonance are given by $Q_{abs} = Z / R_{abs}$ and $Q_{rad} = Z / R_{rad}$ respectively.

From Eq.(19)-(22) it follows that to determine the resonance parameters one simply needs to know the current distribution $\mathbf{j}$ in the resonant coil. Solving Maxwell's equations to rigorously find the current distribution of the resonant electromagnetic eigenmode of a conducting-wire coil is more involved than, for example, of a standard LC circuit, and we can find no exact solutions in the literature for coils of finite length, making an exact solution difficult. One could in principle write down an elaborate transmission-line-like model, and solve it by brute force. We instead present a model that is (as described below) in good agreement (~5%) with experiment. Observing that the finite extent of the conductor forming each coil imposes the boundary condition that the current has to be zero at the ends of the coil, since no current can leave the wire, we assume that the resonant mode of each coil is well approximated by a sinusoidal current profile along the length of the conducting wire. We shall be interested in the lowest mode, so if we denote by x the coordinate along the conductor, such that it runs from $-l/2$ to $+l/2$, then the current amplitude profile would have the form $I(x) = I_o \cos(\pi x / l)$, where we have assumed that the current does not vary significantly along the wire circumference for a particular x, a valid assumption provided $a \ll r$. It immediately follows from the continuity equation for charge that the linear charge density profile should be of the form $\rho_l(x) = \rho_o \sin(\pi x / l)$, and thus $q_o = \int_0^{l/2} dx \rho_o \left|\sin(\pi x / l)\right| = \rho_o l / \pi$. Using these sinusoidal profiles we find the so-called "self-inductance" L_s and "self-capacitance" C_s of the coil by computing numerically the integrals Eq.(19) and (20); the associated frequency and effective impedance are ω_s and Z_s respectively. The "self-resistances" R_s are given analytically by Eq.(21) and (22) using $I_{rms}^2 = \frac{1}{l}\int_{-l/2}^{l/2} dx \left|I_o \cos(\pi x / l)\right|^2 = \frac{1}{2} I_o^2$, $|\mathbf{p}| = q_o \sqrt{\left(\frac{2}{\pi} h\right)^2 + \left(\frac{4N\cos(\pi N)}{(4N^2-1)\pi} r\right)^2}$ and

InductEV, Inc.
Exhibit 1025
Page 525

$|\mathbf{m}| = I_o\sqrt{\left(\frac{2}{\pi}N\pi r^2\right)^2 + \left(\frac{\cos(\pi N)(12N^2-1)-\sin(\pi N)\pi N(4N^2-1)}{(16N^4-8N^2+1)\pi}hr\right)^2}$, and therefore the associated Q_s factors can be calculated.

The results for two examples of resonant coils with subwavelength modes of $\lambda_s / r \geq 70$ (i.e. those highly suitable for near-field coupling and well within the quasi-static limit) are presented in Table 1. Numerical results are shown for the wavelength and absorption, radiation and total loss rates, for the two different cases of subwavelength-coil resonant modes. Note that, for conducting material, copper (σ=5.998•10^-7 S/m) was used. It can be seen that expected quality factors at microwave frequencies are $Q_{s,abs} \geq 1000$ and $Q_{s,rad} \geq 5000$.

Table 1

single coil	λ_s / r	f (MHz)	$Q_{s,rad}$	$Q_{s,abs}$	Q_s
r=30cm, h=20cm, a=1cm, N=4	74.7	13.39	4164	8170	2758
r=10cm, h=3cm, a=2mm, N=6	140	21.38	43919	3968	3639

Referring to Fig. 4, in some examples, energy is transferred between two self-resonant conducting-wire coils. The electric and magnetic fields are used to couple the different resonant conducting-wire coils at a distance D between their centers. Usually, the electric coupling highly dominates over the magnetic coupling in the system under consideration for coils with $h \gg 2r$ and, oppositely, the magnetic coupling highly dominates over the electric coupling for coils with $h \ll 2r$. Defining the charge and current distributions of two coils 1,2 respectively as $\rho_{1,2}(\mathbf{x})$ and $\mathbf{j}_{1,2}(\mathbf{x})$, total charges and peak currents respectively as $q_{1,2}$ and $I_{1,2}$, and capacitances and inductances respectively as $C_{1,2}$ and $L_{1,2}$, which are the analogs of $\rho(\mathbf{x})$, $\mathbf{j}(\mathbf{x})$, q_o, I_o, C and L for the single-coil case and are therefore well defined, we can *define* their mutual capacitance and inductance through the total energy:

InductEV, Inc.
Exhibit 1025
Page 526

$$W \equiv W_1 + W_2 + \frac{1}{2}\left(q_1^* q_2 + q_2^* q_1\right)/M_C + \frac{1}{2}\left(I_1^* I_2 + I_2^* I_1\right)M_L$$

$$\Rightarrow 1/M_C = \frac{1}{4\pi\varepsilon_o q_1 q_2}\iint d\mathbf{x}d\mathbf{x}'\frac{\rho_1(\mathbf{x})\rho_2(\mathbf{x}')}{|\mathbf{x}-\mathbf{x}'|}u, \quad M_L = \frac{\mu_o}{4\pi I_1 I_2}\iint d\mathbf{x}d\mathbf{x}'\frac{\mathbf{j}_1(\mathbf{x})\cdot\mathbf{j}_2(\mathbf{x}')}{|\mathbf{x}-\mathbf{x}'|}u, \quad (23)$$

where $W_1 = \frac{1}{2}q_1^2/C_1 = \frac{1}{2}I_1^2 L_1$, $W_2 = \frac{1}{2}q_2^2/C_2 = \frac{1}{2}I_2^2 L_2$ and the retardation factor of $u = \exp\left(i\omega|\mathbf{x}-\mathbf{x}'|/c\right)$ inside the integral can been ignored in the quasi-static regime $D \ll \lambda$ of interest, where each coil is within the near field of the other. With this definition, the coupling factor is given by $k = \sqrt{C_1 C_2}/M_C + M_L/\sqrt{L_1 L_2}$.

Therefore, to calculate the coupling rate between two self-resonant coils, again the current profiles are needed and, by using again the assumed sinusoidal current profiles, we compute numerically from Eq.(23) the mutual capacitance $M_{C,s}$ and inductance $M_{L,s}$ between two self-resonant coils at a distance D between their centers, and thus $k = 1/Q_\kappa$ is also determined.

Table 2

pair of coils	D/r	Q	$Q_\kappa = 1/k$	U
r=30cm, h=20cm, a=1cm, N=4 $\lambda/r \approx 75$ $Q_s^{abs} \approx 8170$, $Q_s^{rad} \approx 4164$	3	2758	38.9	70.9
	5	2758	139.4	19.8
	7	2758	333.0	8.3
	10	2758	818.9	3.4
r=10cm, h=3cm, a=2mm, N=6 $\lambda/r \approx 140$ $Q_s^{abs} \approx 3968$, $Q_s^{rad} \approx 43919$	3	3639	61.4	59.3
	5	3639	232.5	15.7
	7	3639	587.5	6.2
	10	3639	1580	2.3

Referring to Table 2, relevant parameters are shown for exemplary examples featuring pairs or identical self resonant coils. Numerical results are presented for the average wavelength and loss rates of the two normal modes (individual values not shown), and also the coupling rate and figure-of-merit as a function of the coupling distance D, for the two cases of modes presented in Table1. It can be seen that for

InductEV, Inc.
Exhibit 1025
Page 527

medium distances $D/r = 10-3$ the expected coupling-to-loss ratios are in the range $U \sim 2-70$.

2.1.1 Experimental Results

An experimental realization of an example of the above described system for wireless energy transfer consists of two self-resonant coils of the type described above, one of which (the source coil) is coupled inductively to an oscillating circuit, and the second (the device coil) is coupled inductively to a resistive load, as shown schematically in Fig. 5. Referring to Fig. 5, A is a single copper loop of radius 25cm that is part of the driving circuit, which outputs a sine wave with frequency 9.9MHz. s and d are respectively the source and device coils referred to in the text. B is a loop of wire attached to the load ("light-bulb"). The various κ's represent direct couplings between the objects. The angle between coil d and the loop A is adjusted so that their direct coupling is zero, while coils s and d are aligned coaxially. The direct coupling between B and A and between B and s is negligible.

The parameters for the two identical helical coils built for the experimental validation of the power transfer scheme were $h = 20\,\text{cm}$, $a = 3\,\text{mm}$, $r = 30$ cm and $N = 5.25$. Both coils are made of copper. Due to imperfections in the construction, the spacing between loops of the helix is not uniform, and we have encapsulated the uncertainty about their uniformity by attributing a 10% (2 cm) uncertainty to h. The expected resonant frequency given these dimensions is $f_0 = 10.56 \pm 0.3\,\text{MHz}$, which is about 5% off from the measured resonance at around 9.90 MHz.

The theoretical Q for the loops is estimated to be ~ 2500 (assuming perfect copper of resistivity $\rho = 1/\sigma = 1.7 \times 10^{-8}\,\Omega\,\text{m}$) but the measured value is 950 ± 50. We believe the discrepancy is mostly due to the effect of the layer of poorly conducting copper oxide on the surface of the copper wire, to which the current is confined by the short skin depth ($\sim 20\mu\,\text{m}$) at this frequency. We have therefore used the experimentally observed Q (and $\Gamma_1 = \Gamma_2 = \Gamma = \omega/(2Q)$ derived from it) in all subsequent computations.

The coupling coefficient κ can be found experimentally by placing the two self-resonant coils (fine-tuned, by slightly adjusting h, to the same resonant frequency when isolated) a distance D apart and measuring the splitting in the frequencies of the two

InductEV, Inc.
Exhibit 1025
Page 528

resonant modes in the transmission spectrum. According to Eq.(13) derived by coupled-mode theory, the splitting in the transmission spectrum should be $\delta_p = 2\sqrt{\kappa^2 - \Gamma^2}$, when $\kappa_{A,B}$ are kept very small by keeping A and B at a relatively large distance. The comparison between experimental and theoretical results as a function of distance when the two the coils are aligned coaxially is shown in Fig. 6.

Fig. 7 shows a comparison of experimental and theoretical values for the strong-coupling factor $U = \kappa / \Gamma$ as a function of the separation between the two coils. The theory values are obtained by using the theoretically obtained κ and the experimentally measured Γ. The shaded area represents the spread in the theoretical U due to the $\sim 5\%$ uncertainty in Q. As noted above, the maximum theoretical efficiency depends only on the parameter U, which is plotted as a function of distance in Fig. 7. U is greater than 1 even for $D = 2.4\,\mathrm{m}$ (eight times the radius of the coils), thus the sytem is in the strongly-coupled regime throughout the entire range of distances probed.

The power-generator circuit was a standard Colpitts oscillator coupled inductively to the source coil by means of a single loop of copper wire 25cm in radius (see Fig. 5). The load consisted of a previously calibrated light-bulb, and was attached to its own loop of insulated wire, which was in turn placed in proximity of the device coil and inductively coupled to it. Thus, by varying the distance between the light-bulb and the device coil, the parameter $U_B = \kappa_B / \Gamma$ was adjusted so that it matched its optimal value, given theoretically by Eq.(14) as $U_{B^*} = \sqrt{1 + U^2}$. Because of its inductive nature, the loop connected to the light-bulb added a small reactive component to κ_B which was compensated for by slightly retuning the coil. The work extracted was determined by adjusting the power going into the Colpitts oscillator until the light-bulb at the load was at its full nominal brightness.

In order to isolate the efficiency of the transfer taking place specifically between the source coil and the load, we measured the current at the mid-point of each of the self-resonant coils with a current-probe (which was not found to lower the Q of the coils noticeably.) This gave a measurement of the current parameters I_1 and I_2 defined above. The power dissipated in each coil was then computed from $P_{1,2} = \Gamma L |I_{1,2}|^2$, and the

InductEV, Inc.
Exhibit 1025
Page 529

efficiency was directly obtained from $\eta = P_B / (P_1 + P_2 + P_B)$. To ensure that the experimental setup was well described by a two-object coupled-mode theory model, we positioned the device coil such that its direct coupling to the copper loop attached to the Colpitts oscillator was zero. The experimental results are shown in Fig. 8, along with the theoretical prediction for maximum efficiency, given by Eq.(15).

Using this example, we were able to transmit significant amounts of power using this setup from the source coil to the device coil, fully lighting up a 60W light-bulb from distances more than 2m away, for example. As an additional test, we also measured the total power going into the driving circuit. The efficiency of the wireless power-transmission itself was hard to estimate in this way, however, as the efficiency of the Colpitts oscillator itself is not precisely known, although it is expected to be far from 100%. Nevertheless, this gave an overly conservative lower bound on the efficiency. When transmitting 60W to the load over a distance of 2m, for example, the power flowing into the driving circuit was 400W. This yields an overall wall-to-load efficiency of $\sim 15\%$, which is reasonable given the expected $\sim 40\%$ efficiency for the wireless power transmission at that distance and the low efficiency of the driving circuit.

From the theoretical treatment above, we see that in typical examples it is important that the coils be on resonance for the power transmission to be practical. We found experimentally that the power transmitted to the load dropped sharply as one of the coils was detuned from resonance. For a fractional detuning $\Delta f/f_0$ of a few times the inverse loaded Q, the induced current in the device coil was indistinguishable from noise.

The power transmission was not found to be visibly affected as humans and various everyday objects, such as metallic and wooden furniture, as well as electronic devices large and small, were placed between the two coils, even when they drastically obstructed the line of sight between source and device. External objects were found to have an effect only when they were closer than 10cm from either one of the coils. While some materials (such as aluminum foil, styrofoam and humans) mostly just shifted the resonant frequency, which could in principle be easily corrected with a feedback circuit of the type described earlier, others (cardboard, wood, and PVC) lowered Q when placed

InductEV, Inc.
Exhibit 1025
Page 530

closer than a few centimeters from the coil, thereby lowering the efficiency of the transfer.

This method of power transmission is believed safe for humans. When transmitting 60W (more than enough to power a laptop computer) across 2m, we estimated that the magnitude of the magnetic field generated is much weaker than the Earth's magnetic field for all distances except for less than about 1cm away from the wires in the coil, an indication of the safety of the scheme even after long-term use. The power radiated for these parameters was ~ 5 W, which is roughly an order of magnitude higher than cell phones but could be drastically reduced, as discussed below.

Although the two coils are currently of identical dimensions, it is possible to make the device coil small enough to fit into portable devices without decreasing the efficiency. One could, for instance, maintain the product of the characteristic sizes of the source and device coils constant.

These experiments demonstrated experimentally a system for power transmission over medium range distances, and found that the experimental results match theory well in multiple independent and mutually consistent tests.

The efficiency of the scheme and the distances covered can be appreciably improved by silver-plating the coils, which should increase their Q, or by working with more elaborate geometries for the resonant objects. Nevertheless, the performance characteristics of the system presented here are already at levels where they could be useful in practical applications.

2.2 Capacitively-loaded conducting loops or coils

In some examples, one or more of the resonant objects are capacitively-loaded conducting loops or coils . Referring to Fig. 9 a helical coil with N turns of conducting wire, as described above, is connected to a pair of conducting parallel plates of area A spaced by distance d via a dielectric material of relative permittivity ε, and everything is surrounded by air (as shown, $N=1$ and $h=0$). The plates have a capacitance $C_p = \varepsilon_0 \varepsilon A / d$, which is added to the distributed capacitance of the coil and thus modifies its resonance. Note however, that the presence of the loading capacitor modifies significantly the current distribution inside the wire and therefore the total

InductEV, Inc.
Exhibit 1025
Page 531

effective inductance L and total effective capacitance C of the coil are different respectively from L_s and C_s, which are calculated for a self-resonant coil of the same geometry using a sinusoidal current profile. Since some charge is accumulated at the plates of the external loading capacitor, the charge distribution ρ inside the wire is reduced, so $C < C_s$, and thus, from the charge conservation equation, the current distribution $\mathbf{j}$ flattens out, so $L > L_s$. The resonant frequency for this system is $\omega = 1/\sqrt{L(C + C_p)} < \omega_s = 1/\sqrt{L_s C_s}$, and $I(x) \to I_o \cos(\pi x / l) \Rightarrow C \to C_s \Rightarrow \omega \to \omega_s$, as $C_p \to 0$.

In general, the desired CMT parameters can be found for this system, but again a very complicated solution of Maxwell's Equations is required. Instead, we will analyze only a special case, where a reasonable guess for the current distribution can be made. When $C_p \gg C_s > C$, then $\omega \approx 1/\sqrt{LC_p} \ll \omega_s$ and $Z \approx \sqrt{L/C_p} \ll Z_s$, while all the charge is on the plates of the loading capacitor and thus the current distribution is constant along the wire. This allows us now to compute numerically L from Eq.(19). In the case $h = 0$ and N integer, the integral in Eq.(19) can actually be computed analytically, giving the formula $L = \mu_o r\left[\ln(8r/a) - 2\right]N^2$. Explicit analytical formulas are again available for R from Eq.(21) and (22), since $I_{rms} = I_o$, $|\mathbf{p}| \approx 0$ and $|\mathbf{m}| = I_o N \pi r^2$ (namely only the magnetic-dipole term is contributing to radiation), so we can determine also $Q_{abs} = \omega L / R_{abs}$ and $Q_{rad} = \omega L / R_{rad}$. At the end of the calculations, the validity of the assumption of constant current profile is confirmed by checking that indeed the condition $C_p \gg C_s \Leftrightarrow \omega \ll \omega_s$ is satisfied. To satisfy this condition, one could use a large external capacitance, however, this would usually shift the operational frequency lower than the optimal frequency, which we will determine shortly; instead, in typical examples, one often prefers coils with very small self-capacitance C_s to begin with, which usually holds, for the types of coils under consideration, when $N = 1$, so that the self-capacitance comes from the charge distribution across the single turn, which is almost always very small, or when $N > 1$ and

InductEV, Inc.
Exhibit 1025
Page 532

$h \gg 2Na$, so that the dominant self-capacitance comes from the charge distribution across adjacent turns, which is small if the separation between adjacent turns is large.

The external loading capacitance C_p provides the freedom to tune the resonant frequency (for example by tuning A or d). Then, for the particular simple case $h = 0$, for which we have analytical formulas, the total $Q = \omega L / (R_{abs} + R_{rad})$ becomes highest at the optimal frequency

$$\omega_Q = \left[\frac{c^4}{\pi} \sqrt{\frac{\varepsilon_o}{2\sigma}} \cdot \frac{1}{aNr^3} \right]^{2/7}, \tag{24}$$

reaching the value

$$Q_{\max} = \frac{6}{7\pi} \left(2\pi^2 \eta_o \frac{\sigma a^2 N^2}{r} \right)^{3/7} \cdot \left[\ln\left(\frac{8r}{a} \right) - 2 \right]. \tag{25}$$

At lower frequencies it is dominated by ohmic loss and at higher frequencies by radiation. Note, however, that the formulas above are accurate as long as $\omega_Q \ll \omega_s$ and, as explained above, this holds almost always when $N = 1$, and is usually less accurate when $N > 1$, since $h = 0$ usually implies a large self-capacitance. A coil with large h can be used, if the self-capacitance needs to be reduced compared to the external capacitance, but then the formulas for L and ω_Q, $Q_{\max}$ are again less accurate. Similar qualitative behavior is expected, but a more complicated theoretical model is needed for making quantitative predictions in that case.

The results of the above analysis for two examples of subwavelength modes of $\lambda / r \geq 70$ (namely highly suitable for near-field coupling and well within the quasi-static limit) of coils with $N = 1$ and $h = 0$ at the optimal frequency Eq.(24) are presented in Table 3. To confirm the validity of constant-current assumption and the resulting analytical formulas, mode-solving calculations were also performed using another completely independent method: computational 3D finite-element frequency-domain (FEFD) simulations (which solve Maxwell's Equations in frequency domain exactly apart for spatial discretization) were conducted, in which the boundaries of the conductor were modeled using a complex impedance $\zeta_c = \sqrt{\mu_o \omega / 2\sigma}$ boundary condition, valid as

InductEV, Inc.
Exhibit 1025
Page 533

long as $\zeta_c / \zeta_o \ll 1$ ($<10^{-5}$ for copper in the microwave). Table 3 shows Numerical FEFD (and in parentheses analytical) results for the wavelength and absorption, radiation and total loss rates, for two different cases of subwavelength-loop resonant modes. Note that for conducting material copper ($\sigma=5.998\cdot10^7 S/m$) was used. Specific parameters of the plot in Fig. 4 are highlighted in bold in the table. The two methods (analytical and computational) are in good agreement and show that, in some examples, the optimal frequency is in the low-MHz microwave range and the expected quality factors are $Q_{abs} \geq 1000$ and $Q_{rad} \geq 10000$.

Table 3

single coil	λ / r	f	Q_{rad}	Q_{abs}	Q
r=30cm, a=2cm ε=10, A=138cm², d=4mm	**111.4 (112.4)**	**8.976 (8.897)**	**29546 (30512)**	**4886 (5117)**	**4193 (4381)**
r=10cm, a=2mm ε=10, A=3.14cm², d=1mm	69.7 (70.4)	43.04 (42.61)	10702 (10727)	1545 (1604)	1350 (1395)

Referring to Fig. 10, in some examples, energy is transferred between two capacitively-loaded coils. For the rate of energy transfer between two capacitively-loaded coils 1 and 2 at distance D between their centers, the mutual inductance M_L can be evaluated numerically from Eq.(23) by using constant current distributions in the case $\omega \ll \omega_s$. In the case $h=0$, the coupling is only magnetic and again we have an analytical formula, which, in the quasi-static limit $r \ll D \ll \lambda$ and for the relative orientation shown in Fig. 10, is $M_L \approx \pi\mu_o / 2 \cdot (r_1 r_2)^2 N_1 N_2 / D^3$, which means that $k \propto \left(\sqrt{r_1 r_2} / D\right)^3$ is independent of the frequency ω and the number of turns N_1, N_2. Consequently, the resultant coupling figure-of-merit of interest is

$$U = k\sqrt{Q_1 Q_2} \approx \left(\frac{\sqrt{r_1 r_2}}{D}\right)^3 \cdot \frac{\pi^2 \eta_o \frac{\sqrt{r_1 r_2}}{\lambda} \cdot N_1 N_2}{\prod_{j=1,2}\left(\sqrt{\frac{\pi\eta_o}{\lambda\sigma}} \cdot \frac{r_j}{a_j} N_j + \frac{8}{3}\pi^5 \eta_o \left(\frac{r_j}{\lambda}\right)^4 N_j^2\right)^{1/2}}, \quad (26)$$

InductEV, Inc.
Exhibit 1025
Page 534

which again is more accurate for $N_1 = N_2 = 1$.

From Eq.(26) it can be seen that the optimal frequency ω_U, where the figure-of-merit is maximized to the value $U_{\max}$, is close to the frequency $\omega_{Q_1Q_2}$ at which Q_1Q_2 is maximized, since k does not depend much on frequency (at least for the distances $D \ll \lambda$ of interest for which the quasi-static approximation is still valid). Therefore, the optimal frequency $\omega_U \approx \omega_{Q_1Q_2}$ is mostly independent of the distance D between the two coils and lies between the two frequencies ω_{Q_1} and ω_{Q_2} at which the single-coil Q_1 and Q_2 respectively peak. For same coils, this optimal frequency is given by Eq.(24) and then the strong-coupling factor from Eq.(26) becomes

$$U_{\max} = kQ_{\max} \approx \left(\frac{r}{D}\right)^3 \cdot \frac{3}{7}\left(2\pi^2\eta_o \frac{\sigma a^2 N^2}{r}\right)^{3/7}. \qquad (27)$$

In some examples, one can tune the capacitively-loaded conducting loops or coils, so that their angular eigenfrequencies are close to ω_U within Γ_U, which is half the angular frequency width for which $U > U_{\max}/2$.

Referring to Table 4, numerical FEFD and, in parentheses, analytical results based on the above are shown for two systems each composed of a matched pair of the loaded coils described in Table 3. The average wavelength and loss rates are shown along with the coupling rate and coupling to loss ratio figure-of-merit $U = \kappa / \Gamma$ as a function of the coupling distance D, for the two cases. Note that the average numerical Γ_{rad} shown are slightly different from the single-loop value of Figure 3, analytical results for Γ_{rad} are not shown but the single-loop value is used. (The specific parameters corresponding to the plot in Fig. 10 are highlighted with bold in the table.) Again we chose $N = 1$ to make the constant-current assumption a good one and computed M_L numerically from Eq.(23). Indeed the accuracy can be confirmed by their agreement with the computational FEFD mode-solver simulations, which give κ through the frequency splitting of the two normal modes of the combined system ($\delta_E = 2\kappa$ from Eq.(4)). The results show that for medium distances $D/r = 10 - 3$ the expected coupling-to-loss ratios are in the range $U \sim 0.5 - 50$.

InductEV, Inc.
Exhibit 1025
Page 535

Table 4

pair of coils	D/r	Q^{ohm}	$Q=\omega/2\Gamma$	$Q_c=\omega/2\kappa$	κ/Γ
r=30cm, a=2cm ε=10, A=138cm^2, d=4mm $\lambda/r\approx 112$ $Q^{abs}\approx 4386$	3	30729	4216	62.6 (63.7)	67.4 (68.7)
	5	29577	4194	235 (248)	17.8 (17.6)
	7	**29128**	**4185**	**589 (646)**	**7.1 (6.8)**
	10	28833	4177	1539 (1828)	2.7 (2.4)
r=10cm, a=2mm ε=10, A=3.14cm^2, d=1mm $\lambda/r\approx 70$ $Q^{abs}\approx 1546$	3	10955	1355	85.4 (91.3)	15.9 (15.3)
	5	10740	1351	313 (356)	4.32 (3.92)
	7	10759	1351	754 (925)	1.79 (1.51)
	10	10756	1351	1895 (2617)	0.71 (0.53)

2.2.1 Derivation of optimal power-transmission efficiency

Referring to Fig. 11, to rederive and express Eq.(15) in terms of the parameters which are more directly accessible from particular resonant objects, such as the capacitively-loaded conducting loops, one can consider the following circuit-model of the system, where the inductances L_s, L_d represent the source and device loops respectively, R_s, R_d their respective losses, and C_s, C_d are the required corresponding capacitances to achieve for both resonance at frequency ω. A voltage generator V_g is considered to be connected to the source and a load resistance R_l to the device. The mutual inductance is denoted by M.

Then from the source circuit at resonance ($\omega L_s = 1/\omega C_s$):

$$V_g = I_s R_s - j\omega M I_d \Rightarrow \frac{1}{2}V_g^* I_s = \frac{1}{2}\left|I_s\right|^2 R_s + \frac{1}{2}j\omega M I_d^* I_s, \tag{28}$$

and from the device circuit at resonance ($\omega L_d = 1/\omega C_d$):

$$0 = I_d\left(R_d + R_l\right) - j\omega M I_s \Rightarrow j\omega M I_s = I_d\left(R_d + R_l\right) \tag{29}$$

So by substituting Eq.(29) to Eq.(28) and taking the real part (for time-averaged power) we get:

$$P_g = \mathrm{Re}\left\{\frac{1}{2}V_g^* I_s\right\} = \frac{1}{2}\left|I_s\right|^2 R_s + \frac{1}{2}\left|I_d\right|^2\left(R_d + R_l\right) = P_s + P_d + P_l, \tag{30}$$

where we identified the power delivered by the generator $P_g = \mathrm{Re}\left\{V_g^* I_s / 2\right\}$, the power

InductEV, Inc.
Exhibit 1025
Page 536

lost inside the source $P_s = \left|I_s\right|^2 R_s / 2$, the power lost inside the device $P_d = \left|I_d\right|^2 R_d / 2$ and the power delivered to the load $P_l = \left|I_d\right|^2 R_l / 2$. Then, the power transmission efficiency is:

$$\eta_P \equiv \frac{P_l}{P_g} = \frac{R_l}{\left|\frac{I_s}{I_d}\right|^2 R_s + \left(R_d + R_l\right)} \overset{(29)}{=} \frac{R_l}{\frac{\left(R_d + R_l\right)^2}{\left(\omega M\right)^2} R_s + \left(R_d + R_l\right)}. \tag{31}$$

If we now choose the load impedance R_l to optimize the efficiency by $\eta_P'\left(R_l\right) = 0$, we get the optimal load impedance

$$\frac{R_{l*}}{R_d} = \sqrt{1 + \frac{\left(\omega M\right)^2}{R_s R_d}} \tag{32}$$

and the maximum possible efficiency

$$\eta_{P*} = \frac{R_{l*} / R_d - 1}{R_{l*} / R_d + 1} = \left[\frac{\omega M / \sqrt{R_s R_d}}{1 + \sqrt{1 + \left(\omega M / \sqrt{R_s R_d}\right)^2}}\right]^2. \tag{33}$$

To check now the correspondence with the CMT model, note that $\kappa_l = R_l / 2L_d$, $\Gamma_d = R_d / 2L_d$, $\Gamma_s = R_s / 2L_s$, and $\kappa = \omega M / 2\sqrt{L_s L_d}$, so then $U_l = \kappa_l / \Gamma_d = R_l / R_d$ and $U = \kappa / \sqrt{\Gamma_s \Gamma_d} = \omega M / \sqrt{R_s R_d}$. Therefore, the condition Eq.(32) is identical to the condition Eq.(14) and the optimal efficiency Eq.(33) is identical to the general Eq.(15). Indeed, as the CMT analysis predicted, to get a large efficiency, we need to design a system that has a large strong-coupling factor U.

2.2.2 Optimization of U

The results above can be used to increase or optimize the performance of a wireless energy transfer system, which employs capacitively-loaded coils. For example, from the scaling of Eq.(27) with the different system parameters, one sees that to maximize the system figure-of-merit U, in some examples, one can:

InductEV, Inc.
Exhibit 1025
Page 537

-- Decrease the resistivity of the conducting material. This can be achieved, for example, by using good conductors (such as copper or silver) and/or lowering the temperature. At very low temperatures one could use also superconducting materials to achieve extremely good performance.

-- Increase the wire radius a. In typical examples, this action can be limited by physical size considerations. The purpose of this action is mainly to reduce the resistive losses in the wire by increasing the cross-sectional area through which the electric current is flowing, so one could alternatively use also a Litz wire or a ribbon instead of a circular wire.

-- For fixed desired distance D of energy transfer, increase the radius of the loop r. In typical examples, this action can be limited by physical size considerations, typically especially for the device.

-- For fixed desired distance vs. loop-size ratio D/r, decrease the radius of the loop r. In typical examples, this action can be limited by physical size considerations.

-- Increase the number of turns N. (Even though Eq.(27) is expected to be less accurate for $N>1$, qualitatively it still provides a good indication that we expect an improvement in the coupling-to-loss ratio with increased N.) In typical examples, this action can be limited by physical size and possible voltage considerations, as will be discussed in following paragraphs.

-- Adjust the alignment and orientation between the two coils. The figure-of-merit is optimized when both cylindrical coils have exactly the same axis of cylindrical symmetry (namely they are "facing" each other). In some examples, particular mutual coil angles and orientations that lead to zero mutual inductance (such as the orientation where the axes of the two coils are perpendicular and the centers of the two coils are on one of the two axes) should be avoided.

-- Finally, note that the height of the coil h is another available design parameter, which can have an impact to the performance similar to that of its radius r, and thus the design rules can be similar.

The above analysis technique can be used to design systems with desired parameters. For example, as listed below, the above described techniques can be used to determine the cross sectional radius a of the wire which one should use when designing

InductEV, Inc.
Exhibit 1025
Page 538

as system two same single-turn loops with a given radius in order to achieve a specific performance in terms of $U = \kappa / \Gamma$ at a given D/r between them, when the material is copper (σ=5.998·10^{7}S/m):

$$D/r = 5,\ U \geq 10,\ r = 30cm \Rightarrow a \geq 9mm$$
$$D/r = 5,\ U \geq 10,\ r = 5cm \Rightarrow a \geq 3.7mm$$
$$D/r = 5,\ U \geq 20,\ r = 30cm \Rightarrow a \geq 20mm$$
$$D/r = 5,\ U \geq 20,\ r = 5cm \Rightarrow a \geq 8.3mm$$
$$D/r = 10,\ U \geq 1,\ r = 30cm \Rightarrow a \geq 7mm$$
$$D/r = 10,\ U \geq 1,\ r = 5cm \Rightarrow a \geq 2.8mm$$
$$D/r = 10,\ U \geq 3,\ r = 30cm \Rightarrow a \geq 25mm$$
$$D/r = 10,\ U \geq 3,\ r = 5cm \Rightarrow a \geq 10mm$$

Similar analysis can be done for the case of two dissimilar loops. For example, in some examples, the device under consideration is very specific (e.g. a laptop or a cell phone), so the dimensions of the device object (r_d, h_d, a_d, N_d) are very restricted. However, in some such examples, the restrictions on the source object (r_s, h_s, a_s, N_s) are much less, since the source can, for example, be placed under the floor or on the ceiling. In such cases, the desired distance is often well defined, based on the application (e.g. $D \sim 1m$ for charging a laptop on a table wirelessly from the floor). Listed below are examples (simplified to the case $N_s = N_d = 1$ and $h_s = h_d = 0$) of how one can vary the dimensions of the source object to achieve the desired system performance in terms of $U_{sd} = \kappa / \sqrt{\Gamma_s \Gamma_d}$, when the material is again copper (σ=5.998·10^{7}S/m):

$$D = 1.5m,\ U_{sd} \geq 15,\ r_d = 30cm,\ a_d = 6mm \Rightarrow r_s = 1.158m,\ a_s \geq 5mm$$
$$D = 1.5m,\ U_{sd} \geq 30,\ r_d = 30cm,\ a_d = 6mm \Rightarrow r_s = 1.15m,\ a_s \geq 33mm$$
$$D = 1.5m, U_{sd} \geq 1,\ r_d = 5cm,\ a_d = 4mm \Rightarrow r_s = 1.119m,\ a_s \geq 7mm$$
$$D = 1.5m,\ U_{sd} \geq 2,\ r_d = 5cm,\ a_d = 4mm \Rightarrow r_s = 1.119m,\ a_s \geq 52mm$$
$$D = 2m,\ U_{sd} \geq 10,\ r_d = 30cm,\ a_d = 6mm \Rightarrow r_s = 1.518m,\ a_s \geq 7mm$$
$$D = 2m,\ U_{sd} \geq 20,\ r_d = 30cm,\ a_d = 6mm \Rightarrow r_s = 1.514m,\ a_s \geq 50mm$$
$$D = 2m,\ U_{sd} \geq 0.5,\ r_d = 5cm,\ a_d = 4mm \Rightarrow r_s = 1.491m,\ a_s \geq 5mm$$
$$D = 2m,\ U_{sd} \geq 1,\ r_d = 5cm,\ a_d = 4mm \Rightarrow r_s = 1.491m,\ a_s \geq 36mm$$

InductEV, Inc.
Exhibit 1025
Page 539

2.2.3 Optimization of k

As described below, in some examples, the quality factor Q of the resonant objects is limited from external perturbations and thus varying the coil parameters cannot lead to improvement in Q. In such cases, one can opt to increase the strong-coupling factor U by increasing the coupling factor k. The coupling does not depend on the frequency and the number of turns. Therefore, in some examples, one can:

-- Increase the wire radii a_1 and a_2. In typical examples, this action can be limited by physical size considerations.

-- For fixed desired distance D of energy transfer, increase the radii of the coils r_1 and r_2. In typical examples, this action can be limited by physical size considerations, typically especially for the device.

-- For fixed desired distance vs. coil-sizes ratio $D/\sqrt{r_1 r_2}$, only the weak (logarithmic) dependence of the inductance remains, which suggests that one should decrease the radii of the coils r_1 and r_2. In typical examples, this action can be limited by physical size considerations.

-- Adjust the alignment and orientation between the two coils. In typical examples, the coupling is optimized when both cylindrical coils have exactly the same axis of cylindrical symmetry (namely they are "facing" each other). Particular mutual coil angles and orientations that lead to zero mutual inductance (such as the orientation where the axes of the two coils are perpendicular and the centers of the two coils are on one of the two axes) should obviously be avoided.

-- Finally, note that the heights of the coils h_1 and h_2 are other available design parameters, which can have an impact to the coupling similar to that of their radii r_1 and r_2, and thus the design rules can be similar.

Further practical considerations apart from efficiency, e.g. physical size limitations, will be discussed in detail below.

2.2.4 Optimization of overall system performance

In many cases, the dimensions of the resonant objects will be set by the particular application at hand. For example, when this application is powering a laptop or a cell-phone, the device resonant object cannot have dimensions larger than those of the laptop

InductEV, Inc.
Exhibit 1025
Page 540

or cell-phone respectively. In particular, for a system of two loops of specified dimensions, in terms of loop radii $r_{s,d}$ and wire radii $a_{s,d}$, the independent parameters left to adjust for the system optimization are: the number of turns $N_{s,d}$, the frequency f, the power-load consumption rate $\kappa_l = R_l / 2L_d$ and the power-generator feeding rate $\kappa_g = R_g / 2L_s$, where R_g is the internal (characteristic) impedance of the generator.

In general, in various examples, the primary dependent variable that one wants to increase or optimize is the overall efficiency η. However, other important variables need to be taken into consideration upon system design. For example, in examples featuring capacitively-loaded coils, the design can be constrained by, for example, the currents flowing inside the wires $I_{s,d}$ and the voltages across the capacitors $V_{s,d}$. These limitations can be important because for ~*Watt* power applications the values for these parameters can be too large for the wires or the capacitors respectively to handle. Furthermore, the total loaded (by the load) quality factor of the device $Q_{d[l]} = \omega / 2\left(\Gamma_d + \Gamma_l\right) = \omega L_d / \left(R_d + R_l\right)$ and the total loaded (by the generator) quality factor of the source $Q_{s[g]} = \omega / 2\left(\Gamma_s + \Gamma_g\right) = \omega L_s / \left(R_s + R_g\right)$ are quantities that should be preferably small, because to match the source and device resonant frequencies to within their Q's, when those are very large, can be challenging experimentally and more sensitive to slight variations. Lastly, the radiated powers $P_{s,rad}$ and $P_{d,rad}$ should be minimized for concerns about far-field interference and safety, even though, in general, for a magnetic, non-radiative scheme they are already typically small. In the following, we examine then the effects of each one of the independent variables on the dependent ones.

We define a new variable wp to express the power-load consumption rate for some particular value of U through $U_l = \kappa_l / \Gamma_d = \sqrt{1 + wp \cdot U^2}$. Then, in some examples, values which impact the choice of this rate are: $U_l = 1 \Leftrightarrow wp = 0$ to minimize the required energy stored in the source (and therefore I_s and V_s), $U_l = \sqrt{1 + U^2} > 1 \Leftrightarrow wp = 1$ to maximize the efficiency, as seen earlier, or $U_l \gg 1 \Leftrightarrow wp \gg 1$ to decrease the required

InductEV, Inc.
Exhibit 1025
Page 541

energy stored in the device (and therefore I_d and V_d) and to decrease or minimize $Q_{d[l]}$. Similar is the impact of the choice of the power-generator feeding rate $U_g = \kappa_g / \Gamma_s$, with the roles of the source/device and generator/load reversed.

In some examples, increasing N_s and N_d increases Q_s and Q_d, and thus U and the efficiency significantly, as seen before. It also decreases the currents I_s and I_d, because the inductance of the loops increases, and thus the energy $W_{s,d} = L_{s,d} |I_{s,d}|^2 / 2$ required for given output power P_l can be achieved with smaller currents. However, in some examples, increasing N_d and thus Q_d can increase $Q_{d[l]}$, $P_{d,rad}$ and the voltage across the device capacitance V_d. Similar can be the impact of increasing N_s on $Q_{s[g]}$, $P_{s,rad}$ and V_s. As a conclusion, in some examples, the number of turns N_s and N_d should be chosen large enough (for high efficiency) but such that they allow for reasonable voltages, loaded Q's and/or powers radiated.

With respect to the resonant frequency, again, there is an optimal one for efficiency. Close to that optimal frequency $Q_{d[l]}$ and/or $Q_{s[g]}$ can be approximately maximum. In some examples, for lower frequencies the currents typically get larger but the voltages and radiated powers get smaller. In some examples, one should pick either the frequency that maximizes the efficiency or somewhat lower.

One way to decide on an operating regime for the system is based on a graphical method. Consider two loops of $r_s = 25cm$, $r_d = 15cm$, $h_s = h_d = 0$, $a_s = a_d = 3mm$ and distance $D = 2m$ between them. In Fig. 12, we plot some of the above dependent variables (currents, voltages and radiated powers normalized to $1Watt$ of output power) in terms of frequency f and N_d, given some choice for wp and N_s. Fig. 12 depicts the trend of system performance explained above. In Fig. 13, we make a contour plot of the dependent variables as functions of both frequency and wp but for both N_s and N_d fixed. For example, a reasonable choice of parameters for the system of two loops with the dimensions given above are: $N_s = 2$, $N_d = 6$, $f=10MHz$ and $wp=10$, which gives the following performance characteristics: $\eta = 20.6\%$, $Q_{d[l]} = 1264$, $I_s = 7.2A$, $I_d = 1.4A$,

InductEV, Inc.
Exhibit 1025
Page 542

$V_s = 2.55kV$, $V_d = 2.30kV$, $P_{s,rad} = 0.15W$, $P_{d,rad} = 0.006W$. Note that the results in Figs. 12, 13 and the just above calculated performance characteristics are made using the analytical formulas provided above, so they are expected to be less accurate for large values of N_s, N_d, but still they give a good estimate of the scalings and the orders of magnitude.

Finally, one could additionally optimize for the source dimensions, since usually only the device dimensions are limited, as discussed earlier. Namely, one can add r_s and a_s in the set of independent variables and optimize with respect to these too for all the dependent variables of the problem (we saw how to do this only for efficiency earlier). Such an optimization would lead to improved results.

In this description, we propose that, if one ensures operation in the strongly-coupled regime at mid-range distances, at least medium-power transmission (~W) at mid-range distances with high efficiency is possible.

2.3 Inductively-loaded conducting rods

A straight conducting rod of length $2h$ and cross-sectional radius a has distributed capacitance and distributed inductance, and therefore it supports a resonant mode of angular frequency ω. Using the same procedure as in the case of self-resonant coils, one can define an effective total inductance L and an effective total capacitance C of the rod through formulas Eqs.(19) and (20). With these definitions, the resonant angular frequency and the effective impedance are given again by the common formulas $\omega = 1/\sqrt{LC}$ and $Z = \sqrt{L/C}$ respectively. To calculate the total inductance and capacitance, one can assume again a sinusoidal current profile along the length of the conducting wire. When interested in the lowest mode, if we denote by x the coordinate along the conductor, such that it runs from $-h$ to $+h$, then the current amplitude profile would have the form $I(x) = I_0 \cos(\pi x/2h)$, since it has to be zero at the open ends of the rod. This is the well-known half-wavelength electric dipole resonant mode.

In some examples, one or more of the resonant objects are inductively-loaded conducting rods. Referring to Fig. 14, a straight conducting rod of length $2h$ and cross-sectional radius a, as in the previous paragraph, is cut into two equal pieces of length h,

InductEV, Inc.
Exhibit 1025
Page 543

which are connected via a coil wrapped around a magnetic material of relative permeability μ, and everything is surrounded by air. The coil has an inductance L_c, which is added to the distributed inductance of the rod and thus modifies its resonance. Note however, that the presence of the center-loading inductor modifies significantly the current distribution inside the wire and therefore the total effective inductance L and total effective capacitance C of the rod are different respectively from L_s and C_s, which are calculated for a self-resonant rod of the same total length using a sinusoidal current profile, as in the previous paragraph. Since some current is running inside the coil of the external loading inductor, the current distribution $\mathbf{j}$ inside the rod is reduced, so $L < L_s$, and thus, from the charge conservation equation, the linear charge distribution ρ_l flattens out towards the center (being positive in one side of the rod and negative in the other side of the rod, changing abruptly through the inductor), so $C > C_s$. The resonant frequency for this system is $\omega = 1/\sqrt{(L + L_c)C} < \omega_s = 1/\sqrt{L_s C_s}$, and $I(x) \to I_o \cos(\pi x / 2h) \Rightarrow$ $L \to L_s \Rightarrow \omega \to \omega_s$, as $L_c \to 0$.

In general, the desired CMT parameters can be found for this system, but again a very complicated solution of Maxwell's Equations is generally required. In a special case, a reasonable estimate for the current distribution can be made. When $L_c \gg L_s > L$, then $\omega \approx 1/\sqrt{L_c C} \ll \omega_s$ and $Z \approx \sqrt{L_c / C} \gg Z_s$, while the current distribution is triangular along the rod (with maximum at the center-loading inductor and zero at the ends) and thus the charge distribution is positive constant on one half of the rod and equally negative constant on the other side of the rod. This allows us to compute numerically C from Eq.(20). In this case, the integral in Eq.(20) can actually be computed analytically, giving the formula $1/C = 1/(\pi\varepsilon_o h)\left[\ln(h/a) - 1\right]$. Explicit analytical formulas are again available for R from Eq.(21) and (22), since $I_{rms} = I_o$, $|\mathbf{p}| = q_o h$ and $|\mathbf{m}| = 0$ (namely only the electric-dipole term is contributing to radiation), so we can determine also $Q_{abs} = 1/\omega C R_{abs}$ and $Q_{rad} = 1/\omega C R_{rad}$. At the end of the calculations, the validity of the assumption of triangular current profile is confirmed by checking that indeed the

InductEV, Inc.
Exhibit 1025
Page 544

condition $L_c \gg L_s \Leftrightarrow \omega \ll \omega_s$ is satisfied. This condition is relatively easily satisfied, since typically a conducting rod has very small self-inductance L_s to begin with.

Another important loss factor in this case is the resistive loss inside the coil of the external loading inductor L_c and it depends on the particular design of the inductor. In some examples, the inductor is made of a Brooks coil, which is the coil geometry which, for fixed wire length, demonstrates the highest inductance and thus quality factor. The Brooks coil geometry has N_{Bc} turns of conducting wire of cross-sectional radius a_{Bc} wrapped around a cylindrically symmetric coil former, which forms a coil with a square cross-section of side r_{Bc}, where the inner side of the square is also at radius r_{Bc} (and thus the outer side of the square is at radius $2r_{Bc}$), therefore $N_{Bc} \approx \left(r_{Bc}/2a_{Bc}\right)^2$. The inductance of the coil is then $L_c = 2.0285\mu_o r_{Bc} N_{Bc}^2 \approx 2.0285\mu_o r_{Bc}^5 / 8a_{Bc}^4$ and its resistance $R_c \approx \frac{1}{\sigma}\frac{l_{Bc}}{\pi a_{Bc}^2}\sqrt{1+\frac{\mu_o \omega \sigma}{2}\left(\frac{a_{Bc}}{2}\right)^2}$, where the total wire length is $l_{Bc} \approx 2\pi\left(3r_{Bc}/2\right)N_{Bc} \approx 3\pi r_{Bc}^3 / 4a_{Bc}^2$ and we have used an approximate square-root law for the transition of the resistance from the dc to the ac limit as the skin depth varies with frequency.

The external loading inductance L_c provides the freedom to tune the resonant frequency. For example, for a Brooks coil with a fixed size r_{Bc}, the resonant frequency can be reduced by increasing the number of turns N_{Bc} by decreasing the wire cross-sectional radius a_{Bc}. Then the desired resonant angular frequency $\omega = 1/\sqrt{L_c C}$ is achieved for $a_{Bc} \approx \left(2.0285\mu_o r_{Bc}^5 \omega^2 C\right)^{1/4}$ and the resulting coil quality factor is $Q_c \approx 0.169\mu_o \sigma r_{Bc}^2 \omega / \sqrt{1+\omega^2 \mu_o \sigma \sqrt{2.0285\mu_o \left(r_{Bc}/4\right)^5 C}}$. Then, for the particular simple case $L_c \gg L_s$, for which we have analytical formulas, the total $Q = 1/\omega C\left(R_c + R_{abs} + R_{rad}\right)$ becomes highest at some optimal frequency ω_Q, reaching the value $Q_{\max}$, both determined by the loading-inductor specific design. For example,

InductEV, Inc.
Exhibit 1025
Page 545

for the Brooks-coil procedure described above, at the optimal frequency $Q_{\max} \approx Q_c \approx 0.8\left(\mu_o \sigma^2 r_{Bc}^3 / C\right)^{1/4}$. At lower frequencies it is dominated by ohmic loss inside the inductor coil and at higher frequencies by radiation. Note, again, that the above formulas are accurate as long as $\omega_Q \ll \omega_s$ and, as explained above, this is easy to design for by using a large inductance.

The results of the above analysis for two examples, using Brooks coils, of subwavelength modes of $\lambda / h \geq 200$ (namely highly suitable for near-field coupling and well within the quasi-static limit) at the optimal frequency ω_Q are presented in Table 5.

Table 5 shows in parentheses (for similarity to previous tables) analytical results for the wavelength and absorption, radiation and total loss rates, for two different cases of subwavelength-loop resonant modes. Note that for conducting material copper ($\sigma=5.998 \cdot 10^7 S/m$) was used. The results show that, in some examples, the optimal frequency is in the low-MHz microwave range and the expected quality factors are $Q_{abs} \geq 1000$ and $Q_{rad} \geq 100000$.

Table 5

single rod	λ / h	f (MHz)	Q_{rad}	Q_{abs}	Q
h=30cm, a=2cm μ=1, r_{Bc}=2cm, a_{Bc}=0.88mm, N_{Bc}=129	(403.8)	(2.477)	($2.72*10^6$)	(7400)	(7380)
h=10cm, a=2mm μ=1, r_{Bc}=5mm, a_{Bc}=0.25mm, N_{Bc}=103	(214.2)	(14.010)	($6.92*10^5$)	(3908)	(3886)

In some examples, energy is transferred between two inductively-loaded rods. For the rate of energy transfer between two inductively-loaded rods 1 and 2 at distance D between their centers, the mutual capacitance M_C can be evaluated numerically from Eq.(23) by using triangular current distributions in the case $\omega \ll \omega_s$. In this case, the coupling is only electric and again we have an analytical formula, which, in the quasi-static limit $h \ll D \ll \lambda$ and for the relative orientation such that the two rods are aligned on the same axis, is $1/M_C \approx 1/2\pi\varepsilon_o \cdot \left(h_1 h_2\right)^2 / D^3$, which means that $k \propto \left(\sqrt{h_1 h_2} / D\right)^3$ is independent of the frequency ω. One can then get the resultant strong-coupling factor U.

InductEV, Inc.
Exhibit 1025
Page 546

It can be seen that the optimal frequency ω_U, where the figure-of-merit is maximized to the value $U_{\max}$, is close to the frequency $\omega_{Q_1Q_2}$, where Q_1Q_2 is maximized, since k does not depend much on frequency (at least for the distances $D \ll \lambda$ of interest for which the quasi-static approximation is still valid). Therefore, the optimal frequency $\omega_U \approx \omega_{Q_1Q_2}$ is mostly independent of the distance D between the two rods and lies between the two frequencies ω_{Q_1} and ω_{Q_2} at which the single-rod Q_1 and Q_2 respectively peak. In some typical examples, one can tune the inductively-loaded conducting rods, so that their angular eigenfrequencies are close to ω_U within Γ_U, which is half the angular frequency width for which $U > U_{\max}/2$.

Referring to Table 6, in parentheses (for similarity to previous tables) analytical results based on the above are shown for two systems each composed of a matched pair of the loaded rods described in Table 5. The average wavelength and loss rates are shown along with the coupling rate and coupling to loss ratio figure-of-merit $U = \kappa / \Gamma$ as a function of the coupling distance D, for the two cases. Note that for Γ_{rad} the single-rod value is used. Again we chose $L_c \gg L_s$ to make the triangular-current assumption a good one and computed M_C numerically from Eq.(23). The results show that for medium distances $D/h = 10 - 3$ the expected coupling-to-loss ratios are in the range $U \sim 0.5 - 100$.

Table 6

pair of rods	D/h	$Q_\kappa = 1/k$	U
h=30cm, a=2cm μ=1, r_{Bc}=2cm, a_{Bc}=0.88mm, N_{Bc}=129 $\lambda/h \approx 404$ $Q \approx 7380$	3	(70.3)	(105.0)
	5	(389)	(19.0)
	7	(1115)	(6.62)
	10	(3321)	(2.22)
h=10cm, a=2mm μ=1, r_{Bc}=5mm, a_{Bc}=0.25mm, N_{Bc}=103 $\lambda/h \approx 214$ $Q \approx 3886$	3	(120)	(32.4)
	5	(664)	(5.85)
	7	(1900)	(2.05)
	10	(5656)	(0.69)

InductEV, Inc.
Exhibit 1025
Page 547

2.4 Dielectric disks

In some examples, one or more of the resonant objects are dielectric objects, such as disks. Consider a two dimensional dielectric disk object, as shown in Fig. 15(a), of radius r and relative permittivity ε surrounded by air that supports high-Q "whispering-gallery" resonant modes. The loss mechanisms for the energy stored inside such a resonant system are radiation into free space and absorption inside the disk material. High-Q_{rad} and long-tailed subwavelength resonances can be achieved when the dielectric permittivity ε is large and the azimuthal field variations are slow (namely of small principal number m). Material absorption is related to the material loss tangent: $Q_{abs} \sim \mathrm{Re}\{\varepsilon\} / \mathrm{Im}\{\varepsilon\}$. Mode-solving calculations for this type of disk resonances were performed using two independent methods: numerically, 2D finite-difference frequency-domain (FDFD) simulations (which solve Maxwell's Equations in frequency domain exactly apart for spatial discretization) were conducted with a resolution of *30pts/r*; analytically, standard separation of variables (SV) in polar coordinates was used.

Table 7

single disk	λ / r	Q^{abs}	Q^{rad}	Q
Re{ε}=147.7, m=2	**20.01 (20.00)**	**10103 (10075)**	**1988 (1992)**	**1661 (1663)**
Re{ε}=65.6, m=3	9.952 (9.950)	10098 (10087)	9078 (9168)	4780 (4802)

The results for two TE-polarized dielectric-disk subwavelength modes of $\lambda / r \geq 10$ are presented in Table 7. Table 7 shows numerical FDFD (and in parentheses analytical SV) results for the wavelength and absorption, radiation and total loss rates, for two different cases of subwavelength-disk resonant modes. Note that disk-material loss-tangent $\mathrm{Im}\{\varepsilon\}/\mathrm{Re}\{\varepsilon\}=10^{-4}$ was used. (The specific parameters corresponding to the plot in Fig. 15(a) are highlighted with bold in the table.) The two methods have excellent agreement and imply that for a properly designed resonant low-loss-dielectric object values of $Q_{rad} \geq 2000$ and $Q_{abs} \sim 10000$ are achievable. Note that for the 3D case the computational complexity would be immensely increased, while the physics would not be significantly different. For example, a spherical object of $\varepsilon=147.7$ has a whispering gallery mode with $m=2$, $Q_{rad}=13962$, and $\lambda/r=17$.

InductEV, Inc.
Exhibit 1025
Page 548

The required values of ε, shown in Table 7, might at first seem unrealistically large. However, not only are there in the microwave regime (appropriate for approximately meter-range coupling applications) many materials that have both reasonably high enough dielectric constants and low losses (e.g. Titania, Barium tetratitanate, Lithium tantalite etc.), but also ε could signify instead the effective index of other known subwavelength surface-wave systems, such as surface modes on surfaces of metallic materials or plasmonic (metal-like, negative-ε) materials or metallo-dielectric photonic crystals or plasmono-dielectric photonic crystals.

To calculate now the achievable rate of energy transfer between two disks 1 and 2, as shown in Fig. 15(b) we place them at distance D between their centers. Numerically, the FDFD mode-solver simulations give κ through the frequency splitting of the normal modes of the combined system ($\delta_E = 2\kappa$ from Eq.(4)), which are even and odd superpositions of the initial single-disk modes; analytically, using the expressions for the separation-of-variables eigenfields $\mathbf{E}_{1,2}(\mathbf{r})$ CMT gives κ through

$$\kappa = \omega_1 / 2 \cdot \int d^3 r \varepsilon_2(r) E_2^*(r) E_1(r) / \int d^3 r \varepsilon(r) \left| E_1(r) \right|^2 ,$$

where $\varepsilon_j(\mathbf{r})$ and $\varepsilon(\mathbf{r})$ are the dielectric functions that describe only the disk j (minus the constant ε_0 background) and the whole space respectively. Then, for medium distances D/r =10–3 and for non-radiative coupling such that $D < 2\boldsymbol{r}_C$, where $\boldsymbol{r}_C = m\lambda / 2\pi$ is the radius of the radiation caustic, the two methods agree very well, and we finally find , as shown in Table 8, strong-coupling factors in the range $U \sim 1-50$. Thus, for the analyzed examples, the achieved figure-of-merit values are large enough to be useful for typical applications, as discussed below.

InductEV, Inc.
Exhibit 1025
Page 549

Table 8

two disks	D/r	Q^{rad}	$Q=\omega/2\Gamma$	$\omega/2\pi$	κ/Γ
Re{ε}=147.7, m=2	3	2478	1989	46.9 (47.5)	42.4 (35.0)
$\lambda/r=20$	5	2411	1946	298.0 (298.9)	6.5 (5.6)
$Q^{abs}=10093$	7	2196	1804	769.7 (770.2)	2.3 (2.2)
	10	**2017**	**1681**	**1714 (1601)**	**0.98 (1.04)**
Re{ε}=65.6, m=3	3	7972	4455	144 (140)	30.9 (34.3)
$\lambda/r=30$	5	9240	4824	2242 (2083)	2.2 (2.3)
$Q^{abs}=10096$	7	9187	4810	7485 (7417)	0.64 (0.65)

Note that even though particular examples are presented and analyzed above as examples of systems that use resonant electromagnetic coupling for wireless energy transfer, those of self-resonant conducting coils, capacitively-loaded resonant conducting coils, inductively-loaded resonant conducting rods and resonant dielectric disks, any system that supports an electromagnetic mode with its electromagnetic energy extending much further than its size can be used for transferring energy. For example, there can be many abstract geometries with distributed capacitances and inductances that support the desired kind of resonances. In some examples, the resonant structure can be a dielectric sphere. In any one of these geometries, one can choose certain parameters to increase and/or optimize U or, if the Q's are limited by external factors, to increase and/or optimize for k or, if other system performance parameters are of importance, to optimize those.

3 Coupled-Mode Theory for prediction of far-field radiation interference

The two objects in an energy-transfer system generate radiation, which can sometimes be a significant part of the intrinsic losses, and can interfere in the far field. In the previous Sections, we analyzed systems, where this interference phenomenon was not in effect. In this description, we will repeat the analysis, including the interference effects and will show how it can be used to further enhance the power transmission efficiency and/or the radiated power.

InductEV, Inc.
Exhibit 1025
Page 550

The coupled-mode equations of Eqs.(1) fail to predict such an interference phenomenon. In fact, the inability to predict interference phenomena has often been considered inherent to coupled-mode theory (CMT). However, we show here that making only a simple extension to this model, it can actually very successfully predict such interference. The root of the problem stems from the fact that the coupling coefficients were tacitly assumed to be real. This is usually the case when dealing with proper (real) eigenmodes of a Hermitian (lossless) operator. However, this assumption fails when losses are included, as is for example the current case dealing with generally non-proper (leaky, radiative) eigenmodes of a non-Hermitian (lossy) operator. In this case, the coupling-matrix elements will generally be complex and their imaginary parts will be shown to be directly related to far-field radiation interference.

Imagine a system of many resonators in proximity to each other. When their resonances have close enough frequencies compared to their coupling rates, the CMT assumption is that the total-system field ψ is approximately determined only by these resonances as the superposition $\psi(t) = \sum_n a_n(t)\psi_n$, where ψ_n is the eigenfield of the resonance n normalized to unity energy, and a_n is the field amplitude inside it, which corresponds, due to the normalization, to $|a_n|^2$ stored energy. The fundamental Coupled-Mode Equations (CME) of CMT are then those of the evolution of the vector $\boldsymbol{a} = \{a_n\}$

$$\frac{d}{dt}a = -i\overline{\mathbf{\Omega}} \cdot a + i\overline{\mathbf{K}} \cdot a \tag{34}$$

where the frequency matrix $\overline{\mathbf{\Omega}}$ and the coupling matrix $\overline{\mathbf{K}}$ are found usually using a Perturbation Theory (PT) approach.

We restate here one of the many perturbative formulations of CMT in a system of ElectroMagnetic (EM) resonators: Let $\mu = \mu_o$ and $\epsilon = \epsilon_o + \sum_n \epsilon_n$ be the magnetic-permeability and dielectric-permittivity functions of space that describe the whole system, where ϵ_n is the permittivity of only the dielectric, reciprocal and generally anisotropic object n of volume V_n, in excess to the constant μ_o, ϵ_o background space. Each resonator n, when alone in the background space, supports a resonant eigenmode of complex frequency $\Omega_n = \omega_n - i\Gamma_n$ and field profiles $\psi_n = [\mathbf{E}_n, \mathbf{H}_n]$ normalized to unity energy, satisfying the equations $\nabla \times \mathbf{E}_n = i\Omega_n\mu_o\mathbf{H}_n$ and $\nabla \times \mathbf{H}_n = -i\Omega_n(\epsilon_o + \epsilon_n)\mathbf{E}_n$,

InductEV, Inc.
Exhibit 1025
Page 551

and the boundary condition $\hat{\mathbf{n}} \times \mathbf{E}_n = 0$ on the potential metallic surface S_n of object n. The whole system fields $\psi = [\mathbf{E}, \mathbf{H}]$ satisfy the equations $\nabla \times \mathbf{E} = -\mu \frac{\partial}{\partial t} \mathbf{H}$ and $\nabla \times \mathbf{H} = \epsilon \frac{\partial}{\partial t} \mathbf{E}$, and the boundary condition $\hat{\mathbf{n}} \times \mathbf{E} = 0$ on $S = \sum_n S_n$. Then, start by expanding $\nabla \cdot (\mathbf{E} \times \mathbf{H}_n^- - \mathbf{E}_n^- \times \mathbf{H})$ and integrating over all space, apply the CMT superposition assumption, and finally use the PT argument that, when the coupling-rates between the resonators are small compared to their frequencies, within a sum only terms of lowest order in this small perturbation need to be kept. The result is the CME of Eq.(34), with $\bar{\boldsymbol{\Omega}} = \bar{\mathbf{W}}^{-1} \cdot \bar{\boldsymbol{\Omega}}_o \cdot \bar{\mathbf{W}}$, $\bar{\mathbf{K}} = \bar{\mathbf{W}}^{-1} \cdot \mathbf{K}_o$, where $\bar{\boldsymbol{\Omega}}_o = \mathrm{diag}\{\Omega_n\}$,

$$K_{o,nm} = \frac{\Omega_n}{4} \int_{V_m} dv \left(\mathbf{E}_n^- \cdot \varepsilon_m \cdot \mathbf{E}_m \right) + \frac{i}{4} \oint_{S_m} da \hat{\mathrm{n}} \cdot \left(\mathbf{E}_n^- \times \mathbf{H}_m \right) \quad (35)$$

$$W_{nm} = \frac{1}{4} \int_{V_m} dv \left(\mathbf{E}_n^- \cdot \varepsilon \cdot \mathbf{E}_m + \mathbf{H}_n^- \cdot \mu \cdot \mathbf{H}_m \right) \quad (36)$$

and where $\psi_n = [\mathbf{E}_n^-, \mathbf{H}_n^-]$ satisfy the time-reversed equations (where $\Omega_n \to -\Omega_n$). The choice of these fields in the analysis rather than $\psi_n^* = [\mathbf{E}_n^*, \mathbf{H}_n^*]$ allows to treat also lossy (due to absorption and/or radiation) but reciprocal systems (so $\bar{\mathbf{K}}$ is complex symmetric but non-Hermitian). In the limit, though, of weak loss (high-Q resonances), these two sets of fields can be approximately equal. Therefore, again to lowest order, $\bar{\mathbf{W}} \approx \bar{\mathbf{I}}$, due to the unity-energy normalization, so $\bar{\boldsymbol{\Omega}} \approx \bar{\boldsymbol{\Omega}}_o$ and for $\bar{\mathbf{K}}$ the off-diagonal terms

$$K_{nm} \approx K_{o,mn} \approx \frac{i}{4} \int_{V_m} dv \left(\mathbf{E}_n^* \cdot \mathbf{J}_m \right); \quad n \neq m \quad (37)$$

where $\mathbf{J}_m$ includes both the volume-polarization currents $\mathbf{J}_{p,m} = -i\Omega_m \epsilon_m \mathbf{E}_m$ in V_m and the surface electric currents $\mathbf{J}_{s,m} = \hat{\mathbf{n}} \times \mathbf{H}_m$ on S_m, while the diagonal terms K_{nn} are higher-order small and can often lead to anomalous coupling-induced frequency shifts. The term of Eq.(37) can generally be complex $K_{\mathrm{nm}} = \kappa_{\mathrm{nm}} + i\Lambda_{\mathrm{nm}}$ and, even though the physical interpretation of its real part is well understood, as describing the coupling between the resonators, it is not so the case for its imaginary part

InductEV, Inc.
Exhibit 1025
Page 552

$$\Lambda_{nm} = \frac{1}{4}\mathrm{Re}\left\{\int_{V_m} dv\left[i\omega\mathbf{A}_n - \nabla\phi_n\right]^* \cdot \mathbf{J}_m\right\}$$

$$= \frac{1}{4}\mathrm{Re}\left\{\int_{V_m} dv\left[\int_{V_n} dv \frac{e^{ik|\mathbf{r_m}-\mathbf{r_n}|}}{4\pi|\mathbf{r_m}-\mathbf{r_n}|}\left(i\omega\mu_0\mathbf{J}_n + \frac{\rho_n}{\varepsilon_0}\nabla\right)\right]^* \cdot \mathbf{J}_m\right\} \quad (38)$$

$$= \frac{\omega}{16\pi}\int_{V_m} dv \int_{V_n} dv\,\mathrm{Re}\left\{\left(\frac{\rho_n^*\rho_m}{\varepsilon_0} - \mu_0\mathbf{J}_n^* \cdot \mathbf{J}_m\right)\frac{e^{ik|\mathbf{r}_m-\mathbf{r}_n|}}{4\pi|\mathbf{r}_m-\mathbf{r}_n|}\right\}$$

where integration by parts was used for the $\nabla\phi_n$ term and the continuity equation $\nabla \cdot \mathbf{J} = i\omega\rho$, with ρ being the volume charge density.

Towards understanding this term, let us consider two resonators 1, 2 and evaluate from Eqs.(34) the total power lost from the system

$$\begin{aligned} P_{loss} &= -\frac{d}{dt}\left(|a_1|^2 + |a_2|^2\right) \\ &= 2\Gamma_1|a_1|^2 + 2\Gamma_2|a_2|^2 + 4\Lambda_{12}\,\mathrm{Re}\left\{a_1^* a_2\right\} \end{aligned} \quad (39)$$

Clearly, the term involving an interaction between the two objects should not relate to material absorption, since this is a very localized process inside each object. We therefore split this lost power into absorbed and radiated in the following way

$$P_{abs} = 2\Gamma_{1,abs}|a_1|^2 + 2\Gamma_{2,abs}|a_2|^2 \quad (40)$$

$$P_{rad} = 2\Gamma_{1,rad}|a_1|^2 + 2\Gamma_{2,rad}|a_2|^2 + 4\Lambda_{12}\,\mathrm{Re}\left\{a_1^* a_2\right\} \quad (41)$$

so Λ_{12} is associated with the radiation from the two-object system. However, we have a tool to compute this radiated power separately: Antenna Theory (AT).

Let $\zeta_o = \sqrt{\mu_o/\epsilon_o}$ and $c_o = 1/\sqrt{\mu_o\epsilon_o}$ be the background impedance and light-velocity, and $f = (g, \mathbf{f}) = \int_V dv' J^\nu(\mathbf{r}')e^{-i\mathbf{k}\cdot\mathbf{r}'}$ the moment of the current-distribution 4-vector $J^\nu = (c_o\rho, \mathbf{J})$ of an electromagnetic resonator, where unity-energy normalization is

InductEV, Inc.
Exhibit 1025
Page 553

again assumed for J^ν and $g = \hat{\mathbf{k}} \cdot \mathbf{f}$, as can be shown using the continuity equation and integration by parts. The power radiated from one EM resonator is:

$$P_{rad} = 2\Gamma_{rad}|a|^2 = \frac{\varsigma_o k^2}{32\pi^2}\left(\oint d\Omega |f|^2\right)|a|^2 \tag{42}$$

where $|f|^2 = f^* \cdot f \equiv |\mathbf{f}|^2 - |g|^2$. The power radiated from an 'array' of two resonators 1 and 2, at vector-distance $\mathbf{D}$ between their centers, is given by:

$$\begin{aligned} P_{rad} &= \frac{\varsigma_o k^2}{32\pi^2}\oint d\Omega \left|a_1 f_1 + a_2 f_2 e^{-i\mathbf{k}\cdot\mathbf{D}}\right|^2 \\ &= \frac{\varsigma_o k^2}{32\pi^2}\left[\begin{array}{l}\left(\oint d\Omega |f_1|^2\right)|a_1|^2 + \left(\oint d\Omega |f_2|^2\right)|a_2|^2 \\ +2\,\mathrm{Re}\left\{\oint d\Omega f_1^* \cdot f_2 e^{-i\mathbf{k}\cdot\mathbf{D}} a_1^* a_2\right\}\end{array}\right] \end{aligned} \tag{43}$$

where $f_1^* \cdot f_2 \equiv \mathbf{f}_1^* \cdot \mathbf{f}_2 - g_1^* \cdot g_2$. Thus, by comparing Eqs.(41) and (43), using Eq.(42),

$$\Lambda_{12} = \frac{\varsigma_o k^2}{64\pi^2}\frac{\mathrm{Re}\left\{\oint d\Omega f_1^* \cdot f_2 e^{-i\mathbf{k}\cdot\mathbf{D}} a_1^* a_2\right\}}{\mathrm{Re}\left\{a_1^* a_2\right\}} \tag{44}$$

namely Λ_{12} is exactly the interference term in AT. By substituting for the 4-vector current-moments and making the change of variables $\mathbf{r}_1 = \mathbf{r}_1'$, $\mathbf{r}_2 = \mathbf{r}_2' + \mathbf{D}$,

$$\begin{aligned} \Lambda_{12} &= \frac{\varsigma_o k^2}{64\pi^2}\frac{\mathrm{Re}\left\{\int_{V_1} dv \int_{V_2} dv J_1^* \cdot J_2 \oint d\Omega e^{-i\mathbf{k}\cdot(\mathbf{r_2}-\mathbf{r_1})} a_1^* a_2\right\}}{\mathrm{Re}\left\{a_1^* a_2\right\}} \\ &= \frac{\varsigma_o k}{16\pi}\frac{\mathrm{Re}\left\{\int_{V_1} dv \int_{V_2} dv J_1^* \cdot J_2 \frac{\sin\left(k|\mathbf{r_2}-\mathbf{r_1}|\right)}{|\mathbf{r_2}-\mathbf{r_1}|} a_1^* a_2\right\}}{\mathrm{Re}\left\{a_1^* a_2\right\}} \end{aligned} \tag{45}$$

where we evaluated the integral over all angles of $\mathbf{k}$ with $\mathbf{r}_2 - \mathbf{r}_1$.

InductEV, Inc.
Exhibit 1025
Page 554

Note now that Eqs.(38) and (45) will become identical, if we can take the currents $J_{1,2}^{\nu}$ to be real. This is indeed the case for eigenmodes, where the field solution in bounded regions (such as those where the currents are flowing) is always stationary (in contrast to the leaky part of the eigenmode, which is radiative) and for high enough Q it can be chosen so that it is approximately real in the entire bounded region. Therefore, from either Eq.(38) or (45) we can write

$$\Lambda_{12} = \frac{\zeta_o k}{16\pi} \int_{V_1} dv \int_{V_2} dv J_1 \cdot J_2 \frac{\sin\left(k|\mathbf{r}_2 - \mathbf{r}_1|\right)}{|\mathbf{r}_2 - \mathbf{r}_1|} \tag{46}$$

and from Eq.(44), using Eq.(42), we can define the interference factor

$$V_{\text{rad},12} \equiv \frac{\Lambda_{12}}{\sqrt{\Gamma_{1,\text{rad}}\Gamma_{2,\text{rad}}}} = \frac{\oint d\Omega f_1^* \cdot f_2 e^{-i\mathbf{k}\cdot\mathbf{D}}}{\sqrt{\oint d\Omega |f_1|^2 \oint d\Omega |f_2|^2}} \tag{47}$$

We have shown that, in the high-Q limit, both PT and AT give the same expression for the imaginary part Λ_{nm} of the coupling coefficient, which thus physically describes within CMT the effects of far-field radiation interference. Again, this phenomenon was so far not considered to be predictable from CMT.

4 Efficiency enhancement and radiation suppression by far-field destructive interference

Physically, one can expect that far-field radiation interference can in principle be engineered to be destructive, resulting in reduced overall radiation losses for the two-object system and thus in enhanced system efficiency. In this section, we show that, indeed, in the presence of far-field interference, energy transfer can be more efficient and with less radiated power than what our previous model predicts.

Once more, we will treat the same temporal energy-transfer schemes as before (finite-amount and finite-rate), so that a direct comparison can be made.

4.1 Finite-amount energy-transfer efficiency

Considering again the source and device objects 1,2 to include the interference effects, the same CMT equations as in Eq.(1) can be used, but with the substitutions $\kappa_{\text{nm}} \rightarrow K_{\text{nm}} = \kappa_{\text{nm}} + i\Lambda_{\text{nm}}$; $\text{n,m} = 1,2$. The real parts $\kappa_{11,22}$ can describe, as before, the shift in each object's resonance frequency due to the presence of the other; the imaginary parts $\Lambda_{11,22}$ can describe the change in the losses of each object due to the

InductEV, Inc.
Exhibit 1025
Page 555

presence of the other (due to absorption in it or scattering from it, in which latter case losses could be either increased or decreased); both of these are second-order effects and, for the purposes of our mathematical analysis, can again be absorbed into the complex eigenfrequencies by setting $\omega_{1,2} \to \omega_{1,2} + \kappa_{11,22}$ and $\Gamma_{1,2} \to \Gamma_{1,2} - \Lambda_{11,22}$. The real parts $\kappa_{12,21}$ can denote, as before, the coupling coefficients; the imaginary parts $\Lambda_{12,21}$ can describe the far-field interference, as was shown in Section 3; again, from reciprocity $K_{12} = K_{21} \equiv K \equiv \kappa + i\Lambda$ (note that for a Hermitian problem, the additional requirement $K_{12} = K_{21}^*$ would impose K to be real, which makes sense, since without losses there cannot be any radiation interference).

Substituting $\kappa \to \kappa + i\Lambda$ into Eq.(2), we can find the normal modes of the system including interference effects. Note that, when the two objects are at exact resonance $\omega_1 = \omega_2 \equiv \omega_o$ and $\Gamma_1 = \Gamma_2 \equiv \Gamma_o$, the normal modes are found to be

$$\Omega_+ = (\omega_0 + \kappa) - i(\Gamma_0 - \Lambda) \text{ and } \Omega_- = (\omega_0 - \kappa) - i(\Gamma_0 + \Lambda), \tag{48}$$

which is exactly the typical case for respectively the odd and even normal modes of a system of two coupled objects, where for the even mode the objects' field-amplitudes have the same sign and thus the frequency is lowered and the radiative far-fields interfere constructively so loss is increased, while for the odd mode the situation is the opposite. This is another confirmation for the fact that the coefficient Λ can describe the far-field interference phenomenon under examination.

To treat now again the problem of energy transfer to object 2 from 1, but in the presence of radiative interference, again simply substitute $\kappa \to \kappa + i\Lambda$ into Eq.(3). Note that, at exact resonance $\omega_1 = \omega_2$ and, in the special case $\Gamma_1 = \Gamma_2 \equiv \Gamma_o$, we can just substitute into Eq.(4) $U \to U + iV$, where $U \equiv \kappa/\Gamma_o$ and $V \equiv \Lambda/\Gamma_o$, and then, with $T \equiv \Gamma_o t$, the evolution of the device field-amplitude becomes

$$\frac{a_2(T)}{|a_1(0)|} = \sin[(U + iV)T] \cdot e^{-T} \tag{49}$$

Now the efficiency $\eta_E \equiv |a_2(t)|^2/|a_1(0)|^2$ can be optimized for the normalized time T_* which is the solution of the transcendental equation

InductEV, Inc.
Exhibit 1025
Page 556

$$Re\{(U+iV)\cdot\cot[(U+iV)T_*]\}=1 \tag{50}$$

and the resulting optimal energy-transfer efficiency depends only on U, V and is depicted in Fig. 16(c), evidently increasing with V for a fixed U.

4.2 Finite-rate energy-transfer (power-transmission) efficiency

Similarly, to treat the problem of continuous powering of object 2 by 1, in the presence of radiative interference, simply substitute $U \to U+iV$ into the equations of Section 1.2, where $V \equiv \Lambda/\sqrt{\Gamma_1\Gamma_2}$ we call the strong-interference factor and quantifies the degree of far-field interference that the system experiences compared to loss. In practice, the parameters $D_{1,2}$, $U_{1,2}$ can be designed (engineered), since one can adjust the resonant frequencies $\omega_{1,2}$ (compared to the desired operating frequency ω) and the generator/load supply/drain rates $\kappa_{1,2}$. Their choice can target the optimization of some system performance-characteristic of interest.

In some examples, a goal can be to maximize the power transmission (efficiency) $\eta_P \equiv |S_{21}|^2$ of the system. The symmetry upon interchanging $1 \leftrightarrow 2$ is then preserved and, using Eq.(11), the field-amplitude transmission coefficient becomes

$$S_{21}=\frac{2i(U+iV)U_0}{(1+U_0-iD_0)^2+(U+iV)^2} \tag{51}$$

and from $\eta_P'(D_o)=0$ we get that, for fixed U, V and U_o, the efficiency can be maximized for the symmetric detuning

$$D_0=\begin{cases}2\sqrt{\alpha}\cos\left(\dfrac{\theta+2\nu\pi}{3}\right);\nu=0,1, & if\ \ U^{2/3}-V^{2/3}>(1+U_0)^{2/3}\\ \sqrt[3]{\beta+\sqrt{\beta^2-\alpha^3}}+\sqrt[3]{\beta-\sqrt{\beta^2-\alpha^3}} & if\ \ U^{2/3}-V^{2/3}\le(1+U_0)^{2/3}\end{cases} \tag{52}$$

where $\alpha \equiv [U^2-V^2-(1+U_o)^2]/3$, $\beta \equiv UV(1+U_o)$, $\theta \equiv \tan^{-1}\sqrt{\alpha^3/\beta^2-1}$ and $U^{2/3}-V^{2/3}>(1+U_o)^{2/3} \Leftrightarrow \alpha^3-\beta^2>0 \Leftrightarrow \alpha>0$. Note that, in the first case, the two peaks of the transmission curve are not equal for $V>0$, but the one at higher frequencies ($\nu=0 \Rightarrow$ positive detuning) corresponding to the odd system normal mode is higher, as should be expected, since the odd mode is the one that radiates less. Finally,

InductEV, Inc.
Exhibit 1025
Page 557

by substituting D_o into η_P from Eq.(52), then from $\eta_P'(U_o) = 0$ we get that, for fixed U and V, the efficiency can be maximized for

$$U_{0*} = \sqrt{(1+U^2)(1-V^2)} \quad \text{and} \quad D_{0*} = UV. \tag{53}$$

The dependence of the efficiency on D_o for different U_o (including the new 'critical-coupling' condition) are shown in Figs. 16(a,b). The overall optimal power efficiency using Eqs.(53) is

$$\eta_{P*} \equiv \eta_P(D_{0*}, U_{0*}) = \frac{U^2+V^2}{(U_{0*}+1)^2 + U^2V^2} \tag{54}$$

which depends only on U, $|V|$ and is depicted in Figs. 16 (c,d), increasing with $|V|$ for a fixed U, and actually $\eta_P \to 1$ as $|V| \to 1$ for all values of U.

In some examples, a goal can be to minimize the power reflection at the side of the generator $|S_{11}|^2$ and the load $|S_{22}|^2$. The symmetry upon interchanging $1 \leftrightarrow 2$ is again preserved and, using then Eq.(17), one would require the 'impedance matching' condition

$$(1 - iD_0)^2 - U_0^2 + (U + iV)^2 = 0 \tag{55}$$

from which again we easily find that the values of D_o and U_o that cancel all reflections are exactly those in Eqs.(53).

In some examples, it can be of interest to minimize the power radiated from the system, since e.g. it can be a cause of interference to other communication systems, while still maintaining good efficiency. In some examples, the two objects can be the same, and then, using Eq.(41), we find

$$\eta_{rad} \equiv \frac{P_{rad}}{|S_{+1}|^2} = \frac{4U_0(|1+U_0-iD_0|^2 + |U+iV|^2)\frac{Q}{Q_{rad}} - 2V(V+VU_0+UD_0)}{|(1+U_0-iD_0)^2 + (U+iV)^2|^2} \tag{56}$$

Then, to achieve our goal, we maximize η_P/η_{rad} and find that this can be achieved for

$$U_{0**} = \sqrt{1+U^2-V_{rad}^2U^2+V^2-2VV_{rad}} \quad \text{and} \quad D_{0**} = UV_{rad},$$

InductEV, Inc.
Exhibit 1025
Page 558

(57)

where $V_{\mathrm{rad}} \equiv \Lambda/\sqrt{\Gamma_{1,\mathrm{rad}}\Gamma_{2,\mathrm{rad}}}$, as defined in Eq.(47), we call the interference factor and quantifies the degree of far-field interference that the system experiences compared to the radiative loss, thus $V_{\mathrm{rad}} = V\sqrt{\frac{Q_{1,\mathrm{rad}}}{Q_1}\frac{Q_{2,\mathrm{rad}}}{Q_2}} \geq V$, and $V = V_{\mathrm{rad}}$ when all loss is radiative, in which case Eq.(57) reduces to Eq.(53).

In this description, we suggest that, for any temporal energy-transfer scheme and given some achieved coupling-to-loss ratio, the efficiency can be enhanced and the radiation can be suppressed by shifting the operational frequency away from exact resonance with each object's eigenfrequency and closer to the frequency of the odd normal-mode, which suffers less radiation due to destructive far-field interference. It is the parameters

$$U = \frac{\kappa}{\sqrt{\Gamma_1\Gamma_2}} = k\sqrt{Q_1Q_2} \qquad \text{and} \qquad V = \frac{\Lambda}{\sqrt{\Gamma_1\Gamma_2}} = V_{\mathrm{rad}}\sqrt{\frac{Q_1}{Q_{1,\mathrm{rad}}}\frac{Q_2}{Q_{2,\mathrm{rad}}}} \tag{58}$$

that are the figures-of-merit for any system under consideration for wireless energy-transfer, along with the distance over which large$U$, $|V|$ can be achieved. Clearly, also $|V|$ can be a decreasing function of distance, since two sources of radiation distant by more than a few wavelengths do not interfere substantially. It is important also to keep in mind that the magnitude of V depends on the degree to which radiation dominates the objects' losses, since it is only these radiative losses that can contribute to interference, as expressed from $V_{\mathrm{rad}} \geq V$.

To achieve a large strong-interference factor V, in some examples, the energy-transfer application preferably uses again subwavelength resonances, because, for a given source-device distance, the interference factor V_{rad} will increase as frequency decreases, since naturally the odd mode of two coupled objects, distant much closer than a wavelength, will not radiate at all.

To achieve a large strong-interference factor V, in some examples, the energy-transfer application preferably uses resonant modes of high factors Q/Q_{rad}. This condition can be satisfied by designing resonant modes where the dominant loss

InductEV, Inc.
Exhibit 1025
Page 559

mechanism is radiation. As frequency decreases, radiation losses always decrease and typically systems are limited by absorption losses, as discussed earlier, so Q/Q_{rad} decreases; thus, the advantage of interference can be insignificant at some point compared to the deterioration of absorption-Q.

Therefore, $|V|$ will be maximized at some frequency ω_V, dependent on the source-device distance, and this optimal frequency will typically be different than ω_U, the optimal frequency for U. As seen above, the problem of maximizing the energy-transfer efficiency can require a modified treatment in the presence of interference. The choice of eigenfrequency for the source and device objects as ω_U, where U is maximum, can not be a good one anymore, but also V needs to be considered. The optimization of efficiency occurs then at a frequency ω_η between ω_U and ω_V and is a combined problem, which will be demonstrated below for few examples of electromagnetic systems.

Moreover, note that, at some fixed distance between the source and device objects, the figures U, V can not be maximized for the same set of system parameters; in that case, these parameters could be chosen so that the efficiency of Eq.(54) is maximized.

In the following section, we calculate a magnitude of efficiency improvement and radiation reduction for realistic systems at mid-range distances between two objects, by employing this frequency detuning and by doing a joint optimization for U, V.

5 Far-field interference at mid-range distances for realistic systems

In the case of two objects 1, 2 supporting radiative electromagnetic resonant modes of the same eigenfrequency $\omega_1 = \omega_2 \equiv \omega_o$ and placed at distance D between their arbitrarily-chosen centers, so that they couple in the near field and interfere in the far field, the interference factor V_{rad} is predicted from antenna theory (AT) to be that in Eq.(47).

We have also seen above how to compute the resonance quality factors Q and Q_{rad}, for some example structures, and thus we can compute the factor Q/Q_{rad}.

We will demonstrate the efficiency enhancement and the radiation suppression due to interference for the two examples of capacitively-loaded conducting loops and

InductEV, Inc.
Exhibit 1025
Page 560

dielectric disks. The degree of improvement will be shown to depend on the nature of the system.

5.1 Capacitively-loaded conducting loops

Consider two loops 1, 2 of radius r with N turns of conducting wire with circular cross-section of radius a at distance D, as shown in Fig. 10. It was shown in Section 2.2 how to calculate the quality, coupling and strong-coupling factors for such a system.

Their coupling factor is shown in Fig. 17(a) as a function of the relative distance D/r, for three different dimensions of single-turn ($N = 1$) loops. Their strong-coupling factor at the eigenfrequency $\omega_{Q_1Q_2}$ is shown in Fig. 17(b). The approximate scaling $k, U \propto (r/D)^3$, indicated by Eqs.(26) and (27), is apparent.

We compute the interference parameter between two coupled loops at distance D, using the AT analysis Eq.(47), leading to

Consider two loops 1, 2 of radius r with N turns of conducting wire with circular cross-section of radius a at distance D, as shown in Fig. 10. It was shown in Section 2.2 how to calculate the quality, coupling and strong-coupling factors for such a system. Their coupling factor is shown in Fig. 17(a) as a function of the relative distance D/r, for three different dimensions of single-turn ($N = 1$) loops. Their strong-coupling factor at the eigenfrequency $\omega_{Q_1Q_2}$ is shown in Fig. 17(b). The approximate scaling $k, U \propto (r/D)^3$, indicated by Eqs.(26) and (27), is apparent. We compute the interference parameter between two coupled loops at distance D, using the AT analysis Eq.(47), leading to

$$V_{\text{rad}} = \frac{3}{(kD)^3}\left[\sin(kD) - (kD)\cos(kD)\right], \tag{59}$$

for the orientation of optimal coupling, where one loop is above the other. Their interference factor is shown in Fig. 18 as a function of the normalized distance D/λ, where it can be seen that this factor has nulls only upon reaching the radiative regime. Since the resonant loops are highly subwavelength (in many examples $\lambda/r \geq 50$), at mid-range distances ($D/r \leq 10$), we expect $D/\lambda \leq 0.2$ and thus the interference factor to be very large ($V_{\text{rad}} \geq 0.8$).

InductEV, Inc.
Exhibit 1025
Page 561

At a fixed resonant frequency, in some examples, the factor Q/Q_{rad} can be increased by increasing the radii r of the loops. In some examples, the factor Q/Q_{rad} can be increased by increasing the number N of turns of the loops. In some examples, the factor Q/Q_{rad} can be increased by increasing the radius a of the conducting wire of the loops or by using Litz wire or a ribbon to reduce the absorption losses and thus make radiation more dominant loss mechanism.

We also plot in Fig. 19, for the example $r = 30cm$ and $a = 2cm$, the strong-coupling factor U, the interference factor V_{rad} and the strong-interference factor V as a function of the resonant eigenfrequency of the loops, for a fixed distance $D = 5r$. Indeed, for this example, V_{rad} decreases monotonically with frequency in this subwavelength regime and is always great than 0.8, but V exhibits a maximum, since the term Q/Q_{rad} is increasing towards 1 with frequency, as losses become more and more radiation dominated. It can be seen that the resonant eigenfrequencies f_U and f_V, at which U and V become maximum respectively, are different. This implies that the efficiency will now not necessarily peak at the eigenfrequency f_U, at which U is maximized, as would be the assumption based on prior knowledge, but at a different one f_η between f_U and f_V. This is shown below.

In Fig. 20 the efficiency η_P is plotted as a function of the resonant eigenfrequency of the loops for two different examples of loop dimensions $r = 30cm$, $a = 2cm$ and $r = 1m$, $a = 2cm$, at two different loop distances $D = 5r$ and $D = 10r$, and for the cases:

(i) (solid lines) including interference effects and detuning the driving frequency from the resonant frequency by $D_o = UV$ from Eq.(53) to maximize the power-transmission efficiency and similarly using U_o from Eq.(53), which thus implies optimal efficiency as in Eq.(54).

(ii) (dash-dotted lines) including interference effects and detuning the driving frequency from the resonant frequency by $D_o = UV_{\text{rad}}$ from Eq.(57) to maximize the ratio of power transmitted over power radiated and similarly using U_o from Eq.(57).

(iii) (dashed lines) including interference effects but not detuning the driving frequency from the resonant frequency and using U_o from Eq.(14), as one would do to maximize

InductEV, Inc.
Exhibit 1025
Page 562

efficiency in the absence of interference.
(iv) (dotted lines) truly in the absence of interference effects and thus maximizing efficiency by not detuning the driving frequency from the resonant frequency and using U_o from Eq.(14), which thus implies efficiency as in Eq.(15).

In Fig. 21 we show the amount of driving-frequency detuning that is used in the presence of interference either to maximize efficiency (case (i) (solid lines) of Fig. 20 - $D_o = UV$) or to maximize the ratio of power transmitted over power radiated (case (ii) (dash-dotted lines) of Fig. 20 - $D_o = UV_{\text{rad}}$). Clearly, this driving-frequency detuning can be a non-trivial amount.

It can be seen from Fig. 20 that, for all frequencies, the efficiency of case (i) (solid lines) is larger than the efficiency of case (iii) (dashed lines) which is in turn larger than the efficiency of case (iv) (dotted lines). Therefore, in this description, we suggest that employing far-field interference improves on the power-transmission efficiency (improvement from (iv) (dotted) to (iii) (dashed)) and, furthermore, employing destructive far-field interference, by detuning the driving frequency towards the low-radiation-loss odd normal mode, improves on the power-transmission efficiency even more (improvement from (iii) (dashed) to (i) (solid)).

If f_η is the eigenfrequency, at which the efficiency of case (i) (solid) is optimized, then, in some examples, the resonant eigenfrequency can be designed to be larger than f_η, namely in a regime where the system is more radiation dominated. In this description, we suggest that at such eigenfrequencies, there can be a significant improvement in efficiency by utilizing the destructive far-field interference effects and driving the system at a frequency close to the odd normal mode. This can be seen again from Fig. 20 by comparing the solid lines to the corresponding dashed lines and the dotted lines.

In general, one would tend to design a system resonant at the frequency f_U where the strong-coupling factor U is maximal. However, as suggested above, in the presence of interference, Fig. 20 shows that the maximum of η_P is at an eigenfrequency f_η different than f_U. In some examples, $f_\eta > f_U$. This is because at higher eigenfrequencies, losses are determined more by radiation than absorption, therefore destructive radiation interference can play a more significant role in reducing overall losses and thus $f_V > f_U$ and the efficiency in increased at $f_\eta > f_U$. In this description, we

InductEV, Inc.
Exhibit 1025
Page 563

suggest that, in some examples, the resonant eigenfrequency can be designed to be close to the frequency f_η that optimizes the efficiency rather than the different f_U. In particular, in Fig. 22(a) are plotted these two frequencies f_η (solid line) and f_U (dashed line) as a function of relative distance D/r of two $r = 30cm$ loops. In Fig. 22(b) we show a graded plot of the optimal efficiency from Eq.(54) in the $U - V$ plane. Then, we superimpose the $U - V$ curve of case (i) (solid), parametrized with distance D, for two $r = 30cm$ loops resonant at the optimal frequency f_η for each D. From the path of this curve onto the graded plot the efficiency as a function of distance can be extracted for case (i) (solid). We then also superimpose in Fig. 22(b) the $U - V$ curve of case (iii) (dashed) , parametrized with distance D, for two $r = 30cm$ loops resonant at f_U, and the U range of case (iv) (dotted), parametrized with distance D, for two $r = 30cm$ loops resonant at f_U (note that in this last case there is no interference and thus $V = 0$). In Fig. 22(c) we then show the efficiency enhancement factor achieved by the solid curve of Fig. 22(b), as a function of distance D/r, compared to best that can be achieved without driving-frequency detuning (dashed) and without interference whatsoever (dotted). The improvement by employing interference can reach a factor of 2 at large separation between the loops.

In Fig. 23 we plot the radiation efficiency η_{rad}, using Eq.(39), as a function of the eigenfrequency of the loops for the two different loop dimensions, the two different distances and the four different cases examined in Fig. 20. It can be seen from Fig. 23 that, for all frequencies, η_{rad} of case (ii) (dash-dotted lines) is smaller than η_{rad} of case (i) (solid lines) which is in turn smaller than η_{rad} of case (iii) (dashed lines) and this smaller than η_{rad} of case (iv) (dotted lines). Therefore, in this description, we suggest that employing far-field interference suppresses radiation (improvement from (iv) (dotted) to (iii) (dashed)) and, furthermore, employing destructive far-field interference, by detuning the driving frequency towards the low-radiation-loss odd normal mode, suppress radiation efficiency even more (improvement from (iii) (dashed) to (i) (solid) and (ii) (dash-dotted)), more so in case (ii), specifically optimized for this purpose.

In some examples, the resonant eigenfrequency can be designed to be larger than f_η, namely in a regime where the system is more radiation dominated. In this description, we suggest that at such eigenfrequencies, there can be a significant suppression in

InductEV, Inc.
Exhibit 1025
Page 564

radiation by utilizing the destructive far-field interference effects and driving the system at a frequency close to the odd normal mode. The case (ii)=(dash-dotted) accomplishes the greatest suppression in radiation and, as can be seen in Fig. 20, there is a range of eigenfrequencies (close to f_V), for which the efficiency that this configuration can achieve is only little compromised compared to the maximum possible of configuration (i).

In one example, two single-turn loops of $r = 30cm$ and $a = 2cm$ are at a distance $D/r = 5$ in the orientation shown in Fig. 10 and they are designed to resonate at 30MHz. In the absence of interference, the power-transmission efficiency is 59% and the radiation efficiency is 38%. In the presence of interference and without detuning the driving frequency from 30MHz, the power-transmission efficiency is 62% and the radiation efficiency is 32%. In the presence of interference and detuning the driving frequency from 30MHz to 31.3MHz to maximize efficiency, the power-transmission efficiency is increased to 75% and the radiation efficiency is suppressed to 18%.

In another example, two single-turn loops of $r = 30cm$ and $a = 2cm$ are at a distance $D/r = 5$ in the orientation shown in Fig. 10 and they are designed to resonate at 10MHz. In the absence of interference or in the presence of interference and without detuning the driving frequency from 10MHz, the power-transmission efficiency is approximately 81% and the radiation efficiency is approximately 4%. In the presence of interference and detuning the driving frequency from 10MHz to 10.22MHz to maximize transmission over radiation, the power-transmission efficiency is 42%, reduced by less than a factor of 2, while the radiation efficiency is 0.4%, suppressed by an order of magnitude.

In another example, two single-turn loops of $r = 1m$ and $a = 2cm$ are at a distance $D/r = 5$ in the orientation shown in Fig. 10 and they are designed to resonate at 10MHz. In the absence of interference, the power-transmission efficiency is 48% and the radiation efficiency is 47%. In the presence of interference and without detuning the driving frequency from 10MHz, the power-transmission efficiency is 54% and the radiation efficiency is 37%. In the presence of interference and detuning the driving frequency from 10MHz to 14.8MHz to maximize efficiency, the power-transmission efficiency is increased to 66% and the radiation efficiency is suppressed to 24%.

InductEV, Inc.
Exhibit 1025
Page 565

In another example, two single-turn loops of $r = 1m$ and $a = 2cm$ are at a distance $D/r = 5$ in the orientation shown in Fig. 10 and they are designed to resonate at 4MHz. In the absence of interference or in the presence of interference and without detuning the driving frequency from 4MHz, the power-transmission efficiency is approximately 71% and the radiation efficiency is approximately 8%. In the presence of interference and detuning the driving frequency from 4MHz to 5.06MHz to maximize transmission over radiation, the power-transmission efficiency is 40%, reduced by less than a factor of 2, while the radiation efficiency is approximately 1%, suppressed by almost an order of magnitude.

5.2 Dielectric disks

Consider two dielectric disks 1 and 2 of radius r and dielectric permittivity ϵ placed at distance D between their centers, as shown in Fig. 15(b). Their coupling as a function of distance was calculated in Section 2.4, using analytical and finite-element-frequency-domain (FEFD) methods, and is shown in Fig. 24.

To compute the interference factor between two coupled disks at distance D, we again use two independent methods to confirm the validity of our results: numerically, the FEFD calculations again give Λ (and thus V) by the splitting of the loss-rates of the two normal modes; analytically, calculation of the AT prediction of Eq.(47) gives

$$\begin{aligned} m=1:&\quad V_{\text{rad}} = \frac{2}{(kD)} J_1(kD) \\ m=2:&\quad V_{\text{rad}} = \frac{8}{(kD)^3}\left\{3(kD)J_0(kD)+\left[(kD)^2-6\right]J_1(kD)\right\} \\ m=3:&\quad V_{\text{rad}} = \frac{6}{(kD)^5}\left\{\left[24(kD)^3-320(kD)\right]J_0(kD)+\left[3(kD)^4-128(kD)^2+640\right]J_1(kD)\right\} \end{aligned} \tag{60}$$

The results for the interference of two same disks, for exactly the same parameters for which the coupling was calculated in Fig. 24, are presented in Fig. 25, as a function of frequency (due to varying ϵ) at fixed distances. It can be seen that also the strong-interference factor Γ can have nulls, which can occur even before the system enters the radiative-coupling regime, namely at smaller frequencies than those of U at the same distances, and it decreases with frequency, since then the objects become more and more absorption dominated, so the benefit from radiative interference is suppressed. Both the

InductEV, Inc.
Exhibit 1025
Page 566

above effects result into the fact that, for most distances, U (from Fig. 24(b)) and V (from Fig. 25(b)) can be maximized at different values of the frequency (f_U and f_V respectively), and thus different can also be the optimal frequency f_η for the final energy-transfer efficiency of Eq.(54), which is shown in Fig. 26 again for the same set of parameters. From this plot, it can be seen that interference can significantly improve the transfer efficiency, compared to what Eq.(15) would predict from the calculated values of the coupling figure-of-merit U.

Furthermore, not only does a given energy-transfer system perform better than what a prediction which ignores interference would predict, but also our optimization design will typically lead to different optimal set of parameters in the presence of interference. For example, for the particular distance $D/r = 5$, it turns out from Fig. 26 that the $m = 1$ resonant modes can achieve better efficiency than the $m = 2$ modes within the available range of ϵ, by making use of strong interference which counteracts their weaker U, as viewed in Fig. 24, from which one would have concluded the opposite performance. Moreover, even within the same m-branch, one would naively design the system to operate at the frequency f_U, at which U is maximum. However, the optimization design changes in the presence of interference, since the system should be designed to operate at the different frequency f_η, where the overall efficiency η peaks. In Fig. 27(a), we first calculate those different frequencies where the strong-coupling factor U and the efficiency η (which includes interference) peak, as distance D is changing for the choice of the $m = 2$ disk of Fig. 24, and observe that their difference is actually significant. Then, in Fig. 27(b) we show the peak efficiency for the various frequency choices. For large distances, where efficiency is small and could use a boost, the improvement factor reaches a significant 2 for the particular system under examination. The same result is shown in Fig. 27(c) as a plot of the path of the efficiency on the U - V map, as distance is changing. Similar results are derived for the modes of different m-order. Physically, moving to higher frequencies increases role of radiative losses compared to absorption and thus interference can have a greater influence. At the optimal frequency f_η radiated power including interference is close to what it is at f_U, but absorbed power is much less, therefore the efficiency has been improved.

InductEV, Inc.
Exhibit 1025
Page 567

In some examples, instead of improving efficiency, one might care more about minimizing radiation. In that case, we calculate at the frequency f_U how much power is radiated when optimized under the conditions Eq.(57) compared to the power radiated when simply operating on resonance ($D_0 = 0$) in the cases with and without interference (the latter case can be describing a case where the two disks do not interfere, because they are dissimilar, or due to decoherence issues etc.). We find in Fig. 28 that radiation can be suppressed by a factor of 1.6 by detuning the operating frequency towards the odd sub-radiant mode.

6 System Sensitivity to Extraneous Objects

In general, the overall performance of an example of the resonance-based wireless energy-transfer scheme depends strongly on the robustness of the resonant objects' resonances. Therefore, it is desirable to analyze the resonant objects' sensitivity to the near presence of random non-resonant extraneous objects. One appropriate analytical model is that of "perturbation theory" (PT), which suggests that in the presence of an extraneous perturbing object p the field amplitude $a_1(t)$ inside the resonant object 1 satisfies, to first order:

$$\frac{da_1}{dt} = -i\left(\omega_1 - i\Gamma_1\right)a_1 + i\left(\delta\kappa_{11(p)} + i\delta\Gamma_{1(p)}\right)a_1 \qquad (61)$$

where again ω_1 is the frequency and Γ_1 the intrinsic (absorption, radiation etc.) loss rate, while $\delta\kappa_{11(p)}$ is the frequency shift induced onto 1 due to the presence of p and $\delta\Gamma_{1(p)}$ is the extrinsic due to p (absorption inside p, scattering from p etc.) loss rate. $\delta\Gamma_{1(p)}$ is defined as $\delta\Gamma_{1(p)} \equiv \Gamma_{1(p)} - \Gamma_1$, where $\Gamma_{1(p)}$ is the total perturbed loss rate in the presence of p. The first-order PT model is valid only for small perturbations. Nevertheless, the parameters $\delta\kappa_{11(p)}$, $\delta\Gamma_{1(p)}$ are well defined, even outside that regime, if a_1 is taken to be the amplitude of the exact perturbed mode. Note also that interference effects between the radiation field of the initial resonant-object mode and the field scattered off the extraneous object can for strong scattering (e.g. off metallic objects) result in total $\Gamma_{1,\mathrm{rad}(p)}$ that are smaller than the initial $\Gamma_{1,\mathrm{rad}}$ (namely $\delta\Gamma_{1,\mathrm{rad}(p)}$ is negative).

InductEV, Inc.
Exhibit 1025
Page 568

It has been shown that a specific relation is desired between the resonant frequencies of the source and device-objects and the driving frequency. In some examples, all resonant objects must have the same eigenfrequency and this must be equal to the driving frequency. In some examples, when trying to optimize efficiency or suppress radiation by employing far-field interference, all resonant objects must have the same eigenfrequency and the driving frequency must be detuned from them by a particular amount. In some implementations, this frequency-shift can be "fixed" by applying to one or more resonant objects and the driving generator a feedback mechanism that corrects their frequencies. In some examples, the driving frequency from the generator can be fixed and only the resonant frequencies of the objects can be tuned with respect to this driving frequency.

The resonant frequency of an object can be tuned by, for example, adjusting the geometric properties of the object (e.g. the height of a self-resonant coil, the capacitor plate spacing of a capacitively-loaded loop or coil, the dimensions of the inductor of an inductively-loaded rod, the shape of a dielectric disc, etc.) or changing the position of a non-resonant object in the vicinity of the resonant object.

In some examples, referring to Fig. 29a, each resonant object is provided with an oscillator at fixed frequency and a monitor which determines the eigenfrequency of the object. At least one of the oscillator and the monitor is coupled to a frequency adjuster which can adjust the frequency of the resonant object. The frequency adjuster determines the difference between the fixed driving frequency and the object frequency and acts, as described above, to bring the object frequency into the required relation with respect to the fixed frequency. This technique assures that all resonant objects operate at the same fixed frequency, even in the presence of extraneous objects.

In some examples, referring to Fig. 29(b), during energy transfer from a source object to a device object, the device object provides energy or power to a load, and an efficiency monitor measures the efficiency of the energy-transfer or power-transmission. A frequency adjuster coupled to the load and the efficiency monitor acts, as described above, to adjust the frequency of the object to maximize the efficiency.

In other examples, the frequency adjusting scheme can rely on information exchange between the resonant objects. For example, the frequency of a source object

InductEV, Inc.
Exhibit 1025
Page 569

can be monitored and transmitted to a device object, which is in turn synched to this frequency using frequency adjusters, as described above. In other embodiments the frequency of a single clock can be transmitted to multiple devices, and each device then synched to that frequency using frequency adjusters, as described above.

Unlike the frequency shift, the extrinsic perturbing loss due to the presence of extraneous perturbing objects can be detrimental to the functionality of the energy-transfer scheme, because it is difficult to remedy. Therefore, the total perturbed quality factors $Q_{(p)}$ (and the corresponding perturbed strong-coupling factor $U_{(p)}$ and the perturbed strong-interference factor $V_{(p)}$) should be quantified.

In some examples, a system for wireless energy-transfer uses primarily magnetic resonances, wherein the energy stored in the near field in the air region surrounding the resonator is predominantly magnetic, while the electric energy is stored primarily inside the resonator. Such resonances can exist in the quasi-static regime of operation ($r \ll \lambda$) that we are considering: for example, for coils with $h \ll 2r$, most of the electric field is localized within the self-capacitance of the coil or the externally loading capacitor and, for dielectric disks, with $\epsilon \gg 1$ the electric field is preferentially localized inside the disk. In some examples, the influence of extraneous objects on magnetic resonances is nearly absent. The reason is that extraneous non-conducting objects p that could interact with the magnetic field in the air region surrounding the resonator and act as a perturbation to the resonance are those having significant magnetic properties (magnetic permeability $Re\{\mu\}>1$ or magnetic loss $Im\{\mu\}>0$). Since almost all every-day non-conducting materials are non-magnetic but just dielectric, they respond to magnetic fields in the same way as free space, and thus will not disturb the resonance of the resonator. Extraneous conducting materials can however lead to some extrinsic losses due to the eddy currents induced inside them or on their surface (depending on their conductivity). However, even for such conducting materials, their presence will not be detrimental to the resonances, as long as they are not in very close proximity to the resonant objects.

The interaction between extraneous objects and resonant objects is reciprocal, namely, if an extraneous object does not influence a resonant object, then also the resonant object does not influence the extraneous object. This fact can be viewed in light of safety considerations for human beings. Humans are also non-magnetic and can

InductEV, Inc.
Exhibit 1025
Page 570

sustain strong magnetic fields without undergoing any risk. A typical example, where magnetic fields $B\sim 1T$ are safely used on humans, is the Magnetic Resonance Imaging (MRI) technique for medical testing. In contrast, the magnetic near-field required in typical embodiments in order to provide a few Watts of power to devices is only $B\sim 10^{-4}T$, which is actually comparable to the magnitude of the Earth's magnetic field. Since, as explained above, a strong electric near-field is also not present and the radiation produced from this non-radiative scheme is minimal, the energy-transfer apparatus, methods and systems described herein is believed safe for living organisms.

6.1 Capacitively-loaded conducting loops or coils

In some examples, one can estimate the degree to which the resonant system of a capacitively-loaded conducting-wire coil has mostly magnetic energy stored in the space surrounding it. If one ignores the fringing electric field from the capacitor, the electric and magnetic energy densities in the space surrounding the coil come just from the electric and magnetic field produced by the current in the wire; note that in the far field, these two energy densities must be equal, as is always the case for radiative fields. By using the results for the fields produced by a subwavelength ($r \ll \lambda$) current loop (magnetic dipole) with $h = 0$, we can calculate the ratio of electric to magnetic energy densities, as a function of distance D_p from the center of the loop (in the limit $r \ll D_p$) and the angle θ with respect to the loop axis:

$$\frac{w_e(x)}{w_m(x)} = \frac{\varepsilon_o |E(x)|^2}{\mu_o |H(x)|^2} = \frac{\left(1+\frac{1}{x^2}\right)\sin^2\theta}{\left(\frac{1}{x^2}+\frac{1}{x^4}\right)4\cos^2\theta + \left(1-\frac{1}{x^2}+\frac{1}{x^4}\right)\sin^2\theta}; \; x = 2\pi\frac{D_p}{\lambda}$$
$$\Rightarrow \frac{\oiint_{S_p} w_e(x)\,dS}{\oiint_{S_p} w_m(x)\,dS} = \frac{1+\frac{1}{x^2}}{1+\frac{1}{x^2}+\frac{3}{x^4}}; \; x = 2\pi\frac{D_p}{\lambda} \qquad (62)$$

where the second line is the ratio of averages over all angles by integrating the electric and magnetic energy densities over the surface of a sphere of radius D_p. From Eq.(62) it is obvious that indeed for all angles in the near field ($x \ll 1$) the magnetic energy density

InductEV, Inc.
Exhibit 1025
Page 571

is dominant, while in the far field ($x \gg 1$) they are equal as they should be. Also, the preferred positioning of the loop is such that objects which can interfere with its resonance lie close to its axis ($\theta = 0$), where there is no electric field. For example, using the systems described in Table 4, we can estimate from Eq.(62) that for the loop of $r = 30cm$ at a distance $D_p = 10r = 3m$ the ratio of average electric to average magnetic energy density would be $\sim 12\%$ and at $D_p = 3r = 90cm$ it would be $\sim 1\%$, and for the loop of $r = 10cm$ at a distance $D_p = 10r = 1m$ the ratio would be $\sim 33\%$ and at $D_p = 3r = 30cm$ it would be $\sim 2.5\%$. At closer distances this ratio is even smaller and thus the energy is predominantly magnetic in the near field, while in the radiative far field, where they are necessarily of the same order (ratio $\rightarrow 1$), both are very small, because the fields have significantly decayed, as capacitively-loaded coil systems are designed to radiate very little. Therefore, this is the criterion that qualifies this class of resonant system as a magnetic resonant system.

To provide an estimate of the effect of extraneous objects on the resonance of a capacitively-loaded loop including the capacitor fringing electric field, we use the perturbation theory formula, stated earlier, $\delta\Gamma_{1,abs(p)} = \omega_1 / 4 \cdot \int d^3\mathbf{r}\, \mathrm{Im}\left\{\varepsilon_p(\mathbf{r})\right\} \left|\mathbf{E}_1(\mathbf{r})\right|^2 \Big/ W$ with the computational FEFD results for the field of an example like the one shown in the plot of Fig. 5 and with a rectangular object of dimensions *30cm x 30cm x 1.5m* and permittivity $\varepsilon = 49 + 16i$ (consistent with human muscles) residing between the loops and almost standing on top of one capacitor (~*3cm* away from it) and find $\delta Q_{abs(human)} \sim 10^5$ and for ~*10cm* away $\delta Q_{abs(human)} \sim 5 \cdot 10^5$. Thus, for ordinary distances (~*1m*) and placements (not immediately on top of the capacitor) or for most ordinary extraneous objects *p* of much smaller loss-tangent, we conclude that it is indeed fair to say that $\delta Q_{abs(p)} \rightarrow \infty$. The only perturbation that is expected to affect these resonances is a close proximity of large metallic structures.

Self-resonant coils can be more sensitive than capacitively-loaded coils, since for the former the electric field extends over a much larger region in space (the entire coil)

InductEV, Inc.
Exhibit 1025
Page 572

rather than for the latter (just inside the capacitor). On the other hand, self-resonant coils can be simple to make and can withstand much larger voltages than most lumped capacitors. Inductively-loaded conducting rods can also be more sensitive than capacitively-loaded coils, since they rely on the electric field to achieve the coupling.

6.2 Dielectric disks

For dielectric disks, small, low-index, low-material-loss or far-away stray objects will induce small scattering and absorption. In such cases of small perturbations these extrinsic loss mechanisms can be quantified using respectively the analytical first-order perturbation theory formulas

$$\left[\delta Q_{1,rad(p)}\right]^{-1} \equiv 2\delta\Gamma_{1,rad(p)} / \omega_1 \propto \int d^3\mathbf{r}\left[\mathrm{Re}\left\{\varepsilon_p(\mathbf{r})\right\}\left|\mathbf{E}_1(\mathbf{r})\right|\right]^2 \Big/ W$$

$$\left[\delta Q_{1,abs(p)}\right]^{-1} \equiv 2\delta\Gamma_{1,abs(p)} / \omega_1 = \int d^3\mathbf{r}\,\mathrm{Im}\left\{\varepsilon_p(\mathbf{r})\right\}\left|\mathbf{E}_1(\mathbf{r})\right|^2 \Big/ 2W$$

where $W = \int d^3\mathbf{r}\varepsilon(\mathbf{r})\left|\mathbf{E}_1(\mathbf{r})\right|^2 / 2$ is the total resonant electromagnetic energy of the unperturbed mode. As one can see, both of these losses depend on the square of the resonant electric field tails **E**1 at the site of the extraneous object. In contrast, the coupling factor from object 1 to another resonant object 2 is, as stated earlier,

$$k_{12} = 2\kappa_{12} / \sqrt{\omega_1\omega_2} \approx \int d^3\mathrm{r}\varepsilon_2(\mathrm{r})\mathrm{E}_2^*(\mathrm{r})\mathrm{E}_1(\mathrm{r}) / \int d^3\mathrm{r}\varepsilon(\mathrm{r})\left|\mathrm{E}_1(\mathrm{r})\right|^2$$

and depends *linearly* on the field tails $\mathbf{E}_1$ of 1 inside 2. This difference in scaling gives us confidence that, for, for example, exponentially small field tails, coupling to other resonant objects should be much faster than all extrinsic loss rates ($\kappa_{12} \gg \delta\Gamma_{1,2(p)}$), at least for small perturbations, and thus the energy-transfer scheme is expected to be sturdy for this class of resonant dielectric disks.

However, we also want to examine certain possible situations where extraneous objects cause perturbations too strong to analyze using the above first-order perturbation theory approach. For example, we place a dielectric disk close to another off-resonance object of large $\mathrm{Re}\{\varepsilon\}$, $\mathrm{Im}\{\varepsilon\}$ and of same size but different shape (such as a human being *h*), as shown in Fig. 30a, and a roughened surface of large extent but of small $\mathrm{Re}\{\varepsilon\}$,

InductEV, Inc.
Exhibit 1025
Page 573

$\mathrm{Im}\{\varepsilon\}$ (such as a wall w), as shown in Fig. 30b. For distances $D_{h,w}/r = 10-3$ between the disk-center and the "human"-center or "wall", the numerical FDFD simulation results presented in Figs. 30a and 30b suggest that, the disk resonance seems to be fairly robust, since it is not detrimentally disturbed by the presence of extraneous objects, with the exception of the *very* close proximity of high-loss objects. To examine the influence of large perturbations on an entire energy-transfer system we consider two resonant disks in the close presence of both a "human" and a "wall". Comparing Table 8 to the table in Figure 30c, the numerical FDFD simulations show that the system performance deteriorates from $U \sim 1-50$ to $U_{(hw)} \sim 0.5-10$, i.e. only by acceptably small amounts.

In general, different examples of resonant systems have different degree of sensitivity to external perturbations, and the resonant system of choice depends on the particular application at hand, and how important matters of sensitivity or safety are for that application. For example, for a medical implantable device (such as a wirelessly powered artificial heart) the electric field extent must be minimized to the highest degree possible to protect the tissue surrounding the device. In such cases where sensitivity to external objects or safety is important, one should design the resonant systems so that the ratio of electric to magnetic energy density w_e / w_m is reduced or minimized at most of the desired (according to the application) points in the surrounding space.

7 Applications

The non-radiative wireless energy transfer techniques described above can enable efficient wireless energy-exchange between resonant objects, while suffering only modest transfer and dissipation of energy into other extraneous off-resonant objects. The technique is general, and can be applied to a variety of resonant systems in nature. In this Section, we identify a variety of applications that can benefit from or be designed to utilize wireless power transmission.

Remote devices can be powered directly, using the wirelessly supplied power or energy to operate or run the devices, or the devices can be powered by or through or in addition to a battery or energy storage unit, where the battery is occasionally being charged or re-charged wirelessly. The devices can be powered by hybrid battery/energy storage devices such as batteries with integrated storage capacitors and the like.

InductEV, Inc.
Exhibit 1025
Page 574

Furthermore, novel battery and energy storage devices can be designed to take advantage of the operational improvements enabled by wireless power transmission systems.

Devices can be turned off and the wirelessly supplied power or energy used to charge or recharge a battery or energy storage unit. The battery or energy storage unit charging or recharging rate can be high or low. The battery or energy storage units can be trickle charged or float charged. It would be understood by one of ordinary skill in the art that there are a variety of ways to power and/or charge devices, and the variety of ways could be applied to the list of applications that follows.

Some wireless energy transfer examples that can have a variety of possible applications include for example, placing a source (e.g. one connected to the wired electricity network) on the ceiling of a room, while devices such as robots, vehicles, computers, PDAs or similar are placed or move freely within the room. Other applications can include powering or recharging electric-engine buses and/or hybrid cars and medical implantable devices. Additional example applications include the ability to power or recharge autonomous electronics (e.g. laptops, cell-phones, portable music players, house-hold robots, GPS navigation systems, displays, etc), sensors, industrial and manufacturing equipment, medical devices and monitors, home appliances (e.g. lights, fans, heaters, displays, televisions, counter-top appliances, etc.), military devices, heated or illuminated clothing, communications and navigation equipment, including equipment built into vehicles, clothing and protective-wear such as helmets, body armor and vests, and the like, and the ability to transmit power to physically isolated devices such as to implanted medical devices, to hidden, buried, implanted or embedded sensors or tags, to and/or from roof-top solar panels to indoor distribution panels, and the like.

In some examples, far-field interference can be utilized by a system designer to suppress total radiation loss and/or to increase the system efficiency. In some examples, systems operating optimally closer to the radiative regime can benefit more from the presence of far-field interference, which leads to reduced losses for the sub-radiant normal mode of the coupled objects, and this benefit can be substantial.

A number of examples of the invention have been described. Nevertheless, it will be understood that various modifications can be made without departing from the spirit and scope of the invention.

InductEV, Inc.
Exhibit 1025
Page 575

WHAT IS CLAIMED IS:

1. An apparatus for use in wireless energy transfer, the apparatus comprising:

a first resonator structure configured for energy transfer with a second resonator structure, over a distance D larger than a characteristic size L_1 of said first resonator structure and larger than a characteristic size L_2 of said second resonator structure,

wherein the energy transfer has a rate κ and is mediated by evanescent-tail coupling of a resonant field of the first resonator structure and a resonant field of the second resonator structure, wherein

said resonant field of the first resonator structure has a resonance angular frequency ω_1, a resonance frequency-width Γ_1, and a resonance quality factor $Q_1 = \omega_1 / 2\Gamma_1$ at least larger than 300, and

said resonant field of the second resonator structure has a resonance angular frequency ω_2, a resonance frequency-width Γ_2, and a resonance quality factor $Q_2 = \omega_2 / 2\Gamma_2$ at least larger than 300,

wherein the absolute value of the difference of said angular frequencies ω_1 and ω_2 is smaller than the broader of said resonant widths Γ_1 and Γ_2, and the quantity $\kappa / \sqrt{\Gamma_1 \Gamma_2}$ is at least larger than 20,

and further comprising a power supply coupled to the first structure and configured to drive the first resonator structure or the second resonator structure at an angular frequency away from the resonance angular frequencies and shifted towards a frequency corresponding to an odd normal mode for the resonator structures to reduce radiation from the resonator structures by destructive far-field interference.

2. The apparatus of claim 1, wherein the power supply is configured to drive the first resonator structure or the second resonator structure at the angular frequency away from the resonance angular frequencies and shifted towards the frequency corresponding to an odd normal mode for the resonator structures to substantially suppress radiation from the resonator structures by destructive far-field interference.

InductEV, Inc.
Exhibit 1025
Page 576

3. A method for wireless energy transfer involving a first resonator structure configured for energy transfer with a second resonator structure, over a distance D larger than a characteristic size L_1 of said first resonator structure and larger than a characteristic size L_2 of said second resonator structure, wherein the energy transfer has a rate κ and is mediated by evanescent-tail coupling of a resonant field of the first resonator structure and a resonant field of the second resonator structure, wherein said resonant field of the first resonator structure has a resonance angular frequency ω_1, a resonance frequency-width Γ_1, and a resonance quality factor $Q_1 = \omega_1 / 2\Gamma_1$ at least larger than 300, and said resonant field of the second resonator structure has a resonance angular frequency ω_2, a resonance frequency-width Γ_2, and a resonance quality factor $Q_2 = \omega_2 / 2\Gamma_2$ at least larger than 300, wherein the absolute value of the difference of said angular frequencies ω_1 and ω_2 is smaller than the broader of said resonant widths Γ_1 and Γ_2, and the quantity $\kappa / \sqrt{\Gamma_1 \Gamma_2}$ is at least larger than 20, the method comprising:

driving the first resonator structure or the second resonator structure at an angular frequency away from the resonance angular frequencies and shifted towards a frequency corresponding to an odd normal mode for the resonator structures to reduce radiation from the resonator structures by destructive far-field interference.

4. The method of claim 3, wherein the first resonator structure or the second resonator structure is driven at the angular frequency away from the resonance angular frequencies and shifted towards the frequency corresponding to an odd normal mode for the resonator structures to substantially suppress radiation from the resonator structures by destructive far-field interference.

5. An apparatus for use in wireless energy transfer, the apparatus comprising:

a first resonator structure configured for energy transfer with a second resonator structure, over a distance D larger than a characteristic size L_1 of said first resonator structure and larger than a characteristic size L_2 of said second resonator structure,

wherein the energy transfer has a rate κ and is mediated by evanescent-tail

InductEV, Inc.
Exhibit 1025
Page 577

coupling of a resonant field of the first resonator structure and a resonant field of the second resonator structure, wherein

said resonant field of the first resonator structure has a resonance angular frequency ω_1, a resonance frequency-width Γ_1, and a resonance quality factor $Q_1 = \omega_1 / 2\Gamma_1$ at least larger than 300, and

said resonant field of the second resonator structure has a resonance angular frequency ω_2, a resonance frequency-width Γ_2, and a resonance quality factor $Q_2 = \omega_2 / 2\Gamma_2$ at least larger than 300,

wherein the absolute value of the difference of said angular frequencies ω_1 and ω_2 is smaller than the broader of said resonant widths Γ_1 and Γ_2, and the quantity $\kappa / \sqrt{\Gamma_1 \Gamma_2}$ is at least larger than 20,

and wherein for a desired range of the distances *D*, the resonance angular frequencies for the resonator structures increase transmission efficiency *T* by accounting for radiative interference, wherein the increase is relative to a transmission efficiency *T* calculated without accounting for the radiative interference.

6. The apparatus of claim 5, wherein the resonance angular frequencies for the resonator structures are selected by optimizing the transmission efficiency T to account for both a resonance quality factor *U* and an interference factor *V*.

7. A method for designing a wireless energy transfer apparatus, the apparatus including a first resonator structure configured for energy transfer with a second resonator structure, over a distance *D* larger than a characteristic size L_1 of said first resonator structure and larger than a characteristic size L_2 of said second resonator structure, wherein the energy transfer has a rate κ and is mediated by evanescent-tail coupling of a resonant field of the first resonator structure and a resonant field of the second resonator structure, wherein said resonant field of the first resonator structure has a resonance angular frequency ω_1, a resonance frequency-width Γ_1, and a resonance quality factor $Q_1 = \omega_1 / 2\Gamma_1$ at least larger than 300, and said resonant field of the second

InductEV, Inc.
Exhibit 1025
Page 578

resonator structure has a resonance angular frequency ω_2, a resonance frequency-width Γ_2, and a resonance quality factor $Q_2 = \omega_2 / 2\Gamma_2$ at least larger than 300, wherein the absolute value of the difference of said angular frequencies ω_1 and ω_2 is smaller than the broader of said resonant widths Γ_1 and Γ_2, and the quantity $\kappa / \sqrt{\Gamma_1 \Gamma_2}$ is at least larger than 20, the method comprising:

selecting the resonance angular frequencies for the resonator structures to substantially optimize the transmission efficiency by accounting for radiative interference between the resonator structures.

8. The method of claim 7, wherein the resonance angular frequencies for the resonator structures are selected by optimizing the transmission efficiency T to account for both a resonance quality factor *U* and an interference factor *V*.

9. An apparatus for use in wireless energy transfer, the apparatus comprising:

a first resonator structure configured for energy transfer with a second resonator structure over a distance *D*,

wherein the energy transfer is mediated by evanescent-tail coupling of a resonant field of the first resonator structure and a resonant field of the second resonator structure, with a coupling factor *k*, wherein

said resonant field of the first resonator structure has a resonance angular frequency ω_1, a resonance frequency-width Γ_1, and a resonance quality factor $Q_1 = \omega_1 / 2\Gamma_1$, and is radiative in the far field, with an associated radiation quality factor $Q_{1,\mathrm{rad}} \geq Q_1$, and

said resonant field of the second resonator structure has a resonance angular frequency ω_2, a resonance frequency-width Γ_2, and a resonance quality factor $Q_2 = \omega_2 / 2\Gamma_2$, and is radiative in the far field, with an associated radiation quality factor $Q_{2,\mathrm{rad}} \geq Q_2$,

wherein an absolute value of a difference of said angular frequencies ω_1 and ω_2

InductEV, Inc.
Exhibit 1025
Page 579

is smaller than broader of said resonant widths Γ_1 and Γ_2, and an average resonant angular frequency is defined as $\omega_o = \sqrt{\omega_1 \omega_2}$, corresponding to an average resonant wavelength $\lambda_o = 2\pi c / \omega_o$, where c is the speed of light in free space, and a strong-coupling factor being defined as $U = k\sqrt{Q_1 Q_2}$,

wherein the apparatus is configured to employ interference between said radiative far fields of the resonant fields of the first and second resonator, with an interference factor V_{rad}, to reduce a total amount of radiation from the apparatus compared to an amount of radiation from the apparatus in the absence of interference, a strong-interference factor being defined as $V = V_{rad}\sqrt{\left(Q_1 / Q_{1,rad}\right)\left(Q_2 / Q_{2,rad}\right)}$.

10. The apparatus of claim 9, wherein $Q_1 / Q_{1,rad} \geq 0.01$ and $Q_2 / Q_{2,rad} \geq 0.01$.

11. The apparatus of claim 9, wherein $Q_1 / Q_{1,rad} \geq 0.1$ and $Q_2 / Q_{2,rad} \geq 0.1$.

12. The apparatus of claim 9, wherein D / λ_o is larger than 0.001 and the strong-interference factor V is larger than 0.01.

13. The apparatus of claim 9, wherein D / λ_o is larger than 0.001 and the strong-interference factor V is larger than 0.1.

14. The apparatus of claim 9, further comprising the second resonator structure.

15. The apparatus of claim 9, wherein, during operation, a power generator is coupled to one of the first and second resonant structure, with a coupling rate κ_g, and is configured to drive the resonator structure, to which it is coupled, at a driving frequency f, corresponding to a driving angular frequency $\omega = 2\pi f$,

wherein U_g is defined as κ_g / Γ_1, if the power generator is coupled to the first resonator structure and defined as κ_g / Γ_2, if the power generator is coupled to the second

InductEV, Inc.
Exhibit 1025
Page 580

resonator structure.

16. The apparatus of claim 15, wherein the driving frequency is different from the resonance frequencies of the first and second resonator structures and is closer to a frequency corresponding to an odd normal mode of the system of the two resonator structures,

wherein the detuning of the first resonator from the driving frequency is defined as $D_1 = (\omega - \omega_1)/\Gamma_1$ and the detuning of the second resonator structure from the driving frequency is defined as $D_2 = (\omega - \omega_2)/\Gamma_2$.

17. The apparatus of claim 16, wherein D_1 is approximately equal to UV_{rad} and D_2 is approximately equal to UV_{rad}.

18. The apparatus of claim 15, wherein U_g is chosen to maximize the ratio of the energy-transfer efficiency to the radiation efficiency.

19. The apparatus of claim 17, wherein U_g is approximately equal to $\sqrt{1+U^2-V_{rad}^2U^2+V^2-2VV_{rad}}$.

20. The apparatus of claim 15, wherein f is at least larger than 100 kHz and smaller than 500MHz.

21. The apparatus of claim 15, wherein f is at least larger than 1MHz and smaller than 50MHz.

22. The apparatus of claim 15, further comprising the power generator.

23. The apparatus of claim 15, wherein, during operation, a power load is coupled to the resonant structure to which the power generator is not coupled, with a coupling rate

InductEV, Inc.
Exhibit 1025
Page 581

κ_l, and is configured to receive from the resonator structure, to which it is coupled, a usable power,

wherein U_l is defined as κ_l / Γ_1, if the power load is coupled to the first resonator structure and defined as κ_l / Γ_2, if the power load is coupled to the second resonator structure.

24. The apparatus of claim 23, wherein U_l is chosen to maximize the ratio of the energy-transfer efficiency to the radiation efficiency.

25. The apparatus of claim 24, wherein the driving frequency is different from the resonance frequencies of the first and second resonator structures and is closer to a frequency corresponding to an odd normal mode of the system of the two resonator structures,

wherein the detuning of the first resonator from the driving frequency is defined as $D_1 = (\omega - \omega_1)/\Gamma_1$ and is approximately equal to UV_{rad}, and the detuning of the second resonator structure from the driving frequency is defined as $D_2 = (\omega - \omega_2)/\Gamma_2$ and is approximately equal to UV_{rad},

and U_l is approximately equal to $\sqrt{1 + U^2 - V_{rad}^2 U^2 + V^2 - 2VV_{rad}}$.

26. The apparatus of claim 9, wherein at least one of the first and second resonator structures comprises a capacitively loaded loop or coil of at least one of a conducting wire, a conducting Litz wire, and a conducting ribbon.

27. The apparatus of claim 26, where the characteristic size of said loop or coil is less than 30 cm and the width of said conducting wire or Litz wire or ribbon is less than 2cm.

28. The apparatus of claim 26, where the characteristic size of said loop or coil is less than 1m and the width of said conducting wire or Litz wire or ribbon is less than 2cm.

InductEV, Inc.
Exhibit 1025
Page 582

29. The apparatus of claim 9, further comprising a feedback mechanism for maintaining the resonant frequency of one or more of the resonant objects.

30. The apparatus of claim 29, wherein the feedback mechanism comprises an oscillator with a fixed driving frequency and is configured to adjust the resonant frequency of the one or more resonant objects to be detuned by a fixed amount with respect to the fixed frequency.

31. An apparatus for use in wireless energy transfer, the apparatus comprising:

a first resonator structure configured for energy transfer with a second resonator structure over a distance *D*,

wherein the energy transfer is mediated by evanescent-tail coupling of a resonant field of the first resonator structure and a resonant field of the second resonator structure, with a coupling factor *k*, wherein

said resonant field of the first resonator structure has a resonance angular frequency ω_1, a resonance frequency-width Γ_1, and a resonance quality factor $Q_1 = \omega_1 / 2\Gamma_1$, and is radiative in the far field, with an associated radiation quality factor $Q_{1,\mathrm{rad}} \geq Q_1$, and

said resonant field of the second resonator structure has a resonance angular frequency ω_2, a resonance frequency-width Γ_2, and a resonance quality factor $Q_2 = \omega_2 / 2\Gamma_2$, and is radiative in the far field, with an associated radiation quality factor $Q_{2,\mathrm{rad}} \geq Q_2$,

wherein an absolute value of a difference of said angular frequencies ω_1 and ω_2 is smaller than the broader of said resonant widths Γ_1 and Γ_2, and an average resonant angular frequency is defined as $\omega_o = \sqrt{\omega_1 \omega_2}$, corresponding to an average resonant wavelength $\lambda_o = 2\pi c / \omega_o$, where c is the speed of light in free space, and a strong-coupling factor is defined as $U = k\sqrt{Q_1 Q_2}$,

wherein the apparatus is configured to employ interference between said radiative far fields of the resonant fields of the first and second resonator, with an interference

InductEV, Inc.
Exhibit 1025
Page 583

factor V_{rad}, to increase efficiency of energy transfer for the apparatus compared to efficiency for the apparatus in the absence of interference, the strong-interference factor being defined as $V = V_{rad}\sqrt{(Q_1 / Q_{1,rad})(Q_2 / Q_{2,rad})}$.

32. The apparatus of claim 31, wherein $Q_1 / Q_{1,rad} \geq 0.05$ and $Q_2 / Q_{2,rad} \geq 0.05$.

33. The apparatus of claim 31, wherein $Q_1 / Q_{1,rad} \geq 0.5$ and $Q_2 / Q_{2,rad} \geq 0.5$.

34. The apparatus of claim 31, wherein D / λ_o is larger than 0.01 and the strong-interference factor V is larger than 0.05.

35. The apparatus of claim 31, wherein D / λ_o is larger than 0.01 and the strong-interference factor V is larger than 0.5.

36. The apparatus of claim 31, further comprising the second resonator structure.

37. The apparatus of claim 31, wherein, during operation, a power generator is coupled to one of the first and second resonant structure, with a coupling rate κ_g, and is configured to drive the resonator structure, to which it is coupled, at a driving frequency f, corresponding to a driving angular frequency $\omega = 2\pi f$,

wherein U_g is defined as κ_g / Γ_1, if the power generator is coupled to the first resonator structure and defined as κ_g / Γ_2, if the power generator is coupled to the second resonator structure.

38. The apparatus of claim 37, wherein the driving frequency is different from the resonance frequencies of the first and second resonator structures and is closer to a frequency corresponding to an odd normal mode of the system of the two resonator structures,

wherein the detuning of the first resonator from the driving frequency is defined

InductEV, Inc.
Exhibit 1025
Page 584

as $D_1 = (\omega - \omega_1)/\Gamma_1$ and the detuning of the second resonator structure from the driving frequency is defined as $D_2 = (\omega - \omega_2)/\Gamma_2$.

39. The apparatus of claim 38, wherein D_1 is approximately equal to UV and D_2 is approximately equal to UV.

40. The apparatus of claim 37, wherein U_g is chosen to maximize the energy-transfer efficiency.

41. The apparatus of claim 39, wherein U_g is approximately equal to $\sqrt{(1+U^2)(1-V^2)}$.

42. The apparatus of claim 37, wherein f is at least larger than 100 kHz and smaller than 500MHz.

43. The apparatus of claim 37, wherein f is at least larger than 1MHz and smaller than 50MHz.

44. The apparatus of claim 37, further comprising the power generator.

45. The apparatus of claim 37, wherein, during operation, a power load is coupled to the resonant structure to which the power generator is not coupled, with a coupling rate κ_l, and is configured to receive from the resonator structure, to which it is coupled, a usable power,

wherein U_l is defined as κ_l/Γ_1, if the power load is coupled to the first resonator structure and defined as κ_l/Γ_2, if the power load is coupled to the second resonator structure.

InductEV, Inc.
Exhibit 1025
Page 585

46. The apparatus of claim 45, wherein U_1 is chosen to maximize the energy-transfer efficiency.

47. The apparatus of claim 46, wherein the driving frequency is different from the resonance frequencies of the first and second resonator structures and is closer to a frequency corresponding to an odd normal mode of the system of the two resonator structures,

wherein the detuning of the first resonator from the driving frequency is defined as $D_1 = (\omega - \omega_1)/\Gamma_1$ and is approximately equal to UV, and the detuning of the second resonator structure from the driving frequency is defined as $D_2 = (\omega - \omega_2)/\Gamma_2$ and is approximately equal to UV,

and U_1 is approximately equal to $\sqrt{(1+U^2)(1-V^2)}$.

48. The apparatus of claim 31, wherein at least one of the first and second resonator structures comprises a capacitively loaded loop or coil of at least one of a conducting wire, a conducting Litz wire, and a conducting ribbon.

49. The apparatus of claim 48, where the characteristic size of said loop or coil is less than 30 cm and the width of said conducting wire or Litz wire or ribbon is less than 2cm.

50. The apparatus of claim 48, where the characteristic size of said loop or coil is less than 1m and the width of said conducting wire or Litz wire or ribbon is less than 2cm.

51. The apparatus of claim 31, further comprising a feedback mechanism for maintaining the resonant frequency of one or more of the resonant objects.

52. The apparatus of claim 51, wherein the feedback mechanism comprises an oscillator with a fixed driving frequency and is configured to adjust the resonant frequency of the one or more resonant objects to be detuned by a fixed amount with

InductEV, Inc.
Exhibit 1025
Page 586

respect to the fixed frequency.

53. The apparatus of claim 51, where the feedback mechanism is configured to monitor an efficiency of the energy transfer, and adjust the resonant frequency of the one or more resonant objects to maximize the efficiency.

54. The apparatus of claim 31, wherein the resonance angular frequencies for the resonator structures are selected to optimize the energy-transfer efficiency by accounting for both the strong-coupling factor U and the strong-interference interference factor V.

55. A method for wireless energy transfer, the method comprising:

providing a first resonator structure configured for energy transfer with a second resonator structure over a distance D,

wherein the energy transfer is mediated by evanescent-tail coupling of a resonant field of the first resonator structure and a resonant field of the second resonator structure, with a coupling factor k, wherein

said resonant field of the first resonator structure has a resonance angular frequency ω_1, a resonance frequency-width Γ_1, and a resonance quality factor $Q_1 = \omega_1 / 2\Gamma_1$, and is radiative in the far field, with an associated radiation quality factor $Q_{1,\mathrm{rad}} \geq Q_1$, and

said resonant field of the second resonator structure has a resonance angular frequency ω_2, a resonance frequency-width Γ_2, and a resonance quality factor $Q_2 = \omega_2 / 2\Gamma_2$, and is radiative in the far field, with an associated radiation quality factor $Q_{2,\mathrm{rad}} \geq Q_2$,

wherein an absolute value of a difference of said angular frequencies ω_1 and ω_2 is smaller than broader of said resonant widths Γ_1 and Γ_2, and an average resonant angular frequency is defined as $\omega_o = \sqrt{\omega_1 \omega_2}$, corresponding to an average resonant wavelength $\lambda_o = 2\pi c / \omega_o$, where c is the speed of light in free space, and the strong-coupling factor is defined as $U = k\sqrt{Q_1 Q_2}$, and

InductEV, Inc.
Exhibit 1025
Page 587

employing interference between said radiative far fields of the resonant fields of the first and second resonator, with an interference factor V_{rad}, to reduce a total amount of radiation from the first and second resonator compared to an amount of radiation from the first and second resonator in the absence of interference, a strong-interference factor being defined as $V = V_{rad}\sqrt{(Q_1 / Q_{1,rad})(Q_2 / Q_{2,rad})}$.

56. The method of claim 55, wherein $Q_1 / Q_{1,rad} \geq 0.01$ and $Q_2 / Q_{2,rad} \geq 0.01$.

57. The method of claim 55, wherein, during operation, a power generator is coupled to one of the first and second resonant structure and is configured to drive the resonator structure, to which it is coupled, at a driving frequency *f*, corresponding to a driving angular frequency $\omega = 2\pi f$,

wherein the driving frequency is different from the resonance frequencies of the first and second resonator structures and is closer to a frequency corresponding to an odd normal mode of the system of the two resonator structures.

58. The method of claim 57, wherein, during operation, a power load is coupled to the resonant structure to which the power generator is not coupled and is configured to receive from the resonator structure, to which it is coupled, a usable power.

59. A method for wireless energy transfer, the method comprising:

providing a first resonator structure configured for energy transfer with a second resonator structure over a distance *D*,

wherein the energy transfer is mediated by evanescent-tail coupling of a resonant field of the first resonator structure and a resonant field of the second resonator structure, with a coupling factor *k*, wherein

said resonant field of the first resonator structure has a resonance angular frequency ω_1, a resonance frequency-width Γ_1, and a resonance quality factor $Q_1 = \omega_1 / 2\Gamma_1$, and is radiative in the far field, with an associated radiation quality factor

InductEV, Inc.
Exhibit 1025
Page 588

$Q_{1,\mathrm{rad}} \geq Q_1$, and

said resonant field of the second resonator structure has a resonance angular frequency ω_2, a resonance frequency-width Γ_2, and a resonance quality factor $Q_2 = \omega_2 / 2\Gamma_2$, and is radiative in the far field, with an associated radiation quality factor $Q_{2,\mathrm{rad}} \geq Q_2$,

wherein an absolute value of the difference of said angular frequencies ω_1 and ω_2 is smaller than the broader of said resonant widths Γ_1 and Γ_2,and an average resonant angular frequency is defined as $\omega_o = \sqrt{\omega_1 \omega_2}$, corresponding to an average resonant wavelength $\lambda_o = 2\pi c / \omega_o$, where c is the speed of light in free space, and the strong-coupling factor is defined as $U = k\sqrt{Q_1 Q_2}$, and

employing interference between said radiative far fields of the resonant fields of the first and second resonator, with an interference factor V_{rad}, to increase efficiency of energy transfer between the first and second resonator compared to efficiency of energy transfer between the first and second resonator in the absence of interference, a strong-interference factor being defined as $V = V_{\mathrm{rad}} \sqrt{\left(Q_1 / Q_{1,\mathrm{rad}}\right)\left(Q_2 / Q_{2,\mathrm{rad}}\right)}$.

60. The method of claim 59, wherein $Q_1 / Q_{1,\mathrm{rad}} \geq 0.05$ and $Q_2 / Q_{2,\mathrm{rad}} \geq 0.05$.

61. The method of claim 59, wherein, during operation, a power generator is coupled to one of the first and second resonant structure and is configured to drive the resonator structure, to which it is coupled, at a driving frequency *f*, corresponding to a driving angular frequency $\omega = 2\pi f$,

wherein the driving frequency is different from the resonance frequencies of the first and second resonator structures and is closer to a frequency corresponding to an odd normal mode of the system of the two resonator structures.

62. The method of claim 61, wherein, during operation, a power load is coupled to the resonant structure to which the power generator is not coupled and is configured to

InductEV, Inc.
Exhibit 1025
Page 589

receive from the resonator structure, to which it is coupled, a usable power.

63. The method of claim 59, wherein the resonance angular frequencies for the resonator structures are selected to optimize the energy-transfer efficiency by accounting for both the strong-coupling factor U and the strong-interference interference factor V.

InductEV, Inc.
Exhibit 1025
Page 590

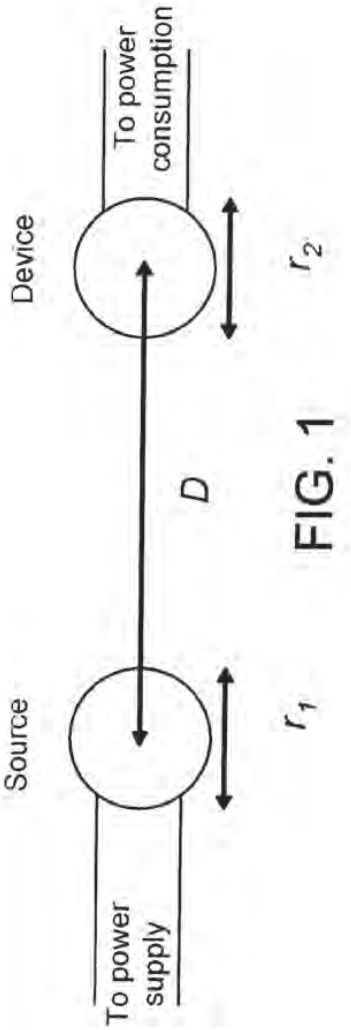


FIG. 1

InductEV, Inc.
Exhibit 1025
Page 591

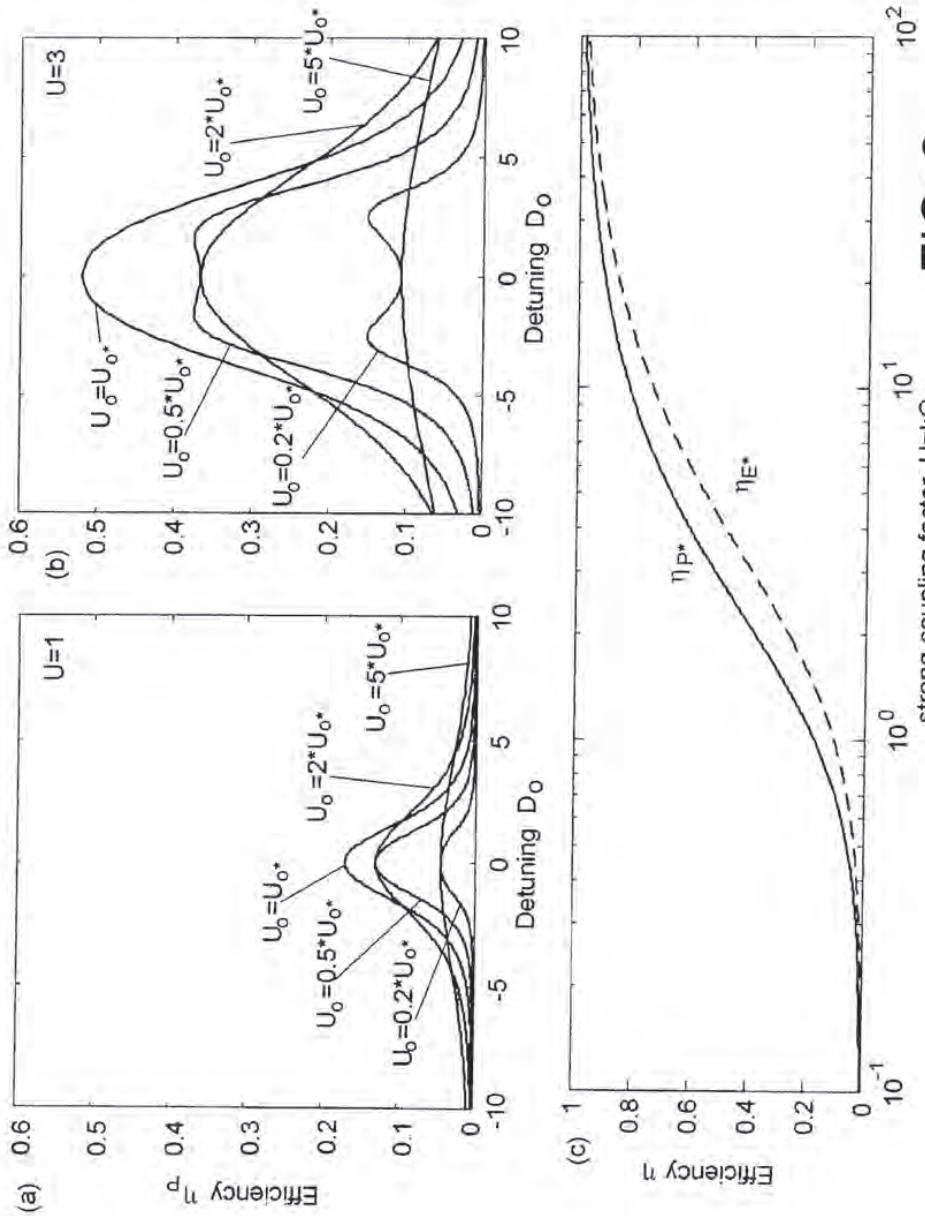


FIG. 2

InductEV, Inc.
Exhibit 1025
Page 592

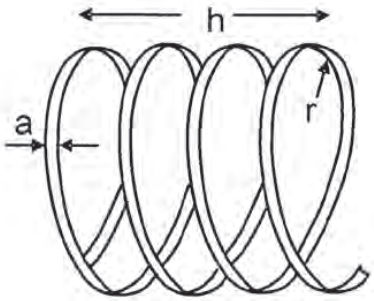


FIG. 3

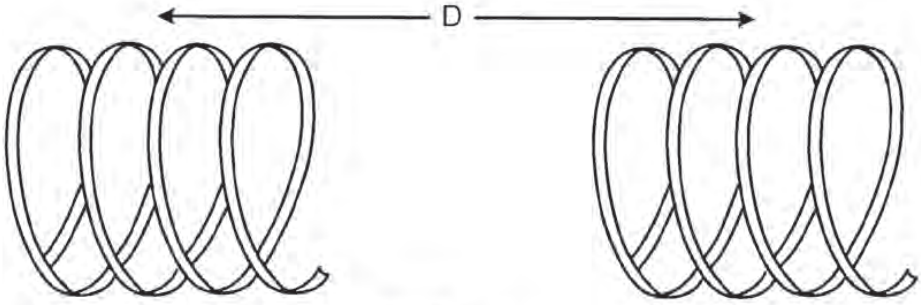


FIG. 4

InductEV, Inc.
Exhibit 1025
Page 593

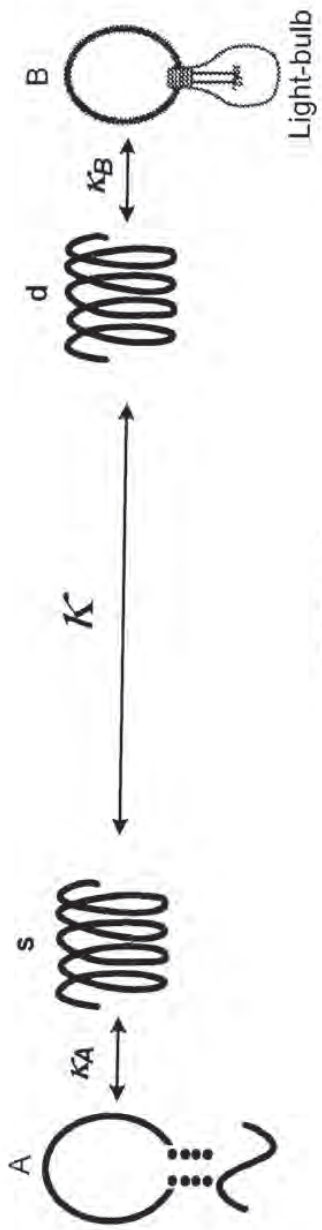
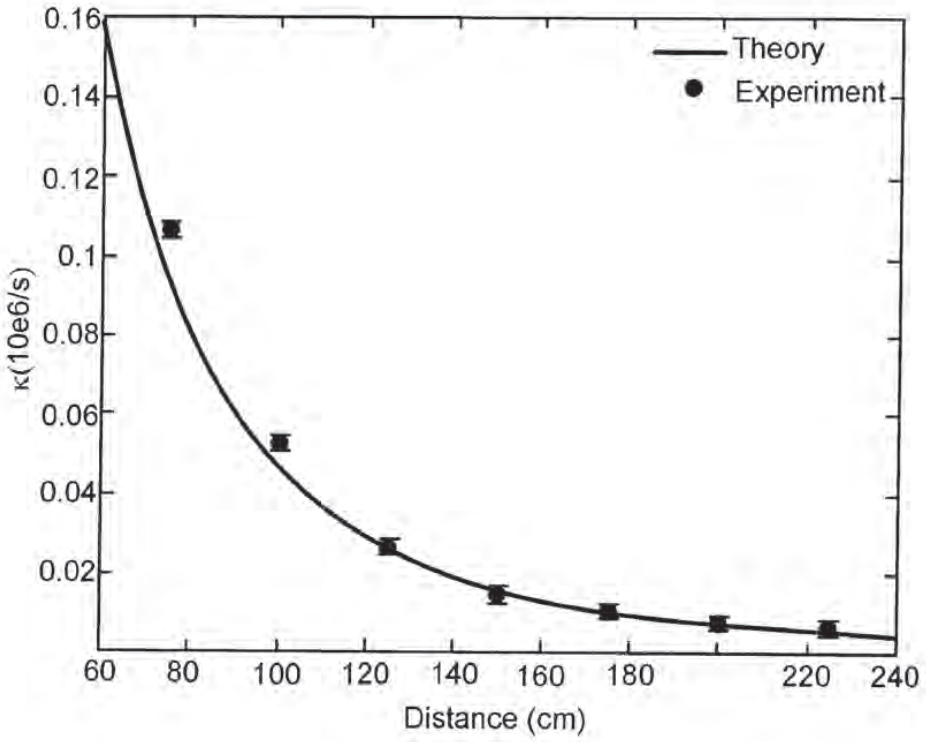


FIG. 5

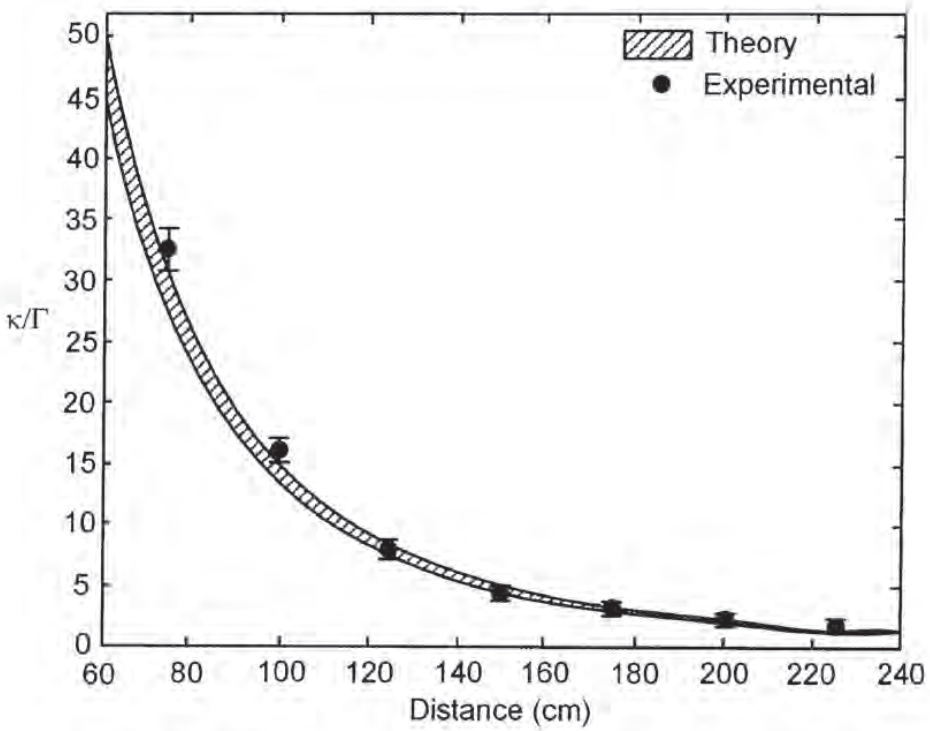
InductEV, Inc.
Exhibit 1025
Page 594



Comparison of experimental and theoretical values for κ as a function of the separation between the source and device coils.

FIG. 6

InductEV, Inc.
Exhibit 1025
Page 595



Comparison of experimental and theoretical values for the parameter κ/Γ as a function of the separation between the two coils. The theory values are obtained by using the theoretically obtained κ and the experimentally measured Γ. The shaded area represents the spread in the theoretical κ/Γ due to the ~5% uncertainty in Q.

FIG.7

InductEV, Inc.
Exhibit 1025
Page 596

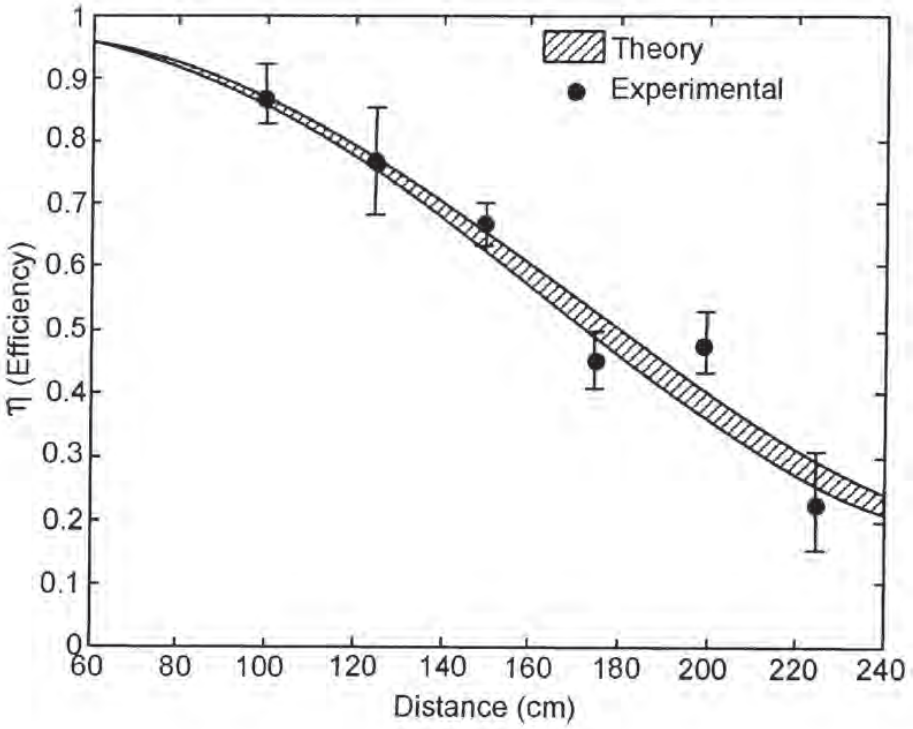


FIG. 8

InductEV, Inc.
Exhibit 1025
Page 597

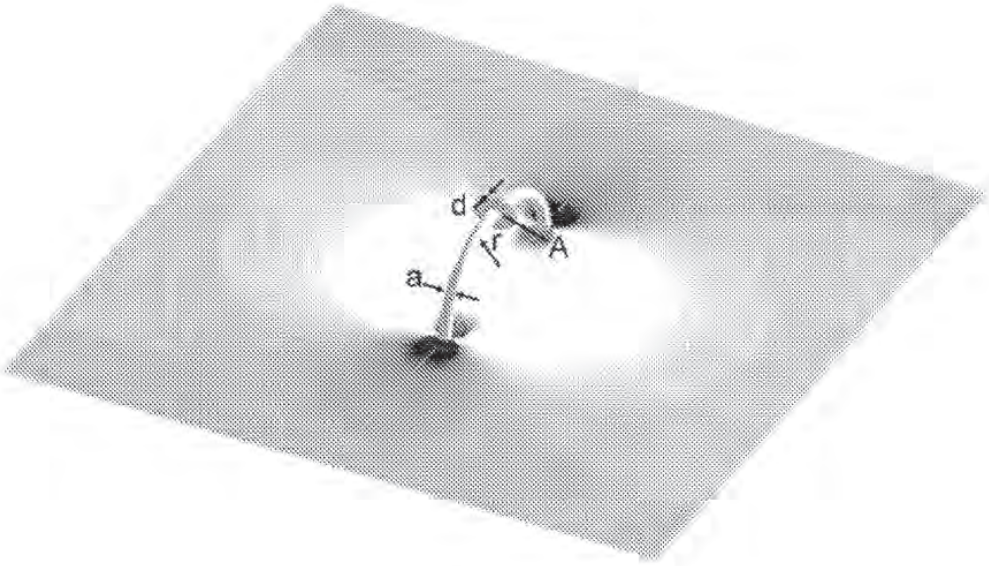


FIG. 9

InductEV, Inc.
Exhibit 1025
Page 598

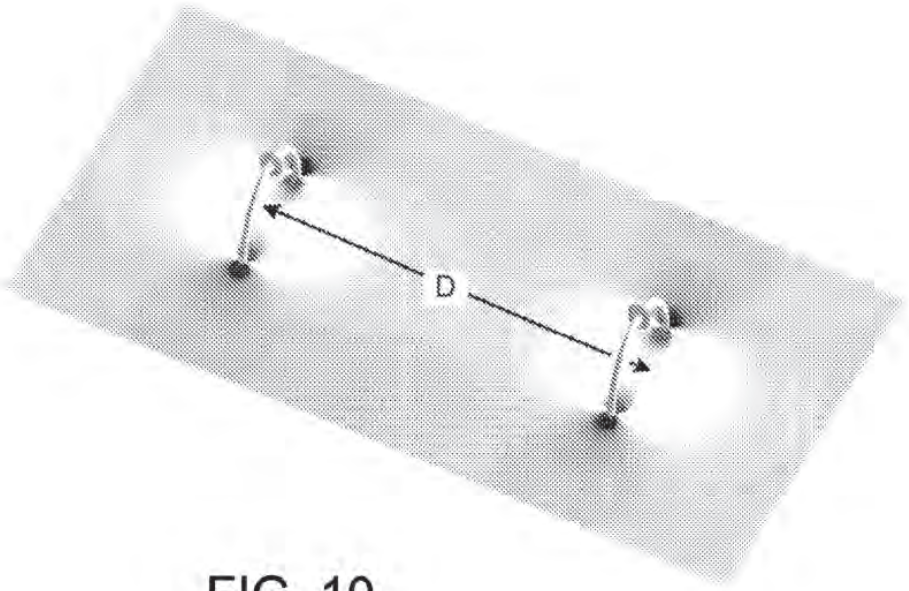


FIG. 10

InductEV, Inc.
Exhibit 1025
Page 599

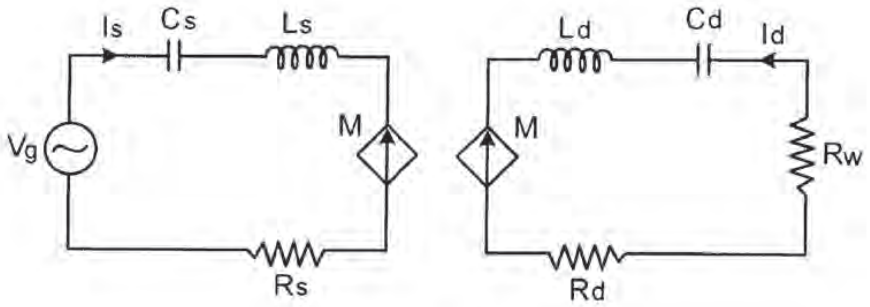


FIG. 11

InductEV, Inc.
Exhibit 1025
Page 600

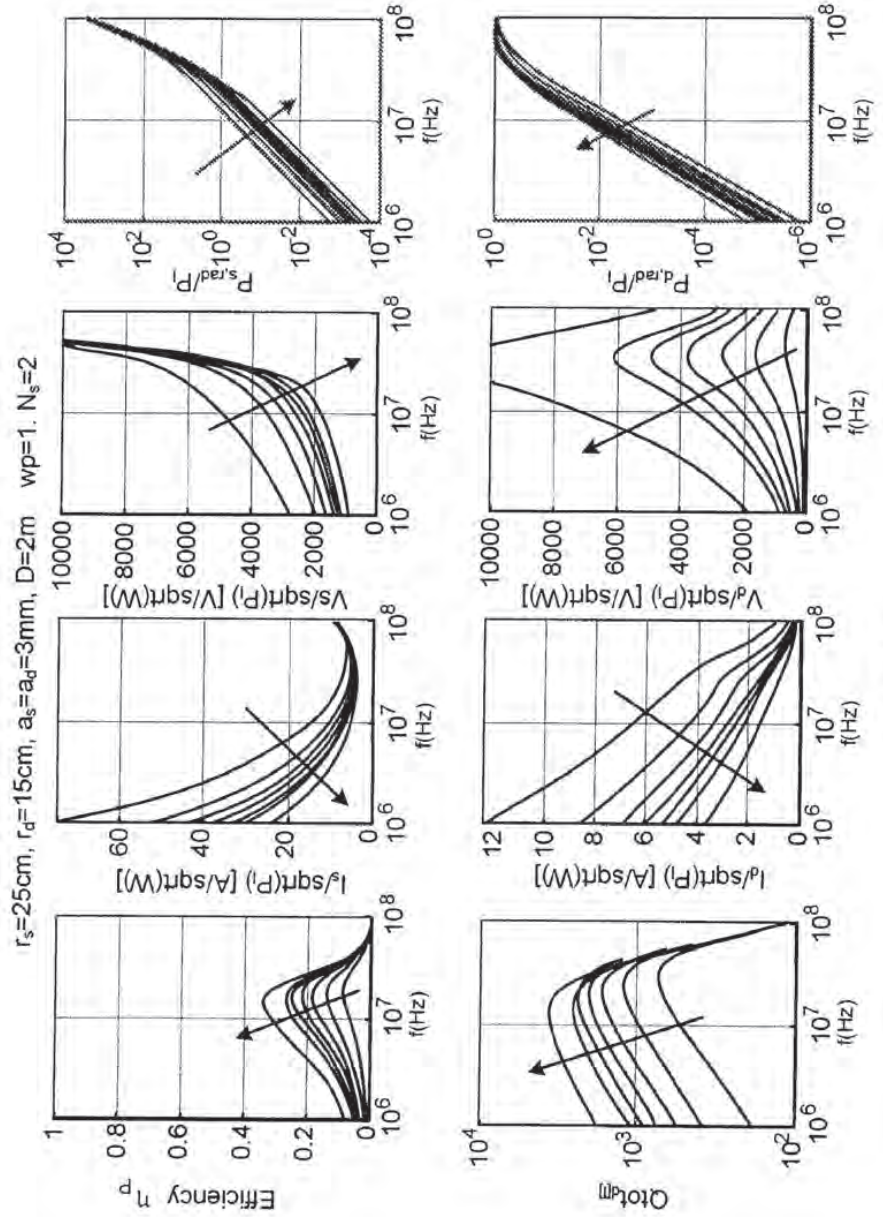


FIG. 12

InductEV, Inc.
Exhibit 1025
Page 601

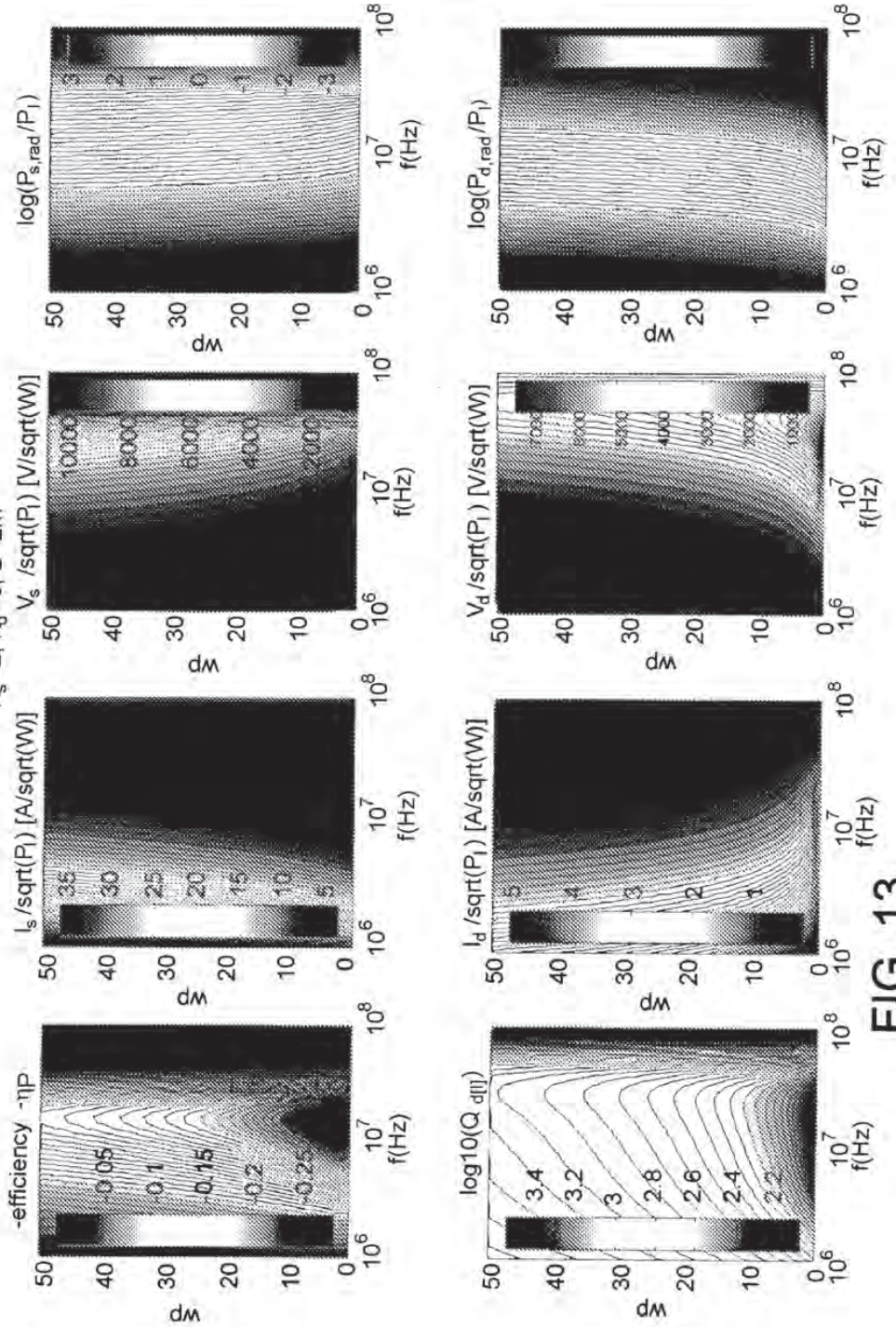


FIG. 13

InductEV, Inc.
Exhibit 1025
Page 602

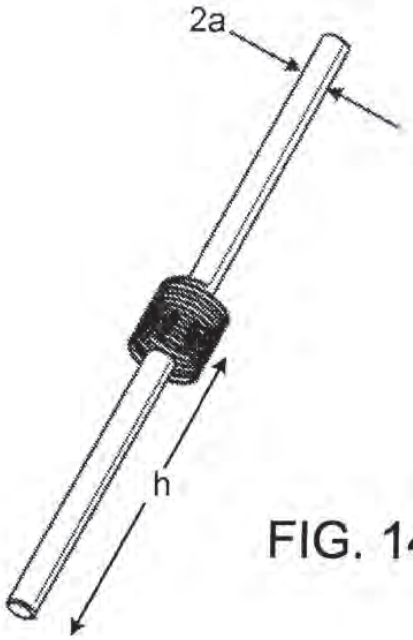


FIG. 14

InductEV, Inc.
Exhibit 1025
Page 603

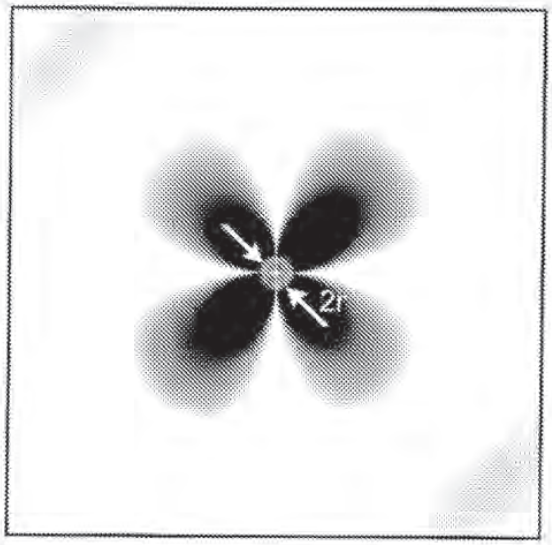


FIG. 15A

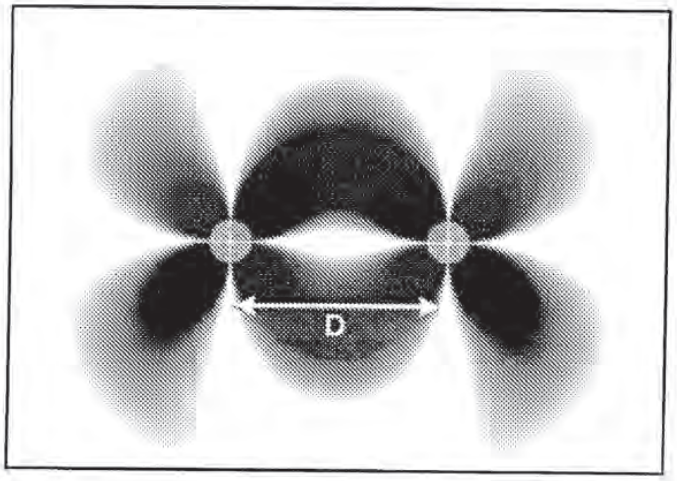


FIG. 15B

InductEV, Inc.
Exhibit 1025
Page 604

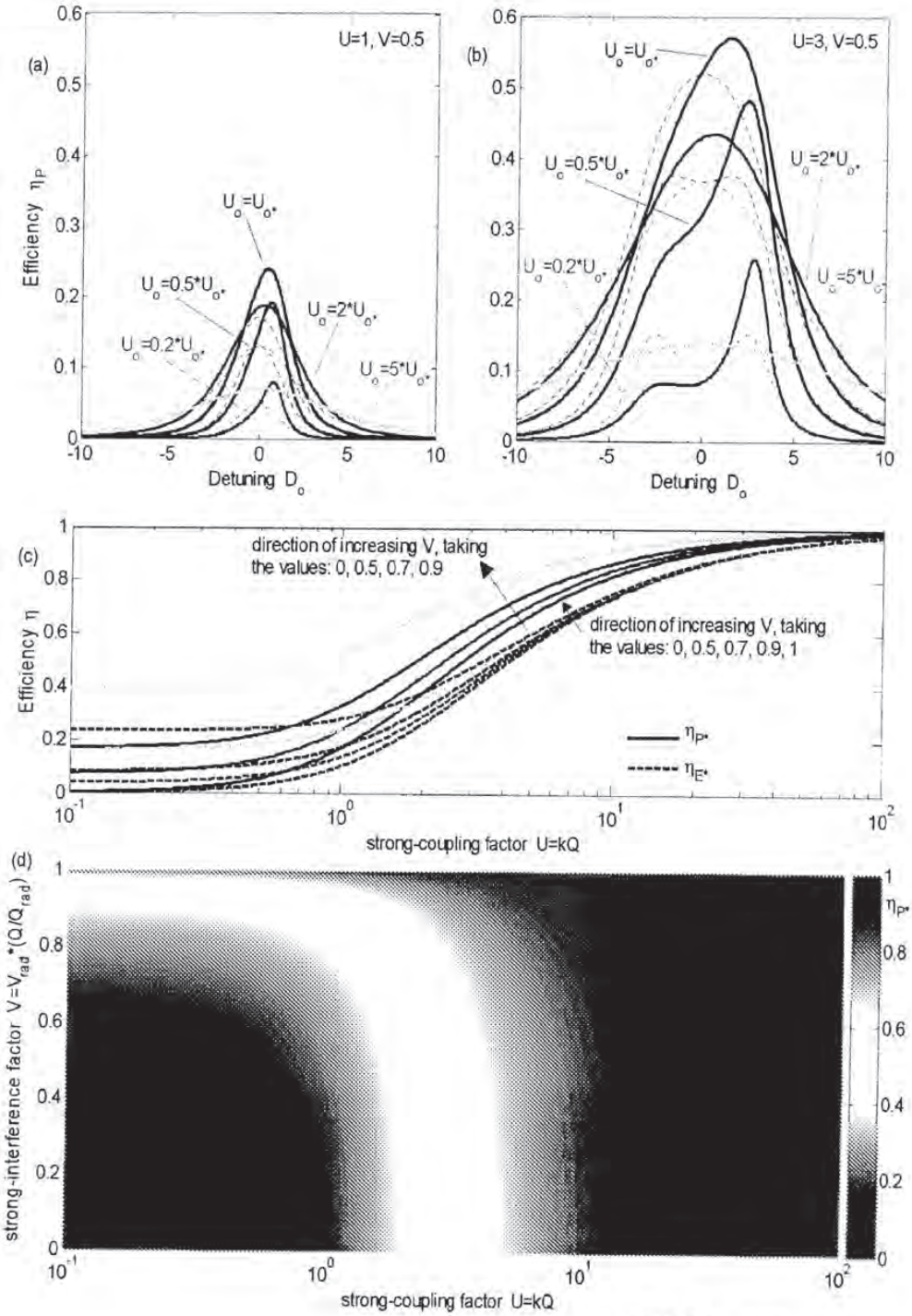


FIG. 16

InductEV, Inc.
Exhibit 1025
Page 605

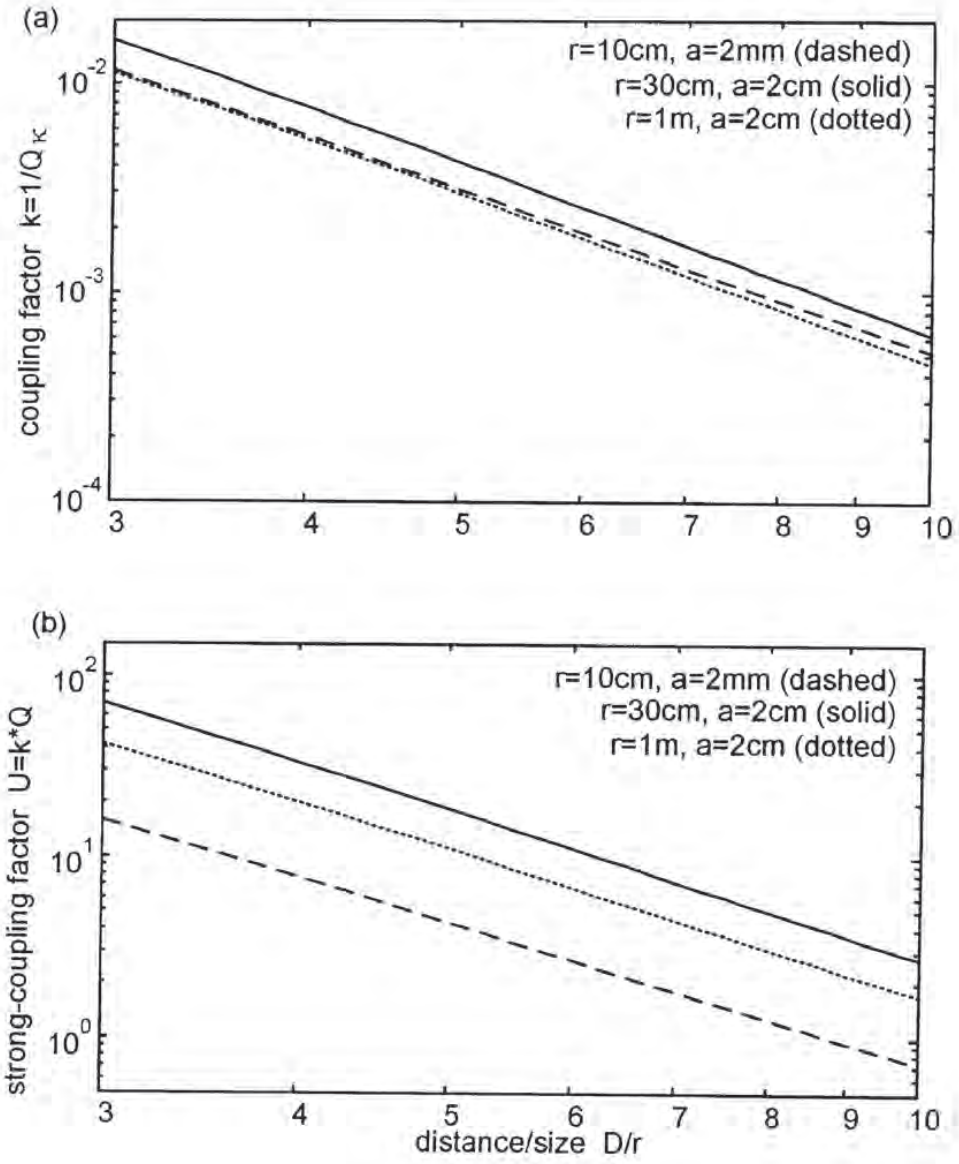


FIG. 17

InductEV, Inc.
Exhibit 1025
Page 606

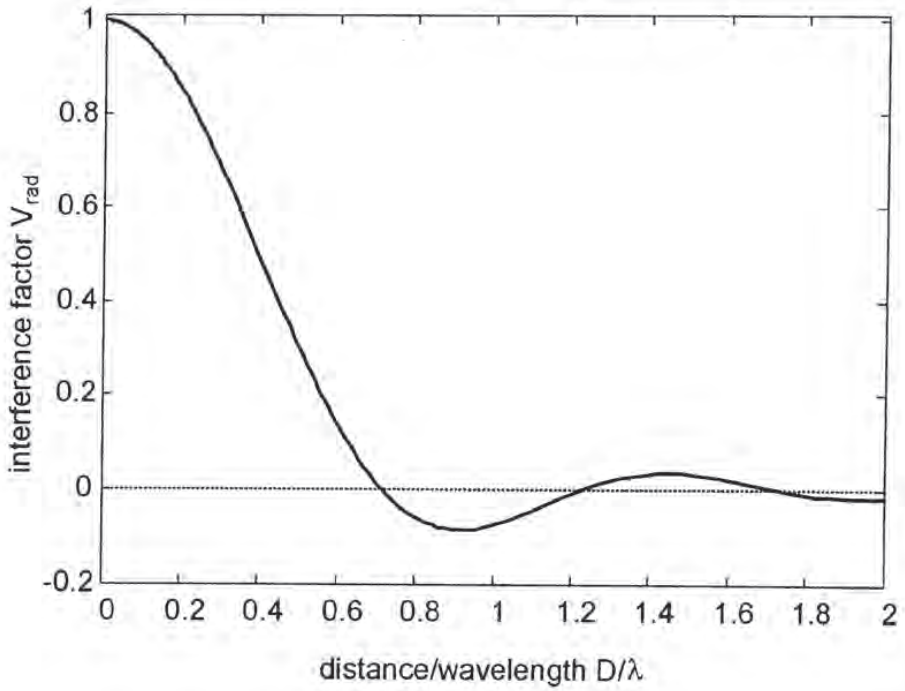


FIG. 18

InductEV, Inc.
Exhibit 1025
Page 607

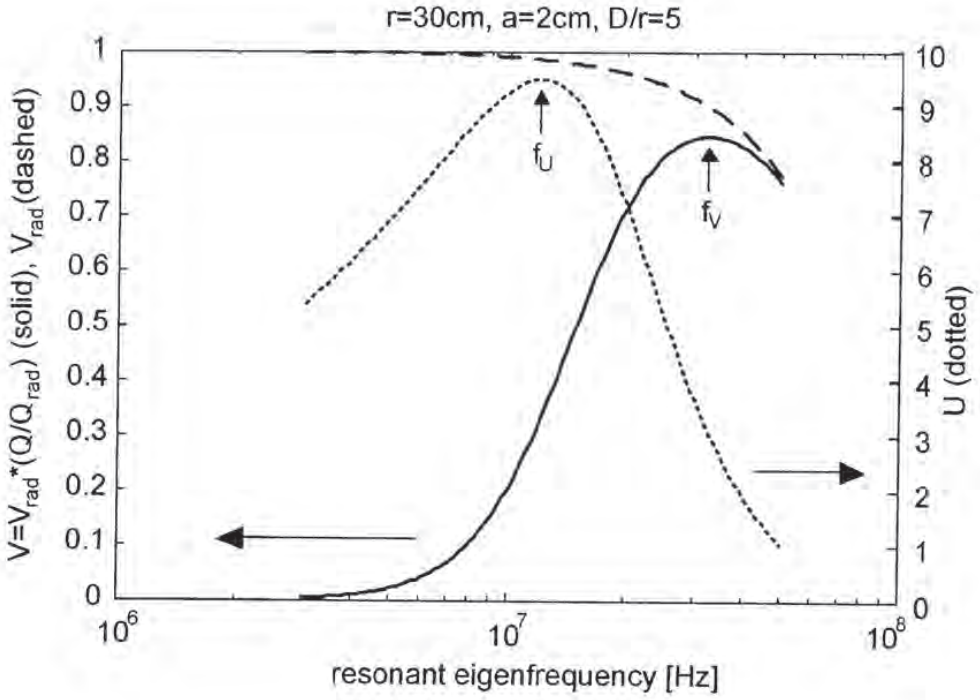


FIG. 19

InductEV, Inc.
Exhibit 1025
Page 608

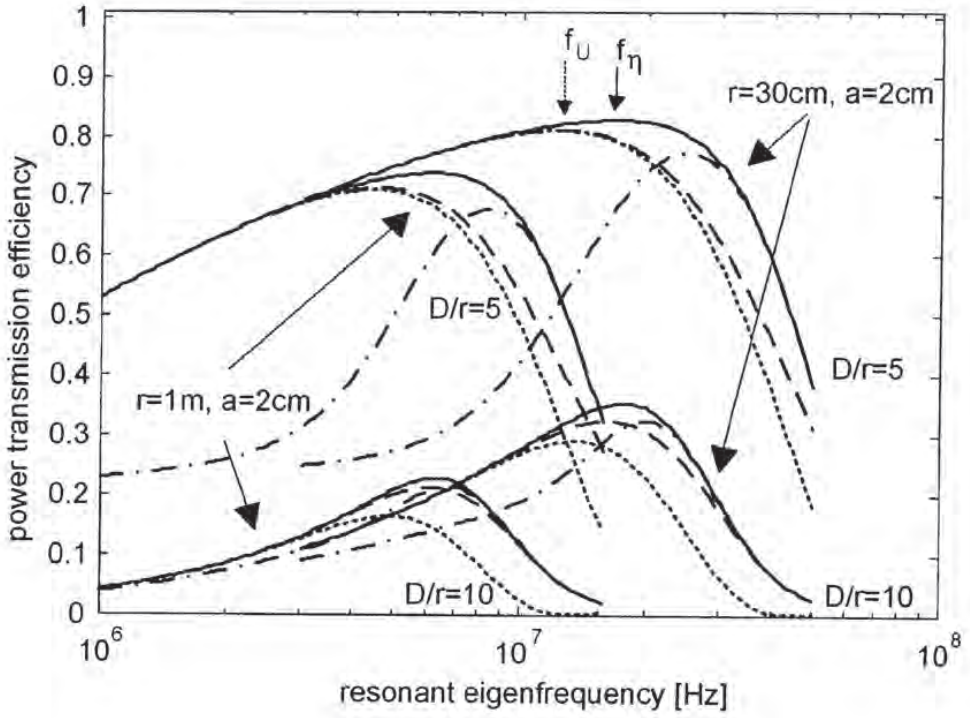


FIG. 20

InductEV, Inc.
Exhibit 1025
Page 609

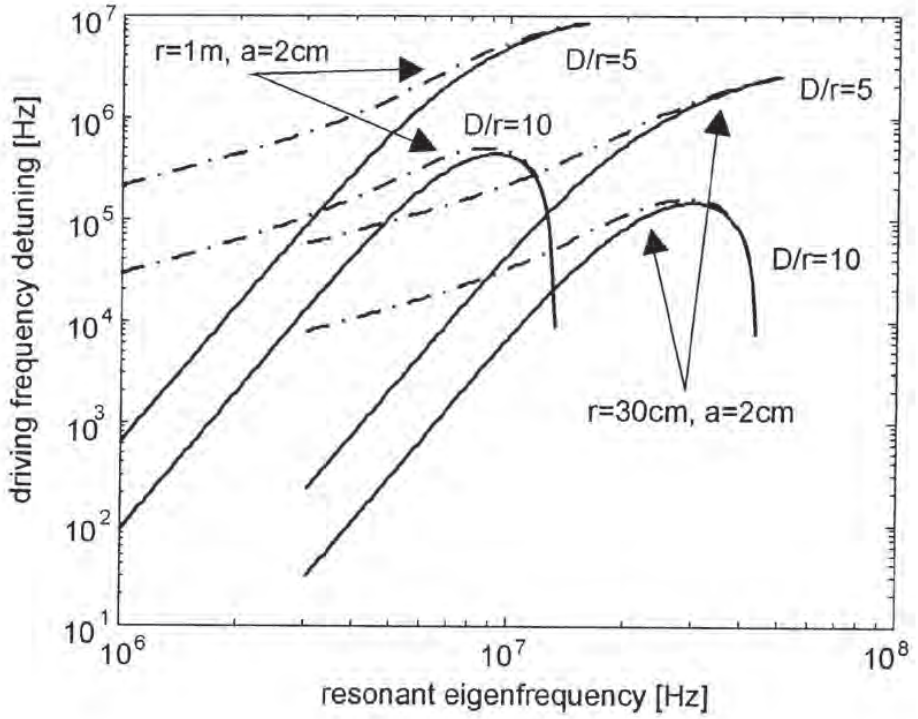


FIG. 21

InductEV, Inc.
Exhibit 1025
Page 610

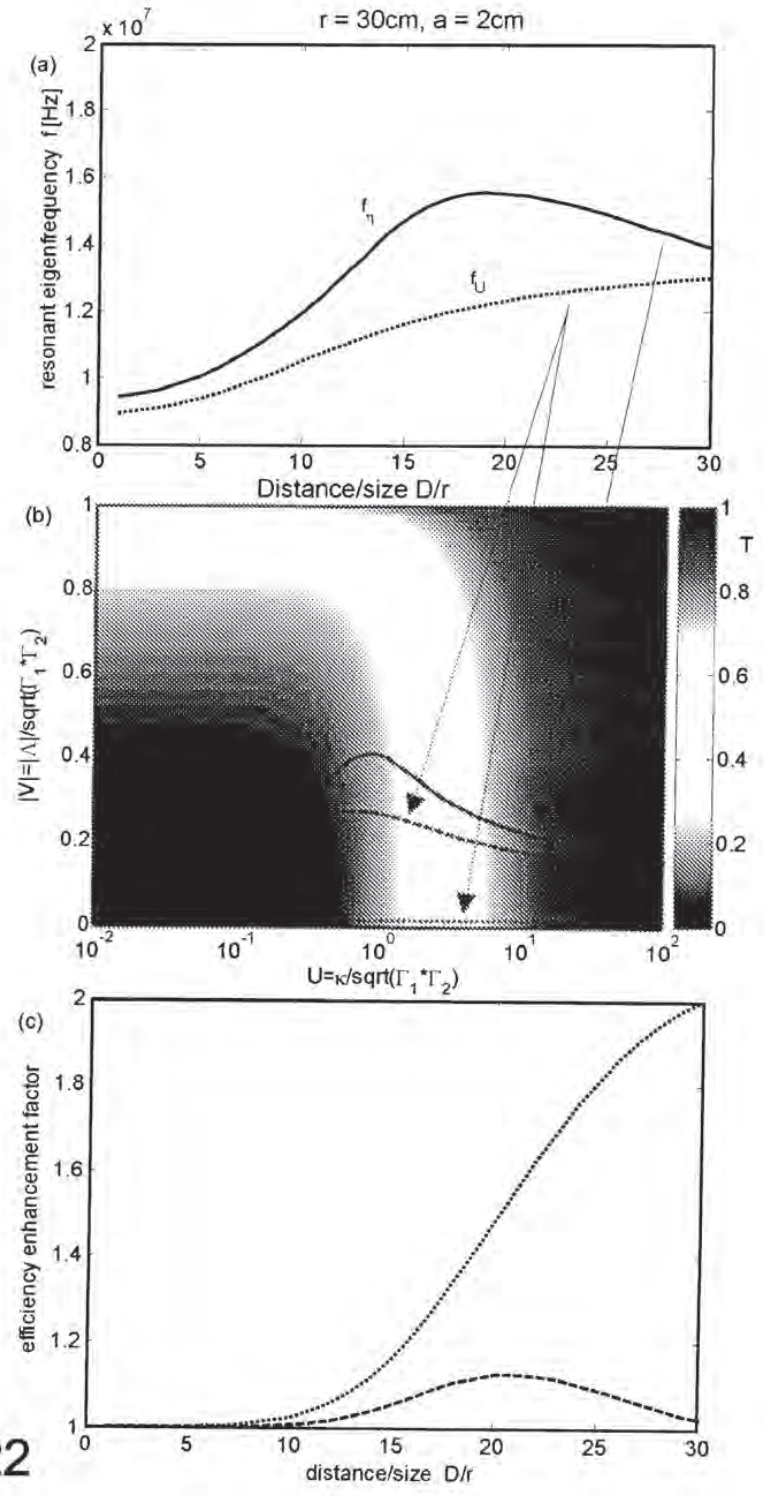


FIG. 22

InductEV, Inc.
Exhibit 1025
Page 611

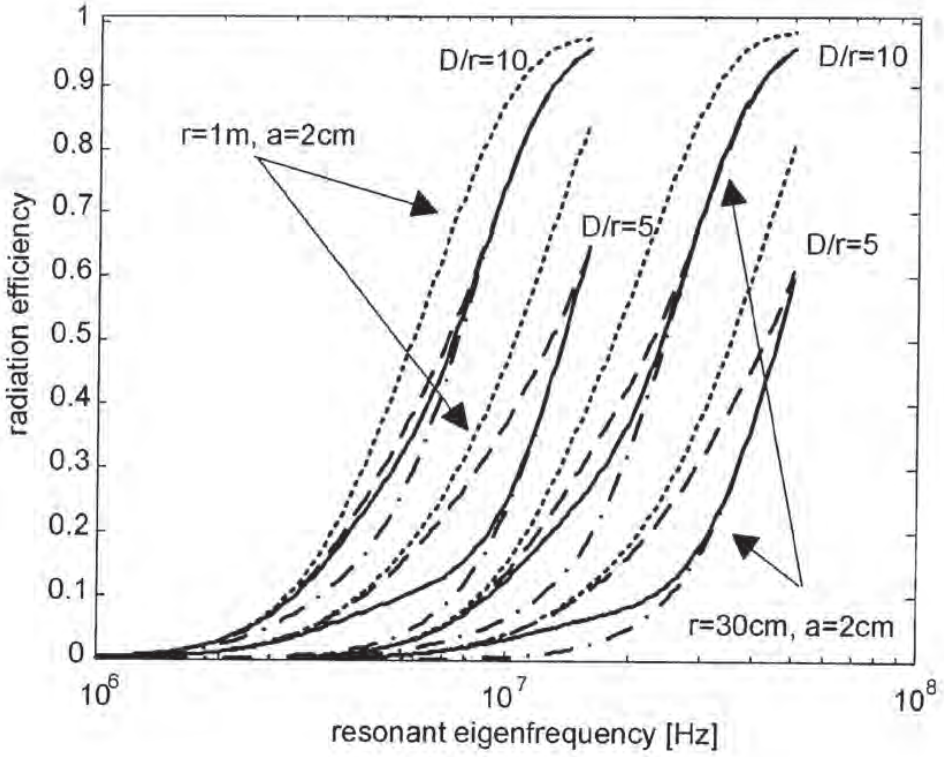


FIG. 23

InductEV, Inc.
Exhibit 1025
Page 612

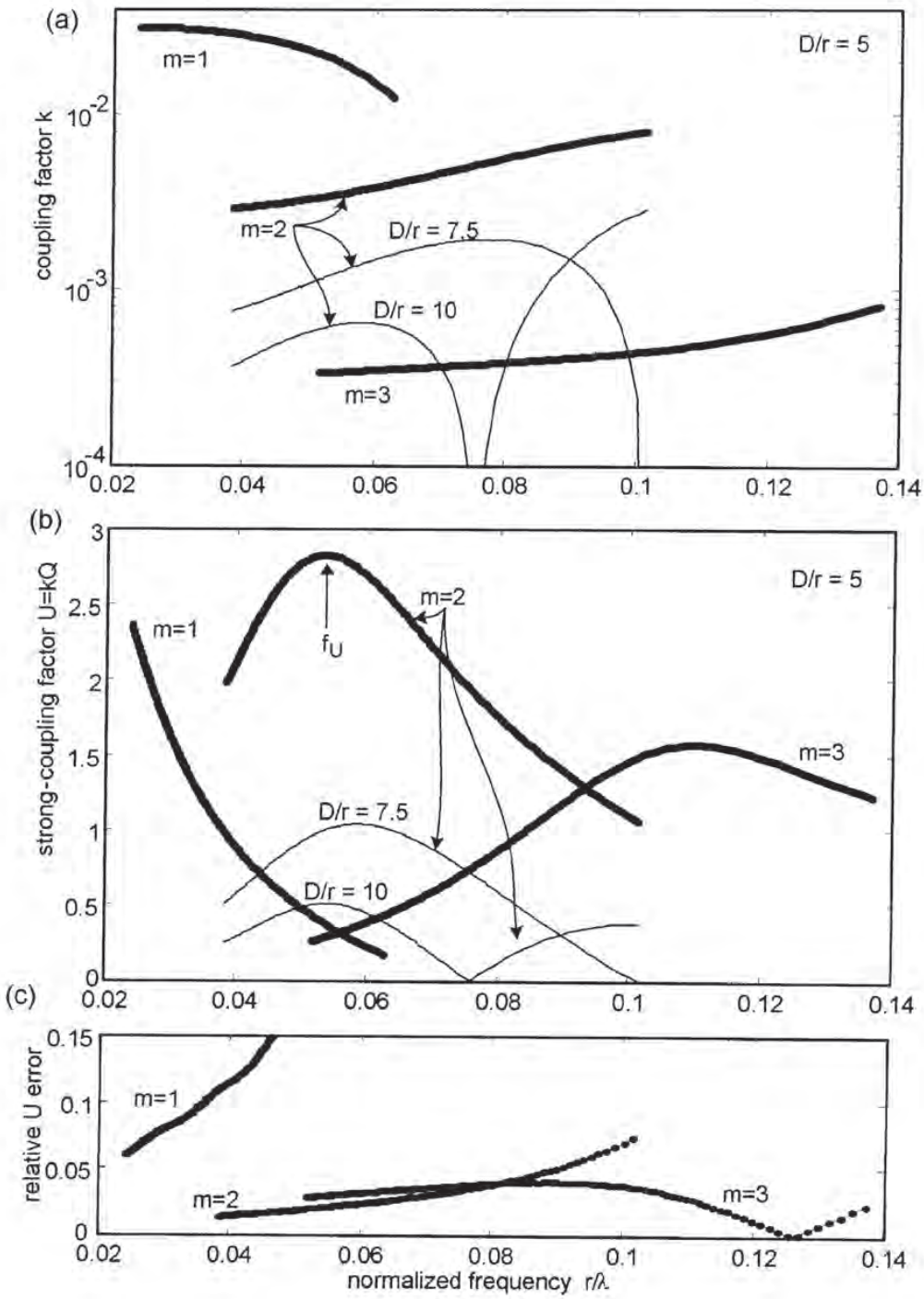


FIG. 24

InductEV, Inc.
Exhibit 1025
Page 613

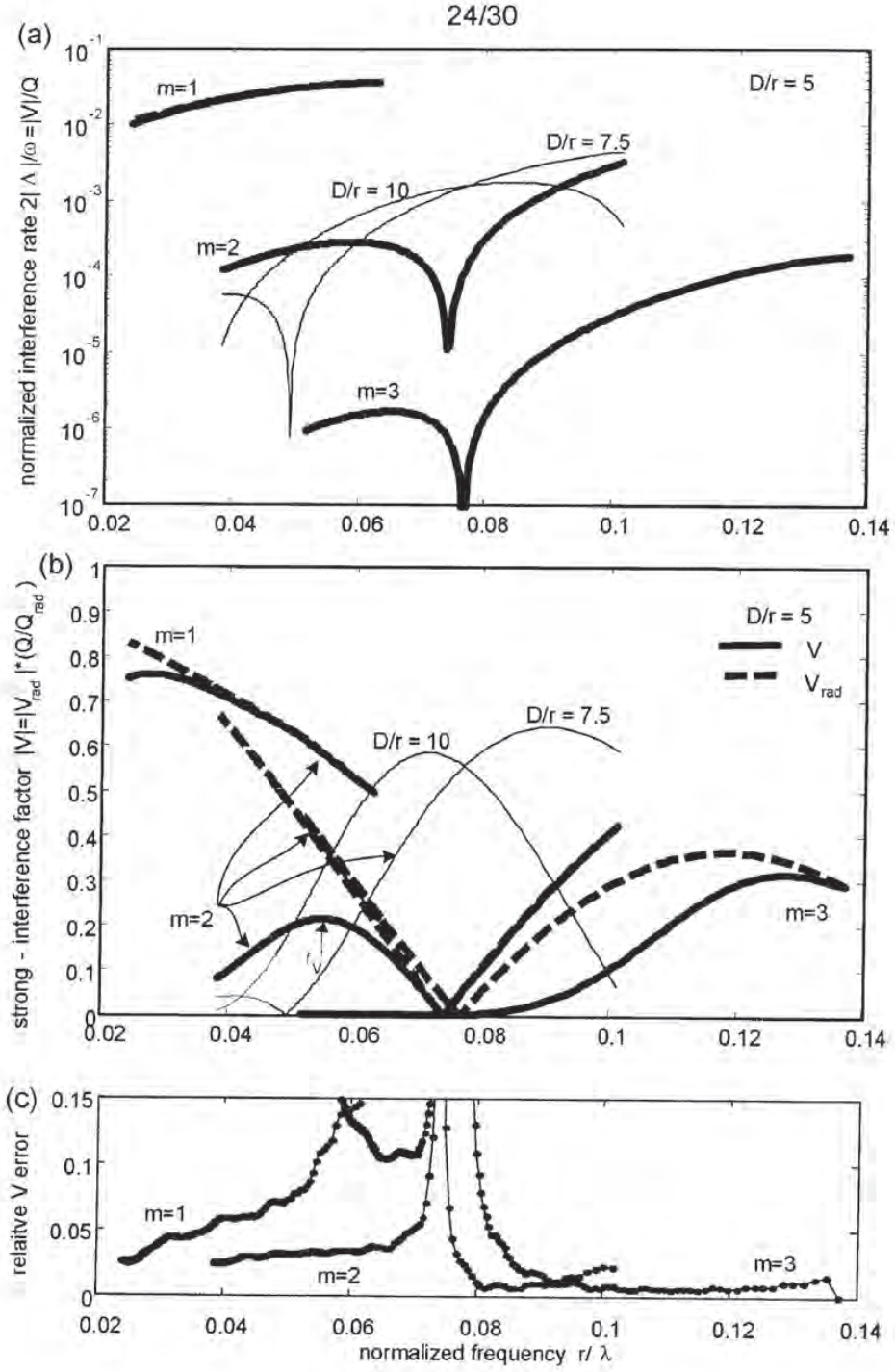


FIG. 25

InductEV, Inc.
Exhibit 1025
Page 614

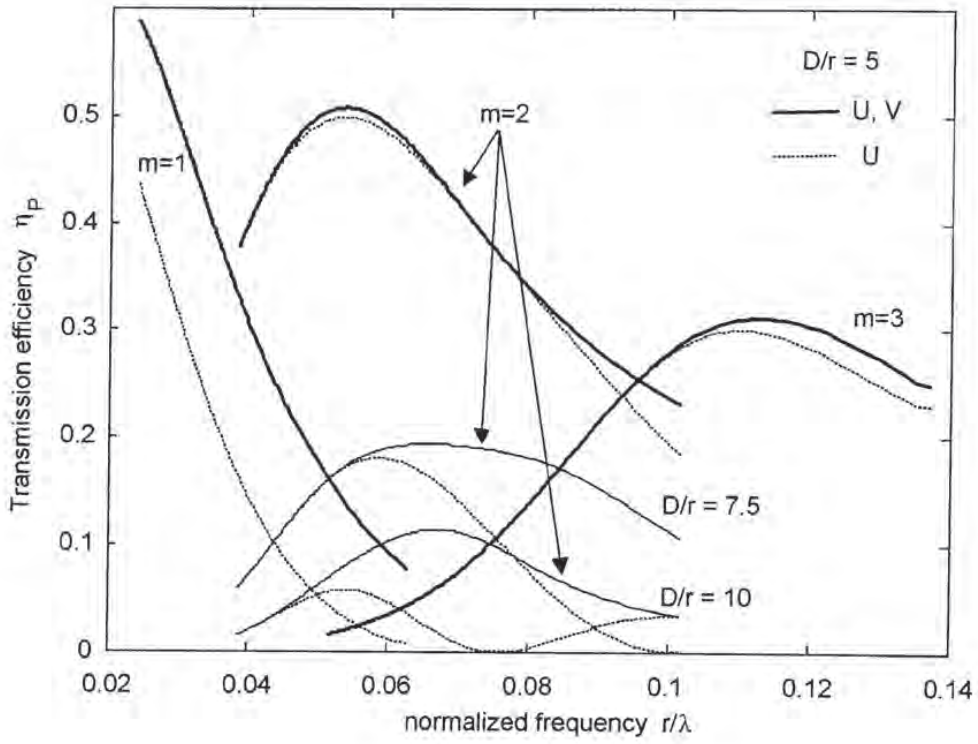


FIG. 26

InductEV, Inc.
Exhibit 1025
Page 615

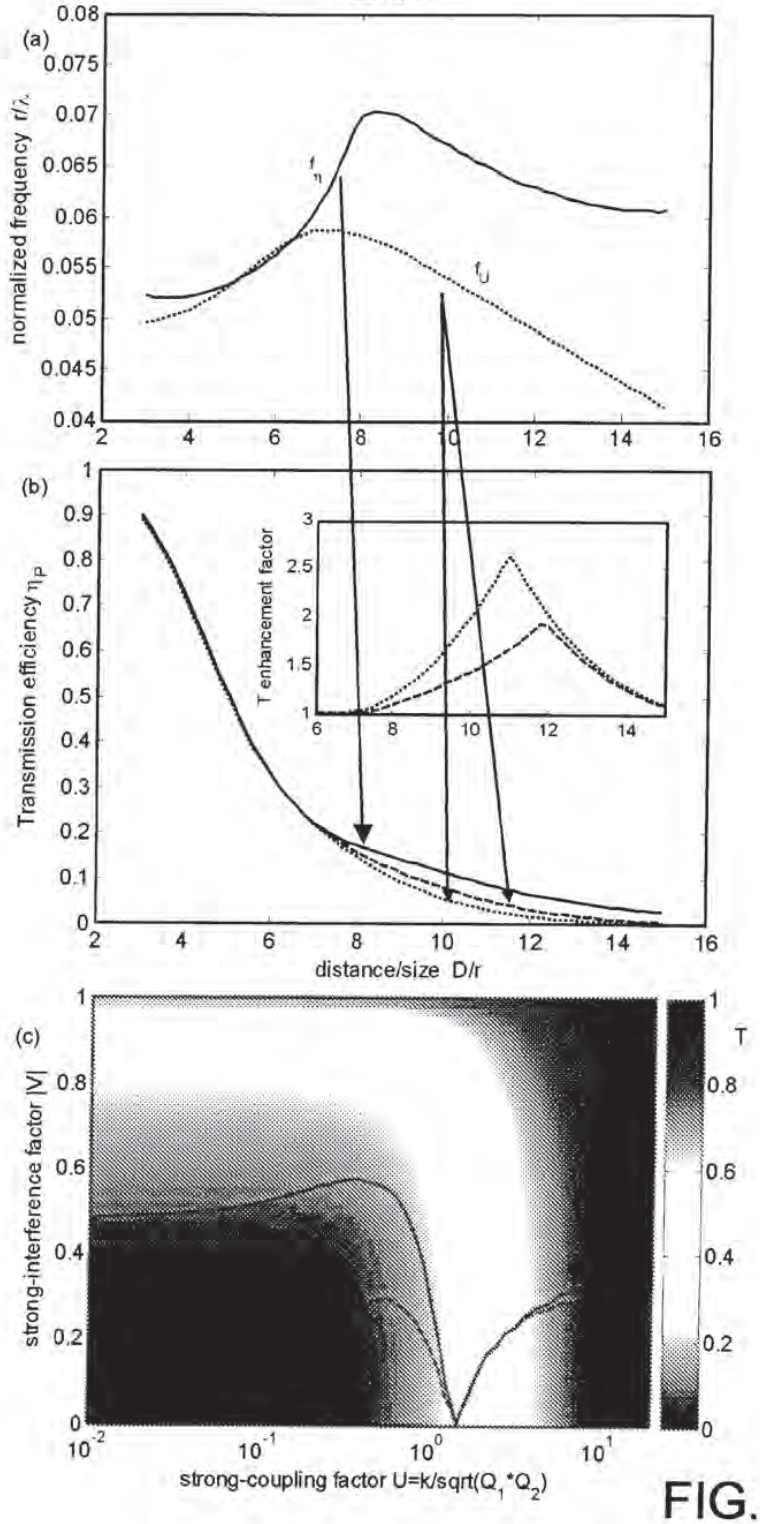


FIG. 27

InductEV, Inc.
Exhibit 1025
Page 616

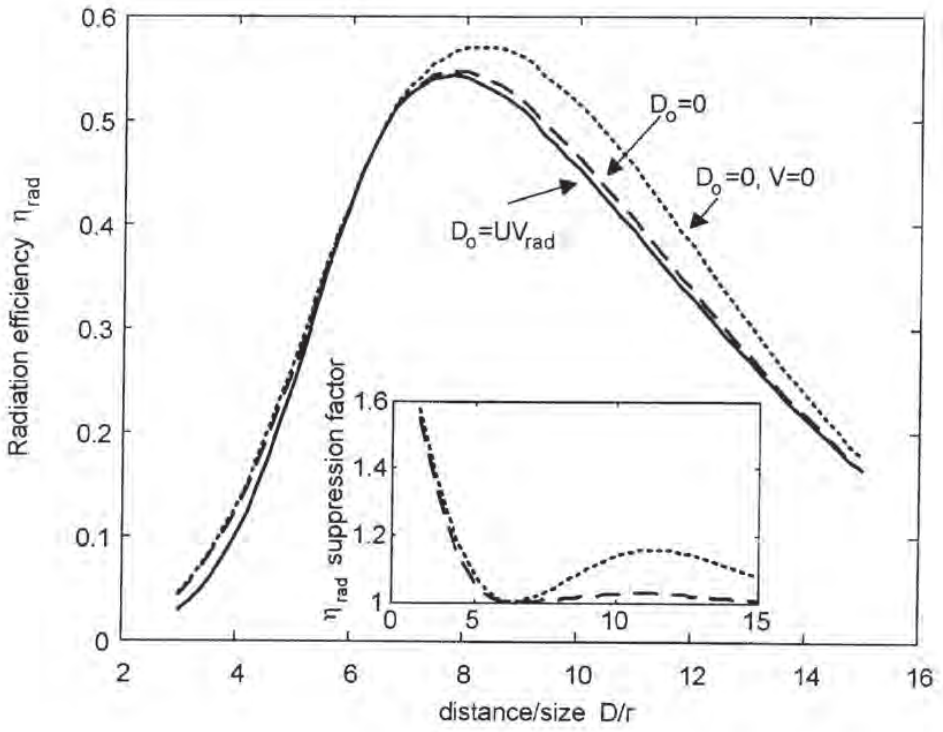


FIG. 28

InductEV, Inc.
Exhibit 1025
Page 617

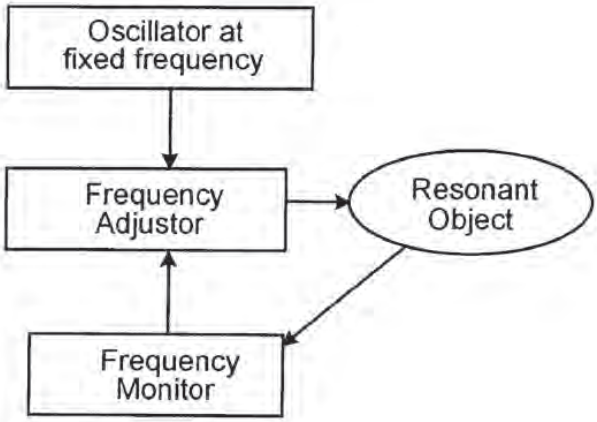


FIG. 29A

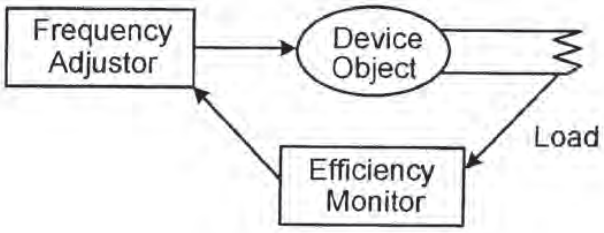
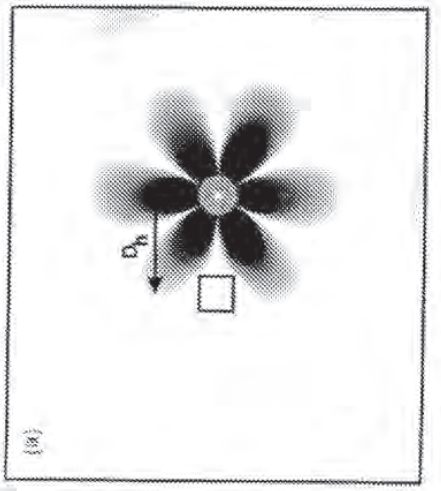


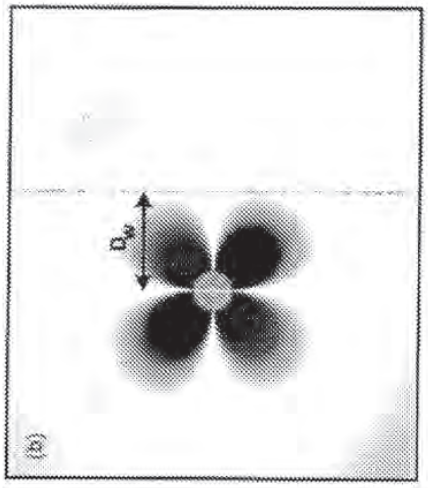
FIG. 29B

InductEV, Inc.
Exhibit 1025
Page 618



Disk with "human"	D_h/r	$Q^{abc}_{c\text{-}h}$	$Q^{rad}_{c[h]}$	$Q_{c[h]}$
Re{ε}=147.7, m=2	3	230	981	
λ /r ≈ 20	5	2917	1984	
Q^{abc}_c≈ 10096	7	11573	2230	
	10	41496	2201	
Re{ε}=65.6, m=3	3	1827	6197	
λ /r ≈10	**5**	**58431**	**11808**	
Q^{abc}_c≈ 10096	7	249748	9931	
	10	867552	9078	

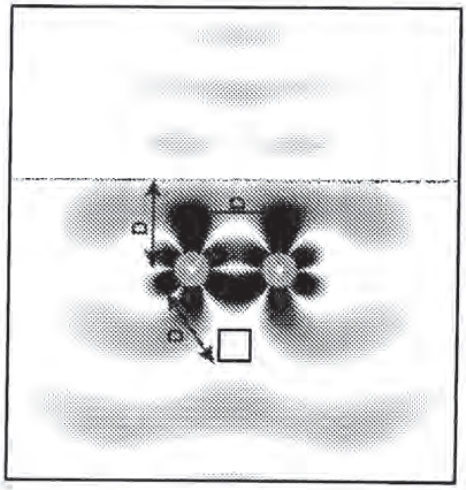
FIG. 30A



Disk with "human"	D_w/r	$Q^{abc}_{c\text{-}w}$	$Q^{rad}_{c[w]}$	$Q_{c[w]}$
Re{ε}=147.7, m=2	3	16725	1235	1033
λ /r ≈ 20	5	**31659**	**1922**	**1536**
Q^{abc}_c≈ 10098	7	49440	2389	1859
	10	82839	2140	1729
Re{ε}=65.6, m=3	3	53154	6228	3592
λ /r ≈10	**5**	127402	10988	5053
Q^{abc}_c≈ 10097	7	159192	10168	4910
	10	191506	9510	4775

FIG. 30B

InductEV, Inc.
Exhibit 1025
Page 619



Two disks with "human" and "wall"	D/r	$Q^{abc}_{c\text{-}h}$	$Q^{abc}_{c\text{-}w}$	$Q^{rad}_{c[hw]}$	$Q_{w[hw]} = \omega/2\Gamma$	$\omega/2\kappa_{[hw]}$	$\kappa_{[hw]}/\Gamma_{c[hw]}$
Re{ε}=147.7, m=2	3	3300	12774	536	426	48	8.8
$\lambda/r \approx 20$	5	5719	26333	1600	1068	322	3.3
$Q^{abc}_c \approx 10100$	7	13248	50161	3542	2097	973	2.2
	10	18447	68460	3624	2254	1768	1.3
Re{ε}=65.6, m=3	3	2088	36661	6764	1328	141	9.4
$\lambda/r \approx 10$	**5**	**72137**	**90289**	**11945**	**4815**	**2114**	**2.3**
$Q^{abc}_c \approx 10100$	7	237822	129094	12261	5194	8307	0.6

FIG. 30C

InductEV, Inc.
Exhibit 1025
Page 620

INTERNATIONAL SEARCH REPORT

International application No.
PCT/US 09/43970

A. CLASSIFICATION OF SUBJECT MATTER
IPC(8) - H01P 7/00 (2009.01)
USPC - 333/219
According to International Patent Classification (IPC) or to both national classification and IPC

B. FIELDS SEARCHED

Minimum documentation searched (classification system followed by classification symbols)
IPC(8) - H01P 7/00 (2009.01)
USPC - 333/219

Documentation searched other than minimum documentation to the extent that such documents are included in the fields searched
USPC - 333/219, 230

Electronic data base consulted during the international search (name of data base and, where practicable, search terms used)
PubWEST (PGPB,USPT,EPAB,JPAB); Google Patents; Google Scholar
Search Terms Used: resonance, resonator, energy, electricity, power, transfer, wireless, frequency, wavelength, angular, width, quality, factor, far, field, interference, generator, source, driving, drive

C. DOCUMENTS CONSIDERED TO BE RELEVANT

Category*	Citation of document, with indication, where appropriate, of the relevant passages	Relevant to claim No.
X — Y	US 2007/0222542 A1 (JOANNOPOULOS et al.) 27 September 2007 (27.09.2007), para [0005], [0006], [0012], [0015], [0016], [0019], [0021], [0022], [0024], [0027], [0028], [0029], [0031], [0035], [0042]	1-8 — 9-63
Y	US 2004/0113847 A1 (QI et al.) 17 June 2004 (17.06.2004), para [0015], [0023]	9-63
Y	US 5,437,057 A (RICHLEY et al.) 25 July 1995 (25.07.1995), col 9, ln 6-18	15-25, 37-47, 57, 58, 61, 62

☐ Further documents are listed in the continuation of Box C. ☐

* Special categories of cited documents:
"A" document defining the general state of the art which is not considered to be of particular relevance
"E" earlier application or patent but published on or after the international filing date
"L" document which may throw doubts on priority claim(s) or which is cited to establish the publication date of another citation or other special reason (as specified)
"O" document referring to an oral disclosure, use, exhibition or other means
"P" document published prior to the international filing date but later than the priority date claimed
"T" later document published after the international filing date or priority date and not in conflict with the application but cited to understand the principle or theory underlying the invention
"X" document of particular relevance; the claimed invention cannot be considered novel or cannot be considered to involve an inventive step when the document is taken alone
"Y" document of particular relevance; the claimed invention cannot be considered to involve an inventive step when the document is combined with one or more other such documents, such combination being obvious to a person skilled in the art
"&" document member of the same patent family

Date of the actual completion of the international search	Date of mailing of the international search report
07 July 2009 (07.07.2009)	14 JUL 2009
Name and mailing address of the ISA/US Mail Stop PCT, Attn: ISA/US, Commissioner for Patents P.O. Box 1450, Alexandria, Virginia 22313-1450 Facsimile No. 571-273-3201	Authorized officer: Lee W. Young PCT Helpdesk: 571-272-4300 PCT OSP: 571-272-7774

Form PCT/ISA/210 (second sheet) (April 2007)

(12) INTERNATIONAL APPLICATION PUBLISHED UNDER THE PATENT COOPERATION TREATY (PCT)

(19) World Intellectual Property Organization
International Bureau

(43) International Publication Date
8 April 2010 (08.04.2010)

PCT

(10) International Publication Number
WO 2010/039967 A1

(51) International Patent Classification:
H01P 7/00 (2006.01)

(21) International Application Number:
PCT/US2009/059244

(22) International Filing Date:
1 October 2009 (01.10.2009)

(25) Filing Language: English

(26) Publication Language: English

(30) Priority Data:
61/101,809 1 October 2008 (01.10.2008) US

(71) Applicant *(for all designated States except US)*: **MASSACHUSETTS INSTITUTE OF TECHNOLOGY** [US/US]; Five Cambridge Center, NE-25-230, Cambridge, Massachusetts 02142-1493 (US).

(72) Inventors; and

(75) Inventors/Applicants *(for US only)*: **HAMAM, Rafif E.** [LB/US]; 550 Memorial Drive, Apt. 9C-2, Cambridge, Massachusetts 02139 (US). **KARALIS, Aristeidis** [GR/US]; 151 Tremont Street, Apt. 21F, Boston, Massachusetts 02111 (US). **JOANNOPOULOS, John D.** [US/US]; 64 Douglas Road, Belmont, Massachusetts 02478 (US). **SOLJACIC, Marin** [HR/US]; 44 Westlund Road, Belmont, Massachusetts 02478 (US).

(74) Agent: **WEFERS, Marc M.**; Fish & Richardson P.C., P.O. Box 1022, Minneapolis, Minnesota 55440-1022 (US).

(81) Designated States *(unless otherwise indicated, for every kind of national protection available)*: AE, AG, AL, AM, AO, AT, AU, AZ, BA, BB, BG, BH, BR, BW, BY, BZ, CA, CH, CL, CN, CO, CR, CU, CZ, DE, DK, DM, DO, DZ, EC, EE, EG, ES, FI, GB, GD, GE, GH, GM, GT, HN, HR, HU, ID, IL, IN, IS, JP, KE, KG, KM, KN, KP, KR, KZ, LA, LC, LK, LR, LS, LT, LU, LY, MA, MD, ME, MG, MK, MN, MW, MX, MY, MZ, NA, NG, NI, NO, NZ, OM, PE, PG, PH, PL, PT, RO, RS, RU, SC, SD, SE, SG, SK, SL, SM, ST, SV, SY, TJ, TM, TN, TR, TT, TZ, UA, UG, US, UZ, VC, VN, ZA, ZM, ZW.

(84) Designated States *(unless otherwise indicated, for every kind of regional protection available)*: ARIPO (BW, GH, GM, KE, LS, MW, MZ, NA, SD, SL, SZ, TZ, UG, ZM, ZW), Eurasian (AM, AZ, BY, KG, KZ, MD, RU, TJ, TM), European (AT, BE, BG, CH, CY, CZ, DE, DK, EE, ES, FI, FR, GB, GR, HR, HU, IE, IS, IT, LT, LU, LV, MC, MK, MT, NL, NO, PL, PT, RO, SE, SI, SK, SM, TR), OAPI (BF, BJ, CF, CG, CI, CM, GA, GN, GQ, GW, ML, MR, NE, SN, TD, TG).

Published:

— *with international search report (Art. 21(3))*

WO 2010/039967 A1

(54) **Title**: EFFICIENT NEAR-FIELD WIRELESS ENERGY TRANSFER USING ADIABATIC SYSTEM VARIATIONS

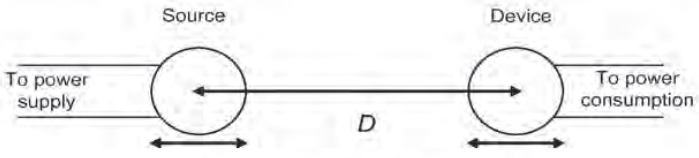


FIG. 1

(57) **Abstract**: Disclosed is a method for transferring energy wirelessly including transferring energy wirelessly from a first resonator structure to an intermediate resonator structure, wherein the coupling rate between the first resonator structure and the intermediate resonator structure is κ_{1B}, transferring energy wirelessly from the intermediate resonator structure to a second resonator structure, wherein the coupling rate between the intermediate resonator structure and the second resonator structure is κ_{B2} and during the wireless energy transfers, adjusting at least one of the coupling rates κ_{1B} and κ_{B2} to reduce energy accumulation in the intermediate resonator structure and improve wireless energy transfer from the first resonator structure to the second resonator structure through the intermediate resonator structure.

Attorney Docket No. 01997-0366WO1
MIT Case No 13441 (WiT MIT 4)

Efficient Near-Field Wireless Energy Transfer Using Adiabatic System Variations

CROSS REFERENCE TO RELATED APPLICATIONS

Pursuant to U.S.C. § 119(e), this application claims priority to U.S. Provisional Application Serial No. 61/101,809, filed October 1, 2008. The contents of the prior application is incorporated herein by reference in its entirety.

BACKGROUND

The disclosure relates to wireless energy transfer. Wireless energy transfer can for example, be useful in such applications as providing power to autonomous electrical or electronic devices.

Radiative modes of omni-directional antennas (which work very well for information transfer) are not suitable for such energy transfer, because a vast majority of energy is wasted into free space. Directed radiation modes, using lasers or highly-directional antennas, can be efficiently used for energy transfer, even for long distances (transfer distance $L_{TRANS} \gg L_{DEV}$, where L_{DEV} is the characteristic size of the device and/or the source), but may require existence of an uninterruptible line-of-sight and a complicated tracking system in the case of mobile objects. Some transfer schemes rely on induction, but are typically restricted to very close-range ($L_{TRANS} \ll L_{DEV}$) or low power (~mW) energy transfers.

The rapid development of autonomous electronics of recent years (e.g. laptops, cell-phones, house-hold robots, that all typically rely on chemical energy storage) has led to an increased need for wireless energy transfer.

SUMMARY

Disclosed is a method for transferring energy wirelessly. The method includes i) transferring energy wirelessly from a first resonator structure to an intermediate resonator structure, wherein the coupling rate between the first resonator structure and the intermediate resonator structure is κ_{1B}; ii) transferring energy wirelessly from the intermediate resonator structure to a second resonator structure, wherein the coupling rate

InductEV, Inc.
Exhibit 1025
Page 623

between the intermediate resonator structure and the second resonator structure is κ_{B2}; and iii) during the wireless energy transfers, adjusting at least one of the coupling rates κ_{1B} and κ_{B2} to reduce energy accumulation in the intermediate resonator structure and improve wireless energy transfer from the first resonator structure to the second resonator structure through the intermediate resonator structure.

Embodiments of the method may include one or more of the following features.

The adjustment of at least one of the coupling rates κ_{1B} and κ_{B2} can be selected to minimize energy accumulation in the intermediate resonator structure and cause wireless energy transfer from the first resonator structure to the second resonator structure.

The adjustment of at least one of the coupling rates κ_{1B} and κ_{B2} can be selected to maintain energy distribution in the field of the three-resonator system in an eigenstate having substantially no energy in the intermediate resonator structure. For example, the adjustment of at least one of the coupling rates κ_{1B} and κ_{B2} can further cause the eigenstate to evolve substantially adiabatically from an initial state with substantially all energy in the resonator structures in the first resonator structure to a final state with substantially all of the energy in the resonator structures in the second resonator structure.

The adjustment of at least one of the coupling rates κ_{1B} and κ_{B2} can be selected to include adjustments of both coupling rates κ_{1B} and κ_{B2} during wireless energy transfer.

The resonator structures can each have a quality factor larger than 10.

The first and second resonator structures can each have a quality factor greater than 50.

The first and second resonator structures can each have a quality factor greater than 100.

The resonant energy in each of the resonator structures can include electromagnetic fields. For example, the maximum value of the coupling rate κ_{1B} and the maximum value of the coupling rate κ_{B2} for inductive coupling between the

InductEV, Inc.
Exhibit 1025
Page 624

intermediate resonator structure and each of the first and second resonator structures can each be larger than twice the loss rate Γ for each of the first and second resonators. Moreover, The maximum value of the coupling rate κ_{1B} and the maximum value of the coupling rate κ_{B2} for inductive coupling between the intermediate resonator structure and each of the first and second resonator structures can each be larger than four (4) times the loss rate Γ for each of the first and second resonators.

Each resonator structure can have a resonant frequency between 50 KHz and 500 MHz.

The maximum value of the coupling rate κ_{1B} and the maximum value of the coupling rate κ_{B2} can each be at least five (5) times greater than the coupling rate between the first resonator structure and the second resonator structure.

The intermediate resonator structure can have a rate of radiative energy loss that is at least twenty (20) times greater than that for either the first resonator structure or the second resonator structure.

The first and second resonator structures can be substantially identical.

The adjustment of at least one of the coupling rates κ_{1B} and κ_{B2} can be selected to cause peak energy accumulation in the intermediate resonator structure to be less than five percent (5%) of the peak total energy in the three resonator structures.

The adjustment of at least one of the coupling rates κ_{1B} and κ_{B2} can be selected to cause peak energy accumulation in the intermediate resonator structure during the wireless energy transfers to be less than ten percent (10%) of the peak total energy in the three resonator structures.

Adjusting at least one of the coupling rates κ_{1B} and κ_{B2} can include adjusting a relative position and/or orientation between one or more pairs of the resonator structures. Moreover, adjusting at least one of the coupling rates κ_{1B} and κ_{B2} can include adjusting a resonator property of one or more of the resonator structures, such as mutual inductance.

The resonator structures can include a capacitively loaded loop or coil of at least one of a conducting wire, a conducting Litz wire, and a conducting ribbon.

InductEV, Inc.
Exhibit 1025
Page 625

The resonator structures can include an inductively loaded rod of at least one of a conducting wire, a conducting Litz wire, and a conducting ribbon.

The wireless energy transfers are non-radiative energy transfers mediated by a coupling of a resonant field evanescent tail of the first resonator structure and a resonant field evanescent tail of the intermediate resonator structure and a coupling of the resonant field evanescent tail of the intermediate resonator structure and a resonant field evanescent tail of the second resonator structure.

The adjustment of the at least one of the coupling rates can define a first mode of operation, wherein the reduction in the energy accumulation in the intermediate resonator structure is relative to energy accumulation in the intermediate resonator structure for a second mode of operation of wireless energy transfer among the three resonator structures having a coupling rate κ'_{1B} for wireless energy transfer from the first resonator structure to the intermediate resonator structure and a coupling rate κ'_{B2} for wireless energy transfer from the intermediate resonator structure to the second resonator structure with κ'_{1B} and κ'_{B2} each being substantially constant during the second mode of wireless energy transfer, and wherein the adjustment of the coupling rates κ_{1B} and κ_{2B} in the first mode of operation can be selected to $\kappa_{1B}, \kappa_{B2} < \sqrt{\left(\kappa'^{2}_{1B} + \kappa'^{2}_{B2}\right)/2}$. Moreover, the first mode of operation can have a greater efficiency of energy transferred from the first resonator to the second resonator compared to that for the second mode of operation. Further, the first and second resonator structures can be substantially identical and each one can have a loss rate Γ_A, the intermediate resonator structure can have a loss rate Γ_B, and wherein Γ_B/Γ_A can be greater than 50.

Also, a ratio of energy lost to radiation and total energy wirelessly transferred between the first and second resonator structures in the first mode of operation is less than that for the second mode of operation. Moreover, the first and second resonator structures can be substantially identical and each one can have a loss rate Γ_A and a loss

InductEV, Inc.
Exhibit 1025
Page 626

rate only due to radiation $\Gamma_{A,rad}$, the intermediate resonator structure can have a loss rate Γ_B and a loss rate only due to radiation $\Gamma_{B,rad}$ and wherein $\Gamma_{B,rad}/\Gamma_B > \Gamma_{A,rad}/\Gamma_A$.

The first mode of operation the intermediate resonator structure interacts less with extraneous objects than it does in the second mode of operation.

During the wireless energy transfer from the first resonator structure to the second resonator structure at least one of the coupling rates can be adjusted so that $\kappa_{1B} << \kappa_{B2}$ at a start of the energy transfer and $\kappa_{1B} >> \kappa_{B2}$ by a time a substantial portion of the energy has been transferred from the first resonator structure to the second resonator structure.

The coupling rate κ_{B2} can be maintained at a fixed value and the coupling rate κ_{1B} is increased during the wireless energy transfer from the first resonator structure to second resonator structure.

The coupling rate κ_{1B} can be maintained at a fixed value and the coupling rate κ_{B2} is decreased during the wireless energy transfer from the first resonator structure to second resonator structure.

During the wireless energy transfer from the first resonator structure to second resonator structure, the coupling rate κ_{1B} can be increased and the coupling rate κ_{B2} is decreased.

The method may further include features corresponding to those listed for one or more of the apparatuses and methods described below.

In another aspect, disclosed is an apparatus including: first, intermediate, and second resonator structures, wherein a coupling rate between the first resonator structure and the intermediate resonator structure is κ_{1B} and a coupling rate between the intermediate resonator structure and the second resonator structure is κ_{B2}; and means for adjusting at least one of the coupling rates κ_{1B} and κ_{B2} during wireless energy transfers among the resonator structures to reduce energy accumulation in the intermediate resonator structure and improve wireless energy transfer from the first resonator structure to the second resonator structure through the intermediate resonator structure.

InductEV, Inc.
Exhibit 1025
Page 627

Embodiments for the apparatus can include one or more of the following features.

The means for adjusting can include a rotation stage for adjusting the relative orientation of the intermediate resonator structure with respect to the first and second resonator structures.

The means for adjusting can include a translation stage for moving the first and/or second resonator structures relative to the intermediate resonator structure.

The means for adjusting can include a mechanical, electro-mechanical, or electrical staging system for dynamically adjusting the effective size of one or more of the resonator structures.

The apparatus may further include features corresponding to those listed for the method described above, and one or more of the apparatuses and methods described below.

In another aspect, a method for transferring energy wirelessly includes i): transferring energy wirelessly from a first resonator structure to a intermediate resonator structure, wherein the coupling rate between the first resonator structure and the intermediate resonator structure is κ_{1B}; ii) transferring energy wirelessly from the intermediate resonator structure to a second resonator, wherein the coupling rate between the intermediate resonator structure and the second resonator structure is κ_{B2}; and iii) during the wireless energy transfers, adjusting at least one of the coupling rates κ_{1B} and κ_{B2} to cause an energy distribution in the field of the three-resonator system to have substantially no energy in the intermediate resonator structure while wirelessly transferring energy from the first resonator structure to the second resonator structure through the intermediate resonator structure.

Embodiments for the method above can include one or more of the following features.

Having substantially no energy in the intermediate resonator structure can mean that peak energy accumulation in the intermediate resonator structure is less than ten percent (10%) of the peak total energy in the three resonator structures throughout the wireless energy transfer.

InductEV, Inc.
Exhibit 1025
Page 628

Having substantially no energy in the intermediate resonator structure can mean that peak energy accumulation in the intermediate resonator structure is less than five percent (5%) of the peak total energy in the three resonator structures throughout the wireless energy transfer.

The adjustment of at least one of the coupling rates κ_{1B} and κ_{B2} can be selected to maintain the energy distribution in the field of the three-resonator system in an eigenstate having the substantially no energy in the intermediate resonator structure.

The adjustment of at least one of the coupling rates κ_{1B} and κ_{B2} can be selected to further cause the eigenstate to evolve substantially adiabatically from an initial state with substantially all energy in the resonator structures in the first resonator structure to a final state with substantially all of the energy in the resonator structures in the second resonator structure.

The adjustment of at least one of the coupling rates κ_{1B} and κ_{B2} can include adjustments of both coupling rates κ_{1B} and κ_{B2} during wireless energy transfers.

The resonant energy in each of the resonator structures comprises electromagnetic fields. For example, the maximum value of the coupling rate κ_{1B} and the maximum value of the coupling rate κ_{B2} for inductive coupling between the intermediate resonator structure and each of the first and second resonator structures can each be larger than twice the loss rate Γ for each of the first and second resonators. Moreover, the maximum value of the coupling rate κ_{1B} and the maximum value of the coupling rate κ_{B2} for inductive coupling between the intermediate resonator structure and each of the first and second resonator structures can each be larger than four (4) times the loss rate Γ for each of the first and second resonators.

The resonator structure can have a resonant frequency between 50 KHz and 500 MHz.

The maximum value of the coupling rate κ_{1B} and the maximum value of the coupling rate κ_{B2} can each be at least five (5) times greater than the coupling rate between the first resonator structure and the second resonator structure.

InductEV, Inc.
Exhibit 1025
Page 629

The intermediate resonator structure can have a rate of radiative energy loss that is at least twenty (20) times greater than that for either the first resonator structure or the second resonator structure.

The first and second resonator structures can be substantially identical.

Adjusting at least one of the coupling rates κ_{1B} and κ_{B2} can include adjusting a relative position and/or orientation between one or more pairs of the resonator structures.

Adjusting at least one of the coupling rates κ_{1B} and κ_{B2} can include adjusting a resonator property of one or more of the resonator structures, such as mutual inductance.

The resonator structures can include a capacitively loaded loop or coil of at least one of a conducting wire, a conducting Litz wire, and a conducting ribbon.

The resonator structures can include an inductively loaded rod of at least one of a conducting wire, a conducting Litz wire, and a conducting ribbon.

The wireless energy transfers can be non-radiative energy transfers mediated by a coupling of a resonant field evanescent tail of the first resonator structure and a resonant field evanescent tail of the intermediate resonator structure and a coupling of the resonant field evanescent tail of the intermediate resonator structure and a resonant field evanescent tail of the second resonator structure.

The first and second resonator structures can each have a quality factor greater than 50.

The first and second resonator structures can each have a quality factor greater than 100.

The adjustment of at least one of the coupling rates κ_{1B} and κ_{B2} can be selected to cause the energy distribution in the field of the three-resonator system to have substantially no energy in the intermediate resonator structure improves wireless energy transfer between the first and second resonator structures.

The adjustment of the at least one of the coupling rates can be selected to define a first mode of operation, wherein energy accumulation in the intermediate resonator structure during the wireless energy transfer from the first resonator structure to second resonator structure is smaller than that for a second mode of operation of wireless energy

InductEV, Inc.
Exhibit 1025
Page 630

transfer among the three resonator structures having a coupling rate κ'_{1B} for wireless energy transfer from the first resonator structure to the intermediate resonator structure and a coupling rate κ'_{B2} for wireless energy transfer from the intermediate resonator structure to the second resonator structure with κ'_{1B} and κ'_{B2} each being substantially constant during the second mode of wireless energy transfer, and wherein the adjustment of the coupling rates κ_{1B} and κ_{B2} in the first mode of operation can be selected to satisfy $\kappa_{1B}, \kappa_{B2} < \sqrt{\left(\kappa'^{2}_{1B} + \kappa'^{2}_{B2}\right)/2}$.

The first mode of operation can have a greater efficiency of energy transferred from the first resonator to the second resonator compared to that for the second mode of operation.

The first and second resonator structures can be substantially identical and each one can have a loss rate Γ_A, the intermediate resonator structure can have a loss rate Γ_B, and wherein Γ_B/Γ_A can be greater than 50.

A ratio of energy lost to radiation and total energy wirelessly transferred between the first and second resonator structures in the first mode of operation can be less than that for the second mode of operation.

The first and second resonator structures can be substantially identical and each one can have a loss rate Γ_A and a loss rate only due to radiation $\Gamma_{A,rad}$, the intermediate resonator structure can have a loss rate Γ_B and a loss rate only due to radiation $\Gamma_{B,rad}$ and wherein $\Gamma_{B,rad}/\Gamma_B > \Gamma_{A,rad}/\Gamma_A$.

The first mode of operation the intermediate resonator structure interacts less with extraneous objects than it does in the second mode of operation.

During the wireless energy transfer from the first resonator structure to the second resonator structure at least one of the coupling rates can be adjusted so that $\kappa_{1B} << \kappa_{B2}$ at a start of the energy transfer and $\kappa_{1B} >> \kappa_{B2}$ by a time a substantial portion of the energy has been transferred from the first resonator structure to the second resonator structure.

InductEV, Inc.
Exhibit 1025
Page 631

The coupling rate κ_{B2} can be maintained at a fixed value and the coupling rate κ_{1B} can be increased during the wireless energy transfer from the first resonator structure to second resonator structure.

The coupling rate κ_{1B} can be maintained at a fixed value and the coupling rate κ_{B2} can be decreased during the wireless energy transfer from the first resonator structure to second resonator structure.

During the wireless energy transfer from the first resonator structure to second resonator structure, the coupling rate κ_{1B} can be increased and the coupling rate κ_{B2} can be decreased.

The method may further include features corresponding to those listed for the apparatus and method described above, and one or more of the apparatuses and methods described below.

In another aspect, disclosed is an apparatus including: first, intermediate, and second resonator structures, wherein a coupling rate between the first resonator structure and the intermediate resonator structure is κ_{1B} and a coupling rate between the intermediate resonator structure and the second resonator structure is κ_{B2}; and means for adjusting at least one of the coupling rates κ_{1B} and κ_{B2} during wireless energy transfers among the resonator structures to cause an energy distribution in the field of the three-resonator system to have substantially no energy in the intermediate resonator structure while wirelessly transferring energy from the first resonator structure to the second resonator structure through the intermediate resonator structure.

Embodiments for the apparatus can include one or more of the following features.

Having substantially no energy in the intermediate resonator structure can mean that peak energy accumulation in the intermediate resonator structure is less than ten percent (10%) of the peak total energy in the three resonator structures throughout the wireless energy transfers.

Having substantially no energy in the intermediate resonator structure can mean that peak energy accumulation in the intermediate resonator structure is less than five

InductEV, Inc.
Exhibit 1025
Page 632

percent (5%) of the peak total energy in the three resonator structures throughout the wireless energy transfers.

The means for adjusting can be configured to maintain the energy distribution in the field of the three-resonator system in an eigenstate having the substantially no energy in the intermediate resonator structure.

The means for adjusting can include a rotation stage for adjusting the relative orientation of the intermediate resonator structure with respect to the first and second resonator structures.

The means for adjusting can include a translation stage for moving the first and/or second resonator structures relative to the intermediate resonator structure.

The means for adjusting can include a mechanical, electro-mechanical, or electrical staging system for dynamically adjusting the effective size of one or more of the resonator structures.

The resonator structures can include a capacitively loaded loop or coil of at least one of a conducting wire, a conducting Litz wire, and a conducting ribbon.

The resonator structures can include an inductively loaded rod of at least one of a conducting wire, a conducting Litz wire, and a conducting ribbon.

A source can be coupled to the first resonator structure and a load can be coupled to the second resonator structure.

The apparatus may further include features corresponding to those listed for the apparatus and methods described above, and the apparatus and method described below.

In another aspect, disclosed is a method for transferring energy wirelessly that includes: i) transferring energy wirelessly from a first resonator structure to a intermediate resonator structure, wherein the coupling rate between the first resonator structure and the intermediate resonator structure is κ_{1B}; ii) transferring energy wirelessly from the intermediate resonator structure to a second resonator, wherein the coupling rate between the intermediate resonator structure and the second resonator structure with a coupling rate is κ_{B2}; and iii) during the wireless energy transfers, adjusting at least one of the coupling rates κ_{1B} and κ_{B2} to define a first mode of operation in which energy

InductEV, Inc.
Exhibit 1025
Page 633

accumulation in the intermediate resonator structure is reduced relative to that for a second mode of operation of wireless energy transfer among the three resonator structures having a coupling rate κ'_{1B} for wireless energy transfer from the first resonator structure to the intermediate resonator structure and a coupling rate κ'_{B2} for wireless energy transfer from the intermediate resonator structure to the second resonator structure with κ'_{1B} and κ'_{B2} each being substantially constant during the second mode of wireless energy transfer, and wherein the adjustment of the coupling rates κ_{1B} and κ_{B2} in the first mode of operation can be selected to satisfy $\kappa_{1B}, \kappa_{B2} < \sqrt{\left(\kappa'^{2}_{1B} + \kappa'^{2}_{B2}\right)/2}$.

The method may further include features corresponding to those listed for the apparatuses and methods described above.

In another aspect, disclosed is an apparatus that includes: first, intermediate, and second resonator structures, wherein a coupling rate between the first resonator structure and the intermediate resonator structure is κ_{1B} and a coupling rate between the intermediate resonator structure and the second resonator structure is κ_{B2}; and means for adjusting at least one of the coupling rates κ_{1B} and κ_{B2} during wireless energy transfers among the resonator structures to define a first mode of operation in which energy accumulation in the intermediate resonator structure is reduced relative to that for a second mode of operation for wireless energy transfer among the three resonator structures having a coupling rate κ'_{1B} for wireless energy transfer from the first resonator structure to the intermediate resonator structure and a coupling rate κ'_{B2} for wireless energy transfer from the intermediate resonator structure to the second resonator structure with κ'_{1B} and κ'_{B2} each being substantially constant during the second mode of wireless energy transfer, and wherein the adjustment of the coupling rates κ_{12} and κ_{B2} in the first mode of operation can be selected to satisfy $\kappa_{1B}, \kappa_{B2} < \sqrt{\left(\kappa'^{2}_{1B} + \kappa'^{2}_{B2}\right)/2}$.

InductEV, Inc.
Exhibit 1025
Page 634

The apparatus may further include features corresponding to those listed for the apparatuses and methods described above.

Unless otherwise defined, all technical and scientific terms used herein have the same meaning as commonly understood by one of ordinary skill in the art. Although methods and materials similar or equivalent to those described herein can be used in the practice or testing of the present disclosure, suitable methods and materials are described below. All publications, patent applications, patents, and other references mentioned herein are incorporated by reference in their entirety. In case of conflict, the present specification, including definitions, will control. In addition, the materials, methods, and examples are illustrative only and not intended to be limiting.

The details of one or more embodiments are set forth in the accompanying drawings and the description below, including the documents appended hereto. Other features and advantages will be apparent from this disclosure and from the claims.

BRIEF DESCRIPTION OF THE DRAWINGS

Fig. 1 shows a schematic of an example wireless energy transfer scheme.

Figs. 2(a)-(b) show the efficiency of power transmission η_P for (a) $U = 1$ and (b) $U = 3$, as a function of the frequency detuning D_o and for different values of the loading rate U_o.

Fig. 2(c) shows the optimal (for zero detuning and under conditions of impedance matching) efficiency for energy transfer η_{E^*} and power transmission η_{P^*}, as a function of the coupling-to-loss figure-of-merit U.

Fig. 3 shows an example of a self-resonant conducting-wire coil.

Fig. 4 shows an example of a wireless energy transfer scheme featuring two self-resonant conducting-wire coils.

Fig. 5 is a schematic of an experimental system demonstrating wireless energy transfer.

Fig. 6 shows a comparison between experimental and theoretical results for the coupling rate of the system shown schematically in Fig. 5.

InductEV, Inc.
Exhibit 1025
Page 635

Fig. 7 shows a comparison between experimental and theoretical results for the strong-coupling factor of the system shown schematically in Fig. 5.

Fig. 8 shows a comparison between experimental and theoretical results for the power-transmission efficiency of the system shown schematically in Fig. 5.

Fig. 9 shows an example of a capacitively-loaded conducting-wire coil, and illustrates the surrounding field.

Fig. 10 shows an example wireless energy transfer scheme featuring two capacitively-loaded conducting-wire coils, and illustrates the surrounding field.

Fig. 11 illustrates an example circuit model for wireless energy transfer.

Fig. 12 shows the efficiency, total (loaded) device Q, and source and device currents, voltages and radiated powers (normalized to 1Watt of output power to the load) as functions of the resonant frequency, for a particular choice of source and device loop dimensions, wp and N_s and different choices of N_d=1,2,3,4,5,6,10.

Fig.13 shows the efficiency, total (loaded) device Q, and source and device currents, voltages and radiated powers (normalized to 1Watt of output power to the load) as functions of frequency and wp for a particular choice of source and device loop dimensions, and number of turns N_s and N_d.

Fig. 14 shows an example of an inductively-loaded conducting-wire coil.

Fig. 15 shows (a) an example of a resonant dielectric disk, and illustrates the surrounding field and (b) a wireless energy transfer scheme featuring two resonant dielectric disks, and illustrates the surrounding field.

Fig. 16 shows a schematic of an example wireless energy transfer scheme with one source resonator and one device resonator exchanging energy indirectly through an intermediate resonator.

Fig. 17 shows an example of a wireless energy transfer system: (a) (Left) Schematic of loops configuration in two-object direct transfer. (Right) Time evolution of energies in the two-object direct energy transfer case. (b) (Left) Schematic of three-loops configuration in the constant-κ case. (Right) Dynamics of energy transfer for the configuration in (b. Left). Note that the total energy transferred E_2 is 2 times larger than in (a. Right), but at the price of the total energy radiated being 4 times larger. (c) (Left)

InductEV, Inc.
Exhibit 1025
Page 636

Loop configuration at t=0 in the adiabatic-κ scheme. (Center) Dynamics of energy transfer with adiabatically rotating loops. (Right) Loop configuration at $t=t_{ETT}$. Note that E_2 is comparable to (b. Right), but the radiated energy is now much smaller: In fact, it is comparable to (a. Right).

Fig. 18 shows a schematic of an example wireless energy transfer scheme with one source resonator and one device resonator exchanging energy indirectly through an intermediate resonator, where an adjustment system is used to rotate the resonator structures to dynamically adjust their coupling rates.

Fig. 19 shows an example of a temporal variation of the coupling rates in a wireless energy transfer system as in Fig. 18 to achieve an adiabatic transfer of energy from the source object R_1 to the device object R_2.

Fig. 20 shows the energy distribution in a wireless energy transfer system as in Fig. 18 as a function of time when the coupling rates are time-varying, for $\Gamma_A=0$, $\kappa/\Gamma_B=10$, $\kappa_{1B}=\kappa\sin[\pi t/(2t_{ETT})]$, and $\kappa_{B2}=\kappa\cos[\pi t/(2t_{ETT})]$.

Figs. 21(a)-(f) show a comparison between the adiabatic-κ and constant-κ energy transfer schemes, in the general case: (a) Optimum E_2 (%) in adiabatic-κ transfer, (b) Optimum E_2 (%) in constant-κ transfer, (c) $(E_2)_{\text{adiabatic-}\kappa}/(E_2)_{\text{constant-}\kappa}$, (d) Energy lost (%) at optimum adiabatic-κ transfer, (e) Energy lost (%) at optimum constant-κ transfer, (f) $(E_{lost})_{\text{constant-}\kappa}/(E_{lost})_{\text{adiabatic-}\kappa}$.

Fig. 22(a)-(e) show a comparison between radiated energies in the adiabatic-κ and constant-κ energy transfer schemes: (a) E_{rad}(%) in the constant-scheme for $\Gamma_B/\Gamma_A=500$ and $\Gamma_{rad}^{A}=0$, (b) E_{rad}(%) in the adiabatic-κ scheme for $\Gamma_B/\Gamma_A=500$ and $\Gamma_{rad}^{A}=0$, (c) $(E_{rad})_{\text{constant-}\kappa}/(E_{rad})_{\text{adiabatic-}\kappa}$ for $\Gamma_B/\Gamma_A=50$, (d) $(E_{rad})_{\text{constant-}\kappa}/(E_{rad})_{\text{adiabatic-}\kappa}$ for $\Gamma_B/\Gamma_A=500$, (e) $[(E_{rad})_{\text{constant-}\kappa}/(E_{rad})_{\text{adiabatic-}\kappa}]$ as function of κ/Γ_B and Γ_B/Γ_A, for $\Gamma_{rad}^{A}=0$.

Figs. 23(a)-(b) show schematics for frequency control mechanisms.

Figs. 24(a)-(c) illustrate a wireless energy transfer scheme using two dielectric disks in the presence of various extraneous objects.

InductEV, Inc.
Exhibit 1025
Page 637

DETAILED DESCRIPTION

Efficient wireless energy-transfer between two similar-frequency resonant objects can be achieved at mid-range distances, provided these resonant objects are designed to operate in the 'strong-coupling' regime. 'Strong coupling' can be realized for a wide variety of resonant objects, including electromagnetic resonant objects such as inductively-loaded conducting rods and dielectric disks. Recently, we have demonstrated wireless energy transfer between strongly coupled electromagnetic self-resonant conducting coils and capacitively-loaded conducting coils, bearing high-Q electromagnetic resonant modes. See, for example, the following commonly owned U.S. Patent Applications, all of which are incorporated herein by reference: U.S. Application Serial No. 11/481,077, filed on July 5, 2006, and published as U.S. Patent Publication No. US 2007-0222542 A1; U.S. Application Serial No. 12/055,963, filed on March 26, 2008, and published as U.S. Patent Publication No. US 2008-0278264 A1; and U.S. Patent Application Serial No. 12/466,065, filed on May 14, 2009, and published as U.S. Patent Publication No. _____. In general, the energy-transfer efficiency between similar-frequency, strongly coupled resonant objects decreases as the distance between the objects is increased.

In this work, we explore a further scheme of efficient energy transfer between resonant objects that extends the range over which energy may be efficiently transferred. Instead of transferring energy directly between two resonant objects, as has been described in certain embodiments of the cross-referenced patents, in certain embodiments, an intermediate resonant object, with a resonant frequency equal or nearly-equal to that of the two energy-exchanging resonant objects is used to mediate the transfer. The intermediate resonant object may be chosen so that it couples more strongly to each of the resonant objects involved in the energy transfer than those two resonant objects couple to each other. One way to design such an intermediate resonator is to make it larger than either of the resonant objects involved in the energy transfer. However, increasing the size of the intermediate resonant object may lower its quality factor, or Q, by increasing its radiation losses. Surprisingly enough, this new "indirect" energy transfer

InductEV, Inc.
Exhibit 1025
Page 638

scheme may be shown to be very efficient and only weakly-radiative by introducing a meticulously chosen time variation of the resonator coupling rates.

The advantage of this method over the prior commonly owned wireless energy transfer techniques is that, in certain embodiments, it can enable energy to be transferred wirelessly between two objects with a larger efficiency and/or with a smaller radiation loss and/or with fewer interactions with extraneous objects.

Accordingly, in certain embodiments, we disclose an efficient wireless energy transfer scheme between two similar resonant objects, strongly coupled to an intermediate resonant object of substantially different properties, but with the same resonance frequency. The transfer mechanism essentially makes use of the adiabatic evolution of an instantaneous (so called 'dark') resonant state of the coupled three-object system. Our analysis is based on temporal coupled mode theory (CMT), and is general. Of particular commercial interest is the application of this technique to strongly-coupled electromagnetic resonators used for mid-range wireless energy transfer applications. We show that in certain parameter regimes of interest, this scheme can be more efficient, and/or less radiative than other wireless energy transfer approaches.

While the technique described herein is primarily directed to tangible resonator structures, the technique shares certain features with a quantum interference phenomenon known in the atomic physics community as Electromagnetically Induced Transparency (EIT). In EIT, three atomic states participate. Two of them, which are non-lossy, are coupled to one that has substantial losses. However, by meticulously controlling the mutual couplings between the states, one can establish a coupled system which is overall non-lossy. This phenomena has been demonstrated using carefully timed optical pulses, referred to as probe laser pulses and Stokes laser pulses, to reduce the opacity of media with the appropriate collection of atomic states. A closely related phenomenon known as Stimulated Raman Adiabatic Passage (STIRAP) may take place in a similar system; namely, the probe and Stokes laser beams may be used to achieve complete coherent population transfer between two molecular states of a medium. Hence, we may refer to the currently proposed scheme as the "EIT-like" energy transfer scheme.

InductEV, Inc.
Exhibit 1025
Page 639

In certain embodiments, we disclose an efficient near-field energy transfer scheme between two similar resonant objects, based on an EIT-like transfer of the energy through a mediating resonant object with the same resonant frequency. In embodiments, this EIT-like energy transfer may be realized using electromagnetic resonators as have been described in the cross-referenced patents, but the scheme is not bound only to wireless energy transfer applications. Rather, this scheme is general and may find applications in various other types of coupling between general resonant objects. In certain embodiments described below, we describe particular examples of electromagnetic resonators, but the nature of the resonators and their coupling mechanisms could be quite different (e.g. acoustic, mechanical, etc.). To the extent that many resonant phenomena can be modeled with nearly identical CMT equations, similar behavior to that described herein would occur.

1. Efficient energy-transfer by two 'strongly coupled' resonances

Fig. 1 shows a schematic that generally describes one example of the invention, in which energy is transferred wirelessly between two resonant objects. Referring to Fig. 1, energy is transferred over a distance D, between a resonant source object having a characteristic size r_1 and a resonant device object of characteristic size r_2. Both objects are resonant objects. The wireless near-field energy transfer is performed using the field (e.g. the electromagnetic field or acoustic field) of the system of two resonant objects.

The characteristic size of an object can be regarded as being equal to the radius of the smallest sphere which can fit around the entire object. The characteristic thickness of an object can be regarded as being, when placed on a flat surface in any arbitrary configuration, the smallest possible height of the highest point of the object above a flat surface. The characteristic width of an object can be regarded as being the radius of the smallest possible circle that the object can pass through while traveling in a straight line. For example, the characteristic width of a cylindrical object is the radius of the cylinder.

Initially, we present a theoretical framework for understanding near-field wireless energy transfer. Note however that it is to be understood that the scope of the invention is not bound by theory.

InductEV, Inc.
Exhibit 1025
Page 640

Different temporal schemes can be employed, depending on the application, to transfer energy between two resonant objects. Here we will consider two particularly simple but important schemes: a one-time finite-amount energy-transfer scheme and a continuous finite-rate energy-transfer (power) scheme.

1.1 Finite-amount energy-transfer efficiency

Let the source and device objects be 1, 2 respectively and their resonance modes, which we will use for the energy exchange, have angular frequencies $\omega_{1,2}$, frequency-widths due to intrinsic (absorption, radiation etc.) losses $\Gamma_{1,2}$ and (generally) vector fields $\mathbf{F}_{1,2}(\mathbf{r})$, normalized to unity energy. Once the two resonant objects are brought in proximity, they can interact and an appropriate analytical framework for modeling this resonant interaction is that of the well-known coupled-mode theory (CMT). This model works well, when the resonances are well defined by having large quality factors and their resonant frequencies are relatively close to each other. In this picture, the field of the system of the two resonant objects 1, 2 can be approximated by $\mathbf{F}(\mathbf{r},t)=a_1(t)\mathbf{F}_1(\mathbf{r})+a_2(t)\mathbf{F}_2(\mathbf{r})$, where $a_{1,2}(t)$ are the field amplitudes, with $|a_{1,2}(t)|^2$ equal to the energy stored inside the object 1, 2 respectively, due to the normalization. Then, using $e^{-i\omega t}$ time dependence, the field amplitudes can be shown to satisfy, to lowest order:

$$\begin{aligned}\frac{d}{dt}a_1(t)&=-i(\omega_1-i\Gamma_1)a_1(t)+i\kappa_{11}a_1(t)+i\kappa_{12}a_2(t)\\ \frac{d}{dt}a_2(t)&=-i(\omega_2-i\Gamma_2)a_2(t)+i\kappa_{21}a_1(t)+i\kappa_{22}a_2(t)\end{aligned} \qquad (1)$$

where $\kappa_{11,22}$ are the shifts in each object's frequency due to the presence of the other, which are a second-order correction and can be absorbed into the resonant frequencies (eigenfrequencies) by setting $\omega_{1,2}\rightarrow\omega_{1,2}+\kappa_{11,22}$, and $\kappa_{12,21}$ are the coupling coefficients, which from the reciprocity requirement of the system satisfy $\kappa_{21}=\kappa_{12}\equiv\kappa$.

InductEV, Inc.
Exhibit 1025
Page 641

The resonant modes of the combined system are found by substituting $[a_1(t), a_2(t)] = [A_1, A_2]e^{-i\bar{\omega}t}$. They have complex resonant frequencies

$$\bar{\omega}_{\pm} = \omega_{12} \pm \sqrt{(\Delta\omega_{12})^2 + \kappa^2} \tag{2a}$$

where $\omega_{12} = \left[(\omega_1 + \omega_2) - i(\Gamma_1 + \Gamma_2)\right]/2$, $\Delta\omega_{12} = \left[(\omega_1 - \omega_2) - i(\Gamma_1 - \Gamma_2)\right]/2$ and whose splitting we denote as $\delta_E \equiv \bar{\omega}_+ - \bar{\omega}_-$, and corresponding resonant field amplitudes

$$\vec{V}_{\pm} = \begin{bmatrix} A_1 \\ A_2 \end{bmatrix}_{\pm} = \begin{bmatrix} \kappa \\ \Delta\omega_{12} \mp \sqrt{(\Delta\omega_{12})^2 + \kappa^2} \end{bmatrix}. \tag{2b}$$

Note that, at exact resonance $\omega_1 = \omega_2 = \omega_A$ and for $\Gamma_1 = \Gamma_2 = \Gamma_A$, we get $\Delta\omega_{12} = 0$, $\delta_E = 2\kappa$, and then

$$\bar{\omega}_{\pm} = \omega_A \pm \kappa - i\Gamma_A$$

$$\vec{V}_{\pm} = \begin{bmatrix} A_1 \\ A_2 \end{bmatrix}_{\pm} = \begin{bmatrix} 1 \\ \mp 1 \end{bmatrix},$$

namely we get the known result that the resonant modes split to a lower frequency even mode and a higher frequency odd mode.

Assume now that at time $t = 0$ the source object 1 has finite energy $|a_1(0)|^2$, while the device object has $|a_2(0)|^2 = 0$. Since the objects are coupled, energy will be transferred from 1 to 2. With these initial conditions, Eqs.(1) can be solved, predicting the evolution of the device field-amplitude to be

$$\frac{a_2(t)}{|a_1(0)|} = \frac{2\kappa}{\delta_E}\sin\left(\frac{\delta_E t}{2}\right) e^{-\frac{\Gamma_1+\Gamma_2}{2}t} e^{-i\frac{\omega_1+\omega_2}{2}t} \tag{3}$$

InductEV, Inc.
Exhibit 1025
Page 642

The energy-transfer efficiency will be $\eta_E \equiv |a_2(t)|^2/|a_1(0)|^2$. The ratio of energy converted to loss due to a specific loss mechanism in resonators 1 and 2, with respective loss rates $\Gamma_{1,\text{loss}}$ and $\Gamma_{2,\text{loss}}$ will be $\eta_{loss,E} = \int_0^t d\tau\left[2\Gamma_{1,\text{loss}}|a_1(\tau)|^2 + 2\Gamma_{2,\text{loss}}|a_2(\tau)|^2\right]/|a_1(0)|^2$. Note that, at exact resonance $\omega_1 = \omega_2 = \omega_A$ (an optimal condition), Eq.(3) can be written as

$$\frac{a_2(T)}{|a_1(0)|} = \frac{\sin\left(\sqrt{1-\Delta^2}T\right)}{\sqrt{1-\Delta^2}} e^{-T/U} e^{-i\omega_A t} \tag{4}$$

where $\equiv \kappa t$, $\Delta^{-1} = 2\kappa/(\Gamma_2 - \Gamma_1)$ and $U = 2\kappa/(\Gamma_1 + \Gamma_2)$.

In some examples, the system designer can adjust the duration of the coupling t at will. In some examples, the duration t can be adjusted to maximize the device energy (and thus efficiency η_E). Then, it can be inferred from Eq.(4) that η_E is maximized for

$$T_* = \frac{\tan^{-1}\left(U\sqrt{1-\Delta^2}\right)}{\sqrt{1-\Delta^2}} \tag{5}$$

resulting in an optimal energy-transfer efficiency

$$\eta_{E^*} \equiv \eta_E(T_*) = \frac{U^2}{1+U^2\left(1-\Delta^2\right)} \exp\left(-\frac{2\tan^{-1}\left(U\sqrt{1-\Delta^2}\right)}{U\sqrt{1-\Delta^2}}\right). \tag{6a}$$

which is a monotonically increasing function of the coupling-to-loss ratio $U = 2\kappa/(\Gamma_1 + \Gamma_2)$ and tends to unity when $U \gg 1 \Longrightarrow |\Delta|^{-1} \gg 1$. Therefore, the energy transfer is nearly perfect, when the coupling rate is much faster than all loss rates ($\kappa/\Gamma_{1,2} \gg 1$). In Fig.2(c) we show the optimal energy-transfer efficiency when $\Gamma_1 = \Gamma_2 = \Gamma_A \Leftrightarrow \Delta = 0$:

$$\eta_E(T_*, \Delta = 0) = \frac{U^2}{1+U^2} \exp\left(-\frac{2\tan^{-1}U}{U}\right). \tag{6b}$$

In a real wireless energy-transfer system, the source object can be connected to a power generator (not shown in Fig.1), and the device object can be connected to a power

InductEV, Inc.
Exhibit 1025
Page 643

consuming load (e.g. a resistor, a battery, an actual device, not shown in Fig.1). The generator will supply the energy to the source object, the energy will be transferred wirelessly and non-radiatively from the source object to the device object, and the load will consume the energy from the device object. To incorporate such supply and consumption mechanisms into this temporal scheme, in some examples, one can imagine that the generator is very briefly but very strongly coupled to the source at time $t = 0$ to almost instantaneously provide the energy, and the load is similarly very briefly but very strongly coupled to the device at the optimal time $t = t_*$ to almost instantaneously drain the energy. For a constant powering mechanism, at time $t = t_*$ also the generator can again be coupled to the source to feed a new amount of energy, and this process can be repeated periodically with a period t_*.

1.2 Finite-rate energy-transfer (power-transmission) efficiency

Let the generator be continuously supplying energy to the source object 1 at a rate κ_1 and the load continuously draining energy from the device object 2 at a rate κ_2. Field amplitudes $s_{\pm 1,2}(t)$ are then defined, so that $|s_{\pm 1,2}(t)|^2$ is equal to the power ingoing to (for the + sign) or outgoing from (for the - sign) the object 1, 2 respectively, and the CMT equations are modified to

$$\begin{aligned}
\frac{d}{dt}a_1(t) &= -i(\omega_1 - i\Gamma_1)a_1(t) + i\kappa_{11}a_1(t) + i\kappa_{12}a_2(t) - \kappa_1 a_1(t) + \sqrt{2\kappa_1}s_{+1}(t) \\
\frac{d}{dt}a_2(t) &= -i(\omega_2 - i\Gamma_2)a_2(t) + i\kappa_{21}a_1(t) + i\kappa_{22}a_2(t) - \kappa_2 a_2(t) \\
s_{-1}(t) &= \sqrt{2\kappa_1}a_1(t) - s_{+1}(t) \\
s_{-2}(t) &= \sqrt{2\kappa_2}a_2(t)
\end{aligned} \qquad (7)$$

where again we can set $\omega_{1,2} \to \omega_{1,2} + \kappa_{11,22}$ and $\kappa_{21} = \kappa_{12} \equiv \kappa$.

Assume now that the excitation is at a fixed frequency ω, namely has the form $s_{+1}(t) = S_{+1}e^{-i\omega t}$. Then the response of the linear system will be at the same frequency, namely $a_{1,2}(t) = A_{1,2}e^{-i\omega t}$ and $s_{-1,2}(t) = S_{-1,2}e^{-i\omega t}$. By substituting these into Eqs.(7), using $\delta_{1,2} \equiv \omega - \omega_{1,2}$, and solving the system, we find the field-amplitude transmitted to the load (S_{21} scattering-matrix element)

InductEV, Inc.
Exhibit 1025
Page 644

$$S_{21} \equiv \frac{S_{-2}}{S_{+1}} = \frac{2i\kappa\sqrt{\kappa_1\kappa_2}}{(\Gamma_1+\kappa_1-i\delta_1)(\Gamma_2+\kappa_2-i\delta_2)+\kappa^2} = \frac{2iU\sqrt{U_1U_2}}{(1+U_1-iD_1)(1+U_2-iD_2)+U^2} \quad (8)$$

and the field-amplitude reflected to the generator (S_{11} scattering-matrix element)

$$S_{11} \equiv \frac{S_{-1}}{S_{+1}} = \frac{(\Gamma_1-\kappa_1-i\delta_1)(\Gamma_2+\kappa_2-i\delta_2)+\kappa^2}{(\Gamma_1+\kappa_1-i\delta_1)(\Gamma_2+\kappa_2-i\delta_2)+\kappa^2} = \frac{(1-U_1-iD_1)(1+U_2-iD_2)+U^2}{(1+U_1-iD_1)(1+U_2-iD_2)+U^2} \quad (9)$$

where $D_{1,2} \equiv \delta_{1,2}/\Gamma_{1,2}$, $U_{1,2} \equiv \kappa_{1,2}/\Gamma_{1,2}$ and $U \equiv \kappa/\sqrt{\Gamma_1\Gamma_2}$. Similarly, the scattering-matrix elementsS_{12}, S_{22} are given by interchanging $1 \leftrightarrow 2$ in Eqs.(8),(9) and, as expected from reciprocity, $S_{21} = S_{12}$. The coefficients for power transmission (efficiency) and reflection and loss are respectively $\eta_P \equiv |S_{21}|^2 = |S_{-2}|^2/|S_{+1}|^2$ and $|S_{11}|^2 = |S_{-1}|^2/|S_{+1}|^2$ and $1 - |S_{21}|^2 - |S_{11}|^2 = (2\Gamma_1|A_1|^2 + 2\Gamma_2|A_2|^2)/|S_{+1}|^2$.

In some implementations, the parameters $D_{1,2}$, $U_{1,2}$ can be designed (engineered), since one can adjust the resonant frequencies $\omega_{1,2}$ (compared to the desired operating frequency ω) and the generator/load supply/drain rates $\kappa_{1,2}$. Their choice can target the optimization of some system performance-characteristic of interest.

In some examples, a goal can be to maximize the power transmission (efficiency) $\eta_P \equiv |S_{21}|^2$ of the system, so one would require

$$\eta_P'(D_{1,2}) = \eta_P'(U_{1,2}) = 0 \quad (10)$$

Since S_{21} (from Eq.(8)) is symmetric upon interchanging $1 \leftrightarrow 2$, the optimal values for $D_{1,2}$ (determined by Eqs.(10)) will be equal, namely $D_1 = D_2 \equiv D_o$, and similarly $U_1 = U_2 \equiv U_o$. Then,

$$S_{21} = \frac{2iUU_o}{(1+U_o-iD_o)^2+U^2} \quad (11)$$

and from the condition $\eta_P'(D_o) = 0$ we get that, for fixed values of U and U_o, the efficiency can be maximized for the following values of the symmetric detuning

InductEV, Inc.
Exhibit 1025
Page 645

$$D_o = \begin{cases} \pm\sqrt{U^2-(1+U_o)^2}, & \text{if } U>1+U_o \\ 0, & \text{if } U\le 1+U_o \end{cases}, \tag{12}$$

which, in the case $U > 1 + U_o$, can be rewritten for the two frequencies at which the efficiency peaks as

$$\omega_\pm = \frac{\omega_1\Gamma_2+\omega_2\Gamma_1}{\Gamma_1+\Gamma_2} \pm \frac{2\sqrt{\Gamma_1\Gamma_2}}{\Gamma_1+\Gamma_2}\sqrt{\kappa^2-(\Gamma_1+\kappa_1)(\Gamma_2+\kappa_2)}, \tag{13}$$

whose splitting we denote as $\delta_P \equiv \bar{\omega}_+ - \bar{\omega}_-$. Note that, at exact resonance $\omega_1 = \omega_2$, and for $\Gamma_1 = \Gamma_2 \equiv \Gamma_o$ and $\kappa_1 = \kappa_2 \equiv \kappa_o$, we get $\delta_P = 2\sqrt{\kappa^2 - (\Gamma_o + \kappa_o)^2} < \delta_E$, namely the transmission-peak splitting is smaller than the normal-mode splitting. Then, by substituting D_o into η_P from Eq.(12), from the condition $\eta_P'(U_o) = 0$ we get that, for fixed value of U, the efficiency can be maximized for

$$U_{o^*} = \sqrt{1+U^2} \quad \overset{\text{Eq(12)}}{\Rightarrow} \quad D_{o^*} = 0 \tag{14}$$

which is known as 'critical coupling' condition, whereas for $U_o < U_{o*}$ the system is called 'undercoupled' and for $U_o > U_{o*}$ it is called 'overcoupled'. The dependence of the efficiency on the frequency detuning D_o for different values of U_o (including the 'critical-coupling' condition) are shown in Fig. 2(a,b). The overall optimal power efficiency using Eqs.(14) is

$$\eta_{P^*} \equiv \eta_P(D_{o^*}, U_{o^*}) = \frac{U_{o^*}-1}{U_{o^*}+1} = \left(\frac{U}{1+\sqrt{1+U^2}}\right)^2, \tag{15}$$

which is again only a function of the coupling-to-loss ratio $U = \kappa/\sqrt{\Gamma_1\Gamma_2}$ and tends to unity when $U \gg 1$, as depicted in Fig. 2(c).

In some examples, a goal can be to minimize the power reflection at the side of the generator $|S_{11}|^2$ and the load $|S_{22}|^2$, so one would then need

$$S_{11,22} = 0 \Rightarrow (1 \mp U_1 - iD_1)(1 \pm U_2 - iD_2) + U^2 = 0, \tag{16}$$

InductEV, Inc.
Exhibit 1025
Page 646

The equations above present 'impedance matching' conditions. Again, the set of these conditions is symmetric upon interchanging $1 \leftrightarrow 2$, so, by substituting $D_1 = D_2 \equiv D_o$ and $U_1 = U_2 \equiv U_o$ into Eqs.(16), we get

$$(1 - iD_o)^2 - U_o^2 + U^2 = 0, \tag{17}$$

from which we easily find that the values of D_o and U_o that cancel all reflections are again exactly those in Eqs.(14).

It can be seen that, the two goals and their associated sets of conditions (Eqs.(10) and Eqs.(16)) result in the same optimized values of the intra-source and intra-device parameters $D_{1,2}$, $U_{1,2}$. Note that for a lossless system this would be an immediate consequence of power conservation (Hermiticity of the scattering matrix), but this is not apparent for a lossy system.

Accordingly, for any temporal energy-transfer scheme, once the parameters specific only to the source or to the device (such as their resonant frequencies and their excitation or loading rates respectively) have been optimally designed, the efficiency monotonically increases with the ratio of the source-device coupling-rate to their loss rates. Using the definition of a resonance quality factor $Q = \omega/2\Gamma$ and defining by analogy the coupling factor $k \equiv 1/Q_\kappa \equiv 2\kappa/\sqrt{\omega_1\omega_2}$, it is therefore exactly this ratio

$$U = \frac{\kappa}{\sqrt{\Gamma_1\Gamma_2}} = k\sqrt{Q_1Q_2} \tag{18}$$

that has been set as a figure-of-merit for any system under consideration for wireless energy-transfer, along with the distance over which this ratio can be achieved (clearly, U will be a decreasing function of distance). The operating regime $U > 1$ is sometimes called 'strong-coupling' regime and is a sufficient condition for efficient energy-transfer. In particular, for $U > 1$ we get, from Eq.(15), $\eta_{P*} > 17\%$, large enough for many practical applications. Note that in some applications, U>0.1 may be sufficient. In applications where it is impossible or impractical to run wires to supply power to a device, U<0.1 may be considered sufficient. One skilled in the art will recognize that the sufficient U is application and specification dependent. The figure-of-merit U may be

InductEV, Inc.
Exhibit 1025
Page 647

called the strong-coupling factor. We will further show how to design systems with a large strong-coupling factor.

To achieve a large strong-coupling factor U, in some examples, the energy-transfer application preferably uses resonant modes of high quality factors Q, corresponding to low (i.e. slow) intrinsic-loss rates Γ. This condition can be satisfied by designing resonant modes where all loss mechanisms, typically radiation and absorption, are sufficiently suppressed.

This suggests that the coupling be implemented using, not the lossy radiative far-field, which should rather be suppressed, but the evanescent (non-lossy) stationary near-field. To implement an energy-transfer scheme, usually more appropriate are finite objects, namely ones that are topologically surrounded everywhere by air, into where the near field extends to achieve the coupling. Objects of finite extent do not generally support electromagnetic states that are exponentially decaying in *all* directions in air away from the objects, since Maxwell's Equations in free space imply that $\mathbf{k}^2=\omega^2/c^2$, where $\mathbf{k}$ is the wave vector, ω the angular frequency, and c the speed of light, because of which one can show that such finite objects cannot support states of infinite Q, rather there always is some amount of radiation. However, very long-lived (so-called "high-Q") states can be found, whose tails display the needed exponential or exponential-like decay away from the resonant object over long enough distances before they turn oscillatory (radiative). The limiting surface, where this change in the field behavior happens, is called the "radiation caustic", and, for the wireless energy-transfer scheme to be based on the near field rather than the far/radiation field, the distance between the coupled objects must be such that one lies within the radiation caustic of the other. One typical way of achieving a high radiation-Q (Q_{rad}) is to design subwavelength resonant objects. When the size of an object is much smaller than the wavelength of radiation in free space, its electromagnetic field couples to radiation very weakly. Since the extent of the near-field into the area surrounding a finite-sized resonant object is set typically by the wavelength, in some examples, resonant objects of subwavelength size have significantly longer evanescent field-tails. In other words, the radiation caustic is pushed far away from the

InductEV, Inc.
Exhibit 1025
Page 648

object, so the electromagnetic mode enters the radiative regime only with a small amplitude.

Moreover, most realistic materials exhibit some nonzero amount of absorption, which can be frequency dependent, and thus cannot support states of infinite Q, rather there always is some amount of absorption. However, very long-lived ("high-Q") states can be found, where electromagnetic modal energy is only weakly dissipated. Some typical ways of achieving a high absorption-Q (Q_{abs}) is to use materials which exhibit very small absorption at the resonant frequency and/or to shape the field to be localized more inside the least lossy materials.

Furthermore, to achieve a large strong-coupling factor U, in some examples, the energy-transfer application may use systems that achieve a high coupling factor k, corresponding to strong (i.e. fast) coupling rate κ, over distances larger than the characteristic sizes of the objects.

Since finite-sized subwavelength resonant objects can often be designed to have high Q, as was discussed above and will be seen in examples later on, such objects may typically be chosen for the resonant device-object. In these cases, the electromagnetic field is, in some examples, of a quasi-static nature and the distance, up to which sufficient coupling can be achieved, is dictated by the decay-law of this quasi-static field.

Note that in some examples, the resonant source-object may be immobile and thus less restricted in its allowed geometry and size. It can be therefore chosen to be large enough that the near-field extent is not limited by the wavelength, and can thus have nearly infinite radiation-Q. Some objects of nearly infinite extent, such as dielectric waveguides, can support guided modes, whose evanescent tails are decaying exponentially in the direction away from the object, slowly if tuned close to cutoff, therefore a good coupling can also be achieved over distances quite a few times larger than a characteristic size of the source- and/or device-object.

2 'Strongly-coupled' resonances at mid-range distances for realistic systems

In the following, examples of systems suitable for energy transfer of the type described above are described. We will demonstrate how to compute the CMT parameters $\omega_{1,2}$, $Q_{1,2}$ and k described above and how to choose or design these

InductEV, Inc.
Exhibit 1025
Page 649

parameters for particular examples in order to produce a desirable figure-of-merit $U = \kappa/\sqrt{\Gamma_1\Gamma_2} = k\sqrt{Q_1Q_2}$ at a desired distance D. In some examples, this figure-of-merit is maximized when $\omega_{1,2}$ are tuned close to a particular angular frequency ω_U.

2.1 Self-resonant conducting coils

In some examples, one or more of the resonant objects are self-resonant conducting coils. Referring to Fig. 3, a conducting wire of length, l, and cross-sectional radius, a, is wound into a helical coil of radius, r, and height, h, (namely with $N = \sqrt{l^2 - h^2}/2\pi r$ number of turns), surrounded by air. As described below, the wire has distributed inductance and distributed capacitance, and therefore it supports a resonant mode of angular frequency ω. The nature of the resonance lies in the periodic exchange of energy from the electric field within the capacitance of the coil, due to the charge distribution $\rho(\mathbf{x})$ across it, to the magnetic field in free space, due to the current distribution $\mathbf{j}(\mathbf{x})$ in the wire. In particular, the charge conservation equation $\nabla \cdot \mathbf{j} = i\omega\rho$ implies that: (i) this periodic exchange is accompanied by a $\pi/2$ phase-shift between the current and the charge density profiles, namely the energy W contained in the coil is at certain points in time completely due to the current and at other points in time completely due to the charge, and (ii) if $\rho_l(x)$ and $I(x)$ are respectively the linear charge and current densities in the wire, where x runs along the wire, $q_o = \frac{1}{2}\int dx|\rho_l(x)|$ is the maximum amount of positive charge accumulated in one side of the coil (where an equal amount of negative charge always also accumulates in the other side to make the system neutral) and $I_o = \max\{|I(x)|\}$ is the maximum positive value of the linear current distribution, then $I_o = \omega q_o$. Then, one can define an effective total inductance L and an effective total capacitance C of the coil through the amount of energy W inside its resonant mode:

InductEV, Inc.
Exhibit 1025
Page 650

$$W \equiv \frac{1}{2} I_o^2 L \Rightarrow L = \frac{\mu_o}{4\pi I_o^2} \iint d\mathbf{x} d\mathbf{x}' \frac{\mathbf{j}(\mathbf{x}) \cdot \mathbf{j}(\mathbf{x}')}{|\mathbf{x} - \mathbf{x}'|}, \tag{19}$$

$$W \equiv \frac{1}{2} q_o^2 \frac{1}{C} \Rightarrow \frac{1}{C} = \frac{1}{4\pi\varepsilon_o q_o^2} \iint d\mathbf{x} d\mathbf{x}' \frac{\rho(\mathbf{x})\rho(\mathbf{x}')}{|\mathbf{x} - \mathbf{x}'|}, \tag{20}$$

where μ_o and ε_o are the magnetic permeability and electric permittivity of free space.

With these definitions, the resonant angular frequency and the effective impedance can be given by the formulas $\omega = 1/\sqrt{LC}$ and $Z = \sqrt{L/C}$ respectively.

Losses in this resonant system consist of ohmic (material absorption) loss inside the wire and radiative loss into free space. One can again define a total absorption resistance R_{abs} from the amount of power absorbed inside the wire and a total radiation resistance R_{rad} from the amount of power radiated due to electric- and magnetic-dipole radiation:

$$P_{abs} \equiv \frac{1}{2} I_o^2 R_{abs} \Rightarrow R_{abs} \approx \zeta_c \frac{l}{2\pi a} \cdot \frac{I_{rms}^2}{I_o^2} \tag{21}$$

$$P_{rad} \equiv \frac{1}{2} I_o^2 R_{rad} \Rightarrow R_{rad} \approx \frac{\zeta_o}{6\pi} \left[\left(\frac{\omega |\mathbf{p}|}{c} \right)^2 + \left(\frac{\omega \sqrt{|\mathbf{m}|}}{c} \right)^4 \right], \tag{22}$$

where $c = 1/\sqrt{\mu_o \varepsilon_o}$ and $\zeta_o = \sqrt{\mu_o / \varepsilon_o}$ are the light velocity and light impedance in free space, the impedance ζ_c is $\zeta_c = 1/\sigma\delta = \sqrt{\mu_o \omega / 2\sigma}$ with σ the conductivity of the conductor and δ the skin depth at the frequency ω, $I_{rms}^2 = \frac{1}{l} \int dx |I(x)|^2$, $\mathbf{p} = \int dx\, \mathbf{r} \rho_l(x)$ is the electric-dipole moment of the coil and $\mathbf{m} = \frac{1}{2} \int dx\, \mathbf{r} \times \mathbf{j}(x)$ is the magnetic-dipole moment of the coil. For the radiation resistance formula Eq.(22), the assumption of operation in the quasi-static regime ($h, r \ll \lambda = 2\pi c/\omega$) has been used, which is the desired regime of a subwavelength resonance. With these definitions, the absorption and radiation quality factors of the resonance may be given by $Q_{abs} = Z/R_{abs}$ and $Q_{rad} = Z/R_{rad}$ respectively.

InductEV, Inc.
Exhibit 1025
Page 651

From Eq.(19)-(22) it follows that to determine the resonance parameters one simply needs to know the current distribution $\mathbf{j}$ in the resonant coil. Solving Maxwell's equations to rigorously find the current distribution of the resonant electromagnetic eigenmode of a conducting-wire coil is more involved than, for example, of a standard LC circuit, and we can find no exact solutions in the literature for coils of finite length, making an exact solution difficult. One could in principle write down an elaborate transmission-line-like model, and solve it by brute force. We instead present a model that is (as described below) in good agreement (~5%) with experiment. Observing that the finite extent of the conductor forming each coil imposes the boundary condition that the current has to be zero at the ends of the coil, since no current can leave the wire, we assume that the resonant mode of each coil is well approximated by a sinusoidal current profile along the length of the conducting wire. We shall be interested in the lowest mode, so if we denote by x the coordinate along the conductor, such that it runs from $-l/2$ to $+l/2$, then the current amplitude profile would have the form $I(x)=I_o\cos(\pi x/l)$, where we have assumed that the current does not vary significantly along the wire circumference for a particular x, a valid assumption provided $a \ll r$. It immediately follows from the continuity equation for charge that the linear charge density profile should be of the form $\rho_l(x)=\rho_o\sin(\pi x/l)$, and thus $q_o=\int_0^{l/2}dx\rho_o\left|\sin(\pi x/l)\right|=\rho_o l/\pi$. Using these sinusoidal profiles we find the so-called "self-inductance" L_s and "self-capacitance" C_s of the coil by computing numerically the integrals Eq.(19) and (20); the associated frequency and effective impedance are ω_s and Z_s respectively. The "self-resistances" R_s are given analytically by Eq.(21) and (22) using $I_{rms}^2=\frac{1}{l}\int_{-l/2}^{l/2}dx\left|I_o\cos(\pi x/l)\right|^2=\frac{1}{2}I_o^2$, $|\mathbf{p}|=q_o\sqrt{\left(\frac{2}{\pi}h\right)^2+\left(\frac{4N\cos(\pi N)}{(4N^2-1)\pi}r\right)^2}$ and $|\mathbf{m}|=I_o\sqrt{\left(\frac{2}{\pi}N\pi r^2\right)^2+\left(\frac{\cos(\pi N)(12N^2-1)-\sin(\pi N)\pi N(4N^2-1)}{(16N^4-8N^2+1)\pi}hr\right)^2}$, and therefore the associated Q_s factors can be calculated.

InductEV, Inc.
Exhibit 1025
Page 652

The results for two examples of resonant coils with subwavelength modes of $\lambda_s / r \geq 70$ (i.e. those highly suitable for near-field coupling and well within the quasi-static limit) are presented in Table 1. Numerical results are shown for the wavelength and absorption, radiation and total loss rates, for the two different cases of subwavelength-coil resonant modes. Note that, for conducting material, copper (σ=5.998•10^-7 S/m) was used. It can be seen that expected quality factors at microwave frequencies are $Q_{s,abs} \geq 1000$ and $Q_{s,rad} \geq 5000$.

Table 1

single coil	λ_s / r	f (MHz)	$Q_{s,rad}$	$Q_{s,abs}$	Q_s
r=30cm, h=20cm, a=1cm, N=4	74.7	13.39	4164	8170	2758
r=10cm, h=3cm, a=2mm, N=6	140	21.38	43919	3968	3639

Referring to Fig. 4, in some examples, energy is transferred between two self-resonant conducting-wire coils. The electric and magnetic fields are used to couple the different resonant conducting-wire coils at a distance D between their centers. Usually, the electric coupling highly dominates over the magnetic coupling in the system under consideration for coils with $h \gg 2r$ and, oppositely, the magnetic coupling highly dominates over the electric coupling for coils with $h \ll 2r$. Defining the charge and current distributions of two coils 1,2 respectively as $\rho_{1,2}(\mathbf{x})$ and $\mathbf{j}_{1,2}(\mathbf{x})$, total charges and peak currents respectively as $q_{1,2}$ and $I_{1,2}$, and capacitances and inductances respectively as $C_{1,2}$ and $L_{1,2}$, which are the analogs of $\rho(\mathbf{x})$, $\mathbf{j}(\mathbf{x})$, q_o, I_o, C and I for the single-coil case and are therefore well defined, we can *define* their mutual capacitance and inductance through the total energy:

$$W \equiv W_1 + W_2 + \frac{1}{2}\left(q_1^* q_2 + q_2^* q_1\right) / M_C + \frac{1}{2}\left(I_1^* I_2 + I_2^* I_1\right) M_L$$

InductEV, Inc.
Exhibit 1025
Page 653

$$\Rightarrow 1/M_C = \frac{1}{4\pi\varepsilon_o q_1 q_2}\iint d\mathbf{x}d\mathbf{x}'\frac{\rho_1(\mathbf{x})\rho_2(\mathbf{x}')}{|\mathbf{x}-\mathbf{x}'|}u, \quad M_L = \frac{\mu_o}{4\pi I_1 I_2}\iint d\mathbf{x}d\mathbf{x}'\frac{\mathbf{j}_1(\mathbf{x})\cdot\mathbf{j}_2(\mathbf{x}')}{|\mathbf{x}-\mathbf{x}'|}u, \quad (23)$$

where $W_1 = \frac{1}{2}q_1^2/C_1 = \frac{1}{2}I_1^2 L_1$, $W_2 = \frac{1}{2}q_2^2/C_2 = \frac{1}{2}I_2^2 L_2$ and the retardation factor of $u = \exp\left(i\omega|\mathbf{x}-\mathbf{x}'|/c\right)$ inside the integral can been ignored in the quasi-static regime $D \ll \lambda$ of interest, where each coil is within the near field of the other. With this definition, the coupling factor is given by $k = \sqrt{C_1 C_2}/M_C + M_L/\sqrt{L_1 L_2}$.

Therefore, to calculate the coupling rate between two self-resonant coils, again the current profiles are needed and, by using again the assumed sinusoidal current profiles, we compute numerically from Eq.(23) the mutual capacitance $M_{C,s}$ and inductance $M_{L,s}$ between two self-resonant coils at a distance D between their centers, and thus $k = 1/Q_\kappa$ is also determined.

Table 2

pair of coils	D/r	Q	$Q_\kappa = 1/k$	U
r=30cm, h=20cm, a=1cm, N=4 $\lambda/r \approx 75$ $Q_s^{abs} \approx 8170$, $Q_s^{rad} \approx 4164$	3	2758	38.9	70.9
	5	2758	139.4	19.8
	7	2758	333.0	8.3
	10	2758	818.9	3.4
r=10cm, h=3cm, a=2mm, N=6 $\lambda/r \approx 140$ $Q_s^{abs} \approx 3968$, $Q_s^{rad} \approx 43919$	3	3639	61.4	59.3
	5	3639	232.5	15.7
	7	3639	587.5	6.2
	10	3639	1580	2.3

Referring to Table 2, relevant parameters are shown for exemplary examples featuring pairs or identical self resonant coils. Numerical results are presented for the average wavelength and loss rates of the two normal modes (individual values not shown), and also the coupling rate and figure-of-merit as a function of the coupling distance D, for the two cases of modes presented in Table1. It can be seen that for

InductEV, Inc.
Exhibit 1025
Page 654

medium distances $D/r = 10-3$ the expected coupling-to-loss ratios are in the range $U \sim 2-70$.

2.1.1 Experimental Results

An experimental realization of an example of the above described system for wireless energy transfer consists of two self-resonant coils, one of which (the source coil) is coupled inductively to an oscillating circuit, and the second (the device coil) is coupled inductively to a resistive load, as shown schematically in Fig. 5. Referring to Fig. 5, A is a single copper loop of radius 25cm that is part of the driving circuit, which outputs a sine wave with frequency 9.9MHz. s and d are respectively the source and device coils referred to in the text. B is a loop of wire attached to the load ("light-bulb"). The various κ's represent direct couplings between the objects. The angle between coil d and the loop A is adjusted so that their direct coupling is zero, while coils s and d are aligned coaxially. The direct coupling between B and A and between B and s is negligible.

The parameters for the two identical helical coils built for the experimental validation of the power transfer scheme were $h = 20\,\text{cm}$, $a = 3\,\text{mm}$, $r = 30$ cm and $N = 5.25$. Both coils are made of copper. Due to imperfections in the construction, the spacing between loops of the helix is not uniform, and we have encapsulated the uncertainty about their uniformity by attributing a 10% (2 cm) uncertainty to h. The expected resonant frequency given these dimensions is $f_0 = 10.56 \pm 0.3\,\text{MHz}$, which is approximately 5% off from the measured resonance at around 9.90 MHz.

The theoretical Q for the loops is estimated to be ~ 2500 (assuming perfect copper of resistivity $\rho = 1/\sigma = 1.7\times10^{-8}\,\Omega\,\text{m}$) but the measured value is 950 ± 50. We believe the discrepancy is mostly due to the effect of the layer of poorly conducting copper oxide on the surface of the copper wire, to which the current is confined by the short skin depth ($\sim 20\mu\,\text{m}$) at this frequency. We have therefore used the experimentally observed Q (and $\Gamma_1 = \Gamma_2 = \Gamma = \omega/(2Q)$ derived from it) in all subsequent computations.

The coupling coefficient κ can be found experimentally by placing the two self-resonant coils (fine-tuned, by slightly adjusting h, to the same resonant frequency when isolated) a distance D apart and measuring the splitting in the frequencies of the two

InductEV, Inc.
Exhibit 1025
Page 655

resonant modes in the transmission spectrum. According to Eq.(13) derived by coupled-mode theory, the splitting in the transmission spectrum should be $\delta_p = 2\sqrt{\kappa^2 - \Gamma^2}$, when $\kappa_{A,B}$ are kept very small by keeping A and B at a relatively large distance. The comparison between experimental and theoretical results as a function of distance when the two the coils are aligned coaxially is shown in Fig. 6.

Fig. 7 shows a comparison of experimental and theoretical values for the strong-coupling factor $U = \kappa/\Gamma$ as a function of the separation between the two coils. The theory values are obtained by using the theoretically obtained κ and the experimentally measured Γ. The shaded area represents the spread in the theoretical U due to the $\sim 5\%$ uncertainty in Q. As noted above, the maximum theoretical efficiency depends only on the parameter U, which is plotted as a function of distance in Fig. 7. U is greater than 1 even for $D = 2.4\,\text{m}$ (eight times the radius of the coils), thus the sytem is in the strongly-coupled regime throughout the entire range of distances probed.

The power-generator circuit was a standard Colpitts oscillator coupled inductively to the source coil by means of a single loop of copper wire 25cm in radius (see Fig. 5). The load consisted of a previously calibrated light-bulb, and was attached to its own loop of insulated wire, which was in turn placed in proximity of the device coil and inductively coupled to it. Thus, by varying the distance between the light-bulb and the device coil, the parameter $U_B = \kappa_B/\Gamma$ was adjusted so that it matched its optimal value, given theoretically by Eq.(14) as $U_{B^*} = \sqrt{1+U^2}$. Because of its inductive nature, the loop connected to the light-bulb added a small reactive component to κ_B which was compensated for by slightly retuning the coil. The work extracted was determined by adjusting the power going into the Colpitts oscillator until the light-bulb at the load was at its full nominal brightness.

In order to isolate the efficiency of the transfer taking place specifically between the source coil and the load, we measured the current at the mid-point of each of the self-resonant coils with a current-probe (which was not found to lower the Q of the coils noticeably.) This gave a measurement of the current parameters I_1 and I_2 defined above.

InductEV, Inc.
Exhibit 1025
Page 656

The power dissipated in each coil was then computed from $P_{1,2} = \Gamma L |I_{1,2}|^2$, and the efficiency was directly obtained from $\eta = P_B / (P_1 + P_2 + P_B)$. To ensure that the experimental setup was well described by a two-object coupled-mode theory model, we positioned the device coil such that its direct coupling to the copper loop attached to the Colpitts oscillator was zero. The experimental results are shown in Fig. 8, along with the theoretical prediction for maximum efficiency, given by Eq.(15).

Using this example, we were able to transmit significant amounts of power using this setup from the source coil to the device coil, fully lighting up a 60W light-bulb from distances more than 2m away, for example. As an additional test, we also measured the total power going into the driving circuit. The efficiency of the wireless power-transmission itself was hard to estimate in this way, however, as the efficiency of the Colpitts oscillator itself is not precisely known, although it is expected to be far from 100%. Nevertheless, this gave an overly conservative lower bound on the efficiency. When transmitting 60W to the load over a distance of 2m, for example, the power flowing into the driving circuit was 400W. This yields an overall wall-to-load efficiency of $\sim 15\%$, which is reasonable given the expected $\sim 40\%$ efficiency for the wireless power transmission at that distance and the low efficiency of the driving circuit.

From the theoretical treatment above, we see that in typical examples it is important that the coils be on resonance for the power transmission to be practical. We found experimentally that the power transmitted to the load dropped sharply as one of the coils was detuned from resonance. For a fractional detuning $\Delta f/f_0$ of a few times the inverse loaded Q, the induced current in the device coil was indistinguishable from noise.

The power transmission was not found to be visibly affected as humans and various everyday objects, such as metallic and wooden furniture, as well as electronic devices large and small, were placed between the two coils, even when they drastically obstructed the line of sight between source and device. External objects were found to have an effect only when they were closer than 10cm from either one of the coils. While some materials (such as aluminum foil, styrofoam and humans) mostly just shifted the

InductEV, Inc.
Exhibit 1025
Page 657

resonant frequency, which could in principle be easily corrected with a feedback circuit of the type described earlier, others (cardboard, wood, and PVC) lowered Q when placed closer than a few centimeters from the coil, thereby lowering the efficiency of the transfer.

This method of power transmission is believed safe for humans. When transmitting 60W (more than enough to power a laptop computer) across 2m, we estimated that the magnitude of the magnetic field generated is much weaker than the Earth's magnetic field for all distances except for less than about 1cm away from the wires in the coil, an indication of the safety of the scheme even after long-term use. The power radiated for these parameters was ~ 5 W, which is roughly an order of magnitude higher than cell phones but could be drastically reduced, as discussed below.

Although the two coils are currently of identical dimensions, it is possible to make the device coil small enough to fit into portable devices without decreasing the efficiency. One could, for instance, maintain the product of the characteristic sizes of the source and device coils constant.

These experiments demonstrated experimentally a system for power transmission over medium range distances, and found that the experimental results match theory well in multiple independent and mutually consistent tests.

The efficiency of the scheme and the distances covered can be improved by silver-plating the coils, which may increase their Q, or by working with more elaborate geometries for the resonant objects. Nevertheless, the performance characteristics of the system presented here are already at levels where they could be useful in practical applications.

2.2 Capacitively-loaded conducting loops or coils

In some examples, one or more of the resonant objects are capacitively-loaded conducting loops or coils. Referring to Fig. 9 a helical coil with N turns of conducting wire, as described above, is connected to a pair of conducting parallel plates of area A spaced by distance d via a dielectric material of relative permittivity ε, and everything is surrounded by air (as shown, $N=1$ and $h=0$). The plates have a capacitance

InductEV, Inc.
Exhibit 1025
Page 658

$C_p = \varepsilon_o \varepsilon A / d$, which is added to the distributed capacitance of the coil and thus modifies its resonance. Note however, that the presence of the loading capacitor may modify the current distribution inside the wire and therefore the total effective inductance L and total effective capacitance C of the coil may be different respectively from L_s and C_s, which are calculated for a self-resonant coil of the same geometry using a sinusoidal current profile. Since some charge may accumulate at the plates of the external loading capacitor, the charge distribution ρ inside the wire may be reduced, so $C < C_s$, and thus, from the charge conservation equation, the current distribution $\mathbf{j}$ may flatten out, so $L > L_s$. The resonant frequency for this system may be $\omega = 1/\sqrt{L(C + C_p)} < \omega_s = 1/\sqrt{L_s C_s}$, and $I(x) \to I_o \cos(\pi x / l) \Rightarrow C \to C_s \Rightarrow \omega \to \omega_s$, as $C_p \to 0$.

In general, the desired CMT parameters can be found for this system, but again a very complicated solution of Maxwell's Equations is required. Instead, we will analyze only a special case, where a reasonable guess for the current distribution can be made. When $C_p \gg C_s > C$, then $\omega \approx 1/\sqrt{LC_p} \ll \omega_s$ and $Z \approx \sqrt{L/C_p} \ll Z_s$, while all the charge is on the plates of the loading capacitor and thus the current distribution is constant along the wire. This allows us now to compute numerically L from Eq.(19). In the case $h = 0$ and N integer, the integral in Eq.(19) can actually be computed analytically, giving the formula $L = \mu_o r\left[\ln(8r/a) - 2\right]N^2$. Explicit analytical formulas are again available for R from Eq.(21) and (22), since $I_{rms} = I_o$, $|\mathbf{p}| \approx 0$ and $|\mathbf{m}| = I_o N \pi r^2$ (namely only the magnetic-dipole term is contributing to radiation), so we can determine also $Q_{abs} = \omega L / R_{abs}$ and $Q_{rad} = \omega L / R_{rad}$. At the end of the calculations, the validity of the assumption of constant current profile is confirmed by checking that indeed the condition $C_p \gg C_s \Leftrightarrow \omega \ll \omega_s$ is satisfied. To satisfy this condition, one could use a large external capacitance, however, this would usually shift the operational frequency lower than the optimal frequency, which we will determine

InductEV, Inc.
Exhibit 1025
Page 659

shortly; instead, in typical examples, one often prefers coils with very small self-capacitance C_s to begin with, which usually holds, for the types of coils under consideration, when $N=1$, so that the self-capacitance comes from the charge distribution across the single turn, which is almost always very small, or when $N>1$ and $h \gg 2Na$, so that the dominant self-capacitance comes from the charge distribution across adjacent turns, which is small if the separation between adjacent turns is large.

The external loading capacitance C_p provides the freedom to tune the resonant frequency (for example by tuning A or d). Then, for the particular simple case $h=0$, for which we have analytical formulas, the total $Q=\omega L/(R_{abs}+R_{rad})$ becomes highest at the optimal frequency

$$\omega_Q = \left[\frac{c^4}{\pi}\sqrt{\frac{\varepsilon_o}{2\sigma}}\cdot\frac{1}{aNr^3}\right]^{2/7} \tag{24}$$

reaching the value

$$Q_{\max} = \frac{6}{7\pi}\left(2\pi^2\eta_o\frac{\sigma a^2N^2}{r}\right)^{3/7}\cdot\left[\ln\left(\frac{8r}{a}\right)-2\right]. \tag{25}$$

At lower frequencies Q is dominated by ohmic loss and at higher frequencies by radiation. Note, however, that the formulas above are accurate as long as $\omega_Q \ll \omega_s$ and, as explained above, this holds almost always when $N=1$, and is usually less accurate when $N>1$, since $h=0$ usually implies a large self-capacitance. A coil with large h can be used, if the self-capacitance needs to be reduced compared to the external capacitance, but then the formulas for L and ω_Q, $Q_{\max}$ are again less accurate. Similar qualitative behavior is expected, but a more complicated theoretical model is needed for making quantitative predictions in that case.

The results of the above analysis for two examples of subwavelength modes of $\lambda/r \geq 70$ (namely highly suitable for near-field coupling and well within the quasi-static limit) of coils with $N=1$ and $h=0$ at the optimal frequency Eq.(24) are presented in Table 3. To confirm the validity of constant-current assumption and the resulting

InductEV, Inc.
Exhibit 1025
Page 660

analytical formulas, mode-solving calculations were also performed using another completely independent method: computational 3D finite-element frequency-domain (FEFD) simulations (which solve Maxwell's Equations in frequency domain exactly apart for spatial discretization) were conducted, in which the boundaries of the conductor were modeled using a complex impedance $\zeta_c = \sqrt{\mu_o \omega / 2\sigma}$ boundary condition, valid as long as $\zeta_c / \zeta_o \ll 1$ ($<10^{-5}$ for copper in the microwave). Table 3 shows Numerical FEFD (and in parentheses analytical) results for the wavelength and absorption, radiation and total loss rates, for two different cases of subwavelength-loop resonant modes. Note that copper was used for the conducting material ($\sigma=5.998 \cdot 10^7 S/m$). Specific parameters of the plot in Fig. 4 are highlighted in bold in the table. The two methods (analytical and computational) are in good agreement and show that, in some examples, the optimal frequency is in the low-MHz microwave range and the expected quality factors are $Q_{abs} \geq 1000$ and $Q_{rad} \geq 10000$.

Table 3

single coil	λ / r	f	Q_{rad}	Q_{abs}	Q
r=30cm, a=2cm ε=10, A=138cm², d=4mm	**111.4 (112.4)**	**8.976 (8.897)**	**29546 (30512)**	**4886 (5117)**	**4193 (4381)**
r=10cm, a=2mm ε=10, A=3.14cm², d=1mm	69.7 (70.4)	43.04 (42.61)	10702 (10727)	1545 (1604)	1350 (1395)

Referring to Fig. 10, in some examples, energy is transferred between two capacitively-loaded coils. For the rate of energy transfer between two capacitively-loaded coils 1 and 2 at distance D between their centers, the mutual inductance M_L can be evaluated numerically from Eq.(23) by using constant current distributions in the case $\omega \ll \omega_s$. In the case $h=0$, the coupling may be only magnetic and again we have an analytical formula, which, in the quasi-static limit $r \ll D \ll \lambda$ and for the relative orientation

InductEV, Inc.
Exhibit 1025
Page 661

shown in Fig. 10, is $M_L \approx \pi\mu_o / 2 \cdot (r_1 r_2)^2 N_1 N_2 / D^3$, which means that $k \propto \left(\sqrt{r_1 r_2} / D\right)^3$ may be independent of the frequency ω and the number of turns N_1, N_2. Consequently, the resultant coupling figure-of-merit of interest is

$$U = k\sqrt{Q_1 Q_2} \approx \left(\frac{\sqrt{r_1 r_2}}{D}\right)^3 \cdot \frac{\pi^2 \eta_o \frac{\sqrt{r_1 r_2}}{\lambda} \cdot N_1 N_2}{\prod_{j=1,2}\left(\sqrt{\frac{\pi\eta_o}{\lambda\sigma}} \cdot \frac{r_j}{a_j} N_j + \frac{8}{3}\pi^5 \eta_o \left(\frac{r_j}{\lambda}\right)^4 N_j^2\right)^{1/2}}, \quad (26)$$

which again is more accurate for $N_1 = N_2 = 1$.

From Eq.(26) it can be seen that the optimal frequency ω_U, where the figure-of-merit is maximized to the value $U_{\max}$, is close to the frequency $\omega_{Q_1 Q_2}$ at which $Q_1 Q_2$ is maximized, since k does not depend much on frequency (at least for the distances $D \ll \lambda$ of interest for which the quasi-static approximation is still valid). Therefore, the optimal frequency $\omega_U \approx \omega_{Q_1 Q_2}$ may be mostly independent of the distance D between the two coils and may lie between the two frequencies ω_{Q_1} and ω_{Q_2} at which the single-coil Q_1 and Q_2 respectively peak. For same coils, this optimal frequency is given by Eq.(24) and then the strong-coupling factor from Eq.(26) becomes

$$U_{\max} = kQ_{\max} \approx \left(\frac{r}{D}\right)^3 \cdot \frac{3}{7}\left(2\pi^2 \eta_o \frac{\sigma a^2 N^2}{r}\right)^{3/7}. \quad (27)$$

In some examples, one can tune the capacitively-loaded conducting loops or coils, so that their angular resonant frequencies are close to ω_U within Γ_U, which is half the angular frequency width for which $U > U_{\max} / 2$.

Referring to Table 4, numerical FEFD and, in parentheses, analytical results based on the above are shown for two systems each composed of a matched pair of the loaded coils described in Table 3. The average wavelength and loss rates are shown along with the coupling rate and coupling to loss ratio figure-of-merit $U = \kappa / \Gamma$ as a function of the coupling distance D, for the two cases. Note that the average numerical Γ_{rad} shown

InductEV, Inc.
Exhibit 1025
Page 662

are slightly different from the single-loop value of Figure 3. Analytical results for Γ_{rad} are not shown but the single-loop value is used. (The specific parameters corresponding to the plot in Fig. 10 are highlighted with bold in the table.) Again we chose $N = 1$ to make the constant-current assumption a good one and computed M_L numerically from Eq.(23). Indeed the accuracy can be confirmed by their agreement with the computational FEFD mode-solver simulations, which give κ through the frequency splitting of the two normal modes of the combined system ($\delta_{\omega} = 2\kappa$ from Eq.(4)). The results show that for medium distances $D/r = 10 - 3$ the expected coupling-to-loss ratios are in the range $U \sim 0.5 - 50$.

Table 4

pair of coils	D/r	Q^{rad}	$Q = \omega/2\Gamma$	$Q_\kappa = \omega/2\kappa$	κ/Γ
r=30cm, a=2cm ε=10, A=138cm², d=4mm $\lambda/r \approx 112$ $Q^{rad} \approx 4886$	3	30729	4216	62.6 (63.7)	67.4 (68.7)
	5	29577	4194	235 (248)	17.8 (17.6)
	7	**29128**	**4185**	**589 (646)**	**7.1 (6.8)**
	10	28833	4177	1539 (1828)	2.7 (2.4)
r=10cm, a=2mm ε=10, A=3.14cm², d=1mm $\lambda/r \approx 70$ $Q^{rad} \approx 1646$	3	10955	1359	85.4 (91.3)	15.9 (15.3)
	5	10740	1351	313 (356)	4.32 (3.92)
	7	10759	1351	754 (925)	1.79 (1.51)
	10	10756	1351	1895 (2617)	0.71 (0.53)

2.2.1 Derivation of optimal power-transmission efficiency

Referring to Fig. 11, to rederive and express Eq.(15) in terms of the parameters which are more directly accessible from particular resonant objects, such as the capacitively-loaded conducting loops, one can consider the following circuit-model of the system, where the inductances L_s, L_d represent the source and device loops respectively, R_s, R_d their respective losses, and C ,C_d are the required corresponding capacitances to achieve for both resonance at frequency ω. A voltage generator V_g is considered to be connected to the source and a load resistance R_l to the device. The mutual inductance is denoted by *M*.

Then from the source circuit at resonance ($\omega L = 1/\omega C$):

InductEV, Inc.
Exhibit 1025
Page 663

$$V_g = I_s R_s - j\omega M I_d \Rightarrow \frac{1}{2} V_g^* I_s = \frac{1}{2}\left|I_s\right|^2 R_s + \frac{1}{2} j\omega M I_d^* I_s, \tag{28}$$

and from the device circuit at resonance ($\omega L_d = 1/\omega C_d$):

$$0 = I_d\left(R_d + R_l\right) - j\omega M I_s \Rightarrow j\omega M I_s = I_d\left(R_d + R_l\right) \tag{29}$$

So by substituting Eq.(29) to Eq.(28) and taking the real part (for time-averaged power) we get:

$$P_g = \mathrm{Re}\left\{\frac{1}{2} V_g^* I_s\right\} = \frac{1}{2}\left|I_s\right|^2 R_s + \frac{1}{2}\left|I_d\right|^2 \left(R_d + R_l\right) = P_s + P_d + P_l, \tag{30}$$

where we identified the power delivered by the generator $P_g = \mathrm{Re}\left\{V_g^* I_s / 2\right.$,the power lost inside the source $P_s = \left|I_s\right|^2 R_s / 2$, the power lost inside the device $P_d = \left|I_d\right|^2 R_d / 2$ and the power delivered to the load $P_l = \left|I_d\right|^2 R_l / 2$. Then, the power transmission efficiency is:

$$\eta_{\mathrm{P}} \equiv \frac{P_l}{P_g} = \frac{R_l}{\left|\frac{I_s}{I_d}\right|^2 R_s + \left(R_d + R_l\right.} \overset{(29)}{=} \frac{R_l}{\frac{\left(R_d + R_l\right)^2}{\left(\omega M\right.^2} R_s + \left(R_d + R_l\right.}. \tag{31}$$

If we now choose the load impedance R_l to optimize the efficiency by $\eta_P'(R_l) = 0$, we get the optimal load impedance

$$\frac{R_{l*}}{R_d} = \sqrt{1 + \frac{\left(\omega M\right)^2}{R_s R_d}} \tag{32}$$

and the maximum possible efficiency

$$\eta_{P*} = \frac{R_{l*}/R_d - 1}{R_{l*}/R_d + 1} = \left[\frac{\omega M / \sqrt{R_s R_d}}{1 + \sqrt{1 + \left(\omega M / \sqrt{R_s R_d}\right)^2}}\right]^2. \tag{33}$$

InductEV, Inc.
Exhibit 1025
Page 664

To check now the correspondence with the CMT model, note that $\kappa_l = R_l / 2L_d$, $\Gamma_d = R_d / 2L_d$, $\Gamma_s = R_s / 2L_s$, and $\kappa \quad \omega M / 2\sqrt{L_s L_d}$, so then $U_l = \kappa_l / \Gamma_d = R_l / R_d$ and $U = \kappa / \sqrt{\Gamma_s \Gamma_d} = \omega M / \sqrt{R_s R_d}$. Therefore, the condition Eq.(32) is identical to the condition Eq.(14) and the optimal efficiency Eq.(33) is identical to the general Eq.(15). Indeed, as the CMT analysis predicted, to get a large efficiency, we need to design a system that has a large strong-coupling factor U.

2.2.2 Optimization of U

The results above can be used to increase or optimize the performance of a wireless energy transfer system, which employs capacitively-loaded coils. For example, from the scaling of Eq.(27) with the different system parameters, one sees that to maximize the system figure-of-merit U, in some examples, one can:

-- Decrease the resistivity of the conducting material. This can be achieved, for example, by using good conductors (such as copper or silver) and/or lowering the temperature. At very low temperatures one could use also superconducting materials to achieve extremely good performance.

-- Increase the wire radius a. In typical examples, this action can be limited by physical size considerations. The purpose of this action is mainly to reduce the resistive losses in the wire by increasing the cross-sectional area through which the electric current is flowing, so one could alternatively use also a Litz wire, or ribbon, or any low AC-resistance structure, instead of a circular wire.

-- For fixed desired distance D of energy transfer, increase the radius of the loop r. In typical examples, this action can be limited by physical size considerations.

-- For fixed desired distance vs. loop-size ratio D/r, decrease the radius of the loop r. In typical examples, this action can be limited by physical size considerations.

-- Increase the number of turns N. (Even though Eq.(27) is expected to be less accurate for $N > 1$, qualitatively it still provides a good indication that we expect an improvement in the coupling-to-loss ratio with increased N.) In typical examples, this

InductEV, Inc.
Exhibit 1025
Page 665

action can be limited by physical size and possible voltage considerations, as will be discussed in following paragraphs.

-- Adjust the alignment and orientation between the two coils. The figure-of-merit is optimized when both cylindrical coils have exactly the same axis of cylindrical symmetry (namely they are "facing" each other). In some examples, particular mutual coil angles and orientations that lead to zero mutual inductance (such as the orientation where the axes of the two coils are perpendicular and the centers of the two coils are on one of the two axes) should be avoided.

-- Finally, note that the height of the coil h is another available design parameter, which can have an impact on the performance similar to that of its radius *r*, and thus the design rules can be similar.

The above analysis technique can be used to design systems with desired parameters. For example, as listed below, the above described techniques can be used to determine the cross sectional radius *a* of the wire used to design a system including two same single-turn loops with a given radius in order to achieve a specific performance in terms of $U = \kappa / \Gamma$ at a given D / r between them, when the loop material is copper (σ=5.998·10^{7}S/m):

$$D / r = 5,\ U \geq 10,\ r = 30cm \Rightarrow a \geq 9mm$$
$$D / r = 5,\ U \geq 10,\ r = 5cm \Rightarrow a \geq 3.7mm$$
$$D / r = 5,\ U \geq 20,\ r = 30cm \Rightarrow a \geq 20mm$$
$$D / r = 5,\ U \geq 20,\ r = 5cm \Rightarrow a \geq 8.3mm$$
$$D / r = 10,\ U \geq 1,\ r = 30cm \Rightarrow a \geq 7mm$$
$$D / r = 10,\ U \geq 1,\ r = 5cm \Rightarrow a \geq 2.8mm$$
$$D / r = 10,\ U \geq 3,\ r = 30cm \Rightarrow a \geq 25mm$$
$$D / r = 10,\ U \geq 3,\ r = 5cm \Rightarrow a \geq 10mm$$

Similar analysis can be done for the case of two dissimilar loops. For example, in some examples, the device under consideration may be identified specifically (e.g. a laptop or a cell phone), so the dimensions of the device object (r_d, h_d, a_d, N_d) may be restricted. However, in some such examples, the restrictions on the source object (r_s, h_s, a_s, N_s) may be much less, since the source can, for example, be placed under the

InductEV, Inc.
Exhibit 1025
Page 666

floor or on the ceiling. In such cases, the desired distance between the source and device may be fixed; in other cases it may be variable. Listed below are examples (simplified to the case $N_s = N_d = 1$ and $h_s = h_d = 0$) of how one can vary the dimensions of the source object to achieve a desired system performance in terms of $U_{sd} = \kappa / \sqrt{\Gamma_s \Gamma_d}$, when the material is again copper (σ=5.998·10^{7}S/m):

$$D = 1.5m,\ U_{sd} \geq 15,\ r_d = 30cm,\ a_d = 6mm \Rightarrow r_s = 1.158m,\ a_s \geq 5mm$$
$$D = 1.5m,\ U_{sd} \geq 30,\ r_d = 30cm,\ a_d = 6mm \Rightarrow r_s = 1.15m,\ a_s \geq 33mm$$
$$D = 1.5m, U_{sd} \geq 1,\ r_d = 5cm,\ a_d = 4mm \Rightarrow r_s = 1.119m,\ a_s \geq 7mm$$
$$D = 1.5m,\ U_{sd} \geq 2,\ r_d = 5cm,\ a_d = 4mm \Rightarrow r_s = 1.119m,\ a_s \geq 52mm$$
$$D = 2m,\ U_{sd} \geq 10,\ r_d = 30cm,\ a_d = 6mm \Rightarrow r_s = 1.518m,\ a_s \geq 7mm$$
$$D = 2m,\ U_{sd} \geq 20,\ r_d = 30cm,\ a_d = 6mm \Rightarrow r_s = 1.514m,\ a_s \geq 50mm$$
$$D = 2m,\ U_{sd} \geq 0.5,\ r_d = 5cm,\ a_d = 4mm \Rightarrow r_s = 1.491m,\ a_s \geq 5mm$$
$$D = 2m,\ U_{sd} \geq 1,\ r_d = 5cm,\ a_d = 4mm \Rightarrow r_s = 1.491m,\ a_s \geq 36mm$$

2.2.3 Optimization of k

As described below, in some examples, the quality factor Q of the resonant objects may be limited from external perturbations and thus varying the coil parameters may not lead to significant improvements in Q. In such cases, one can opt to increase the strong-coupling factor U by increasing the coupling factor k. The coupling does not depend on the frequency and may weakly depend on the number of turns. Therefore, in some examples, one can:

-- Increase the wire radii a_1 and a_2. In typical examples, this action can be limited by physical size considerations.

-- For fixed desired distance D of energy transfer, increase the radii of the coils r_1 and r_2. In typical examples, this action can be limited by physical size considerations.

-- For fixed desired distance vs. coil-sizes ratio $D/\sqrt{r_1 r_2}$, only the weak (logarithmic) dependence of the inductance remains, which suggests that one should decrease the radii of the coils r_1 and r_2. In typical examples, this action can be limited by physical size considerations.

InductEV, Inc.
Exhibit 1025
Page 667

-- Adjust the alignment and orientation between the two coils. In typical examples, the coupling is optimized when both cylindrical coils have exactly the same axis of cylindrical symmetry (namely they are "facing" each other). Particular mutual coil angles and orientations that lead to zero mutual inductance (such as the orientation where the axes of the two coils are perpendicular and the centers of the two coils are on one of the two axes) should obviously be avoided.

-- Finally, note that the heights of the coils h_1 and h_2 are other available design parameters, which can have an impact to the coupling similar to that of their radii r_1 and r_2, and thus the design rules can be similar.

Further practical considerations apart from efficiency, e.g. physical size limitations, will be discussed in detail below.

2.2.4 Optimization of overall system performance

In embodiments, the dimensions of the resonant objects may be determined by the particular application. For example, when the application is powering a laptop or a cell-phone, the device resonant object cannot have dimensions that exceed those of the laptop or cell-phone respectively. For a system of two loops of specified dimensions, in terms of loop radii $r_{s,d}$ and wire radii $a_{s,d}$, the independent parameters left to adjust for the system optimization are: the number of turns $N_{s,d}$, the frequency f, the power-load consumption rate $\kappa_l = R_l / 2L_d$ and the power-generator feeding rate $\kappa_g = R_g / 2L_s$, where R_g is the internal (characteristic) impedance of the generator.

In general, in various examples, the dependent variable that one may want to increase or optimize may be the overall efficiency η. However, other important variables may need to be taken into consideration upon system design. For example, in examples featuring capacitively-loaded coils, the designs can be constrained by, the currents flowing inside the wires $I_{s,d}$ and other components and the voltages across the capacitors $V_{s,d}$. These limitations can be important because for ~*Watt* power applications the values for these parameters can be too large for the wires or the capacitors respectively to handle. Furthermore, the total loaded (by the load) quality factor of the

InductEV, Inc.
Exhibit 1025
Page 668

device $Q_{d[l]} = \omega / 2(\Gamma_d + \Gamma_l) = \omega L_d / (R_d + R_l)$ and the total loaded (by the generator) quality factor of the source $Q_{s[g]} = \omega / 2(\Gamma_s + \Gamma_g) = \omega L_s / (R_s + R_g)$ are quantities that should be preferably small, because to match the source and device resonant frequencies to within their Q's, when those are very large, can be challenging experimentally and more sensitive to slight variations. Lastly, the radiated powers $P_{s,rad}$ and $P_{d,rad}$ may need to be minimized for concerns about far-field interference and safety, even though, in general, for a magnetic, non-radiative scheme they are already typically small. In the following, we examine then the effects of each one of the independent variables on the dependent ones.

We define a new variable wp to express the power-load consumption rate for some particular value of U through $U_l = \kappa_l / \Gamma_d = \sqrt{1 + wp \cdot U^2}$. Then, in some examples, values which may impact the choice of this rate are: $U_l = 1 \Leftrightarrow wp = 0$ to minimize the required energy stored in the source (and therefore I_s and V_s), $U_l = \sqrt{1+U^2} > 1 \Leftrightarrow wp = 1$ to maximize the efficiency, as seen earlier, or $U_l \gg 1 \Leftrightarrow wp \gg 1$ to decrease the required energy stored in the device (and therefore I_d and V_d) and to decrease or minimize $Q_{d[l]}$. Similar is the impact of the choice of the power-generator feeding rate $U_g = \kappa_g / \Gamma_s$, with the roles of the source/device and generator/load reversed.

In some examples, increasing N_s and N_d may increase Q_s and Q_d, and thus U and the efficiency significantly. It also may decrease the currents I_s and I_d, because the inductance of the loops may increase, and thus the energy $W_{s,d} = L_{s,d} |I_{s,d}|^2 / 2$ required for given output power P_l can be achieved with smaller currents. However, in some examples, increasing N_d and thus Q_d can increase $Q_{d[l]}$, $P_{d,rad}$ and the voltage across the device capacitance V_d. Similar can be the impact of increasing N_s on $Q_{s[g]}$, $P_{s,rad}$ and V_s. As a conclusion, in some examples, the number of turns N_s and N_d may be chosen

InductEV, Inc.
Exhibit 1025
Page 669

large enough (for high efficiency) but such that they allow for reasonable voltages, loaded Q's and/or powers radiated.

With respect to the resonant frequency, again, there may be an optimal one for efficiency. Close to that optimal frequency $Q_{d[l]}$ and/or $Q_{s[g]}$ can be approximately maximum. In some examples, for lower frequencies the currents may typically get larger but the voltages and radiated powers may get smaller. In some examples, one may choose the resonant frequency to maximize any of a number of system parameters or performance specifications, such as efficiency.

One way to decide on an operating regime for the system may be based on a graphical method. Consider two loops of $r_s = 25cm$, $r_d = 15cm$, $h_s = h_d = 0$, $a_s = a_d = 3mm$ and distance $D = 2m$ between them. In Fig. 12, we plot some of the above dependent variables (currents, voltages and radiated powers normalized to *1Watt* of output power) in terms of frequency f and N_d, given some choice for wp and N_s. Fig. 12 depicts the trend of system performance explained above. In Fig. 13, we make a contour plot of the dependent variables as functions of both frequency and *wp* but for both N_s and N_d fixed. For example, in embodiments, a reasonable choice of parameters for the system of two loops with the dimensions given above may be: $N_s = 2$, $N_d = 6$, *f=10MHz* and *wp=10*, which gives the following performance characteristics: $\eta = 20.6\%$, $Q_{d[l]} = 1264$, $I_s = 7.2A$, $I_d = 1.4A$, $V_s = 2.55kV$, $V_d = 2.30kV$, $P_{s,rad} = 0.15W$, $P_{d,rad} = 0.006W$. Note that the results in Figs. 12, 13 and the calculated performance characteristics are made using the analytical formulas provided above, so they are expected to be less accurate for large values of N_s, N_d, but still may give a good estimate of the scalings and the orders of magnitude.

Finally, in embodiments, one could additionally optimize for the source dimensions, if, for example, only the device dimensions are limited. Namely, one can add r_s and a_s in the set of independent variables and optimize with respect to these all the

InductEV, Inc.
Exhibit 1025
Page 670

dependent variables of the system. In embodiments, such an optimization may lead to improved results.

2.3 Inductively-loaded conducting rods

A straight conducting rod of length $2h$ and cross-sectional radius a has distributed capacitance and distributed inductance, and therefore can support a resonant mode of angular frequency ω. Using the same procedure as in the case of self-resonant coils, one can define an effective total inductance L and an effective total capacitance C of the rod through formulas Eqs.(19) and (20). With these definitions, the resonant angular frequency and the effective impedance may be given again by the common formulas $\omega = 1/\sqrt{LC}$ and $Z = \sqrt{L/C}$ respectively. To calculate the total inductance and capacitance, one can assume again a sinusoidal current profile along the length of the conducting wire. When interested in the lowest mode, if we denote by x the coordinate along the conductor, such that it runs from $-h$ to $+h$, then the current amplitude profile may have the form $I(x) = I_o \cos(\pi x/2h)$, since it has to be zero at the open ends of the rod. This is the well-known half-wavelength electric dipole resonant mode.

In some examples, one or more of the resonant objects may be inductively-loaded conducting rods. Referring to Fig. 14, a straight conducting rod of length $2h$ and cross-sectional radius a, as in the previous paragraph, is cut into two equal pieces of length h, which may be connected via a coil wrapped around a magnetic material of relative permeability μ, and everything is surrounded by air. The coil has an inductance L_c, which is added to the distributed inductance of the rod and thus modifies its resonance. Note however, that the presence of the center-loading inductor may modify the current distribution inside the wire and therefore the total effective inductance L and total effective capacitance C of the rod may be different respectively from L_s and C_s, which are calculated for a self-resonant rod of the same total length using a sinusoidal current profile, as in the previous paragraph. Since some current may be running inside the coil of the external loading inductor, the current distribution $\mathbf{j}$ inside the rod may be reduced,

InductEV, Inc.
Exhibit 1025
Page 671

so $L < L_s$, and thus, from the charge conservation equation, the linear charge distribution ρ_l may flatten out towards the center (being positive in one side of the rod and negative in the other side of the rod, changing abruptly through the inductor), so $C > C_s$. The resonant frequency for this system may be $\omega = 1/\sqrt{(L + L_c\ C} < \omega_s = 1/\sqrt{L_s C_s}$, and $I(x) \to I_o \cos(\pi x/2h) \Rightarrow\ L \to L_s \Rightarrow\ \omega \to \omega_s$, as $L_c \to 0$.

In general, the desired CMT parameters can be found for this system, but again a very complicated solution of Maxwell's Equations is generally required. In a special case, a reasonable estimate for the current distribution can be made. When $L_c \gg L_s > L$, then $\omega \approx 1/\sqrt{L_c C} \ll \omega_s$ and $Z \approx \sqrt{L_c/C} \gg Z_s$, while the current distribution is triangular along the rod (with maximum at the center-loading inductor and zero at the ends) and thus the charge distribution may be positive constant on one half of the rod and equally negative constant on the other side of the rod. This allows us to compute numerically C from Eq.(20). In this case, the integral in Eq.(20) can actually be computed analytically, giving the formula $1/C = 1/(\pi\varepsilon_o h)\left[\ln(h/a) - 1\right]$. Explicit analytical formulas are again available for R from Eq.(21) and (22), since $I_{rms} = I_o$, $|\mathbf{p}| = q_o h$ and $|\mathbf{m}| = 0$ (namely only the electric-dipole term is contributing to radiation), so we can determine also $Q_{abs} = 1/\omega C R_{abs}$ and $Q_{rad} = 1/\omega C R_{rad}$. At the end of the calculations, the validity of the assumption of triangular current profile may be confirmed by checking that indeed the condition $L_c \gg L_s \Leftrightarrow \omega \ll \omega_s$ is satisfied. This condition may be relatively easily satisfied, since typically a conducting rod has very small self-inductance L_s to begin with.

Another important loss factor in this case is the resistive loss inside the coil of the external loading inductor L_c and it may depend on the particular design of the inductor. In some examples, the inductor may be made of a Brooks coil, which is the coil geometry which, for fixed wire length, may demonstrate the highest inductance and thus quality factor. The Brooks coil geometry has N_{Bc} turns of conducting wire of cross-sectional

InductEV, Inc.
Exhibit 1025
Page 672

radius a_{Bc} wrapped around a cylindrically symmetric coil former, which forms a coil with a square cross-section of side r_{Bc}, where the inner side of the square is also at radius r_{Bc} (and thus the outer side of the square is at radius $2r_{Bc}$), therefore $N_{Bc} \approx (r_{Bc}/2a_{Bc})^2$. The inductance of the coil is then $L_c = 2.0285\mu_o r_{Bc} N_{Bc}^2 \approx 2.0285\mu_o r_{Bc}^5 / 8a_{Bc}^4$ and its resistance $R_c \approx \frac{1}{\sigma}\frac{l_{Bc}}{\pi a_{Bc}^2}\sqrt{1+\frac{\mu_o\omega\sigma}{2}\left(\frac{a_{Bc}}{2}\right)^2}$, where the total wire length is $l_{Bc} \approx 2\pi(3r_{Bc}/2)N_{Bc} \approx 3\pi r_{Bc}^3/4a_{Bc}^2$ and we have used an approximate square-root law for the transition of the resistance from the dc to the ac limit as the skin depth varies with frequency.

The external loading inductance L_c provides the freedom to tune the resonant frequency. For example, for a Brooks coil with a fixed size r_{Bc}, the resonant frequency can be reduced by increasing the number of turns N_{Bc} by decreasing the wire cross-sectional radius a_{Bc}. Then the desired resonant angular frequency $\omega = 1/\sqrt{L_c C}$ may be achieved for $a_{Bc} \approx \left(2.0285\mu_o r_{Bc}^5 \omega^2 C\right)^{1/4}$ and the resulting coil quality factor may be $Q_c \approx 0.169\mu_o\sigma r_{Bc}^2\omega/\sqrt{1+\omega^2\mu_o\sigma\sqrt{2.0285\mu_o(r_{Bc}/4)^5 C}}$. Then, for the particular simple case $L_c \gg L_s$, for which we have analytical formulas, the total $Q = 1/\omega C(R_c + R_{abs} + R_{rad})$ becomes highest at some optimal frequency ω_Q, reaching the value $Q_{\max}$, that may be determined by the loading-inductor specific design. For example, for the Brooks-coil procedure described above, at the optimal frequency $Q_{\max} \approx Q_c \approx 0.8\left(\mu_o\sigma^2 r_{Bc}^3 / C\right)^{1/4}$. At lower frequencies it is dominated by ohmic loss inside the inductor coil and at higher frequencies by radiation. Note, again, that the above formulas are accurate as long as $\omega_Q \ll \omega_s$ and, as explained above, this may be easy to design for by using a large inductance.

InductEV, Inc.
Exhibit 1025
Page 673

The results of the above analysis for two examples, using Brooks coils, of subwavelength modes of $\lambda / h \geq 200$ (namely highly suitable for near-field coupling and well within the quasi-static limit) at the optimal frequency ω_Q are presented in Table 5.

Table 5 shows in parentheses (for similarity to previous tables) analytical results for the wavelength and absorption, radiation and total loss rates, for two different cases of subwavelength-rod resonant modes. Note that copper was used for the conducting material ($\sigma=5.998\cdot10^7 S/m$). The results show that, in some examples, the optimal frequency may be in the low-MHz microwave range and the expected quality factors may be $Q_{abs} \geq 1000$ and $Q_{rad} \geq 100000$.

Table 5

single rod	λ / h	f (MHz)	Q_{rad}	Q_{abs}	Q
h=30cm, a=2cm μ=1, r_{Bc}=2cm, a_{Bc}=0.88mm, N_{Bc}=129	(403.8)	(2.477)	($2.72*10^6$)	(7400)	(7380)
h=10cm, a=2mm μ=1, r_{Bc}=5mm, a_{Bc}=0.25mm, N_{Bc}=103	(214.2)	(14.010)	($6.92*10^5$)	(3908)	(3886)

In some examples, energy may be transferred between two inductively-loaded rods. For the rate of energy transfer between two inductively-loaded rods 1 and 2 at distance D between their centers, the mutual capacitance M_C can be evaluated numerically from Eq.(23) by using triangular current distributions in the case $\omega \ll \omega_s$. In this case, the coupling may be only electric and again we have an analytical formula, which, in the quasi-static limit $h \ll D \ll \lambda$ and for the relative orientation such that the two rods are aligned on the same axis, is $1/M_C \approx 1/2\pi\varepsilon_o \cdot (h_1 h_2)^2 / D^3$, which means that $k \propto \left(\sqrt{h_1 h_2} / D\right)^3$ is independent of the frequency ω. One can then get the resultant strong-coupling factor U,

InductEV, Inc.
Exhibit 1025
Page 674

It can be seen that the frequency ω_U, where the figure-of-merit is maximized to the value $U_{\max}$, is close to the frequency $\omega_{Q_1Q_2}$, where Q_1Q_2 is maximized, since k does not depend much on frequency (at least for the distances $D \ll \lambda$ of interest for which the quasi-static approximation is still valid). Therefore, the optimal frequency $\omega_U \approx \omega_{Q_1Q_2}$ may be mostly independent of the distance D between the two rods and may lie between the two frequencies ω_{Q_1} and ω_{Q_2} at which the single-rod Q_1 and Q_2 respectively peak. In some typical examples, one can tune the inductively-loaded conducting rods, so that their angular eigenfrequencies are close to ω_U within Γ_U, which is half the angular frequency width for which $U > U_{\max}/2$.

Referring to Table 6, in parentheses (for similarity to previous tables) analytical results based on the above are shown for two systems each composed of a matched pair of the loaded rods described in Table 5. The average wavelength and loss rates are shown along with the coupling rate and coupling to loss ratio figure-of-merit $U = \kappa / \Gamma$ as a function of the coupling distance D, for the two cases. Note that for Γ_{rad} the single-rod value is used. Again we chose $L_c \gg L_s$ to make the triangular-current assumption a good one and computed M_C numerically from Eq.(23). The results show that for medium distances $D/h = 10-3$ the expected coupling-to-loss ratios are in the range $U \sim 0.5-100$.

Table 6

pair of rods	D/h	$Q_\kappa = 1/k$	U
h=30cm, a=2cm μ=1, r_{Bc}=2cm, a_{Bc}=0.88mm, N_{Bc}=129 $\lambda/h \approx 404$ $Q \approx 7380$	3	(70.3)	(105.0)
	5	(389)	(19.0)
	7	(1115)	(6.62)
	10	(3321)	(2.22)
h=10cm, a=2mm μ=1, r_{Bc}=5mm, a_{Bc}=0.25mm, N_{Bc}=103 $\lambda/h \approx 214$ $Q \approx 3886$	3	(120)	(32.4)
	5	(664)	(5.85)
	7	(1900)	(2.05)
	10	(5656)	(0.69)

InductEV, Inc.
Exhibit 1025
Page 675

2.4 Dielectric disks

In some examples, one or more of the resonant objects are dielectric objects, such as disks. Consider a two dimensional dielectric disk object, as shown in Fig. 15(a), of radius r and relative permittivity ε surrounded by air that supports high-Q "whispering-gallery" resonant modes. The loss mechanisms for the energy stored inside such a resonant system are radiation into free space and absorption inside the disk material. High-Q_{rad} and long-tailed subwavelength resonances can be achieved when the dielectric permittivity ε is large and the azimuthal field variations are slow (namely of small principal number m). Material absorption is related to the material loss tangent: $Q_{abs} \sim \mathrm{Re}\{\varepsilon\}/\mathrm{Im}\{\varepsilon\}$. Mode-solving calculations for this type of disk resonances were performed using two independent methods: numerically, 2D finite-difference frequency-domain (FDFD) simulations (which solve Maxwell's Equations in frequency domain exactly apart for spatial discretization) were conducted with a resolution of *30pts/r*; analytically, standard separation of variables (SV) in polar coordinates was used.

Table 7

single disk	λ/r	Q^{abs}	Q^{rad}	Q
Re{ε}=147.7, m=2	**20.01 (20.00)**	**10103 (10075)**	**1988 (1992)**	**1661 (1663)**
Re{ε}=65.6, m=3	9.952 (9.950)	10098 (10087)	9078 (9168)	4780 (4802)

The results for two TE-polarized dielectric-disk subwavelength modes of $\lambda/r \geq 10$ are presented in Table 7. Table 7 shows numerical FDFD (and in parentheses analytical SV) results for the wavelength and absorption, radiation and total loss rates, for two different cases of subwavelength-disk resonant modes. Note that disk-material loss-tangent $\mathrm{Im}\{\varepsilon\}/\mathrm{Re}\{\varepsilon\}=10^{-4}$ was used. (The specific parameters corresponding to the plot in Fig. 15(a) are highlighted with bold in the table.) The two methods have excellent agreement and imply that for a properly designed resonant low-loss-dielectric object values of $Q_{rad} \geq 2000$ and $Q_{abs} \sim 10000$ are achievable. Note that for the 3D

InductEV, Inc.
Exhibit 1025
Page 676

case the computational complexity would be immensely increased, while the physics would not be significantly different. For example, a spherical object of $\varepsilon=147.7$ has a whispering gallery mode with $m=2$, $Q_{rad}=13962$, and $\lambda/r=17$.

The required values of ε, shown in Table 7, might at first seem unrealistically large. However, not only are there in the microwave regime (appropriate for approximately meter-range coupling applications) many materials that have both reasonably high enough dielectric constants and low losses (e.g. Titania, Barium tetratitanate, Lithium tantalite etc.), but also ε could signify instead the effective index of other known subwavelength surface-wave systems, such as surface modes on surfaces of metallic materials or plasmonic (metal-like, negative-ε) materials or metallo-dielectric photonic crystals or plasmono-dielectric photonic crystals.

To calculate now the achievable rate of energy transfer between two disks 1 and 2, as shown in Fig. 15(b) we place them at distance D between their centers. Numerically, the FDFD mode-solver simulations give κ through the frequency splitting of the normal modes of the combined system ($\delta_E = 2\kappa$ from Eq.(4)), which are even and odd superpositions of the initial single-disk modes; analytically, using the expressions for the separation-of-variables eigenfields $\mathbf{E}_{1,2}(\mathbf{r})$ CMT gives κ through

$$\kappa = \omega_1 / 2 \cdot \int d^3 r \varepsilon_2(r) E_2^*(r) E_1(r) / \int d^3 r \varepsilon(r) |E_1(r)|^2 ,$$

where $\varepsilon_j(\mathbf{r})$ and $\varepsilon(\mathbf{r})$ are the dielectric functions that describe only the disk j (minus the constant ε_o background) and the whole space respectively. Then, for medium distances D/r =10−3 and for non-radiative coupling such that $D<2r_C$, where $r_C = m\lambda/2\pi$ is the radius of the radiation caustic, the two methods agree very well, and we finally find , as shown in Table 8, strong-coupling factors in the range $U \sim 1-50$. Thus, for the analyzed examples, the achieved figure-of-merit values are large enough to be useful for typical applications, as discussed below.

InductEV, Inc.
Exhibit 1025
Page 677

Table 8

two disks	D/r	Q^{rad}	$Q=\omega/2\Gamma$	$\omega/2\kappa$	κ/Γ
Re{s}=147.7, m=2	3	2478	1989	46.9 (47.5)	42.4 (35.0)
$\lambda/r \approx 20$	5	2411	1946	298.0 (298.0)	6.5 (5.6)
$Q^{abs} \approx 10093$	7	2196	1804	769.7 (770.2)	2.3 (2.2)
	10	**2017**	**1681**	**1714 (1601)**	**0.98 (1.04)**
Re{s}=65.6, m=3	3	7972	4455	144 (140)	30.9 (34.3)
$\lambda/r \approx 30$	5	9240	4824	2242 (2083)	2.2 (2.3)
$Q^{abs} \approx 10096$	7	9187	4810	7485 (7417)	0.64 (0.65)

Note that even though particular examples are presented and analyzed above as examples of systems that use resonant electromagnetic coupling for wireless energy transfer, those of self-resonant conducting coils, capacitively-loaded resonant conducting coils, inductively-loaded resonant conducting rods and resonant dielectric disks, any system that supports an electromagnetic mode with its electromagnetic energy extending much further than its size can be used for transferring energy. For example, there can be many abstract geometries with distributed capacitances and inductances that support the desired kind of resonances. In some examples, the resonant structure can be a dielectric sphere. In any one of these geometries, one can choose certain parameters to increase and/or optimize U or, if the Q's are limited by external factors, to increase and/or optimize for k or, if other system performance parameters are of importance, to optimize those.

Illustrative example

In one example, consider a case of wireless energy transfer between two identical resonant conducting loops, labeled by L_1 and L_2. The loops are capacitively-loaded and couple inductively via their mutual inductance. Let r_A denote the loops' radii, N_A their numbers of turns, and b_A the radii of the wires making the loops. We also denote by D_{12} the center-to-center separation between the loops.

InductEV, Inc.
Exhibit 1025
Page 678

Resonant objects of this type have two main loss mechanisms: ohmic absorption and far-field radiation. Using the same theoretical method as in previous sections, we find that for r_A=7cm, b_A=6mm, and N_A=15 turns, the quality factors for absorption, radiation and total loss are respectively, $Q_{A,abs} = \pi f / \Gamma_{A,abs} = 3.19\times10^{4}$, $Q_{A,rad} = \pi f / \Gamma_{A,rad} = 2.6\times10^{8}$ and $Q_A = \pi f / \Gamma_A = 2.84\times10^{4}$ at a resonant frequency $f = 1.8\times10^{7}$ Hz (remember that L_1 and L_2 are identical and have the same properties). $\Gamma_{A,abs}$, $\Gamma_{A,rad}$ are respectively the rates of absorptive and radiative loss of L_1 and L_2, and the rate of coupling between L_1 and L_2 is denoted by κ_{12}.

When the loops are in fixed distinct parallel planes separated by D_{12} =1.4m and have their centers on an axis (C) perpendicular to their planes, as shown in Fig. 17a(Left), the coupling factor for inductive coupling (ignoring retardation effects) is $k_{12} \equiv \kappa_{12} / \pi f = 7.68\times10^{-5}$, independent of time, and thus the strong-coupling factor is $U_{12} \equiv k_{12} Q_A = 2.18$. This configuration of parallel loops corresponds to the largest possible coupling rate κ_{12} at the particular separation D_{12}.

We find that the energy transferred to L_2 is maximum at time $\boldsymbol{T_* = \kappa t_* = \tan^{-1}(2.18) = 1.14 \Rightarrow t_* = 4775(1/f)}$ from Eq.(5), and constitutes $\boldsymbol{\eta_{E*} = 29\%}$ of the initial total energy from Eq.(6a), as shown in Fig. 17a(Right). The energies radiated and absorbed are respectively $\boldsymbol{\eta_{rad,E}(t_*) = 7.2\%}$ and $\boldsymbol{\eta_{abs,E}(t_*) = 58.1\%}$ of the initial total energy, with $\boldsymbol{5.8\%}$ of the energy remaining in L_1.

We would like to be able to further increase the efficiency of energy transfer between these two resonant objects at their distance D_{12}. In some examples, one can use an intermediate resonator between the source and device resonators, so that energy is transferred more efficiently from the source to the device resonator indirectly through the intermediate resonator.

InductEV, Inc.
Exhibit 1025
Page 679

3. Efficient energy-transfer by a chain of three 'strongly coupled' resonances

Fig. 16 shows a schematic that generally describes one example of the invention, in which energy is transferred wirelessly among three resonant objects. Referring to Fig. 16, energy is transferred, over a distance D_{1B}, from a resonant source object R_1 of characteristic size r_1 to a resonant intermediate object R_B of characteristic size r_B, and then, over an additional distance D_{B2}, from the resonant intermediate object R_B to a resonant device object R_2 of characteristic size r_2, where $D_{1B}+D_{B2}=D$. As described above, the source object R_1 can be supplied power from a power generator that is coupled to the source object R_1. In some examples, the power generator can be wirelessly, e.g., inductively, coupled to the source object R_1. In some examples, the power generator can be connected to the source object R_1 by means of a wire or cable. Also, the device object R_2 can be connected to a power load that consumes energy transferred to the device object R_2. For example, the device object can be connected to e.g. a resistor, a battery, or other device. All objects are resonant objects. The wireless near-field energy transfer is performed using the field (e.g. the electromagnetic field or acoustic field) of the system of three resonant objects.

Different temporal schemes can be employed, depending on the application, to transfer energy among three resonant objects. Here we will consider a particularly simple but important scheme: a one-time finite-amount energy-transfer scheme

3.1 Finite-amount energy-transfer efficiency

Let again the source, intermediate and device objects be 1, B, 2 respectively and their resonance modes, which we will use for the energy exchange, have angular frequencies $\omega_{1,B,2}$, frequency-widths due to intrinsic (absorption, radiation etc.) losses $\Gamma_{1,B,2}$ and (generally) vector fields $\mathbf{F}_{1,B,2}(\mathbf{r})$, normalized to unity energy. Once the three resonant objects are brought in proximity, they can interact and an appropriate analytical framework for modeling this resonant interaction is again that of the well-known coupled-mode theory (CMT), which can give a good description of the system for resonances having quality factors of at least, for example, 10. Then, using $e^{-i\omega t}$ time

InductEV, Inc.
Exhibit 1025
Page 680

dependence, for the chain arrangement shown in Fig.16, the field amplitudes can be shown to satisfy, to lowest order:

$$\begin{aligned}\frac{d}{dt}a_1(t) &= -i(\omega_1 - i\Gamma_1)a_1(t) + i\kappa_{11}a_1(t) + i\kappa_{1B}a_B(t)\\ \frac{d}{dt}a_B(t) &= -i(\omega_B - i\Gamma_B)a_B(t) + i\kappa_{BB}a_B(t) + i\kappa_{B1}a_1(t) + i\kappa_{B2}a_2(t)\\ \frac{d}{dt}a_2(t) &= -i(\omega_2 - i\Gamma_2)a_2(t) + i\kappa_{22}a_2(t) + i\kappa_{2B}a_B(t)\end{aligned} \quad (34)$$

where $\kappa_{11,BB,22}$ are the shifts in each object's frequency due to the presence of the other, which are a second-order correction and can be absorbed into the eigenfrequencies by setting $\omega_{1,B,2} \to \omega_{1,B,2} + \kappa_{11,BB,22}$, and κ_{ij} are the coupling coefficients, which from the reciprocity requirement of the system must satisfy $\kappa_{ij} = \kappa_{ji}$. Note that, in some examples, the direct coupling coefficient κ_{12} between the resonant objects 1 and 2 may be much smaller than the coupling coefficients κ_{1B} and κ_{B2} between these two resonant objects with the intermediate object B, implying that the direct energy transfer between 1 and 2 is substantially dominated by the indirect energy transfer through the intermediate object. In some examples, if the coupling rates κ_{1B} and κ_{B2} are at least 5 times larger than the direct coupling rate κ_{12}, using an intermediate resonator may lead to an improvement in terms of energy transfer efficiency, as the indirect transfer may dominate the direct transfer. Therefore, in the CMT Eqs.(34) above, the direct coupling coefficient κ_{12} has been ignored, to analyze those particular examples.

The three resonant modes of the combined system are found by substituting $[a_1(t)\ a_B(t), a_2(t)] = [A_1, A_B, A_2]e^{-i\bar{\omega}t}$. When the resonators 1 and 2 are at exact resonance $\omega_1 = \omega_2 = \omega_A$ and for $\Gamma_1 = \Gamma_2 = \Gamma_A$, the resonant modes have complex resonant frequencies

$$\bar{\omega}_{\pm} = \omega_{AB} \pm \sqrt{(\Delta\omega_{AB})^2 + \kappa_{1B}^2 + \kappa_{B2}^2} \text{ and } \bar{\omega}_{ds} = \omega_A - i\Gamma_A \quad (35a)$$

InductEV, Inc.
Exhibit 1025
Page 681

where $\omega_{AB}=\left[\left(\omega_A+\omega_B\right)-i\left(\Gamma_A+\Gamma_B\right)\right]/2$, $\Delta\omega_{AB}=\left[\left(\omega_A-\omega_B\right)-i\left(\Gamma_A-\Gamma_B\right)\right]/2$ and whose splitting we denote as $\tilde{\delta}_E \equiv \bar{\omega}_+ - \bar{\omega}_-$, and corresponding resonant field amplitudes

$$\vec{V}_\pm=\begin{bmatrix}A_1\\A_B\\A_2\end{bmatrix}_\pm=\begin{bmatrix}\kappa_{1B}\\\Delta\omega_{AB}\mp\sqrt{\left(\Delta\omega_{AB}\right)^2+\kappa_{1B}^2+\kappa_{B2}^2}\\\kappa_{B2}\end{bmatrix} \text{ and } \vec{V}_{ds}=\begin{bmatrix}A_1\\A_B\\A_2\end{bmatrix}_{ds}=\begin{bmatrix}-\kappa_{B2}\\0\\\kappa_{1B}\end{bmatrix} \quad (35b)$$

Note that, when all resonators are at exact resonance $\omega_1=\omega_2(=\omega_A)=\omega_B$ and for $\Gamma_1=\Gamma_2(=\Gamma_A)=\Gamma_B$, we get $\Delta\omega_{AB}=0$, $\tilde{\delta}_E=2\sqrt{\kappa_{1B}^2+\kappa_{B2}^2}$, and then

$$\bar{\omega}_\pm=\omega_A\pm\sqrt{\kappa_{1B}^2+\kappa_{B2}^2}-i\Gamma_A \text{ and } \bar{\omega}_{ds}=\omega_A-i\Gamma_A \quad (36a)$$

$$\vec{V}_\pm=\begin{bmatrix}A_1\\A_B\\A_2\end{bmatrix}_\pm=\begin{bmatrix}\kappa_{1B}\\\mp\sqrt{\kappa_{1B}^2+\kappa_{B2}^2}\\\kappa_{B2}\end{bmatrix} \text{ and } \vec{V}_{ds}=\begin{bmatrix}A_1\\A_B\\A_2\end{bmatrix}_{ds}=\begin{bmatrix}-\kappa_{B2}\\0\\\kappa_{1B}\end{bmatrix}, \quad (36b)$$

namely we get that the resonant modes split to a lower frequency, a higher frequency and a same frequency mode.

Assume now that at time $t=0$ the source object 1 has finite energy $|a_1(0)|^2$, while the intermediate and device objects have $|a_B(0)|^2=|a_2(0)|^2=0$. Since the objects are coupled, energy will be transferred from 1 to B and from B to 2. With these initial conditions, Eqs.(34) can be solved, predicting the evolution of the field-amplitudes. The energy-transfer efficiency will be $\tilde{\eta}_E \equiv |a_2(t)|^2/|a_1(0)|^2$. The ratio of energy converted to loss due to a specific loss mechanism in resonators 1, B and 2, with respective loss rates $\Gamma_{1,\text{loss}}$, $\Gamma_{B,\text{loss}}$ and $\Gamma_{2,\text{loss}}$ will be $\tilde{\eta}_{loss,E}=\int_0^t d\tau\left[2\Gamma_{1,\text{loss}}|a_1(\tau)|^2+2\Gamma_{B,\text{loss}}|a_B(\tau)|^2+2\Gamma_{2,\text{loss}}|a_2(\tau)|^2\right]/|a_1(0)|^2$. At exact

InductEV, Inc.
Exhibit 1025
Page 682

resonance $\omega_1 = \omega_2 (= \omega_A) = \omega_B$ (an optimal condition) and in the special symmetric case $\Gamma_1 = \Gamma_2 = \Gamma_A$ and $\kappa_{1B} = \kappa_{B2} = \kappa$, the field amplitudes are

$$a_1(\tilde{T}) = \frac{1}{2} e^{-i\omega_A t} e^{-\tilde{T}/\tilde{U}} \left[\tilde{\Delta} \frac{\sin(\sqrt{1-\tilde{\Delta}^2}\tilde{T})}{\sqrt{1-\tilde{\Delta}^2}} + \cos(\sqrt{1-\tilde{\Delta}^2}\tilde{T}) + e^{-\tilde{\Delta}\tilde{T}} \right] \quad (37a)$$

$$a_B(\tilde{T}) = \frac{1}{2} e^{-i\omega_A t} e^{-\tilde{T}/\tilde{U}} \frac{\sin(\sqrt{1-\tilde{\Delta}^2}\tilde{T})}{\sqrt{1-\tilde{\Delta}^2}} \quad (37b)$$

$$a_2(\tilde{T}) = \frac{1}{2} e^{-i\omega_A t} e^{-\tilde{T}/\tilde{U}} \left[\tilde{\Delta} \frac{\sin(\sqrt{1-\tilde{\Delta}^2}\tilde{T})}{\sqrt{1-\tilde{\Delta}^2}} + \cos(\sqrt{1-\tilde{\Delta}^2}\tilde{T}) - e^{-\tilde{\Delta}\tilde{T}} \right] \quad (37c)$$

where $\tilde{T} \equiv \sqrt{2}\kappa t$, $\tilde{\Delta}^{-1} = 2\sqrt{2}\kappa/(\Gamma_B - \Gamma_A)$ and $\tilde{U} = 2\sqrt{2}\kappa/(\Gamma_A + \Gamma_B)$.

In some examples, the system designer can adjust the duration of the coupling t at will. In some examples, the duration t can be adjusted to maximize the device energy (and thus efficiency $\tilde{\eta}_E$). Then, in the special case above, it can be inferred from Eq.(37c) that $\tilde{\eta}_E$ is maximized for the $\tilde{T} = \tilde{T}_*$ that satisfies

$$\left[\tilde{\Delta} - \tilde{U}\left(1-\tilde{\Delta}^2\right) \right] \frac{\sin(\sqrt{1-\tilde{\Delta}^2}\tilde{T})}{\sqrt{1-\tilde{\Delta}^2}} + \left(1 - \tilde{\Delta}\tilde{U}\right) \left[\cos(\sqrt{1-\tilde{\Delta}^2}\tilde{T}) - e^{\tilde{\Delta}\tilde{T}} \right] = 0 \quad (38)$$

In general, this equation may not have an obvious analytical solution, but it does admit a simple solution in the following two cases:

When $\Gamma_A = \Gamma_B \Leftrightarrow \tilde{\Delta} = 0, \tilde{U} = \sqrt{2}\kappa/\Gamma_B$, the energy transfer from resonator 1 to resonator 2 is maximized at

$$\tilde{T}_*\left(\tilde{\Delta} = 0\right) = 2\tan^{-1}\tilde{U} \quad (39)$$

resulting in an energy-transfer efficiency

$$\tilde{\eta}_E\left(\tilde{T}_*, \tilde{\Delta} = 0\right) = \left[\frac{\tilde{U}^2}{1+\tilde{U}^2} \exp\left(-\frac{2\tan^{-1}\tilde{U}}{\tilde{U}} \right) \right]^2, \quad (40)$$

which has the form of the two-object energy-transfer efficiency of Eq.(6b) but squared.

InductEV, Inc.
Exhibit 1025
Page 683

When $\Gamma_A = 0 \Leftrightarrow \tilde{\Delta}^{-1} = \tilde{U} = 2\sqrt{2}\kappa/\Gamma_B$, the energy transfer from resonator 1 to resonator 2 is maximized at

$$\tilde{T}_* \left(\tilde{\Delta}^{-1} = \tilde{U}\right) = \begin{cases} \pi\tilde{U}/\sqrt{\tilde{U}^2 - 1}, \tilde{U} > 1 \\ \infty, \tilde{U} \le 1 \end{cases} \quad (41)$$

resulting in an energy-transfer efficiency

$$\eta_E \left(\tilde{T}_*, \tilde{\Delta}^{-1} = \tilde{U}\right) = \frac{1}{4} \cdot \begin{cases} \left[1 + \exp\left(-\pi/\sqrt{\tilde{U}^2 - 1}\right)\right]^2, \tilde{U} > 1 \\ 1, \tilde{U} \le 1 \end{cases}. \quad (42)$$

In both cases, and in general for any $\tilde{\Delta}$, the efficiency is an increasing function of $\tilde{U}$. Therefore, once more resonators that have high quality factors are preferred. In some examples, one may design resonators with Q>50. In some examples, one may design resonators with Q>100.

Illustrative example

Returning to our illustrative example, in order to improve the ~29% efficiency of the energy transfer from L_1 to L_2, while keeping the distance D_{12} separating them fixed, we propose to introduce an intermediate resonant object that couples strongly to both L_1 and L_2, while having the same resonant frequency as both of them. In one example, we take that mediator to also be a capacitively-loaded conducting-wire loop, which we label by L_B. We place L_B at equal distance (D_{1B}=D_{B2}=D_{12}/2=0.7m) from L_1 and L_2 such that its axis also lies on the same axis (C), and we orient it such that its plane is parallel to the planes of L_1 and L_2, which is the optimal orientation in terms of coupling. A schematic diagram of the three-loops configuration is depicted in Fig. 17b(Left).

In order for L_B to couple strongly to L_1 and L_2, its size needs to be substantially larger than the size of L_1 and L_2. However, this increase in the size of L_B has considerable drawback in the sense that it may also be accompanied by significant decrease in its radiation quality factor. This feature may often occur for the resonant systems of this type: stronger coupling can often be enabled by increasing the objects' size, but it may imply stronger radiation from the object in question. Large radiation may often be undesirable, because it could lead to far-field interference with other RF systems, and in

InductEV, Inc.
Exhibit 1025
Page 684

some systems also because of safety concerns. For r_B=70cm, b_B=1.5cm, and N_B=1 turn, we get $Q_{B,abs} = \pi f / \Gamma_{B,abs} = 7706$, $Q_{B,rad} = \pi f / \Gamma_{B,rad} = 400$, so $Q_B = \pi f / \Gamma_B = 380$, and $k_{1B} \equiv \kappa_{1B} / \pi f = k_{B2} = 0.0056$, so $\tilde{U} = 2\sqrt{2}\kappa / (\Gamma_A + \Gamma_B) = 5.94$ and $\tilde{\Delta}^{-1} = 2\sqrt{2}\kappa / (\Gamma_B - \Gamma_A) = 6.1$, at $f = 1.8 \times 10^7$ Hz. Note that since the coupling rates κ_{1B} and κ_{B2} are $\approx$70 times larger than κ_{12}, indeed we can ignore the direct coupling between L_1 and L_2, and focus only on the indirect energy transfer through the intermediate loop L_B, therefore the analysis of the previous section can be used.

The optimum in energy transferred to L_2 occurs at time $\tilde{T}_* = \sqrt{2}\kappa t_* = 3.21 \Rightarrow t_* = 129(1/f)$, calculated from Eq.(38), and is equal to $\tilde{\eta}_{E*} = 61.5\%$ of the initial energy from Eq.(37c). [Note that, since $Q_A \gg Q_B$, we could have used the analytical conclusions of the case $\tilde{\Delta}^{-1} = \tilde{U}$ and then we would have gotten a very close approximation of $\tilde{T}_* = 3.19$ from Eq.(41).] The energy radiated is $\tilde{\eta}_{rad,E}(t_*) = 31.1\%$, while the energy absorbed is $\tilde{\eta}_{abs,E}(t_*) = 3.3\%$, and 4.1% of the initial energy is left in L_1. Thus, the energy transferred, now indirectly, from L_1 to L_2 has increased by factor of 2 relative to the two-loops direct transfer case. Furthermore, the transfer time in the three-loops case is now $\approx$35 times shorter than in the two-loops direct transfer, because of the stronger coupling rate. The dynamics of the energy transfer in the three-loops case is shown in Fig. 17b(Right).

Note that the energy radiated in the three-loop system has undesirably increased by factor of 4 compared to the two-loop system. We would like to be able to achieve a similar improvement in energy-transfer efficiency, while not allowing the radiated energy to increase. In this specification, we disclose that, in some examples, this can be achieved by appropriately varying the values of the coupling strengths between the three resonators.

InductEV, Inc.
Exhibit 1025
Page 685

4. Efficient energy-transfer by a chain of three resonances with adiabatically varying coupling strengths

Consider again the system of a source resonator R_1, a device resonator R_2 and an intermediate resonator R_B. For the purposes of the present analysis, R_1 and R_2 will be assumed to have negligible mutual interactions with each other, while each of them can be strongly coupled to R_B, with coupling rates κ_{1B} and κ_{B2} respectively. Note that, in some examples of wireless energy transfer systems, for the resonant object R_B to be able to have strong coupling with other resonant objects, it may be accompanied with inferior loss properties compared to R_1 and R_2, usually in terms of substantially larger radiation losses.

It was seen in a previous section that, when the resonators 1 and 2 are at exact resonance $\omega_1 = \omega_2 = \omega_A$ and for $\Gamma_1 = \Gamma_2 = \Gamma_A$, the system supports a resonant state (eigenstate) with resonant frequency (eigenfrequency) $\tilde{\omega}_{ds} = \omega_A - i\Gamma_A$ and resonant field amplitudes $\vec{V}_{ds} = \left[-\kappa_{B2} \quad 0 \quad \kappa_{1B}\right]^T / \sqrt{\kappa_{1B}^2 + \kappa_{B2}^2}$, where here we normalized it. This eigenstate $\vec{V}_{ds}$ we call the "dark state" in analogy with atomic systems and the related phenomenon of Electromagnetically Induced Transparency (EIT), wherein complete population transfer between two quantum states through a third lossy state, coupled to each of the other two states, is enabled. The dark state is the most essential building block of our proposed efficient weakly-radiative energy-transfer scheme, because it has no energy at all in the intermediate (lossy) resonator R_B, i.e. $a_B(t)=0 \ \forall$ t whenever the three-object system is in state $\vec{V}_{ds}$. In fact, if $\Gamma_A \to 0$, then this state is completely lossless, or if $\Gamma_{A,rad} \to 0$, then this state is completely non-radiative. Therefore, we disclose using predominantly this state to implement the wireless energy transfer. By doing that, the proposed energy transfer scheme can be made completely lossless, in the limit $\Gamma_A \to 0$, no matter how large is the loss rate Γ_B, as shown in Fig. 20, or completely non-radiative, in the limit $\Gamma_{A,rad} \to 0$, no matter how large is the radiative loss rate $\Gamma_{B,rad}$. Since the energy transfer efficiency increases as the quality factors of the first (source) and second (device) resonances increase, one may design these resonators to have a high quality

InductEV, Inc.
Exhibit 1025
Page 686

factor. In some examples, one may design resonators with Q_A>50. In some examples, one may design resonators with Q_A>100.

Let us demonstrate how it is possible to use the dark state for energy transfer with minimal loss. From the expression of $\vec{V}_{ds}$ one can see that, if the three-object system is in the state $\vec{V}_{ds}$, then, in general, there is energy in the source resonator with field amplitude proportional to the coupling rate κ_{B2} between the device resonator and the intermediate resonator, and there is also energy in the device resonator with field amplitude proportional to the coupling rate κ_{1B} between the source resonator and the intermediate resonator. Then, κ_{1B}=0 corresponds to all the system's energy being in R_1, while κ_{B2}=0 corresponds to all the system's energy being in R_2.

So, the important considerations necessary to achieve efficient weakly-radiative energy transfer, consist of preparing the system initially in state $\vec{V}_{ds}$ and varying the coupling rates in time appropriately to evolve this state $\vec{V}_{ds}$ in a way that will cause energy transfer. Thus, if at t=0 all the energy is in R_1, then one should have $\kappa_{1B}(t=0) << \kappa_{B2}(t=0)$, for example $\kappa_{1B}(t=0)=0$ and $\kappa_{B2}(t=0) \neq 0$. In order for the total energy of the system to end up in R_2, at a time t_{EIT} when the full variation of the coupling rates has been completed, we should have $\kappa_{1B}(t= t_{EIT}) >> \kappa_{B2}(t= t_{EIT})$, for example $\kappa_{1B}(t=t_{EIT}) \neq 0$ and $\kappa_{B2}(t=t_{EIT})=0$. This ensures that the initial and final states of the three-object system are parallel to $\vec{V}_{ds}$. However, a second important consideration is to keep the three-object system at all times in $\vec{V}_{ds}(t)$, even as $\kappa_{1B}(t)$ and $\kappa_{B2}(t)$ are varied in time. This is crucial in order to prevent the system's energy from getting into any of the two other eigenstates $\vec{V}_{\pm}$ and thus getting into the intermediate object R_B, which may be highly radiative or lossy in general, as in the example of Fig. 17. This consideration requires changing $\kappa_{1B}(t)$ and $\kappa_{B2}(t)$ slowly enough so as to make the entire three-object system adiabatically follow the time evolution of $\vec{V}_{ds}(t)$. The criterion for adiabatic following can be expressed, in analogy to the population transfer case as

InductEV, Inc.
Exhibit 1025
Page 687

$$\left|\left\langle \bar{V}_{\pm}\left|\frac{d\bar{V}_{ds}}{dt}\right\rangle\right| \ll \left|\bar{\omega}_{\pm}-\bar{\omega}_{ds}\right| \qquad (43)$$

where $\vec{V}_{\pm}$ are the remaining two eigenstates of the system, with corresponding eigenvalues $\bar{\omega}_{\pm}$, as shown earlier. Note that any functional dependence of the coupling rates with time (with duration parameter t_{EIT}) will work, provided it satisfies the adiabaticity criterion Eq.(43) above. The time functional can be linear, sinusoidal (as in the illustrative example to follow) or the temporal analog of a Butterworth (maximally flat) taper, a Chebyshev taper, an exponential taper and the like.

Referring to Fig. 18, an example coupling rate adjustment system 300 for adjusting coupling rates for the one or more of the resonator structures R_1, R_2, or R_B is shown. As described, the coupling rates between the first and intermediate resonator structures and the intermediate and second resonator structures are characterized by κ_{1B} and κ_{B2} respectively. These coupling rates, κ_{1B} and κ_{B2}, are several times (e.g., 70 times) greater than the coupling rate κ_{12} between the first and second resonator structure. In some examples, the coupling rate adjustment system can be a mechanical, electrical, or electro-mechanical system for dynamically adjusting, e.g., rotating, or effecting a translational movement, of the one or more resonator structures with respect to each other.

In some examples, the coupling rate κ_{1B} is much smaller than the coupling rate the coupling rate κ_{B2} at the beginning of the energy transfer. By the end, i.e., when a substantial amount of energy has been transferred from the first resonator structure R_1 to the second resonator structure, R_2, the coupling rate κ_{1B} is much greater than the coupling rate κ_{B2}. In some examples, the coupling rate κ_{1B} can be set to a fixed value while the coupling rate κ_{B2} is being varied from its maximum to its minimum value. In some examples, the coupling rate κ_{B2} can be set to a fixed value while the coupling rate κ_{1B} is being varied from its minimum to its maximum value. In some examples, the

InductEV, Inc.
Exhibit 1025
Page 688

coupling rate κ_{1B} can be varied from a minimum to a maximum value while the coupling rate κ_{B2} is being varied from its maximum to minimum value.

Referring now to Fig. 19, a graph for implementing an example coupling rate adjustment system 300 is shown. As shown, in some examples, the coupling rate κ_{1B} is set at its minimum value at time, t=0, and increased as a function of time (see, for example, equation 44), while the coupling rate κ_{B2} is at its maximum value at t=0 and decreased as a function of time (see, for example, equation 45). Accordingly, at the beginning (t=0), the value of κ_{1B} is much smaller than the value of κ_{B2}. In some examples, the value of κ_{1B} can be selected to be any value much smaller than the value of κ_{B2}. During the wireless energy transfer, the value of κ_{1B} is increased, while the value of κ_{B2} is decreased. After a predetermined amount of time t_{ETT} has elapsed (e.g., after a substantial amount of energy has been transferred to the second resonator), the value of κ_{1B} becomes much greater than the value of κ_{B2}.

In some implementations, the coupling rate adjustment system 300 can effect an adjustment of coupling rates between the resonator structures by changing a relative orientation of one or more of the resonator structures with respect to each other. For example, referring again to Fig. 18, the first and second resonator structures, R_1 and R_2, can be rotated about their respective axes (e.g., varying angles θ_1 and θ_2), with respect to the intermediate resonator structure R_B to simultaneously change κ_{1B} and κ_{B2}. Alternatively, the orientation of the intermediate resonator structure, R_B, can be adjusted, e.g., rotated about an axis, with respect to the first and second resonator structures to simultaneously change κ_{1B} and κ_{B2}. Alternatively, the orientation of only the first resonator structure R_1 can be rotated about its respective axis to change κ_{1B}, while the orientations of R_2 and R_B are fixed and thus κ_{B2} is fixed to a value intermediate between the minimum and maximum values of κ_{1B}. Alternatively, the orientation of only the second resonator structure R_2 can be rotated about its respective axis to change κ_{B2},

InductEV, Inc.
Exhibit 1025
Page 689

while the orientations of R_1 and R_B are fixed and thus κ_{1B} is fixed to a value intermediate between the minimum and maximum values of κ_{B2}.

In some implementations, the coupling rate adjustment system 300 can effect an adjustment of coupling rates between the resonator structures by translationally moving one or more of the resonator structures with respect to each other. For example, the positions of the first and second resonator structures, R_1 and R_2, can be adjusted, e.g., moved along an axis, with respect to the intermediate resonator structure R_B to simultaneously change κ_{1B} and κ_{B2}. Alternatively, a position of the intermediate resonator structure, R_B, can be adjusted, e.g., moved along an axis, with respect to the first and second resonator structures to simultaneously change κ_{1B} and κ_{B2}. Alternatively, a position of only the first resonator structure, R_1, can be adjusted, e.g., moved along an axis, with respect to the intermediate R_B resonator structure to change κ_{1B}, while the positions of R_2 and R_B are fixed and thus κ_{B2} is fixed to a value intermediate between the minimum and maximum values of κ_{1B}. Alternatively, a position of only the second resonator structure, R_2, can be adjusted, e.g., moved along an axis, with respect to the intermediate R_B resonator structure to change κ_{B2}, while the positions of R_1 and R_B are fixed and thus κ_{1B} is fixed to a value intermediate between the minimum and maximum values of κ_{B2}.

In some examples, the coupling rate adjustment system 300 can dynamically adjust an effective size of the resonator objects to effect adjustments in the coupling rates κ_{1B} and κ_{B2} similar to that described above. The effective size can be adjusted by changing a physical size of the resonator objects. For example, the physical size can be adjusted by effecting mechanical changes in area, length, or other physical aspect of one or more of the resonator structures. The effective size can also be adjusted through non-mechanical changes, such as, but not limited to, applying a magnetic field to change the permeability of the one or more of the resonator structures.

In principle, one would think of making the transfer time t_{EIT} as long as possible to ensure adiabaticity. However there is limitation on how slow the transfer process can

InductEV, Inc.
Exhibit 1025
Page 690

optimally be, imposed by the losses in R_1 and R_2. Such a limitation may not be a strong concern in typical atomic EIT case, because the initial and final states there can be chosen to be non-lossy ground states. However, in our case, losses in R_1 and R_2 are not avoidable, and can be detrimental to the energy transfer process whenever the transfer time t_{EIT} is not less than $1/\Gamma_A$. This is because, even if the three-object system is carefully kept in $\vec{V}_{ds}$ at all times, the total energy of the system will decrease from its initial value as a consequence of losses in R_1 and R_2. Thus the duration of the transfer may be a compromise between these two limits: the desire to keep t_{EIT} long enough to ensure near-adiabaticity, but short enough not to suffer from losses in R_1 and R_2.

Given a particular functional variation of the coupling rates with time with variation duration parameter t_{EIT}, one may calculate the optimal energy transfer efficiency in the following way: First, for each t_{EIT}, determine the optimal time t_*, at which the energy at R_2 is maximized and the transfer process may be be terminated. Then find the optimal variation time t_{EIT^*} based on the counteracting mechanisms discussed above. The optimal efficiency of energy transfer $\tilde{\eta}_{EIT,E^*}$ can then be calculated. In most cases, this procedure may need to be done numerically using the CMT Eqs.(34) as analytical solutions may not be possible. With respect to optimizing the functional dependence of the coupling rates with time, one may choose one that minimizes the coupling of energy to the eigenstates $\vec{V}_{\pm}$ for a given t_{EIT}, which may lead to the temporal analog of a Chebyshev taper.

In some examples, the optimal t_{EIT} may not be long enough for the adiabadicity criterion of Eq.(43) to be always satisfied. In those cases, some energy may get into at least one of the lossy states $\vec{V}_{\pm}$. Still significant improvement in efficiency and radiation loss may be achieved by the mode of operation where the coupling rates are variable, compared to the mode of operation where the coupling rates are constant, provided the maximum energy that enters the states $\vec{V}_{\pm}$ is much less in the variable rate scenario than in the constant rate scenario. In examples, using the proposed scheme of time-varying coupling rates may be advantageous as long as the maximum energy stored in the intermediate resonator is substantially small. In some examples, substantially small may

InductEV, Inc.
Exhibit 1025
Page 691

be at most 5% of the peak total energy of the system. In some examples, substantially small may be at most 10% of the peak total energy of the system.

We can now also see why the mode of operation of the system where the coupling rates are kept constant in time may cause a considerable amount of lost (and especially radiated) energy, compared to the proposed mode of operation where the coupling rates are varied adiabatically in time. The reason is that, when $\kappa_{1B}=\kappa_{B2}$=const, the energies in R_1 and R_2 will always be equal to each other if the three-object system is to stay in $\vec{V}_{ds}$. So one cannot transfer energy from R_1 to R_2 by keeping the system purely in state $\vec{V}_{ds}$; note that even the initial state of the system, in which all the energy is in R_1 and there is no energy in R_3, cannot be solely in $\vec{V}_{ds}$ for fixed nonzero κ_{1B} and κ_{B2}, and has nonzero components along the eigenstates $\vec{V}_{\pm}$ which implies a finite energy will build up in R_B, and consequently result in an increased radiation, especially if $\Gamma_{B,rad} \gg \Gamma_{A,rad}$, which may be the case if the resonator R_B is chosen large enough to couple strongly to R_1 and R_2, as explained earlier.

Illustrative example

The previous analysis explains why a considerable amount of energy was radiated when the inductive coupling rates of the loops were kept constant in time, like in Fig. 17b. Let us now consider the modifications necessary for an adiabatically-varied-κ three-loops indirect transfer scheme, as suggested in the previous section, aiming to reduce the total radiated energy back to its reasonable value in the two-loops direct transfer case (Fig.17a), while maintaining the total energy transfer at level comparable to the constant-κ three-loops indirect transfer case (Fig. 17b). In one example, shown in Fig. 17c(Left and Right), we will keep the orientation of L_B fixed, and start initially (t=0) with L_1 perpendicular to L_B for κ_{1B}=0 and L_2 parallel to L_B for κ_{B2}=max, then uniformly rotate L_1 and L_2, at the same rates, until finally, at ($t=t_{ETT}$), L_1 becomes parallel to L_B for κ_{1B}=max and L_2 perpendicular to L_B for κ_{B2}=0, where we stop the rotation process. In this example, we choose a sinusoidal temporal variation of the coupling rates:

InductEV, Inc.
Exhibit 1025
Page 692

$$\kappa_{1B}(t) = \kappa \sin(\pi t / 2t_{EIT}) \quad (44)$$

$$\kappa_{B2}(t) = \kappa \cos(\pi t / 2t_{EIT}) \quad (45)$$

for $0<t<t_{EIT}$, and $k_{1B} \equiv \kappa_{1B} / \pi f = k_{B2} = 0.0056$ as before. By using the same CMT analysis as in Eq. (34), we find, in Fig. 17c(Center), that for an optimal $t_{EIT*} = 1989(1/f)$, an optimum transfer of $\tilde{\eta}_{EIT,E*} = 61.2\%$ can be achieved at $t_* = 1796(1/f)$, with only 8.2% of the initial energy being radiated, 28.6% absorbed, and 2% left in L_1. This is quite remarkable: by simply rotating the loops during the transfer, the energy radiated has dropped by factor of 4, while keeping the same 61% level of the energy transferred.

This considerable decrease in radiation may seem surprising, because the intermediate resonator L_B, which mediates all the energy transfer, is highly radiative ($\approx$ 650 times more radiative than L_1 and L_2), and there is much more time to radiate, since the whole process lasts 14 times longer than in Fig. 17b. Again, the clue to the physical mechanism behind this surprising result can be obtained by observing the differences between the curves describing the energy in R_B in Fig. 17b and Fig. 17c. Unlike the case of constant coupling rates, depicted in Fig. 17b, where the amount of energy ultimately transferred to L_2 goes first through the intermediate loop L_B, with peak energy storage in L_B as much as 30% of the peak total energy of the system, in the case of time-varying coupling rates, shown in Fig. 17c, there is almost little or no energy in L_B at all times during the transfer. In other words, the energy is transferred quite efficiently from L_1 to L_2, mediated by L_B without considerable amount of energy ever being in the highly radiative intermediate loop L_B. (Note that direct transfer from L_1 to L_2 is identically zero here since L_1 is always perpendicular to L_2, so all the energy transfer is indeed mediated through L_B). In some examples, improvement in efficiency and/or radiated energy can still have been accomplished if the energy transfer had been designed with a time t_{EIT} smaller than its optimal value (perhaps to speed up the process), if the maximum energy accumulated inside the intermediate resonator was less than 30%. For example, improvement can have been achieved for maximum energy accumulation inside the intermediate resonator of 5% or even 10%.

InductEV, Inc.
Exhibit 1025
Page 693

An example implementation of the coupling rate adjustment system 300 is described below, where the resonators are capacitively-loaded loops, which couple to each other inductively. At the beginning (t=0), the coupling rate adjustment system 300 sets the relative orientation of the first resonator structure L_1 to be perpendicular to the intermediate resonator structure L_B. At this orientation, the value of the coupling rate κ_{1B} between the first and intermediate resonator structure is at its minimum value. Also, the coupling rate adjustment system 300 can set the relative orientation of the second resonator structure L_2 to be parallel to the intermediate resonator structure L_B. At this orientation, the value of the coupling rate κ_{B2} is at a maximum value. During wireless energy transfer, the coupling rate adjustment system 300 can effect the rotation of the first resonator structure L_1 about its axis so that the value of κ_{1B} is increased. In some examples, the coupling rate adjustment system 300 can also effect the rotation of the second resonator structure, L_2, about its axis so that the value of κ_{B2} is decreased. In some examples, a similar effect can be achieved by fixing L_1 and L_2 to be perpendicular to each other and rotating only L_B to be parallel to L_2 and perpendicular to L_1 at t=0 and parallel to L_1 and perpendicular to L_2 at $t=t_{ETT}$. In some examples, a similar effect can be achieved by fixing L_B and one of L_1 and L_2 (e.g., L_1) at a predetermined orientation (e.g. at 45 degrees with respect to the intermediate resonator L_B) and rotating only the other of L_1 and L_2 (e.g., L_2 from parallel to L_B at t=0 to perpendicular to L_B at $t=t_{ETT}$).

Similarly, in some implementations, at the beginning (t=0), the coupling rate adjustment system 300 can set the position of the first resonator structure L_1 at a first large predetermined distance from the intermediate resonator structure L_B so that the value of the coupling rate κ_{1B} is at its minimum value. Correspondingly, the coupling rate adjustment system 300 can set the position of the second resonator structure L_2 at a second small predetermined distance from the intermediate resonator structure L_B so that the value of the coupling rate κ_{B2} between the first and intermediate resonator structure is at its maximum value. During wireless energy transfer, the coupling rate adjustment system 300 can affect the position of the first resonator structure L_1 to bring it closer to

InductEV, Inc.
Exhibit 1025
Page 694

L_B so that the value of κ_{1B} is increased. In some examples, the coupling rate adjustment system 300 can also effect the position of the second resonator structure, L_2, to take it away from L_B so that the value of κ_{B2} is decreased. In some examples, a similar effect can be achieved by fixing L_1 and L_2 to be at a fixed distance to each other and effecting the position of only L_B to be close to L_2 and away from L_1 at t=0 and close to L_1 and away from L_2 at $t=t_{EIT}$. In some examples, a similar effect can be achieved by fixing L_B and one of L_1 and L_2 (e.g., L_1) at a predetermined (not too large but not too small) distance and effecting the position only the other of L_1 and L_2 (e.g., L_2 from close to L_B at t=0 to away from L_B at $t=t_{EIT}$).

5. Comparison of static and adiabatically dynamic systems

In the abstract case of energy transfer from R_1 to R_2, where no constraints are imposed on the relative magnitude of κ, Γ_{rad}^{A}, Γ_{rad}^{B}, Γ_{abs}^{A}, and Γ_{abs}^{B}, it is not certain that the adiabatic-κ (EIT-like) system will always perform better than the constant-κ one, in terms of the transferred and radiated energies. In fact, there could exist some range of the parameters ($\kappa, \Gamma_{rad}^{A}, \Gamma_{rad}^{B}, \Gamma_{abs}^{A}, \Gamma_{abs}^{B}$), for which the energy radiated in the constant-κ transfer case is less than that radiated in the EIT-like case. For this reason, we investigate both the adiabatic-κ and constant-κ transfer schemes, as we vary some of the crucial parameters of the system. The percentage of energies transferred and lost (radiated+absorbed) depends only on the relative values of κ, $\Gamma_A = \Gamma_{rad}^{A} + \Gamma_{abs}^{A}$ and $\Gamma_B = \Gamma_{rad}^{B} + \Gamma_{abs}^{B}$. Hence we first calculate and visualize the dependence of these energies on the relevant parameters κ/Γ_B and Γ_B/Γ_A, in the contour plots shown in Fig. 21.

The way the contour plots are calculated is as follows. For each value of (κ/Γ_B, Γ_B/Γ_A) in the adiabatic case, where $\kappa_{1B}(t)$ and $\kappa_{B2}(t)$ are given by Eq. (44)-(45), one tries range of values of t_{EIT}. For each t_{EIT}, the maximum energy transferred $E_2(\%)$ over $0< t <t_{EIT}$, denoted by $\max(E_2, t_{EIT})$, is calculated together with the total energy lost at that maximum transfer. Next the maximum of $\max(E_2, t_{EIT})$ over all values of t_{EIT} is selected

InductEV, Inc.
Exhibit 1025
Page 695